UCSF

UC San Francisco Electronic Theses and Dissertations

Title
The low pH-induced conformational change in the influenza hemagglutinin

Permalink
https://escholarship.org/uc/item/6d96c0gv

Author
Hoffman, Lucas R.

Publication Date
1997

Peer reviewed|Thesis/dissertation

eScholarship.org Powered by the California Digital Library
University of California

The low pH-induced conformational change in the influenza hemagglutinin: Inhibitor design

by

Lucas R. Hoffman

DISSERTATION

Submitted in partial satisfaction of the requirements for the degree of

DOCTOR OF PHILOSOPHY

in

Biochemistry

in the

GRADUATE DIVISION

of the

UNIVERSITY OF CALIFORNIA

San Francisco

[redacted]

Date **University Librarian**

Degree Conferred: . . . .

© Copyright 1996
by
Lucas R. Hoffman

To my lovely and mysterious (who has the flu)

Preface

When I came to UCSF to interview for the MD/PhD program, I was sent to have a low-key, no-pressure "talk" with a faculty member (who shall remain nameless) before the real grilling began. This man chatted easily about the research he was engaged in and the virtues of UCSF in general; he had, after all, been here for a while. He asked me about the research I had done as an undergraduate, and when I described my bioinorganic chemical synthesis project, he shook his head in surprise. He looked over my application. "Well, I have to be honest," he said, "I don't think you'd be very happy here. We don't have anyone doing much like that." He went on to tell me that my background wouldn't be much good in biomedical sciences. My first two interviews were with Charly Craik and Irwin "Tack" Kuntz, each of whom told me that my background would serve me well in a place like UCSF, and each of whom is largely responsible for my surviving graduate school.

The project described in this thesis is multidisciplinary; this means I was forced to learn something about many fields but everything about nothing. This is exactly the sort of work I wanted to do. I found that I had to meet nearly everybody in the school in order to get through the project, and I quickly became an expert in shamelessly leeching time, information, and resources from anyone in any department. Therefore, this section is the most difficult of all to write. I owe everything to everybody, and I have to thank them all. I'm afraid, however, I'll have to hit the biggest ones only, keeping the hugest ones for last. I'll try to organize this by department.

In biophysics and pharmaceutical chemistry, Fred Cohen and the members of his lab literally babysat me after one of my advisors, Judy White, moved away. They gave me computer resources, Doom games, and most importantly, food. Bob Keenan, Earl Rutenber, Nick Sauter and Reuben Peters have been indispensable friends and advisors on the crystallographic end of things. And, as mentioned above, Charly Craik has always made time for me when I needed it and supported me during the troughs of graduate school. Dave Agard has always done the same. And I often needed their time. The Kuntz lab (especially Elaine Meng, Dan Gschwend, Connie Oshiro and Todd Ewing) taught me about the strengths and weaknesses of DOCK; Donna Hendrix, Malin Young, and Keith Burdick have been the backbone of the Integrase project.

In biochemistry, the White lab (especially Joanna Gilbert, Lorrie Hernandez, Paul Straight, Tsafi Danieli, Carol Weiss, Paul Straight, Hui Qiao and Jill Hacker) took a chemist who'd never used a pipetman and taught him the mysteries of cell biology. My discussions with them have been some of my most useful, and I simply wouldn't know how to do anything without them. Paul Wilson, Pablo Garcia and the Bourne lab were also very helpful on the cell biology front. Dave Leonardo, Jose de la Torre, Kayvan Roayaie, Chen Ming Fan and pretty much the whole 14th floor taught me how to sequence from scratch and always let me use equipment they couldn't easily spare.

And now for the big ones: Don Ganem and his lab took me in after Judy left; without them, my project would undoubtedly be a different one with much less rigorous microbiological study. Simply put, they were my lab and my friends during the last year and a half of this project. Don gave me space in the lab for no reason other than kindness, and he treated me as his own student without expecting any recognition. Judy White and Tack Kuntz taught me more than I've ever learned about more subjects than ever before. I have learned about the politics of science, about bench science, about theoretical science, and most importantly, about how nice people do science. They have been infinitely patient with me and given me more rein than I deserved in what was, again, an atypical project. They sent me nearly everywhere to help along the project and my education. And they did it together, with one on each coast. I doubt this could have worked with anyone else at the helm. Dale Bodian began this project over 8 years ago with even less of an indication that it would work than I had. She worked the kinks out of many of the techniques I've used, and her flawless memory has made her a key advisor even as she was working on her postdoc in England. Finally, my family has been an ocean of support, especially during orals and my (gulp) wedding, which brings me to my newest family member and my most ardent supporter: Ellen Kuwana married me during this strange project with the odd lab situation, an act of inexplicable understanding and patience.

To everyone mentioned here and even everyone not mentioned: THANK YOU. I loved this project not only for the science; the people it brought me to made it much more worth it.

Abstract

Fusion Mechanism of the Influenza Hemagglutinin: Inhibitor Design

Past structure-based design of an inhibitor of the fusion-inducing conformational change in the influenza hemagglutinin (HA) identified several small molecule inhibitors. The most potent of these, t-butyl hydroquinone (TBHQ), inhibits both the conformational change in HA *in vitro* and viral infectivity in tissue culture with IC_{50} values in the micromolar range. Further effort to use these molecules to design more potent inhibitors requires an understanding of their sites of binding and modes of action. A genetic approach was taken to characterize the site and mode of TBHQ inhibition. Several lines of evidence suggest a TBHQ binding site. Based on how DOCK predicts that TBHQ binds to this site, a derivative of TBHQ was predicted and shown to be a more potent inhibitor. In addition, a fresh round of structure-based inhibitor design was begun using (i) the recently refined BHA crystal structure (2.1 Å resolution), (ii) a greater understanding of the mechanism of the conformational change, and (iii) improvements in the macromolecular docking program, DOCK. The fresh design work has yielded new inhibitors with varying potencies and actions. A group of new inhibitors actually promote the conformational change yet still inhibit viral infectivity.

Using the recently determined crystallographic structures of the core region of HIV-1 and ASV integrase (IN), we have undertaken efforts to identify and develop structure-based inhibitors of IN activity. Potential integrase inhibitors were selected using the DOCK structure-based searching program based on three putative sites on the ASV integrase central domain. We searched the Available Chemical Directory and carried out similarity searches of known integrase inhibitors. Compounds identified in this way were then tested *in vitro* for inhibition of HIV-1 IN purified from yeast. An IC_{50} was determined for each compound that showed inhibitory activity. In this manner, several lead compounds have been identified.

Table of Contents

Chapter 1. Introduction 1

Chapter 2. Phenolic Inhibitors of the fusion-inducing conformational change in the influenza hemagglutinin: Improved potency and mechanism of action 18

Chapter 3. Structure-based identification of an inducer of the low-pH conformational change in the influenza hemagglutinin that inhibits infectivity 69

Chapter 4 A specific proline substitution in the coiled-coil region of the influenza hemagglutinin impairs its membrane fusion activity 115

Chapter 5 Recent developments in elucidating the mechanism of action of HA inhibitors 160

Chapter 6 Perspectives on HA function 181

Chapter 7 Preliminary structure-based searches for ASV/HIV integrase inhibitors . 184

Appendix A Sample computer files used in this work 204

Appendix B Protocols for methods developed or altered in this work 231

Appendix C Top 100 compounds selected by DOCK targeted to the alternate candidate TBHQ site 263

List of Tables

Chapter 2

Table I Effect of TBHQ on influenza viruses of various subtypes......42
Table II Inhibition of membrane fusion by TBHQ......46
Table III HA mutations in TBHQ-resistant viruses......51
Table IV TBHQ vs. TBP......58

Chapter 3

Table I Input parameters for DOCK-related programs......79
Table II Effects of compounds targeted to new DOCK sites.....83
Table III Effect of C22 on fusion......95
Table IV Sensitivity of HA mutants to C22......103

Chapter 4

Table I Summary of mutation data for HA2 55-81......128

Chapter 7

Table I Results to date: HIV-1 IN......199

List of Figures

Chapter 1

Figure 1 Entry of enveloped viruses into host cells 5

Figure 2 BHA trimer 7

Figure 3 Alpha-carbon tracings of trimeric BHA and TBHA2...10

Figure 4 Residues visible in TBHA2 in three conformations 12

Chapter 2

Figure 1 Thermolysin digestion assay 29

Figure 2 Effect of TBHQ on the conformational change of HA.32

Figure 3 Activities of TBHQ and its tautomer(s)........................37

Figure 4 Effect of TBHQ on infectivity: Time of addition.........39

Figure 5 Effect of TBHQ on BHA from Japan virus.................44

Figure 6 Effect of 10 μM TBHQ on fusion................................46

Figure 7 Locations of HA mutations in TBHQ-resistant isolates48

Figure 8 Location of TBHQ difference density..........................55

Chapter 3

Figure 1 Locations of new DOCK sites.....................................76

Figure 2 Structures of DOCK-selected potential inhibitors.........81

Figure 3 Effect of S22 and C22 on HA conformational change.85

Figure 4 Effect of C22 on the conformational change of HA.....88

Figure 5 Effect of C22 on infectivity and cell viability................91

Figure 6 Inhibition of fusion and hemolysis by 10 μM C22.......95

Figure 7 HA mutations in C22-resistant isolates 99

Figure 8 Reversibility of C22 effect on infectivity 105

Chapter 4

Figure 1 HA2 55-81 in pre- and post- fusion forms.................126

Figure 2 Migration of wt and mutant HA0s on SDS gels........132
Figure 3 Proteolytic processing of wt and mutant HA0s..........135
Figure 4 Sucrose gradient analysis of wt and pro-substituted HAs........138
Figure 5 Proteinase K sensitivity of wt and mutant HAs..........141
Figure 6 Reactivity of wt, ala- and pro- substituted HAs to C-HA1........143
Figure 7 Fusion activity of pro-substituted HAs: Lipid mixing........146
Figure 8 Fusion activity of pro-substituted HAs: Content mixing........148
Figure 9 Cell surface expression of wt vs. V55P HA..............151
Figure 10 Normalized fusion activity of wt and V55P HA........154
Figure 11 Fusion activity of V55P/S71P HA............................156

Chapter 5

Figure 1 Effect of TBHQ and C22 on proteinase K sensitivity of BHA........163
Figure 2 Effect of TBHQ and C22 on trypsin sensitivity of BHA........164
Figure 3 Effect of TBHQ on immunoprecipitation by site A and N2........166
Figure 4 Effect of C22 on immunoprecipitation by site A and N2........167
Figure 5 Effect of TBHQ on immunoprecipitation by interface168
Figure 6 Effect of C22 on immunoprecipitation by interface....169
Figure 7 Effect of S22 and TBHQ mixtures in the thermolysin

assay 170
Figure 8 Effect of S22 and TBHQ mixture on infectivity......... 171
Figure 9 Effect of C22 and TBHQ mixtures in the thermolysin assay 172
Figure 10 Effect of C22 and TBHQ mixture on infectivity 173

Chapter 7

Figure 1 Structures of the catalytic domains of HIV-1 and ASV IN 188
Figure 2 Locations of DOCK sites on ASV IN........................ 191
Figure 3 A hypothetical similarity search using 2 methods 198

Chapter 1:

Introduction

Portions of this chapter are being published as:

White, J.M., Hoffman, L.R., Arevalo, J.H., and Wilson, I.A. (1996) Attachment and entry of influenza virus into host cells: pivotal roles of the hemagglutinin. in: *Structural Biology of Viruses*, W. Chu, R. Burnatt, R.Garcea (eds.), Oxford University Press. in press.

and

Hernandez, L. D., Hoffman, L. R., Wolfsberg, T. G., & White, J. M. (1996) *Ann. Rev. Cell Devel. Biol. 12*, in press.

Introduction

Structure-based inhibitor design and antivirals

Structure-based drug design represents a relatively new technology in the search for novel chemotherapeutics. This technique uses the three-dimensional structure of a macromolecular target as well as experimentally determined information regarding the function of the macromolecule to identify small molecules that inhibit its function. One of the earliest and most-used computer algorithms developed to aid in such pursuits is DOCK ((Kuntz et al., 1982),(Shoichet, 1991),(Shoichet, 1992),(Meng, 1992)), a program that both identifies potential binding sites on a receptor and searches databases of small molecules for chemicals predicted to interact with these sites. The use of DOCK to identify enzyme inhibitors is well-documented ((DesJarlais, 1990),(Shoichet, 1993),(Yamamoto, 1994),(Rose, 1994)); DOCK has also been used to identify molecules that bind non-enzyme macromolecules (Bodian et al., 1993).

Viruses present a particularly enticing case for structure-based inhibitor design because they often encode proteins not encountered in the host cell. For example, retroviruses direct the production of integrases and reverse transcriptases, both enzymes with no cellular homolog (Katz, 1994). As the structures of a growing number of viral proteins are solved, structure-based antiviral design has become a useful tool in the search for new therapeutics. In addition, in the case of at least one virus, HIV-1 (Carpenter, 1996), a high viral mutational rate has necessitated the use of a combination antiviral therapy that targets more than one enzyme target; the use of "rational" drug-design methods in the exploration of new targets has already proven fruitful (Lam, 1994). The use of small molecules to maintain viruses in their coated, pre-infectious state is also a relatively new idea ((Bodian et al., 1993),(Mosser & Rueckert, 1993)).

Influenza and hemagglutinin

Influenza viruses cause acute and highly contagious respiratory illnesses. It is likely that the viruses have been with us since ancient times, and major epidemics, such as the "Spanish" influenza of 1918, the "Asian" influenza of 1957, and the "Hong Kong" influenza of 1968 led to the deaths of millions of individuals. In addition, nearly annual outbreaks of the virus continue to impart significant morbidity and excess mortality around the world. Hence influenza remains a major unconquered viral disease (Kingsbury, 1990),(Murphy & Webster, 1990),(Wilson & Cox, 1990)).

Influenza virus is membrane-bound, or enveloped. Enveloped viruses employ two routes of entry into host cells (Fig. 1). One route involves binding to cell surface receptors, endocytosis through clathrin coated pits and vesicles, delivery to endosomes, and finally fusion with the endosomal membrane in response to the low pH therein (Fig. 1A). This is the route taken by influenza. The other route is conceptually simpler: following binding to cell surface receptors, the virus fuses directly with the plasma membrane at neutral pH (Fig. 1B). In either case, the membrane fusion reaction is kinetically extremely unfavorable, and thus each virus encodes a protein to facilitate the process. The fusion protein encoded by influenza virus is known as hemagglutinin (HA), which has been well-studied (for reviews, see (White, 1996), (Hernandez et al., 1996)), and is thus considered a paradigm for virus membrane fusion in general.

The fusion-inducing conformational change of HA

The influenza HA is a trimeric, transmembrane glycoprotein that projects 130 Å from the virus membrane (Fig. 2). Each monomer is composed of HA1, a globular receptor binding subunit and HA2, a fibrous subunit which houses the fusion peptide. The two subunits arise by a proteolytic cleavage event that is essential for fusion activity. In

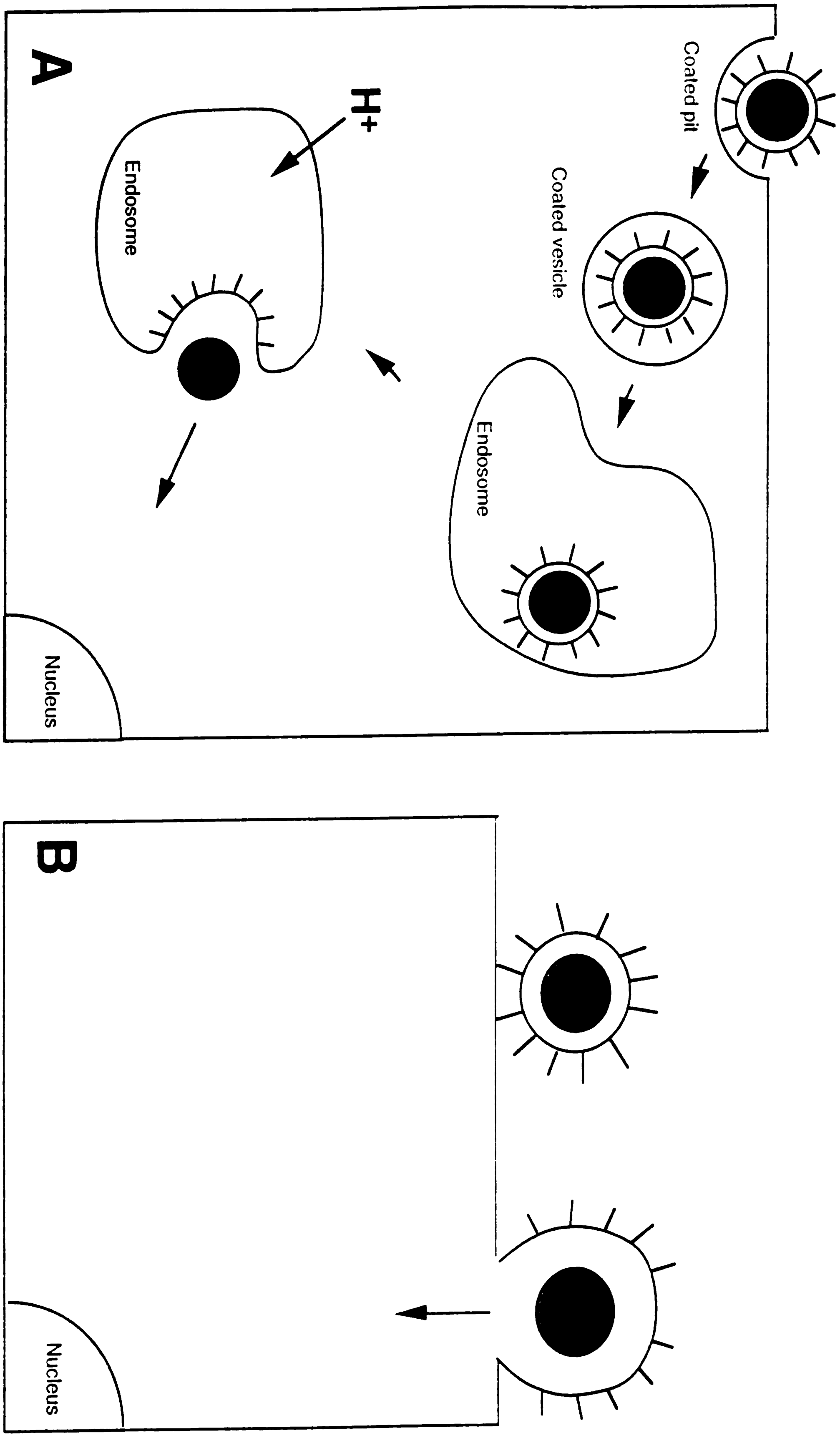
A
Coated pit
Coated vesicle
Endosome
H+
Endosome
Nucleus
B
Nucleus

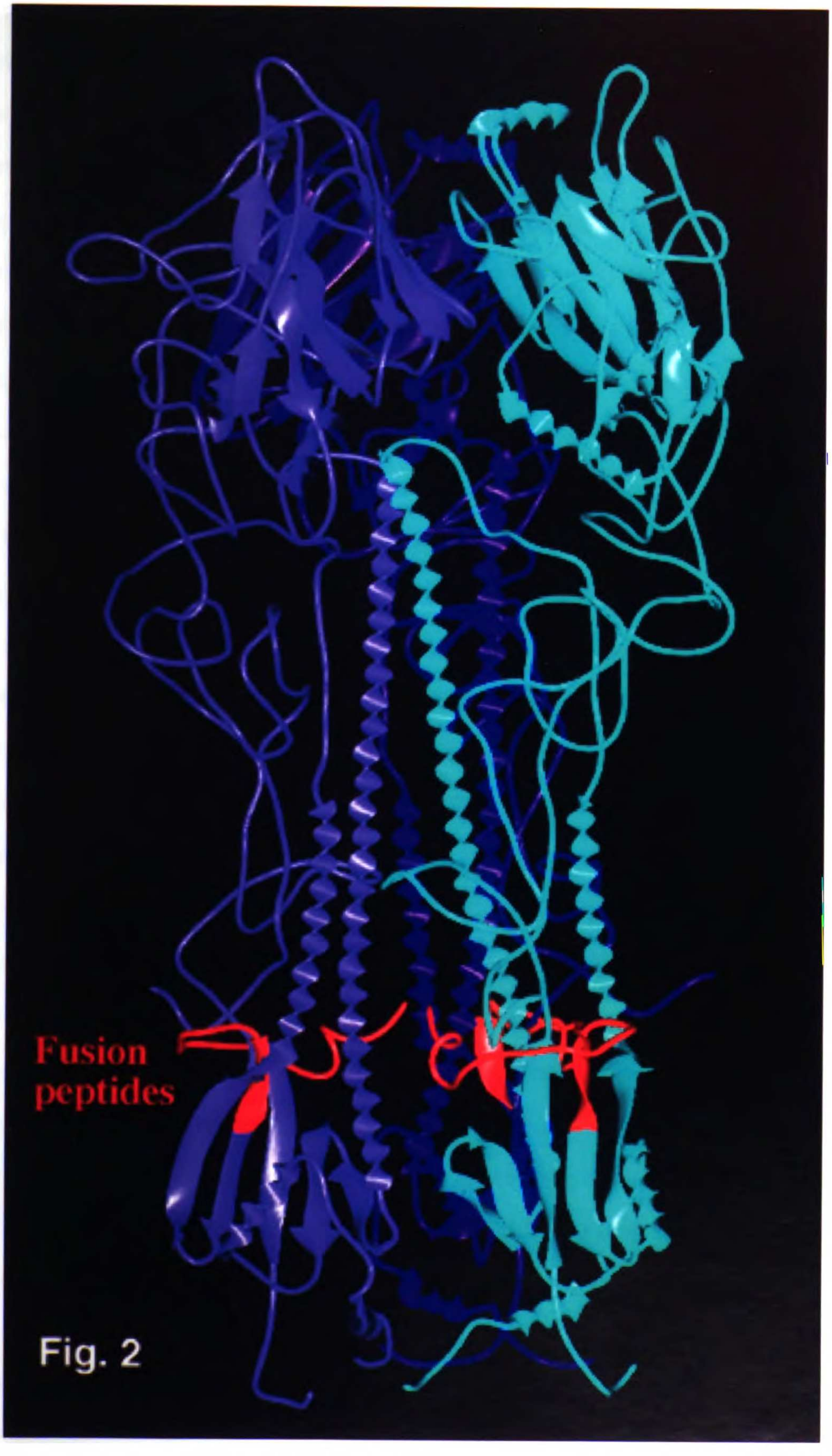
Fusion peptides

Fig. 2

response to the acidity of the endosome, HA undergoes a drastic, irreversible conformational change that triggers the fusion reaction. Treatment of whole, active influenza virus with the protease bromelain releases a soluble, trimeric form of HA known as BHA. This protein was crystallized in is neutral-pH form (inactive for fusion), and the crystal structure was solved to 3.0Å resolution in 1981 (Wilson et al., 1981); the resolution of this structure was recently extended to 2.1Å resolution (Watowich et al., 1994). Upon exposure to low pH, however, BHA and HA irreversibly inactivate through aggregation or interaction with membranes (Wharton et al., 1995). In the neutral pH structure, the three fusion peptides, one from each monomer, are located ~ 100 Å from the target membrane, where they are tucked in the trimer interface by a network of hydrogen bonds and lie approximately parallel to the plane of the virus membrane (Wiley & Skehel, 1987). In response to low pH, HA exposes its fusion peptides and binds hydrophobically to target membranes. Many conformational changes, including exposure of the fusion peptides and separation of the globular head domains, were illuminated using biochemical, biophysical, and immunological probes ((Doms, 1993); (Gaudin et al., 1995)). None, however, foreshadowed the massive rearrangements in HA2 that were revealed by the x-ray structure of a derivative of low pH HA called TBHA2 (Bullough et al., 1994). TBHA2 is made by treating the bromelain released HA ectodomain (BHA) with low pH, and then treating it with trypsin to cleave off the globular head domains and with thermolysin, to digest the fusion peptides. The resulting structure (Figs. 3, 4B) revealed three major changes in the HA2 stem. Firstly, a prominent loop, designated "B", has been transformed into a helix, thereby connecting the existing helical regions, "A" and "C" and, presumably, propelling the N-terminal fusion peptide upwards towards the target membrane. Secondly, residues 106-112 convert from helical form to a loop, thereby causing the rest of the "D" helix to be flipped 180 deg. and to run antiparallel to the "C" helix. The third notable feature is that ~20 C-terminal amino acids, which are present in

Fig. 3. Alpha-carbon tracings of trimer BHA and TBHA2. Left, BHA trimer; HA1 of one monomer is colored red, HA2 is colored green, yellow, cyan and red going from the N-terminus to C-terminus. The yellow region corresponds to HA2 55-81, which undergoes a loop to helix transformation at low pH, while the cyan region corresponds to the long helix (HA2 82-127) which undergoes a helix-to-loop transformation at low pH.

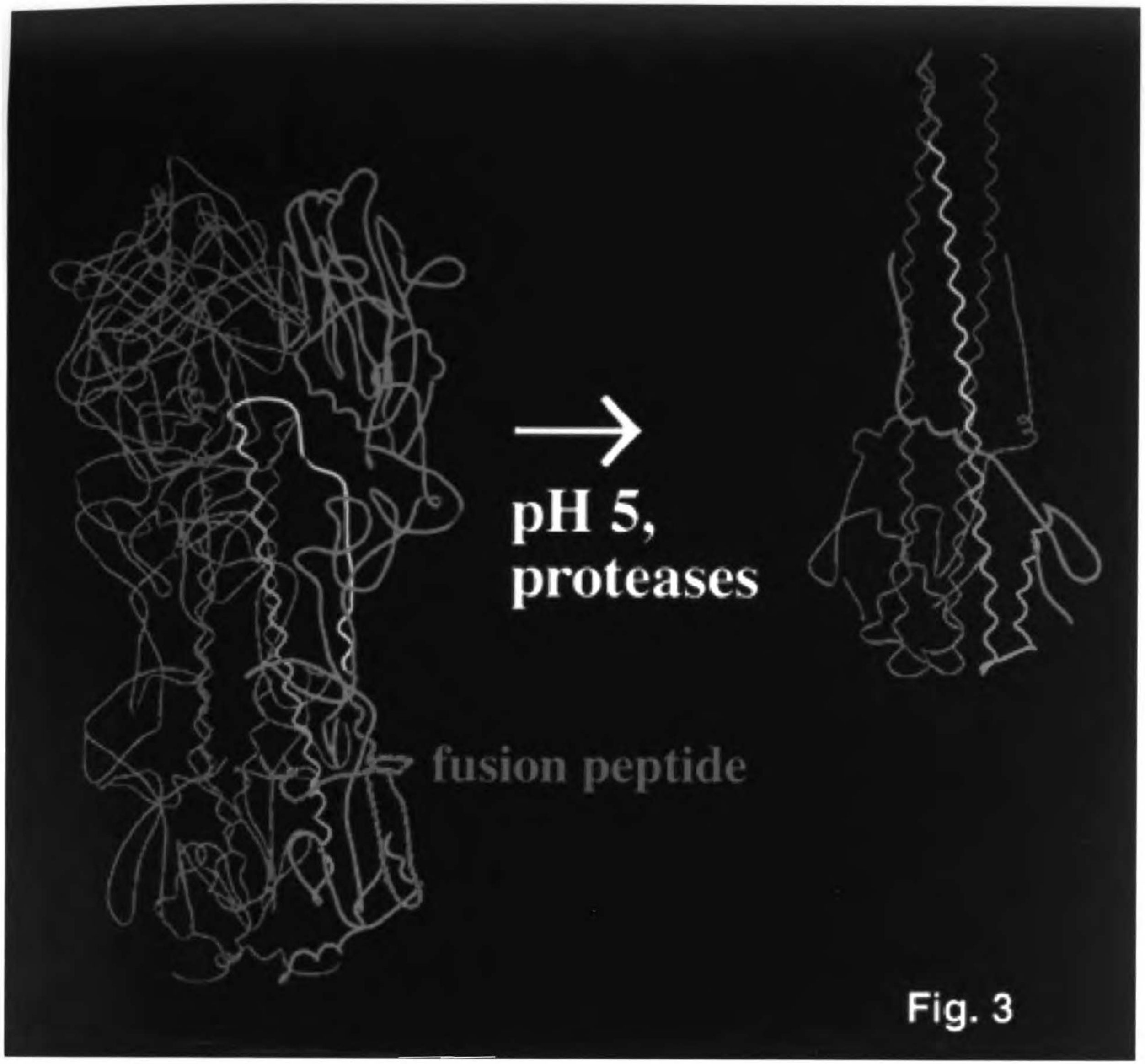
pH 5,
proteases
fusion peptide

Fig. 3

Fig. 4. Schematic of all of the residues visible in a TBHA2 monomer in each of three conformations: (a) In the neutral-pH conformation (inactive for fusion), (b) in the low-pH conformation (possibly active for fusion), and (c) in an inverted conformation in which fusion peptides are inserted into the viral membrane (inactive for fusion).

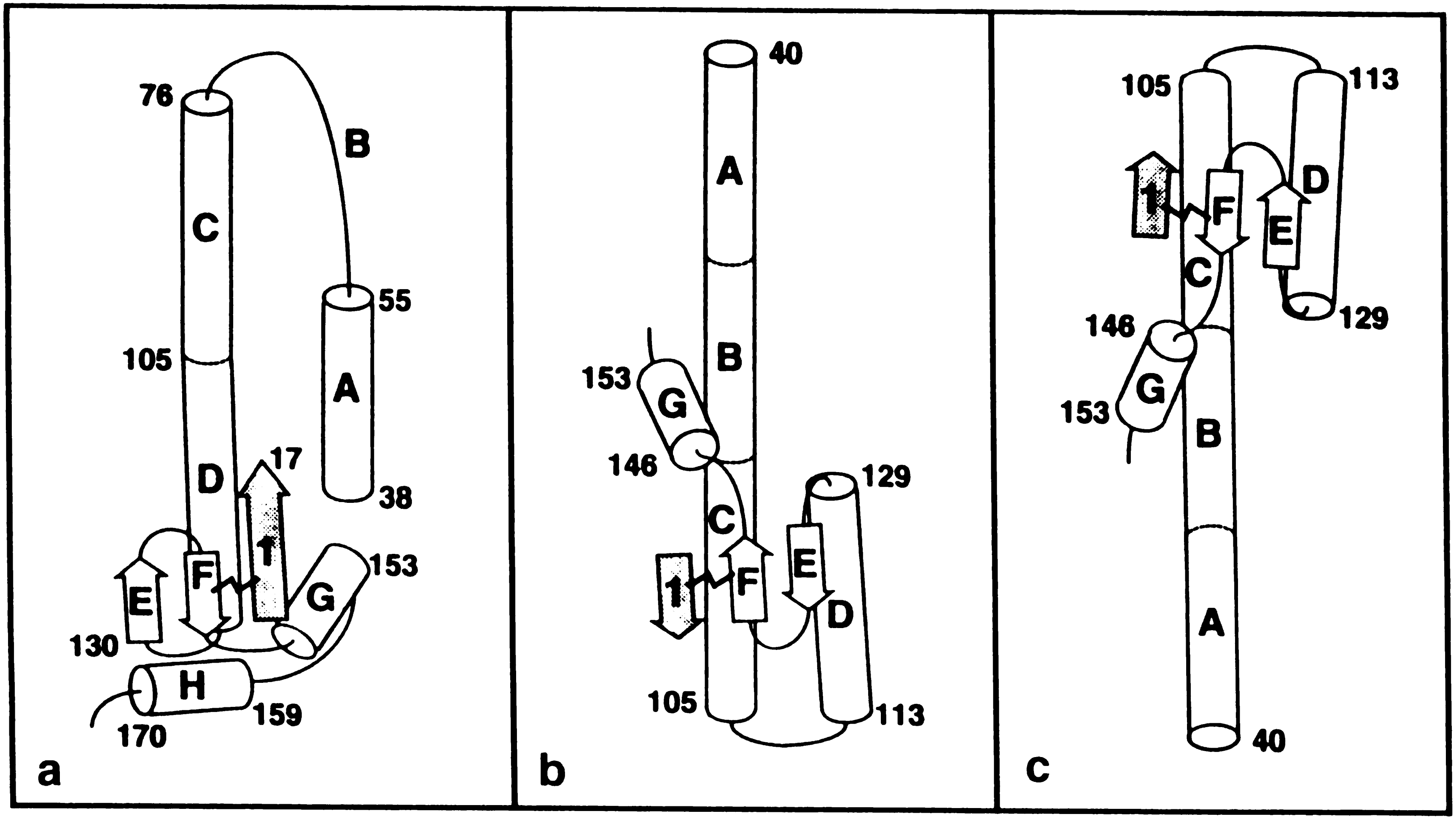
76
B
C
55
105
A
D
17
38
1
153
F
E
G
130
H
159
170
a
40
A
B
153
G
146
129
C
E
1
F
D
105
113
b
105
113
D
1
F
E
C
129
146
G
153
B
A
40
c

the TBHA2 protein, cannot be seen in the x-ray structure, indicating that they are in a disordered, perhaps extended, conformation. Although the "B" loop-to-helix transition had been proposed from structure prediction ((Carr & Kim, 1993); (Ward & Dopheide, 1980)), and synthetic peptide (Carr & Kim, 1993) studies, the latter two changes had not been predicted.

A critical question is how the structure reflected by TBHA2, the final low pH and most stable form of HA (Ruigrok et al., 1988), participates in fusion. Insight into this question can be garnered by considering how TBHA2 is oriented vis-à-vis the virus membrane, which in the fused state is united with the target membrane. Two recent studies have addressed this issue. If X:31 influenza (the strain whose BHA structure has been solved (Wilson et al., 1981) is pretreated at low pH in the absence of a target membrane, it becomes irreversibly inactivated for fusion (White, 1995). In other words, it has prematurely undergone its conformational change and is driven into a fusion-incompetent form. In the first study, ^{125}I-labeled photoactivatable phospholipids were incorporated into influenza viral membranes. The virus particles were then exposed to low pH, and the HA isolated and analyzed for radioactive labeling. Label was found only in the fusion peptide. Hence in the fusion-inactive form, the fusion peptide is in the virus membrane, as is its transmembrane domain ((Weber et al., 1994), Fig. 4C). In short, the two available crystal structures of HA represent fusion-inactive forms.

Structure-based antiviral design

The work presented in this thesis concerns the structure-based design of small-molecule antivirals. In this analysis, two questions are addressed regarding HA function: First, how do the conformational changes revealed by the two crystal structures relate to the intermediate structure of HA that mediates fusion? Second, can we use the current understanding of HA structure and function to design inhibitors of viral fusion and define their modes of action? In Chapter 2 of this thesis, I describe recent progress in understanding the mechanism of influenza inhibition by a family of small molecules identified by earlier work in the White and Kuntz laboratories (Bodian et al., 1993). Chapter 3 details the identification of several new influenza inhibitors with interesting properties and their utility in understanding the mechanism of HA-mediated fusion. In Chapter 4, an examination of the role of HA2 55-81 in converting HA to its fusion-active form is presented. Chapter 5 describes recent progress in elucidating the mechanism of action of the inhibitors examined in Chapters 2 and 3 and, and Chapter 6 synthesizes this material in a general conclusion section.

Continuing the theme of structure-based inhibitor design, Chapter 7 presents a brief description of preliminary searches for novel molecules that inhibit retroviral integrases. These searches have employed both DOCK and computer database searches for molecules structurally similar to known integrase inhibitors.

References

Bodian, D. L., Yamasaki, R. B., Buswell, R. L., Stearns, J. F., White, J. M., & Kuntz, I. D. (1993) *Biochemistry 32*, 2967-2978.

Bullough, P. A., Hughson, F. M., Skehel, J. J., & Wiley, D. C. (1994) *Nature 371*, 37-43.

Carpenter, C, Fischl, MA; Hammer, SM; Hirsch, MS; Jacobsen, DM; Katzenstein, DA; Montaner, JS; Richman, DD; Saag, MS; Schooley, RT et al. (1996) *JAMA 276*, 146-54.

Carr, C. M., & Kim, P. S. (1993) *Cell 73*, 823-832.

DesJarlais, R. Seibel, GL; Kuntz, ID; Furth, PS; Alvarez, JC; Ortiz de Montellano, PR; DeCamp, DL; Babe, LM; et al. (1990) *PNAS 87*, 6644-6648.

Doms, R. W. (1993) in *Meth. Enzymol* (Duzgunes, N., Ed.) pp 61-82, Academic Press, San Diego.

Gaudin, Y., Ruigrok, R. W. H., & Brunner, J. (1995) *J. Gen. Virol. 76*, 1541-1556.

Hernandez, L. D., Hoffman, L. R., Wolfsberg, T. G., & White, J. M. (1996) *Ann. Rev. Cell Devel. Biol. 12*, in press.

Katz, R, Skalka, AM. (1994) *Annu. Rev. Biochem. 63*, 133-73.

Kingsbury, D. W. (1990) in *Virology* (Fields, B. N., Knipe, D. M., Chanock, R. M., Hirsch, M. S., Melnick, J. L., Monath, T. P., & Roizman, B., Eds.) pp 1075-1089, Raven Press, Ltd., New York.

Kuntz, I., Blaney, J., Oatley, S., Langridge, R., & Ferrin, T. (1982) *J. Mol. Biol. 161*, 269-288.

Lam, P, Jadhav, PK; Eyermann CJ; Hodge, CN; Ru, Y; Bacheler, LT; Meek, JL; Otto, MJ; Rayner, MM; Wong, YN; et al. (1994) *Science 263*, 380-4.

Meng, E. Shoichet, BK; Kuntz, ID. (1992) *Journal of Computational Chemistry 13*, 505-524.

Mosser, A., & Rueckert, R. (1993) *J. Virol. 67*, 1246-1254.

Murphy, B. R., & Webster, R. G. (1990) in *Virology* (Fields, B. N., Knipe, D. M., Chanock, R. M., Hirsch, M. S., Melnick, J. L., Monath, T. P., & Roizman, B., Eds.) pp 1091-1152, Raven Press, New York, NY.

Rose, J, Craik, CS. (1994) *American Journal of Respiratory and Critical Care Medicine 150*, S176-82.

Ruigrok, R. W. H., Aitken, A., Calder, L. J., Martin, S. R., Skehel, J. J., Wharton, S. A., Weis, W., & Wiley, D. C. (1988) *J. gen. Virol. 69*, 2785-2795.

Shoichet, B, Bodian, DL; Kuntz, ID. (1992) *Journal of Computational Chemistry 13*, 380-397.

Shoichet, B, Kuntz, ID. (1991) *Journal of Molecular Biology 221*, 327-346.

Shoichet, B, Stroud, RM; Santi, DV; Kuntz, ID; Perry, KM. (1993) *Science 259*, 1445-50.

Ward, C. W., & Dopheide, T. A. (1980) *Aust. J. Biol. Sci. 33*, 449-455.

Watowich, S. J., Skehel, J. J., & Wiley, D. C. (1994) *Structure 2*, 719-731.

Weber, T., Paesold, G., Mischler, R., Semenza, G., & Brunner, J. (1994) *J. Biol. Chem. 269*, 18353-18358.

Wharton, S. A., Calder, L. J., Ruigrok, R. W. H., Skehel, J. J., Steinhauer, D. A., & Wiley, D. C. (1995) *EMBO J. 14*, 240-246.

White, J.M., Hoffman, LR; Arevalo, JH; Wilson, IA. (1996) .

White, J. M. (1995) *CSHSQB 60*, 581-588.

Wiley, D. C., & Skehel, J. J. (1987) *Annu. Rev. Biochem. 56*, 365-394.

Wilson, I. A., & Cox, N. J. (1990) *Annu. Rev. Immunol. 8*, 737-771.

Wilson, I. A., Skehel, J. J., & Wiley, D. C. (1981) *Nature 289*, 366-372.

Chapter 2:

Phenolic inhibitors of the fusion-inducing conformational change in the influenza hemagglutinin: Improved potency and mechanism of action

Note: Crystallographic data with TBHQ mentioned herein were collected by Stan Watowich in the laboratory of Don Wiley, Harvard University, and are preliminary.

Introduction

Enveloped virus penetration into host cells relies on fusion of the viral envelope and the host cell membrane. The orthomyxovirus influenza enters host cells by receptor-mediated endocytosis. Upon delivery to endosomes, the low pH therein triggers an irreversible conformational change in the viral transmembrane protein hemagglutinin (HA). This conversion, in turn, induces fusion of the viral and host endocytic membranes, thus allowing the viral genetic material to enter the cell to initiate an infection (Wiley & Skehel, 1987). HA exists on the surface of the virus as a trimer, and each monomer consists of two chains, HA1 and HA2. In terms of virus entry, the HA1 subunit is largely responsible for binding the virus to host cell sialic acid-containing receptors whereas the HA2 subunit, which houses the "fusion peptide", is responsible for fusion.

When virus is treated with the protease bromelain, a soluble, trimeric HA ectodomain, known as BHA, is released. The X-ray structure of the neutral-pH form of BHA has been solved to 2.1Å resolution ((Wilson et al., 1981),(Watowich et al., 1994)). In this structure, the fusion peptides are inserted into the center of the trimer, largely inaccessible to solvent and approximately 100Å away from the sialic acid binding sites and thus the target membrane (Wilson et al., 1981). Recently, the structure of a proteolyzed form of low-pH treated BHA (known as TBHA2) was solved by X-ray analysis (Bullough et al., 1994). According to this model, the fusion peptides (although themselves not present in the structure) have been transported via the conformational change to the top of the molecule and to the target membrane.

Since the HA conformational change (and its direct result, membrane fusion) is absolutely required for successful influenza infection and occurs early in the viral life cycle, this event is an attractive target for pharmacologic intervention. We have previously reported an approach used to identify inhibitors of the HA conformational change (Bodian et al., 1993) that used a 3Å resolution structure of BHA and a structure-based computer searching algorithm known as DOCK ((Desjarlais, 1988),(Shoichet, 1992)). Given the three-dimensional coordinates of a target macromolecule, DOCK will characterize the molecular surface chemically and geometrically and scan a database for small molecules predicted to interact with a user-defined target site on that surface. Our original search for HA inhibitors focused on the region around the fusion peptide. We applied DOCK to a pocket on HA that is formed partially by residues of the fusion peptide with the expectation that a molecule that binds to the site would stabilize the region in its pre-fusion conformation. From the compounds suggested by DOCK, we identified a family of related benzoquinones and hydroquinones that inhibit the acid-induced conformational change of BHA *in vitro* as well as viral infectivity in cell culture at micromolar concentrations. The most potent of these inhibitors is tert-butyl hydroquinone (TBHQ), a small molecule that inhibits both the conformational change and viral infectivity in the range of 5-10 μM. Our prior work, however, did not establish the actual site or mechanism of action of TBHQ. In the present study, we present results that strongly suggest that TBHQ inhibits influenza virus infectivity by stabilizing the HA structure under acidic conditions that lead to fusion, and this analysis has suggested an alternate candidate site of action by the inhibitor. Our further characterization of the mechanism of action of TBHQ has also led us to identify a more potent derivative of the inhibitor.

Materials and Methods

Cells and Viruses

Madin-Darby Canine Kidney clone 2 (MDCK2) cells and the HA-expressing cells, HA300A^{++}, were cultivated as described previously ((Bodian et al., 1993),(Kemble et al., 1994)). Influenza viruses X:31 (clone C-22), Victoria, and A/Japan/57 were grown as described (Bodian et al., 1993). Viruses resistant to TBHQ were isolated by two procedures. In the first procedure, allantoic fluid from eggs infected with plaque-purified virus was used to infect MDCK2 monolayers at a multiplicity of infection (MOI) of 0.01 PFU/cell. Allantoic fluid was diluted in Minimal essential medium with Earle's basic salts (MEM-EBSS) containing 25 mM HEPES, penicillin/streptomycin and 1% FBS (hereafter referred to as diluent). TBHQ (100 µM or 10 µM) was added, and the mixture was adsorbed to cells for 1 hour at 37^{0}C. The medium was then replaced with primary overlay medium (2x MEM-EBSS with 2x penicillin/streptomycin, 50 mM HEPES, and 5% FBS mixed with an equal volume of 1% SeaPlaque agarose). Trypsin was added to a final concentration of 10 µg/mL, and the overlay was allowed to harden at room temperature. The cells were then returned to a 37^{o}C, 5% CO_2 incubator. The infection was allowed to proceed for 36 hours, at which time 2.5 mL of second overlay medium (equal volumes 2x MEM-EBSS with 2x penicillin/streptomycin, 50 mM HEPES, 5% FBS and 1.8% SeaPlaque agarose, also containing 0.003% neutral red solution (Sigma) was allowed to harden over the first overlay, and the cells were returned to the incubator for an additional 4 h. Plaques containing virus were harvested with sterile 200 µL pipet tips and resuspended in 2 mL diluent for further passaging. This process was repeated 8 times with the exception that in passages 2 to 8, inhibitor was added to the overlay as well. TBHQ-resistant virus was then amplified by one passage on MDCK2 cells in virus-free, TBHQ-free diluent instead of agarose and omitting trypsin. After 48 hours of infection, the diluent containing virus was harvested and cleared of cellular debris. The resultant virus stock was then tested for sensitivity to TBHQ by both plaque assay and ELISA assay, and prepared for sequencing as described below. In the second procedure, the initial infection was carried out as above but with an MOI of 1 PFU/cell and in the presence of 3 mM TBHQ, a concentration that is nontoxic to MDCK2 cells as assessed by trypan blue exclusion assay (Ausubel, 1994). After 1 hour of adsorption, the diluent containint virus and inhibitor was removed and replaced with liquid diluent overlay containing 100 µM TBHQ. After 48 hours of incubation at 37°C, 5% CO_2, the overlay containing virus was harvested. This stock was then used to isolate TBHQ-resistant viruses through one round of plaque-purification, and these isolates were amplified and processed as above.

Inhibitors

TBHQ was purchased from Aldrich, and 4-bromo 2-tert-butyl phenol (TBP) from the Aldrich Library of Rare Chemicals (also known as Salor).

Infectivity Assays

Plaque assays on MDCK2 cells were carried out as described (Tobita, 1975) with the following modifications: Virus released from MDCK2 cells (which express the inactive precursor, HA0, form of HA) was pretreated with 10 µg/mL trypsin for 30 minutes at RT. Monolayers of MDCK2 cells in 6-well plates were washed twice with PBS and inoculated with 0.25 mL of virus in diluent for 1 hour at 37 °C with rocking every 15 min. At this time, 2.5 mL of primary overlay medium containing 10 µg/mL trypsin was added. After the overlay was allowed to harden at room temperature, the cells were returned to a 37°C, 5% CO_2 incubator for 36 h. At this time, 2.5 mL of second overlay medium containing 0.003% neutral red was added and allowed to harden, and the cells were returned to the incubator. Plaques were counted 6 hours later. For the single-cycle infection assay, virus was adsorbed to cells for 1 hr at 4°C. The medium was then removed and replaced with fresh, prewarmed diluent.. The cells were then returned to the 37°C, 5% CO_2 incubator. After 15 hours, the medium was removed, treated with 10 µg/mL trypsin for 30 min at RT, and assayed for virus concentration by plaque assay.

ELISA assays for single-cycle growth and MTT cell viability assays were carried out as described (Bodian et al., 1993).

Hemolysis Assay

The pH at which the different viruses lysed fresh, human type A^+ erythrocytes was determined as described (Daniels et al., 1985) with the following modifications: Incubations at low pH were conducted for 15 minutes at 37°C; hemoglobin was detected spectrophotometrically at 550 nm.

Virus Genome Sequencing

Virus isolates harvested in liquid media were pelleted and their RNA genomes purified as described (Xu, 1993). The HA genes were then reverse transcribed using a primer corresponding to coding strand nucleotides 15-35 numbered according to the cDNA sequence of X:31 HA given in Genbank accession #J02090 using the method of (Xu, 1993). The cDNAs were then amplified by PCR using one primer corresponding to coding strand nucleotides 36-56 and another complementary to coding strand nucleotides 1693-1712 in the non-coding direction. The products of this amplification were then sequenced using the *fmol* cycle sequencing kit (Promega). The ten primers used for X-31 mutant and wild-type viruses correspond to coding strand nucleotides 36-56, 282-306, 454-477, 677-700, 857-881, 1025-1048, 1191-1214, 1350-1373, 1497-1520, and 1596-1640.

Preparation and Purification of Biotinylated BHA

X-31 virus was biotinylated and its HA released with bromelain as described for HA-expressing cells (Kemble et al., 1992) with the following modifications: 13 mg of virus was suspended in 3 mL ice-cold PBS containing 1 mg/mL NHS-LC-biotin (Amersham) and incubated at 4°C for 45 minutes. The virus was then pelleted by centrifugation in a

TLA100.3 rotor at 55,000 rpm for 30 minutes at 4°C. The supernatant was aspirated, and the virus pellet was resuspended in 50 mM glycine in ice-cold PBS. The virus was pelleted as before and resuspended in 1 mL 0.1 M Tris-HCl, pH 8. Bromelain was added to give a final concentration of 2.5 mg/mL. 7.7 µL concentrated β-mercaptoethanol was added and the mixture was incubated at 37°C overnight. The virus was then pelleted as above. Biotinylated BHA was then purified from the supernatant on a column of agarose-conjugated ricin-I (Sigma). The column was washed with Mes-saline-succinate-hepes buffer (MSSH: 10 mM HEPES, 10 mM MES, 10 mM succinate, 0.10 M NaCl, pH 7.0), and the bound BHA was eluted with 0.2 M galactose in MSSH. Biotinylated BHA was detected following SDS-PAGE on 12% gels and blotting of proteins transferred to Immobilon-P membrane (Millipore) with streptavidin-conjugated horseradish peroxidase (Kemble et al., 1992).

BHA from Japan virus was the kind gift of Dr. Don Wiley.

Protease Assays for the HA Conformational Change

Thermolysin Digestion:

Thermolysin has been shown to digest exposed fusion peptides in the final low-pH conformation of BHA (Bullough et al., 1994). To assay for this conformational change, 100 µL aliquots of purified, biotinylated BHA (1 µg/mL in MSSH) were adjusted to the indicated pH value by the addition of 1 M acetic acid for the indicated time and then reneutralized using 1 M NaOH. Equivalent amounts of MSSH buffer were added to pH 7 controls. $CaCl_2$ and thermolysin (Sigma) were added to final concentrations of 1 mM and 10 µg/mL, respectively, the mixture was incubated at 37°C for 2 hours, and the reaction was then quenched with EDTA (10 mM final). Samples were then processed for and analyzed by SDS-PAGE, transferred to Immobilon-P membranes, and probed with streptavidin-HRP as described in (Kemble et al., 1992) and above. Films of each gel were analyzed by densitometry. Four standards, containing 100%, 60%, 20%, and 10% of the input biotinylated BHA used in each analysis, were loaded on each gel and used to generate a standard curve of the percent protein versus the HA2 signal.

Trypsin Assay

Low pH-treated BHA is cleaved by trypsin at HA1 residues 27 and 224 (Skehel et al., 1982). To assay for this conformational change, biotinylated BHA was treated at low pH and reneutralized as described above and then incubated with trypsin (1000:1 BHA:trypsin, w:w) for 20 minutes at RT. Samples were then processed for SDS gels and streptavidin-HRP blotting as described above. Digestion of the HA1 band was used as a qualitative assay for the conformational change.

K_d Determination

The dissociation constant, K_d, for the binding of TBHQ to BHA was determined using an equilibrium dialysis method as described (Legler, 1986). From the known initial concentrations, $[TBHQ]_i$ and $[BHA]_i$ (trimer), and the assumption of 3 binding sites per trimer ,

$$Kd = [TBHQ]_u ([BHA]_i-1/3\ [TBHQ]_b) / 1/3\ [TBHQ]_b.$$

where $[TBHQ]_u$ is the concentration of unbound hydroquinone measured directly via a standard curve of concentration versus absorbance at 381 nm and $[TBHQ]_b$ is the bound concentration of the hydroquinone, found from $[TBHQ]_i$ as

$$[TBHQ]_b=[TBHQ]_i - [TBHQ]_u .$$

Fusion Assays

Fresh, type A^+ human erythrocytes (RBCs) were lysed by hypotonic shock and resealed in the presence of either ethidium bromide or β-galactosidase as described ((Melikyan et al., 1995), (Ellens et al., 1989)). RBCs were then washed and adsorbed onto monolayers of HA300a^{++} cells. Prior to RBC addition, HA300a^{++} cells were treated with either neuraminidase (Melikyan et al., 1995) or a mixture of neuraminidase and trypsin (to cleave HAO to HA1 and HA2 (Melikyan et al., 1995)). After washing to remove unbound RBCs, the preparation was exposed either to pH 4.9 or pH 7 buffer as described (Melikyan et al., 1995), reneutralized and processed for microscopy: For the ethidium bromide (EtBr) assay, cells were visualized in a fluorescent microscope to detect transfer of EtBr to the HA300A^{++} cells (Melikyan et al., 1995). For the β-galactosidase assay, cell-RBC complexes were treated with 20 mg/mL neuraminidase (with shaking) to remove bound but unfused RBCs. The cells were then fixed in 0.05% glutaraldehyde in PBS for 10 min. at RT and processed for the detection of β–galactosidase activity as described (Ausubel, 1994).

DOCK

DOCK was carried out as described (Gschwend, 1996), using the X-ray crystallographic coordinates of BHA solved to 2.1Å resolution (Watowich et al., 1994). User-defined variables are listed in Appendices. Coordinates for small molecules were obtained from the Available Chemicals Directory (Molecular Design Limited, San Leandro, CA).

Substructure Searching

Searches for molecules similar to TBHQ were performed using the substructure search function of ISIS/BASE (Molecular Design Limited, San Leandro, CA).

Computer Modeling of HA

HA drawings were produced using the MidasPlus software system from the Computer Graphics Laboratory, University of California, San Francisco (Ferrin et al., 1988). Coordinates of HA used in figures are from entry 5hmg (Weis et al., 1990a) in the Brookhaven protein data bank (Bernstein et al., 1977).

Results

Effects of TBHQ on the low pH-induced conformational change of BHA

We have previously shown, using a scintillation proximity assay (SPA), that benzoquinones and hydroquinones inhibit the fusion-inducing conformational change in the influenza HA. The most potent inhibitor identified was TBHQ, which displayed an IC_{50} in the SPA of 5 μM. As a starting point for our study we have developed a new quantitative assay for the HA conformational change and have used it to assess the effects of TBHQ. The assay employs purified, biotinylated BHA and relies on the observation that following treatment at low pH, the exposed fusion peptide is sensitive to thermolysin resulting in the decrease in apparent molecular weight of HA2 from approximately 20 KD to 18 KD ((Skehel et al., 1982), (Daniels et al., 1983)). As seen in Fig. 1, when low pH-treated BHA is treated with thermolysin, the HA2 band is fully digested and a band, labelled HA2*, appears (lane 2). However, if TBHQ is included during the low pH treatment, the HA2 band is largely protected (lane 4). If TBHQ is added after the low pH treatment (post control), the HA2 band is not protected (lane 6). Quantitative analysis of the HA2 band proved to be a more reproducible measure than quantitation of the relatively faint HA2* band. The HA2* band is likely faint due to loss of biotinylated residues

Fig. 1. Thermolysin digestion assay for the HA conformational change: protection by TBHQ. Biotinylated BHA was incubated without (-, lanes 1,2,7 and 8) or with (+, lanes 3,4,5, and 6) 100 μM TBHQ at pH 7 (lanes 1,3,5, and 7) or pH 5 (lanes 2,4,6, and 8) for 7 minutes at room temperature. Samples were then reneutralized and processed for the thermolysin digestion assay as described in the Materials and Methods section. In treatments labeled "post" (lanes 5 and 6), 100 μM TBHQ was added after reneutralization but before the addition of thermolysin to assay for inhibition of thermolysin activity.

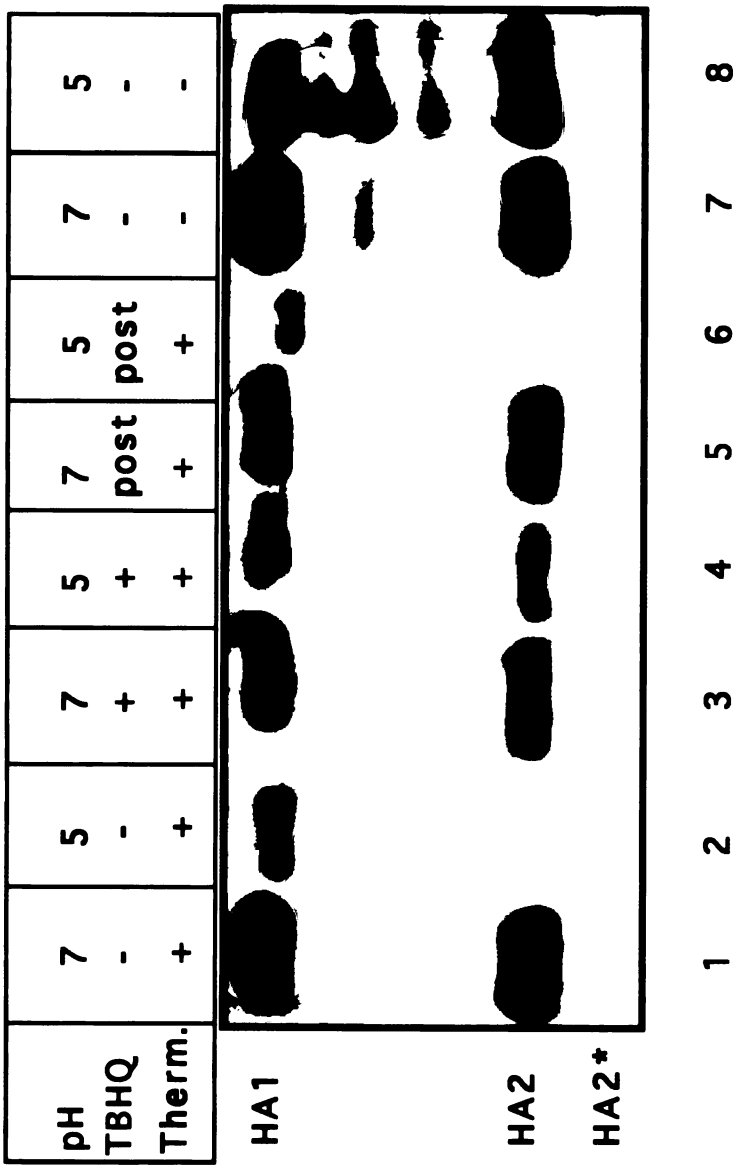
pH
TBHQ
Therm.
7 - +
5 - +
7 + +
5 + +
7 post +
5 post +
7 - -
5 - -
HA1
HA2
HA2*
1
2
3
4
5
6
7
8

Fig. 1

(relative to HA2) and because, in our hands (for comparison, see (Daniels et al., 1983)), the HA2* band is not stable but becomes further digested by thermolysin. Analysis of the concentration of TBHQ required to inhibit the conformational change revealed an IC_{50} in the range of 12 µM (Fig. 2A), in close agreement with our prior results (Bodian et al., 1993). Inhibition of the BHA conformational change was also observed using intrinsic tryptophan fluorescence (as in (Wharton et al., 1988), data not shown) or trypsin sensitivity as an assay (data not shown). The effect and concentration dependence of TBHQ was also recently confirmed in a study employing bis-ANS as a probe for the HA conformational change (Bethell, 1995).

The extent of the low pH-induced conformational change in HA is a function of both time and pH (Doms et al., 1985). To explore our hypothesis that TBHQ stabilizes BHA with respect to low pH, we compared the time (Fig. 2B) and pH (Fig. 2C) dependence of the conformational change in the absence and presence of 100 µM TBHQ. As seen in Fig. 2B, TBHQ prevented BHA from undergoing the conformational change for at least 10 min. As seen in Fig. 2C, TBHQ decreased the pH at which 50% of BHA converted to its low-pH form by 0.7 pH units under the conditions tested.

Binding of TBHQ to BHA

TBHQ might alter the kinetics of the conversion of HA to its fusion-active form by any of several methods. For example, it could bind to BHA at neutral pH and stabilize the protein in its native conformation, or it could bind only at low pH and halt the conformational change at an inactive intermediate stage. To test whether TBHQ binds directly to BHA at neutral pH, we conducted an equilibrium dialysis experiment as described in the Materials and Methods section. The calculated dissociation constant (Fig. 3) was 5 µM, and this value was reproducible in experiments conducted with low concentrations of TBHQ ($\leq$ 10 µM) for a constant time of 20 hours. We noted a loss of binding on longer incubations,

Fig. 2 Effect of TBHQ on the conformational change of HA: (A) Concentration, (B) time and (C) pH dependence. In (A), samples of biotinylated BHA were treated with TBHQ at the indicated concentration and then incubated at pH 5.2 at RT for 7 minutes. In (B) and (C), samples of biotinylated BHA were treated without (filled boxes) or with (open boxes) 100 μM TBHQ, and then incubated at (B) pH 5.2 at room temperature for the indicated time or (C) at the indicated pH for 7 minutes at room temperature. For all treatments, following reneutralization, samples were treated with thermolysin, subjected to reducing SDS-PAGE, and analyzed for biotinylated BHA2 as described in the Materials and Methods section.

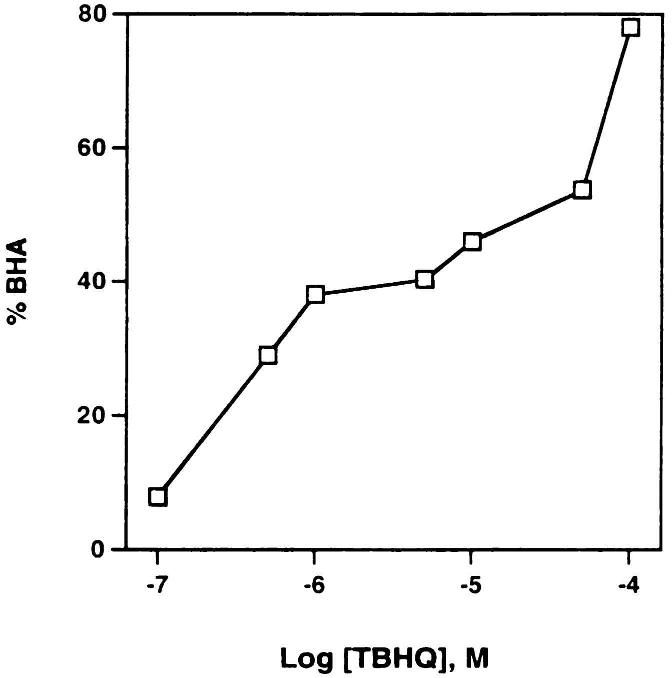

Fig. 2A

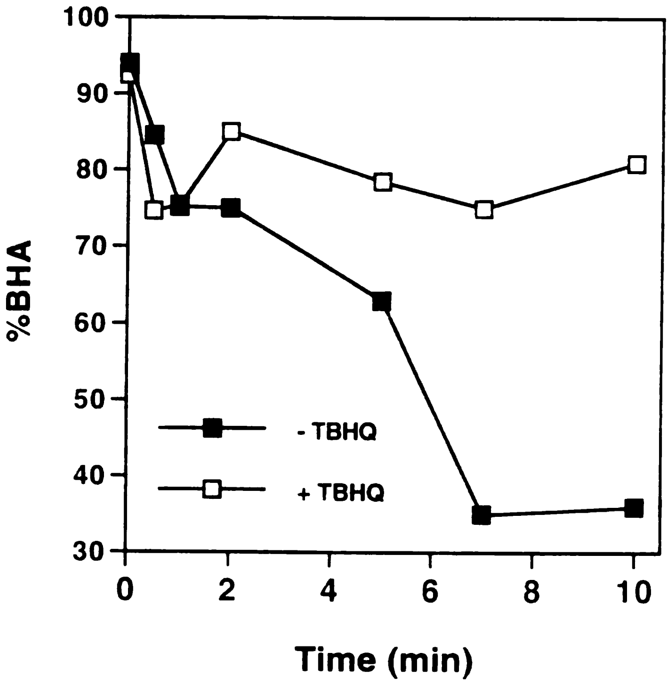

Fig. 2B

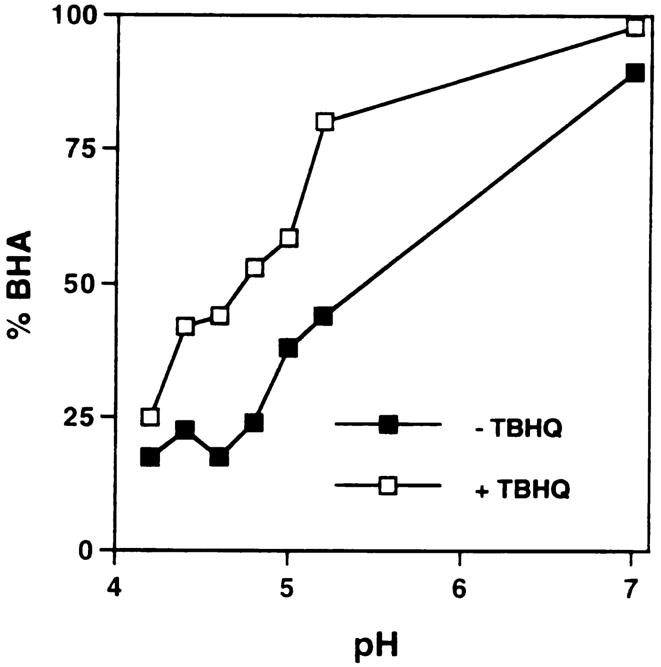

Fig. 2C

and TLC and spectroscopic absorbance analysis indicated the formation of a new species (referred to hereafter as TBHQ*) under these conditions. This conversion of TBHQ to TBHQ* was not affected by the presence or absence of oxygen but was strongly affected by pH, TBHQ concentration, solvent polarity and temperature. The likely reaction, a tautomerization, is diagrammed in Fig. 3; as indicated in this figure, TBHQ* is not active in inhibiting the conversion of BHA to its low-pH conformation and binds more poorly to BHA than does TBHQ. Because of the tautomerization reaction, which occurs on the time scale of the dialysis experiment, the reported dissociation constants are upper limits only on the true values. Nevertheless, the results demonstrate that TBHQ binds to neutral pH BHA with a micromolar binding constant.

Effects of TBHQ on Viral Infectivity

We have previously shown that TBHQ inhibits infectivity of X:31 influenza virus with an IC_{50} of 20 μM in a single-cycle infectivity assay (Bodian et al., 1993). To characterize further the mechanism of inhibition of infectivity, we determined the time interval during which TBHQ had to be added to exert its inhibitory effect. As seen in Fig. 4, TBHQ appears to act primarily during an early stage of the infection cycle; maximal inhibition is seen only if the compound is added within the first 15 minutes of initiation of infection. Inhibitory activity begins to wane if TBHQ is added 30 minutes post adsorption and disappears if added after 2 hours. The fact that TBHQ must be added early in the infection cycle is consistent with the notion that it inhibits a conformational change required for virus entry (or cannot cross cellular membranes).

TBHQ was identified using a structure-based inhibitor search against the crystal structure of BHA from X:31, which is an H3 influenza subtype. We next tested whether TBHQ is effective against other influenza viruses of the same subtype and other influenza subtypes.

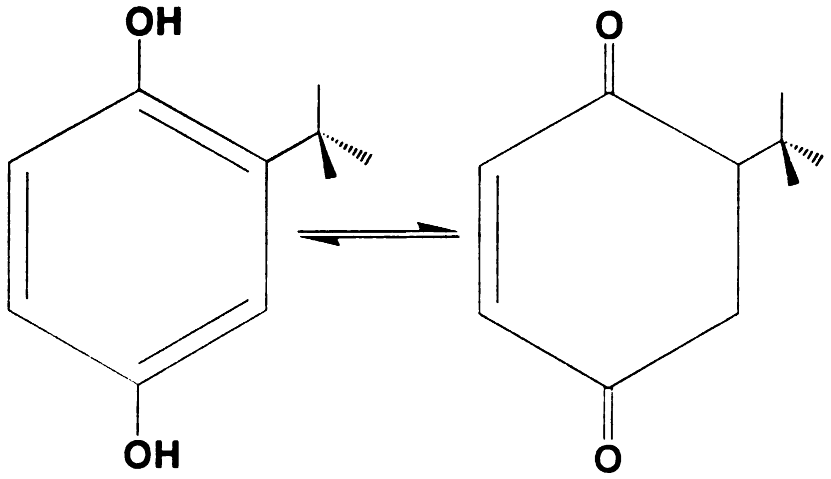

$IC_{50,\ infect}$	8 μM	100 μM
Inhibits conf. Δ	Yes	No
$K_{d,\ HA}$	$\sim 2\ \mu$M	$> 10\ \mu$M

Fig. 3

Fig. 4. Effect of TBHQ on infectivity when added at various times during the viral life cycle. 10 mM TBHQ was added to virus at the indicated times during a single cycle of influenza infection of MDCK2 cells, and the amount of virus produced after 15 hours (the time required for a single cycle of infection, (Gaush, 1968) was assessed as described in the Materials and Methods section. A control experiment showed that TBHQ at 10 or 100 μM does not inhibit hemagglutination (data not shown).

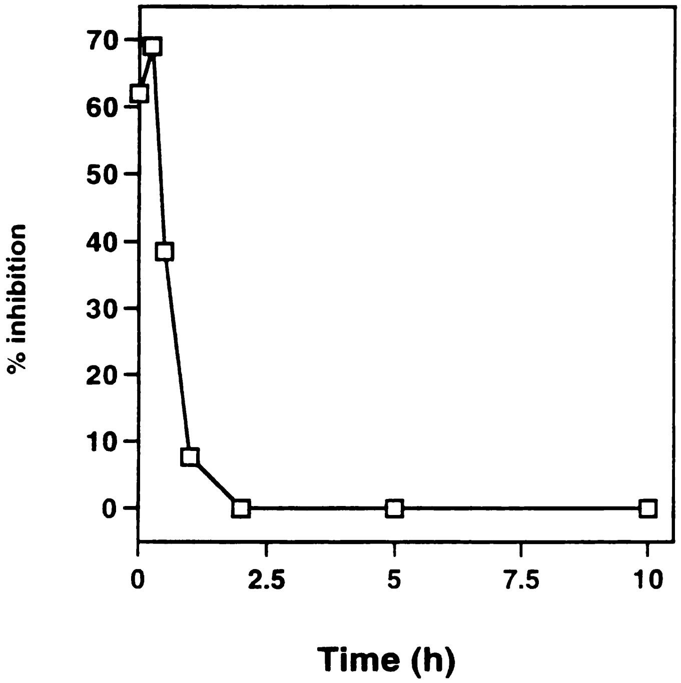

Fig. 4

As seen in Table I, TBHQ is equally effective at inhibiting the infectivity of Victoria, another H3 influenza virus. An H2 subtype virus, Japan, was ~2.3-fold less sensitive (see Discussion for further analysis). Moreover, TBHQ did not appear to protect purified BHA from Japan virus from undergoing the low pH-induced conformational change (Fig. 5)

Effect of TBHQ on HA-mediated Membrane Fusion

We previously showed that TBHQ inhibits influenza virus-induced syncytia formation, suggesting that it inhibits membrane fusion (Bodian et al., 1993). Here we tested this prediction using a more direct assay. Cells that stably express the influenza HA can be induced to fuse with RBCs ((Doxsey et al., 1985), (Kemble et al., 1994)). As shown in Fig. 6 and Table II, TBHQ inhibits this activity at both 100 and 10 μM.

TBHQ-resistant Mutants

The locations of mutations in HA in viruses resistant to TBHQ might shed light on the binding site for TBHQ, its mechanism of action, or both. We therefore isolated viruses resistant to TBHQ and sequenced their HA genes. Table III lists each isolate, the HA residues mutated, and their sensitivities to TBHQ as compared to wild-type virus. When mapped onto the neutral-pH crystal structure of X:31 BHA (Wilson et al., 1981), the mutations clustered in two regions: in the vicinity of the fusion peptide and in the globular head domain interface (Fig. 7A), a distribution strikingly similar to that of mutations conferring resistance to high doses of amantadine ((Daniels et al., 1985), (Steinhauer et al., 1992)). As expected, all of the resistant isolates were destabilized with respect to the pH at which their HA changes conformation (Table III), as measured by an hemolysis assay using intact virus (Daniels et al., 1985). Five mutations occur at residues that, in wild-type virus, make interactions with the fusion peptide ((Daniels et al., 1985), (Steinhauer et

Table I: Effect of TBHQ on infectivity of influenza viruses of various subtypes. Plaque assays were conducted as in the Materials and Methods section; plaque number/well are averaged over 4 wells in a 6-well tissue culture plate.

Virus	**X:31**	**Victoria**	**Japan**
Subtype	H3	H3	H2
# plaques/well when [TBHQ]= :			
0	50	34	37
1 μM	45	31	36
10 μM	34	25	37
100 μM	2	3	8
[TBHQ], 50% inhibition (μM)	19	22	44
$IC_{50}/IC_{50,X:31}$	1	1.1	2.3

Table I: Effect of TBHQ on infectivity of various virus subtypes

Fig. 5. Effect of TBHQ on BHA from Japan influenza virus. Coomassie-stained gel showing that Japan BHA is not protected from thermolysin digestion by 100 μM TBHQ. Samples were treated as in Figure 1 with the exception that the gel was stained with Coomassie brilliant blue.

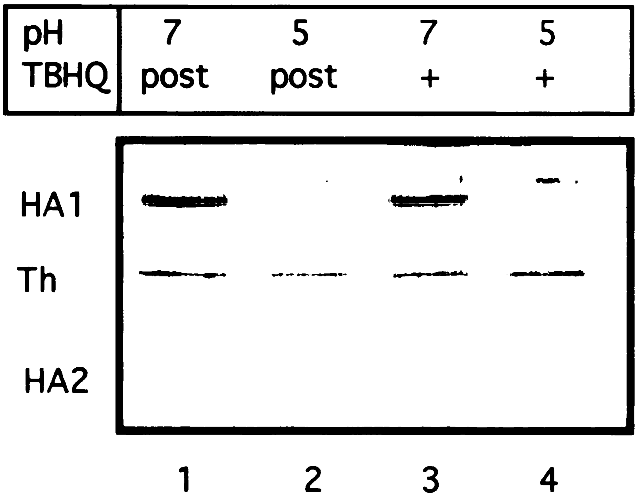
pH 7 5 7 5
TBHQ post post + +
HA1
Th
HA2
1 2 3 4

Fig. 5

Table II: Inhibition of membrane fusion by TBHQ. Fusion assays using HA-expressing cells and erythrocyte ghosts loaded with β-galactosidase were performed as described in the Materials and Methods section. Column 1: Where indicated, cells were pretreated with trypsin to cleave the inactive precursor HA0 into active HA. Column 2: pH of 2 minute buffer incubation. Column 3: Concentration of TBHQ present during incubations. Column 4: Number of nuclei in blue (fused) areas per field at 100X magnification. Results were confirmed with an assay identical to that described above but using RBCs loaded with ethidium bromide. Column 5: % inhibition by TBHQ compared to no inhibitor.

Fig. 6. Effect of 10 μM TBHQ in β-galactosidase-loaded RBC fusion assay, performed as described in the Materials and Methods section. Fusion events can be seen as dark patches; cell-cell fusion allows these patches to become larger.

HA or HA0	pH	[TBHQ], μM	# fusions/field	% inhibition
HA0	7	0	0	
HA0	5	0	0	
HA	7	0	0	
HA	5	0	20 +/- 2	
HA	5	10	9 +/- 2	55
HA	5	100	5 +/- 2	75
HA0	5	100	0	
HA	7	100	0	

Table II: Inhibition of membrane fusion by TBHQ

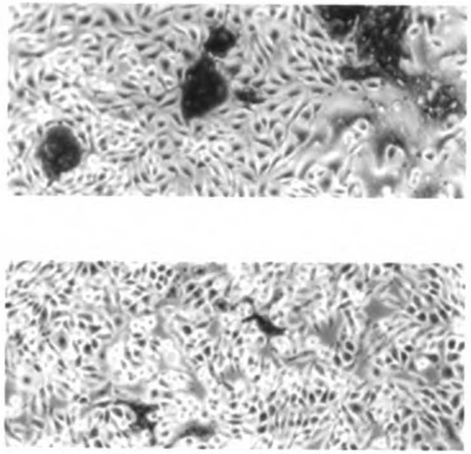

No TBHQ

10 μM TBHQ

Figure 6

Fig. 7. (a) Locations of HA mutations in TBHQ-resistant influenza viruses. BHA is shown in its neutral-pH form (coordinates are from the Brookhaven Protein Databank entry 5HMG); subunits in the trimeric protein are colored white, green, and yellow. Fusion peptide of one monomer is shown in black. Wild-type residues mutated in TBHQ-resistant isolates are indicated in magenta, CPK-rendered side-chains. (b) Protein residues surrounding the residue HA2 R124 (magenta), which is mutated to Gly in a TBHQ-resistant isolate. BHA monomers are colored as in (a).

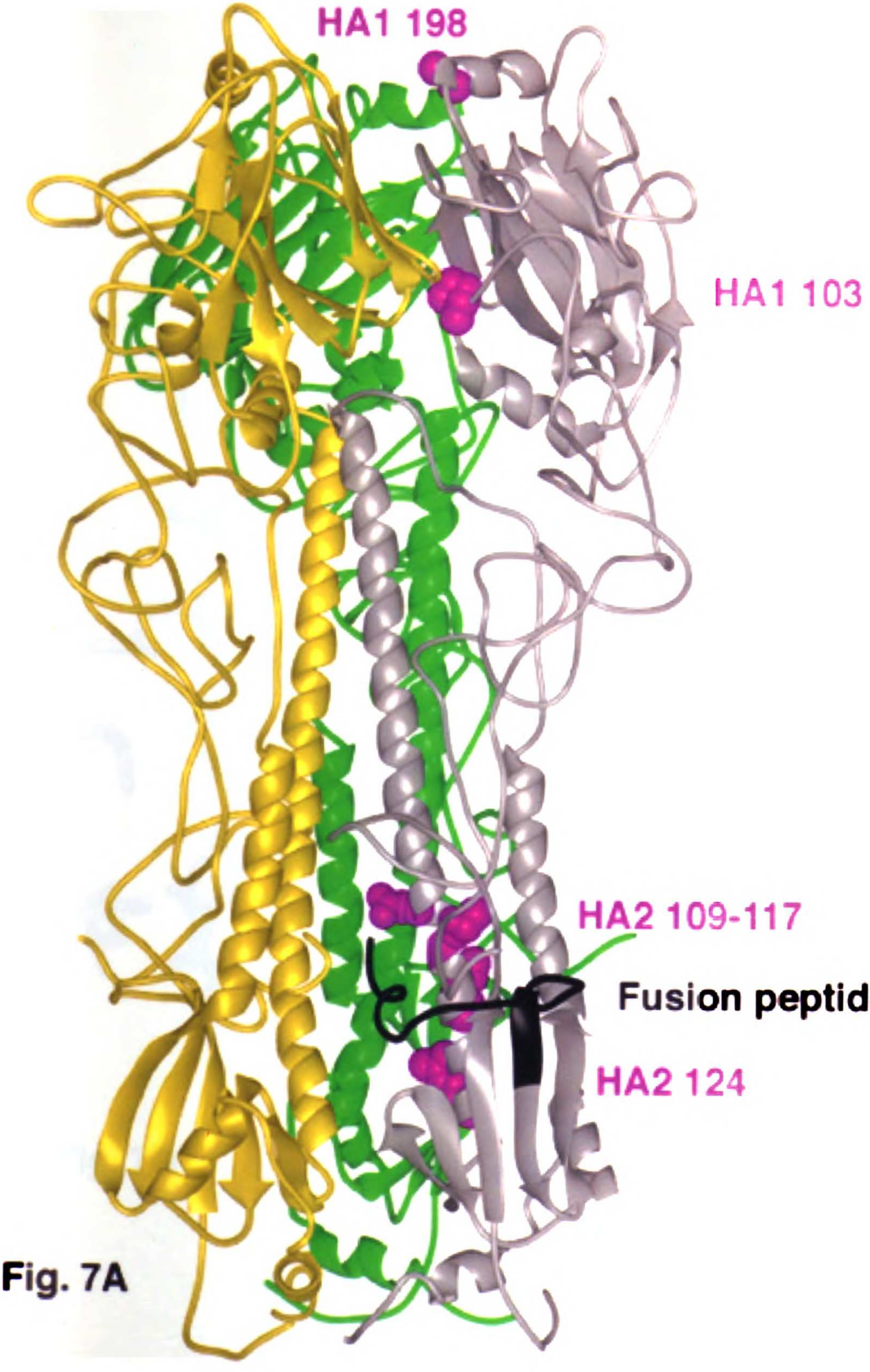
HA1 198
HA1 103
HA2 109-117
Fusion peptide
HA2 124

Fig. 7A

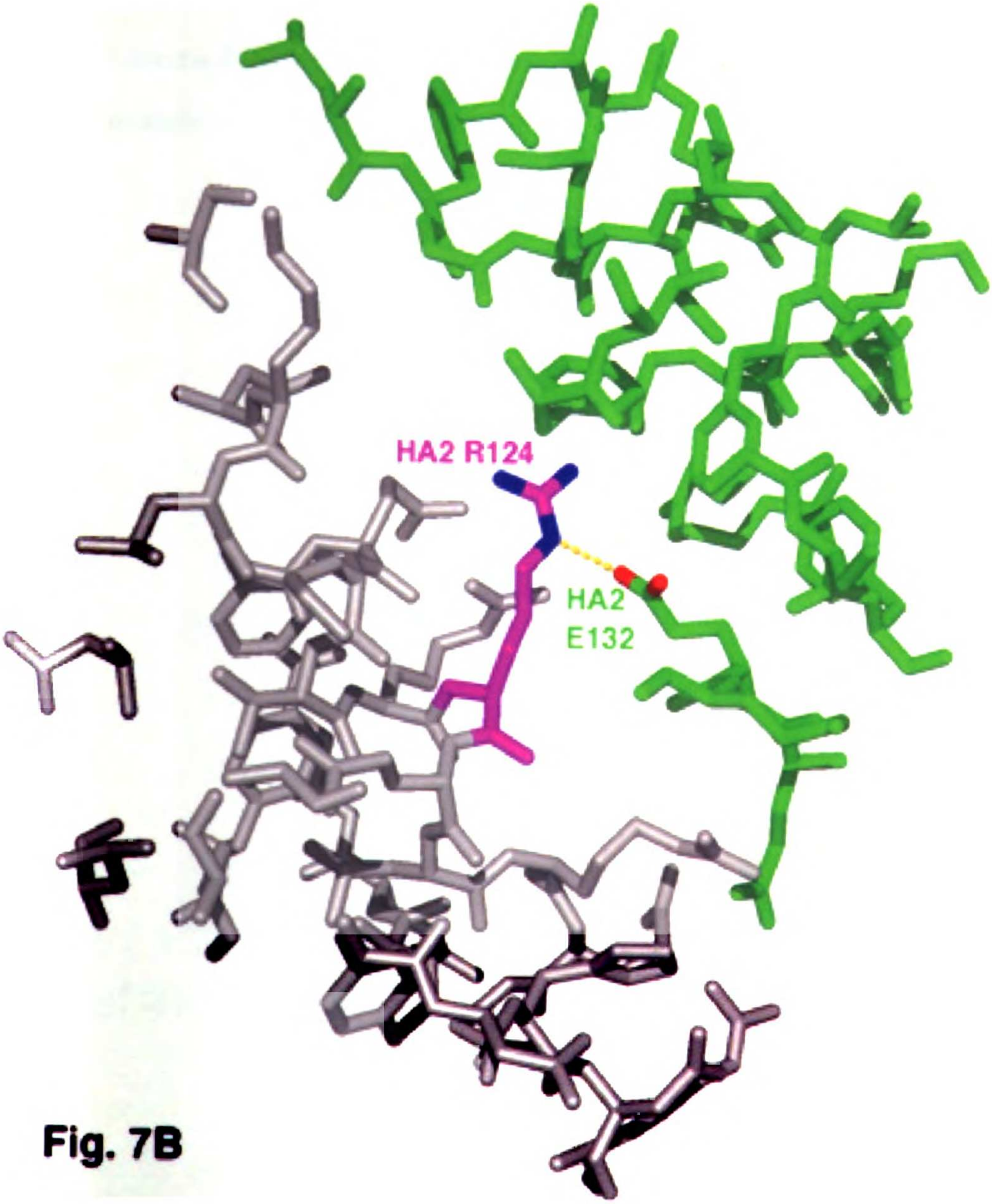
HA2 R124
HA2
E132

Fig. 7B

Table III: HA mutations in TBHQ-resistant viruses.

Each entry indicates the mutations in a single isolate; HA1 P103K and HA2 T111A occur in a single isolate. Column 2 indicates the fold difference in IC_{50} when compared to wild-type, X:31 virus. Column 3 indicates the shift in the pH of 50% hemolysis of each isolate as compared to wild-type virus, measured as described in the Materials and Methods section. Column 4 indicates whether each mutation was identified previously in X:31 virus resistant to high concentrations of amantadine.

Residue	$IC_{50}/IC_{50,wt}$	ΔpH_{hem}	amant.^{r} [1]
HA2 D112E	10	.4 units[1]	yes
HA2 D112N	2	.4[1]	yes
HA2 D109G	2	.1[1]	yes
HA2 K117E	10	.4[1]	yes
HA2 R124G	11	.3[2]	no
HA1 P103K HA2 T111A	3	.1[2]	no
HA1 A198E	7	None detected[2]	no

[1] Reference: Steinhauer, D.A. *et al* (1992) *Seminars in Virology* 3, 91-100
[2] This work

Table III: HA mutations in TBHQ-resistant viruses

al., 1992), (Weis et al., 1990b)); these mutations likely allow the fusion peptide to become exposed more easily, thereby facilitating the conformational change and subsequent fusion (Daniels et al., 1985). Four of the mutations that we identified in the fusion peptide region, HA2 D112E, D112N, D109G, and K117E, were the same as previously-identified amantadine-resistant mutants (Daniels et al., 1985). A fifth mutation, T111A, occurs in the same region as these others but was not identified as a high-dose amantadine resistance mutation. It occurs in a double mutant with HA1 P103K; this latter residue resides in the intermonomer region in the heads of HA, which are known to separate during the conformational change (Kemble et al., 1992). Another mutation, HA1 A198E, maps to the interface region of the heads. Both of these head mutations (HA1 A198E and P103K) occur near to, but not at the same loci as, the sites of amantadine-resistant mutations; the HA1 P103K/HA2 T111A double mutant was shown to be destabilized with respect to the pH of its HA conformational change as well (Table III) while the isolate with the mutation HA1 A198E was not detectably destabilized. The final mutation, HA2 R124G, occurs well away from the fusion peptide and even farther from the heads in the neutral structure (Fig. 7A). This mutation also destabilizes HA with respect to pH (Table III), and it occurs at the site of an intermonomer salt bridge in wild-type virus with aspartate HA2 132 (Fig. 7B). A charge reversal mutation at HA2 132 was identified earlier in a virus that induces fusion at relatively elevated pH (Doms et al., 1986), and the mutation at HA2 124 presumably has the same effect.

Crystallography and structure-based selection of improved inhibitors

Another method used to investigate the mode of TBHQ inhibition, crystallography, was begun in a collaborative effort with the laboratory of Dr. Don Wiley at Harvard University. Crystal soaks at high concentrations of TBHQ yielded preliminary, low-resolution X-ray crystallographic evidence of inhibitor binding to HA at a site distinct from the target site used for structure-based design (Fig. 8A, Stan Watowich, personal communication). These preliminary results have, as yet, not been confirmed. DOCK was used to predict a binding orientation within this alternate candidate site; this analysis revealed a small pocket adjacent to this site making no predicted interactions with TBHQ (Fig. 8B). A molecule with a slightly larger substituent in one region (Br for OH) but otherwise identical to TBHQ (tert-butyl bromophenol, or TBP) was predicted by DOCK to bind to the alternate site more tightly than does TBHQ; both molecules were computed to bind to this alternate site better than to the original DOCK site (site 1A). Table IV details the relevant data. TBP displays roughly 6-fold higher potency in inhibiting viral infectivity than TBHQ. These data support the hypothesis that this site is the site of TBHQ inhibition.

Discussion

Mechanism of TBHQ Inhibition of Infectivity

TBHQ was originally identified as an inhibitor of fusion peptide exposure (Bodian et al., 1993). The concurrence of the IC_{50} values for inhibition of both fusion and viral infectivity suggests a causal relationship between the two properties. We have described in this paper several lines of evidence that further support this mechanism of TBHQ inhibition of influenza virus infection. Firstly, the striking similarity between the HA mutations in TBHQ-resistant and high dose amantadine-resistant viruses indicates a shared mode of action. It has been shown that the concentrations of amantadine used to isolate these earlier mutants (100 μg/mL) raise the pH of intracellular vesicles to levels incompatible with the conformational change of wild-type HA (Daniels et al., 1985). Furthermore, the amantadine-resistant viral isolates possess mutations that destabilize HA

Fig. 8. Location of difference electron density in crystals of neutral BHA soaked with 1 mM TBHQ. (a) BHA is displayed as in Fig. 7A; TBHQ oriented into the site of difference density by DOCK is colored magenta. The site used for the original DOCK search is colored black on the two front monomers. (b) Close-up of the pocket containing the TBHQ elctron density with TBHQ in the orientation scored highest by DOCK for interaction with the protein pocket. HA2 K58 is colored cyan; other colors are as in (a).

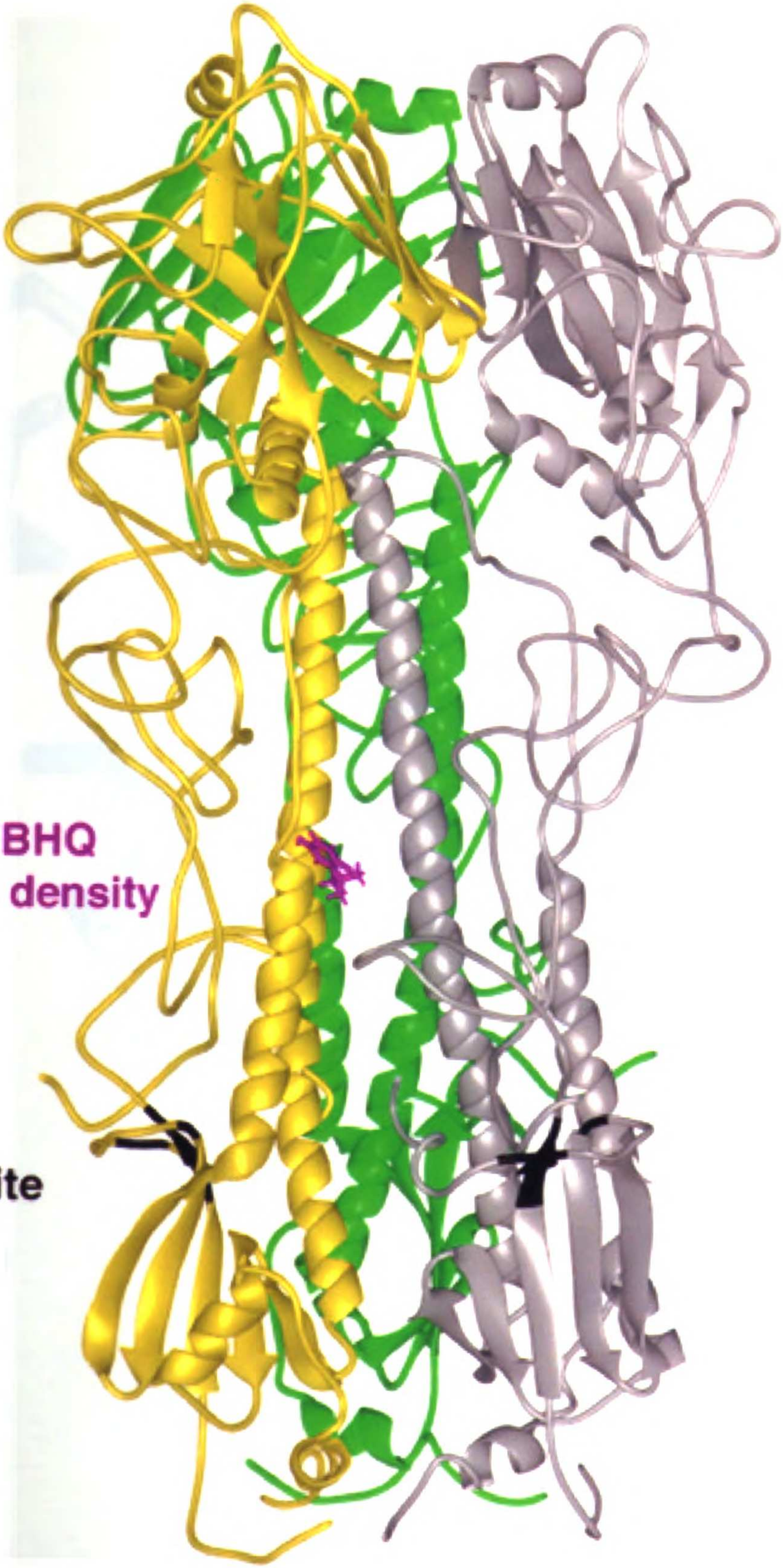
Site of TBHQ electron density
DOCK site

Fig. 8A

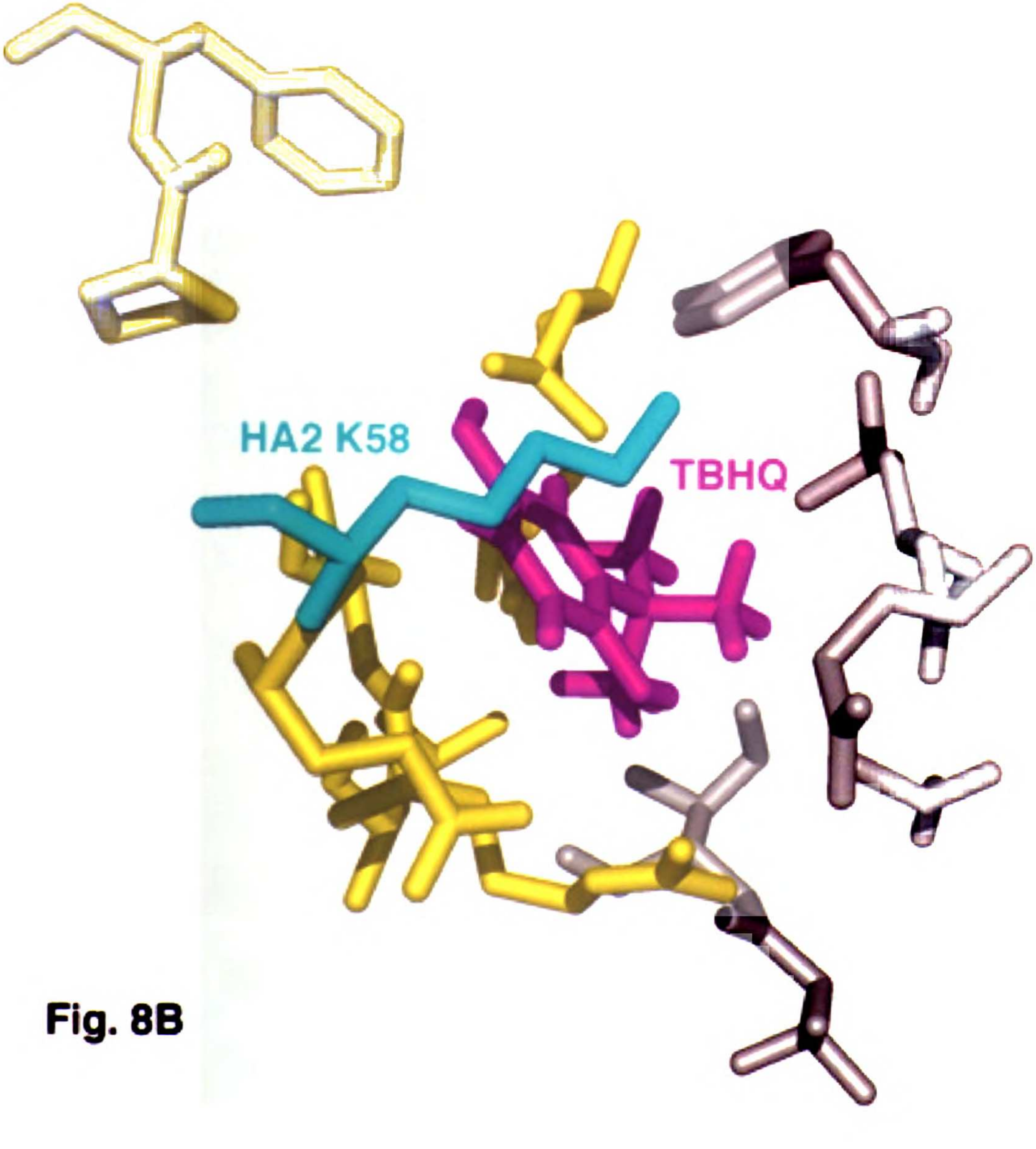
HA2 K58
TBHQ

Fig. 8B

Table IV: TBHQ vs. TBP. DOCK force-field scores of TBHQ and TBP docked to both the site of crystallographic density (preliminary data; as of yet unconfirmed) and to the site of the original DOCK search are listed. Lower (more negative) numbers indicate a higher predicted affinity. Inhibition of virus infectivity and cell viability were performed as described in the Materials and Methods section. TBP is more toxic to MDCK2 cells at a given concentration than is TBHQ, yet its effect on infectivity at its IC_{50} cannot be accounted for by this toxicity.

	TBHQ	TBP
DOCK score to new site	-21.89	-23.81
DOCK score to orig. site*	-15.41	-13.76
IC_{50}, infectivity	12 μM	~2 μM
IC_{50}, cell viability	3 mM	~25 μM (No toxicity at 2 μM)

* Reference=Bodian et al., 1992, *Biochemistry*. 32: 2967-2978

Table IV: TBHQ vs. TBP

with respect to pH, indicating that the drug was acting to inhibit the HA conformational change, and the same is true for the TBHQ-resistant isolates ((Daniels et al., 1985), (Steinhauer et al., 1992). The use of TBHQ to select destabilized HA mutants is, however, more specific than the use of high-doses of amantadine. Amantadine does not interact directly with BHA (Bodian, 1992) and, moreover, given that the drug directly inhibits the virus proton channel M2 (Wharton et al., 1994), it is likely to have pleiotropic effects on the virus at the high concentrations. The HAs of all of the TBHQ resistant mutants are detectably destabilized with respect to pH except for one: HA1 A198E. It is not yet clear how this mutation leads to resistance, since it does not destabilize HA and it does not lie near the presumed binding site. This case aside, the finding that the other six virus isolates resistant to TBHQ all have hemagglutinins that change conformation at an elevated pH indicates that TBHQ acts to stabilize HA during the course of an infection, and that this stabilization impedes infectivity.

Another line of evidence that TBHQ acts by inhibiting the conformational change in HA is that it only inhibits viral infectivity (at its IC_{50}; see below) if added during the first 15-30 minutes of infection. This time dependence places the level of action at the earliest portions of the influenza life cycle, namely cell surface binding, endocytosis, and membrane fusion. Earlier observations have demonstrated that endocytosis and fusion of influenza virus occurs between 25-30 minutes after cell binding (Stegmann et al., 1987). TBHQ does not inhibit receptor binding (Fig. 4 legend), strongly suggesting that its inhibitory action is at the level of fusion.

Finally, the fusion assays presented here directly demonstrate that TBHQ alone inhibits fusion between erythrocyte ghosts and cells expressing influenza hemagglutinin. Taken together, the above evidence strongly suggests that TBHQ inhibits influenza infectivity by the mechanism for which it was selected: inhibition of membrane fusion by the stabilization of an inactive form of HA.

In single-cycle infectivity assays using 100 μM TBHQ (data not shown), the compound retained its inhibitory activity even when added late in the infectivity cycle, while the results presented in Fig. 4 show that the effect of 10 μM TBHQ is only manifested during the first 30 minutes of infection. Furthermore, 10 μM TBHQ does not inhibit infectivity of Japan (H2) virus, while 100 μM does reduce plaque number, as indicated by the result presented in Table I. Taken together, these data suggest that TBHQ at 100 μM inhibits infectivity by an additional mechanism not exhibited at 10 μM.

Site of TBHQ Action and Identification of a TBHQ Derivative With Improved Potency

Three lines of evidence presented here suggest that TBHQ inhibits the low-pH conformational change of HA at a site distinct from the site used in the original inhibitor search: The first, and most critical, is the preliminary (as of yet unconfirmed) observation of electron density at a new site in BHA crystals soaked with TBHQ (Fig. 8; similar results were obtained previously with two related compounds, 1,4 naphthoquinone and 2,3-dimethyl hydroquinone (Bodian, 1992). The second is the use of the candidate alternate site in a successful structure-based prediction that a derivative of TBHQ, TBP, would be a more potent inhibitor. The third is the DOCK computation, using the refined BHA structure, that both TBHQ and TBP should both have higher affinities for the new site than for the targeted site. The original search for inhibitors of the HA conformational change used a relatively low-resolution structure of the protein, an early version of the program DOCK, and a very limited portion of the BHA structure (Site 1A (Bodian et al., 1993)). Since the original search, the resolution of the neutral-pH BHA structure has been improved to 2.1 Å (Watowich et al., 1994), and DOCK has improved as well ((Kuntz, 1992),(Meng, 1992),(Gschwend, 1996)). This combination of improvements has generated a more accurate description of TBHQ binding.

Preliminary results examining the binding of conformation-specific antibodies to and protease sensitivity of BHA suggest that TBHQ inhibits significant head movement, but not movement of the area of HA1 27 (Chapter 5). These results await further analysis.

Further support for the notion that TBHQ acts by binding to the alternate candidate site comes from an analysis of a mutant HA selected for resistance to low doses of amantadine (Steinhauer et al., 1991). The HA with this mutation, HA2 K58I, is stabilized with respect to wild type HA; it undergoes its conformational change at a lower pH (Steinhauer et al., 1991). HA2 K58I forms a portion of the alternate candidate TBHQ site (Fig.8B). More recently, another mutation in X-31 HA has been shown to stabilize the trimer with respect to pH (Ch. 3); this mutation, at HA1 27, is believed to form a salt bridge with HA2 54, which also forms part of the putative TBHQ-binding site. The two stabilizing mutations and the TBHQ data suggest a critical role for this pocket in controlling the kinetics of the fusion-inducing conformational change. A mutation at HA2 55, as described in Chapter 4 and (Qiao et al., in prep), affects the kinetics of the conformational change; this residue also forms a side of the site. The pocket has also attracted attention in the past due to the existence of "unexplained electron density" in the area by X-ray crystallographic analysis (Steinhauer et al., 1991); the possibility that some other, unknown ligand normally binds to this area is enticing in light of the mechanistic role of the pocket. Site 1A was originally chosen partially for its excellent conservation between subtypes (Bodian et al., 1993), but the site at HA2 58 is not so well-conserved (based on data derived from (Bodian, 1992), Appendix B). The observation that an H2 virus is less sensitive than is an H3 virus is consistent with the hypothesis that TBHQ acts at the alternate candidate site as opposed to the original targeted pocket, site 1A. Further crystallographic analysis is necessary to substantiate this hypothesis.

Mechanism of the BHA low-pH conformational change

The proposed site of action of TBHQ and the locations of the mutations in TBHQ-resistant viruses also support a current working model of the HA conformational change (for reviews, see (Hernandez et al., 1996), (White, 1995)). According to this model, the HA1 globular heads must separate; the occurrence of destabilizing mutations in the interface between heads is consistent with this aspect of the model. Another aspect of the conformational change predicted by the model is the conversion of the region HA2 55-81 from a random coil to a helix ((Carr & Kim, 1993), (Bullough et al., 1994)). This tenet of the model is supported by our recent evidence that a proline mutation at HA2 55 alters the kinetics of fusion and that a double mutant with prolines at HA2 55 and 71 exhibits no fusion activity (Chapter 4 and Qiao et al, in prep). The presumed site of TBHQ action is formed partially from residues of this region, most notably HA2 K58; TBHQ may stabilize the random-coil form of HA2 55-81. Another area of the protein, HA2 106-117, undergoes two related changes in the model. In the neutral pH form of BHA, this segment is helical and makes contacts with the fusion peptide, tethering it into the center of the trimer. In the low-pH form of the protein, most of this region has assumed the form of a loop, and the contacts with the fusion peptide have been broken (Bullough et al., 1994). Mutations that remove these contacts (e.g. at HA2 109, 111, 112, and 117) probably allow the fusion peptide to be exposed more easily ((Steinhauer et al., 1992), (Weis et al., 1990b)) while also facilitating the helix-to-loop conversion. Further support for the requisite role of this conversion is the fact that one of the TBHQ-resistant viruses that we isolated had the mutation HA2 R124G. In the neutral-pH form of BHA, arginine at this position makes contacts with HA2 D132 on another subunit, the location of a previously-identified destabilizing mutation (Doms et al., 1986). This interaction is one of the few intermonomer contacts involving the helical region HA2 117-127, a region that is reoriented via the helix-to-loop transformation to rotate 180 degrees and to pack against the N-terminal half of the central helix (which it had previously been a part of, see Ch. 1, Fig. 4) at low pH. A mutation that removes the interaction between HA2 R124 and HA2 D132 would therefore remove this tethering interaction, and possibly allow the helix-to-loop transformation to proceed more easily. The destabilization of HA containing mutations at either of these residues supports this model.

Taken together, our data indicate that the best candidate site of action of TBHQ and its relatives is a pocket near HA2 58. In addition, the mutations we identified in TBHQ-resistant viruses occur in regions of HA implicated in all aspects of the conformational change: fusion peptide exposure, head separation, the loop-to-helix transformation, and the helix-to-loop transformation. Future experiments are needed to determine the temporal order of these transitions, and which stage of the fusion reaction is mediated by each transition.

Inhibitors of Virus Fusion

The results presented in this report suggest three future directions. The first entails further examination of the site of action of TBHQ by crystallographic analysis. Second is a structure-based search using the proposed site of action of TBHQ for other, possibly unrelated, inhibitors. The residues comprising the alternate candidate site are more varied between influenza subtypes than those of the original target site. This greater variability may account for the observation that HA from an H2 subtype virus is less sensitive to TBHQ than is HA from H3 viruses. An inhibitor may, however, be designed that maintains contacts with the well-conserved residues in the pocket. Such an inhibitor could be a variant of the phenolic inhibitors described in this report, but the instability of TBHQ and toxicity of TBP argue for a new structure-based search to the area. Currently, only two closely related antiinfluenza drugs that act by inhibiting a viral ion channel are approved for clinical use in the United States: amantadine and rimantidine, both of which cause undesirable side effects (Wintermeyer, 1995) and suffer from clinical resistance ((Houck, 1995), (Wintermeyer, 1995)). A promising new drug, 4-guanidino-Neu5Ac2en (4-GuDANA), was designed to inhibit the viral enzyme neuraminidase (Woods, 1993), and it is currently being evaluated for clinical use, but resistance has already been encountered in laboratory settings (Staschke, 1995). The addition of inhibitors of influenza-mediated membrane fusion to the Pharmacopeia would therefore be welcome.

The third direction is extension of the strategy presented here to other viruses. All enveloped viruses must fuse their membranes with those of the host cell during infection; it is conceivable that, employing a similar strategy of stabilization of an inactive conformation, inhibitors of other virus fusion proteins, such as HIV-env, could be developed. Peptides that specifically inhibit HIV and paramyxovirus fusion have already been identified ((Wild et al., 1994), (Lambert, 1996)); it remains to be seen whether the mechanism of action of these peptides is related to that of TBHQ inhibition of HA.

References

Ausubel, F. et al, eds. (1994) *Current Protocols in Molecular Biology*, Vol. 2, Wiley, Brooklyn, NY.

Bernstein, F. C., Koetzle, T. F., Williams, G. J. B., Meyer, J., E.F., Brice, M. C., Rodgers, J. R., Kennard, O., Shimanouchi, T., & Tasumi, M. (1977) *J. Mol. Biol. 112*, 535-542.

Bethell, R, Gray, NM; Penn, CR. (1995) *Biochemical and Biophysical Research Communications 206*, 355-361.

Bodian, D. (1992) *Ph.D. Thesis, University of California, San Francisco.*

Bodian, D. L., Yamasaki, R. B., Buswell, R. L., Stearns, J. F., White, J. M., & Kuntz, I. D. (1993) *Biochemistry 32*, 2967-2978.

Bullough, P. A., Hughson, F. M., Skehel, J. J., & Wiley, D. C. (1994) *Nature 371*, 37-43.

Carr, C. M., & Kim, P. S. (1993) *Cell 73*, 823-832.

Daniels, R. S., Douglas, A. R., Skehel, J. J., Waterfield, M. D., Wilson, I. A., & Wiley, D. c. (1983) in *The Origin of Pandemic Influenza Viruses* (Laver, W. G., Ed.) pp 1-7, Elsevier Science Publishing Co., Inc., New York.

Daniels, R. S., Downie, J. C., Hay, A. J., Knossow, M., Skehel, J. J., Wang, M. L., & Wiley, D. C. (1985) *Cell 40*, 431-439.

Desjarlais, R, Sheridan, RP; Seibel, GL; Dixon, JS; Kuntz, ID; Venkataraghavan, R. (1988) *Journal of Medicinal Chemistry 31*, 722-729.

Doms, R. W., Gething, M.-J., Henneberry, J., White, J., & Helenius, A. (1986) *J. Virol. 57*, 603-613.

Doms, R. W., Helenius, A., & White, J. (1985) *J. Biol. Chem. 260*, 2973-2981.

Doxsey, S., Sambrook, J., Helenius, A., & White, J. (1985) *J. Cell Biol. 101*, 19-27.

Ellens, H., Doxsey, S., Glenn, J. S., & White, J. M. (1989) *Meth. Cell Biol. 31*, 155-176.

Ferrin, T. E., Huang, C. C., Jarvis, L. E., & Langridge, R. (1988) *J. Mol. Graphics 6*, 13-27.

Gschwend, DA, Kuntz, ID. (1996) *Journal of Computer-aided Molecular Design 10*, 123-132.

Hernandez, L. D., Hoffman, L. R., Wolfsberg, T. G., & White, J. M. (1996) *Ann. Rev. Cell Devel. Biol. 12*, in press.

Houck, P, Hemphill, M; LaCroix, S; Hirsch, D; Cox, N. (1995) *Archives of Internal Medicine 155*, 533-7.

Kemble, G. W., Bodian, D. L., Rosé, J., Wilson, I. A., & White, J. M. (1992) *J. Virol. 66*, 4940-4950.

Kemble, G. W., Danieli, T., & White, J. M. (1994) *Cell 76*, 383-391.

Kuntz, ID (1992) *Science 257*, 1078-1082.

Lambert, D, Barney, S; Lambert, AL; Guthrie, K; Medinas, R; Davis, DE; Bucy, T; Erickson, J; Merutka, G; Pettesay, SR Jr. (1996) *PNAS 93*, 2186-2191.

Legler, U, Benet, LZ. (1986) *European Journal of Clinical Pharmacology 30*, 51-55.

Melikyan, G. B., White, J. M., & Cohen, F. S. (1995) *J. Cell Biol. 131*, 679-691.

Meng, EC, Shoichet, BK; Kuntz, ID. (1992) *Journal of Computational Chemistry 13*, 505-524.

Shoichet, B, Bodian, DL; Kuntz, ID. (1992) *Journal of Computational Chemistry 13*, 380-397.

Skehel, J. J., Bayley, P. M., Brown, E. B., Martin, S. R., Waterfield, M. D., White, J. M., Wilson, I. A., & Wiley, D. C. J. (1982) *Proc. Natl. Acad. Sci. USA 79*, 968-972.

Staschke, K, Colacino, JM; Baxter, AJ; Air, GM; Bansal, A; Hornback, WJ; Munroe, JE, and Laver, WG. (1995) *Virology 214*, 642-646.

Stegmann, T., Morselt, W., Scholma, J., & Wilschut, J. (1987) *Biochim. Biophys. Acta 904*, 165-170.

Steinhauer, D. A., Sauter, N. K., Skehel, J. J., & Wiley, D. C. (1992) *Receptor binding and cell entry by influenza viruses*, Vol. 3, Saunders Scientific Publications, Academic Press, London, U.K.

Steinhauer, D. A., Wharton, S. A., Skehel, J. J., Wiley, D. C., & Hay, A. J. (1991) *Proc. Natl. Acad. Sci. USA 88*, 11525-11529.

Tobita, K, Sugiura, A; Enomoto, C; Furuyama, M. (1975) *Med. Microbiol. Immunol. 162*, 9-14.

Watowich, S. J., Skehel, J. J., & Wiley, D. C. (1994) *Structure 2*, 719-731.

Weis, W. I., Bruenger, A. T., Skehel, J. J., & Wiley, D. C. (1990a) *J. Mol. Biol. 212*, 737-761.

Weis, W. I., Cusack, S. C., Brown, J. H., Daniels, R. W., Skehel, J. J., & Wiley, D. C. (1990b) *EMBO J. 9*, 17-24.

Wharton, S. A., Belshe, R. B., Skehel, J. J., & Hay, A. J. (1994) *J. Gen. Virol. 75*, 945-948.

Wharton, S. A., Ruigrok, R. W. H., Martin, S. R., Skehel, J. J., Bayley, P. M., Weis, W., & Wiley, D. C. (1988) *J. Biol. Chem. 263*, 4474-4480.

White, J. M. (1995) *CSHSQB 60*, 581-588.

Wild, C. T., Shugars, D. C., Greenwell, T. K., McDanal, C. B., & Matthews, T. J. (1994) *Proc Natl Acad Sci U S A 91*, 9770-9774.

Wiley, D. C., & Skehel, J. J. (1987) *Annu. Rev. Biochem. 56*, 365-394.

Wilson, I. A., Skehel, J. J., & Wiley, D. C. (1981) *Nature 289*, 366-372.

Wintermeyer, SM, Nahata, MC. (1995) *Annals of Pharmacotherapy 29*, 299-310.

Woods, JM, Bethell, RC; Coates, JAV; Healy, N; Hiscox, SA; Pearson, BA; Ryan, DM; Ticehurst, J; Tilling, J; Walcott, SM; Penn, CR. (1993) *Antimicrobial Agents and Chemotherapy 37*, 1473-1479.

Xu, X., Rocha, EP; Regnery, HL; Kendai, AP; Cox, NJ. (1993) *Virus Research 28*, 37-35.

Chapter 3:

Structure-based identification of an inducer of the low-pH conformational change in the influenza hemagglutinin that inhibits infectivity

Introduction

Penetration of influenza virus into host cells requires fusion between the viral envelope and the host cell membrane. The membrane fusion reaction is triggered by a low pH-induced conformational change in a viral glycoprotein, the hemagglutinin (HA). Since HA-mediated membrane fusion is absolutely required for successful influenza infection and occurs early in its life cycle, virus-cell fusion is an attractive target for pharmacologic intervention. Initial structure-based efforts to identify inhibitors of the fusion activity of HA yielded a family of small benzoquinones and hydroquinones that impede not only the conformational change of HA, but also virus infectivity and syncytium formation ((Bodian et al., 1993), Ch. 2); the most potent of these compounds is tert-butyl hydroquinone (TBHQ).

Since the identification of TBHQ as an inhibitor of the low pH-induced conformational change in HA, considerable progress has been made in both the structure of HA and the structure-based search tools. The availability of higher-resolution structural data on the ectodomain of hemagglutinin (BHA, (Watowich et al., 1994)) enabled the structure-based searching program DOCK to represent potential target sites more accurately. In addition, DOCK itself improved, having gained a more chemically descriptive scoring function for ranking potential inhibitors (Meng, 1992), and the database of compounds searched has grown approximately 3-fold (Molecular Design Limited, San Leandro, CA). The most recent version of DOCK employs a rigid-body minimization step designed to model a more exhaustive search of possible ligand binding orientations (Gschwend, 1996). Recent advances in the understanding of the HA conformational change have also been made; the probable low-pH conformation of BHA was identified crystallographically (Bullough et al., 1994), and evidence of the importance of regions distal to the fusion peptide in achieving this conformation and membrane fusion have been presented ((Kemble et al., 1992),(Carr & Kim, 1993), (Wharton et al., 1995), Qiao et al, in prep). Separation of the globular head regions of HA is now known to be necessary for fusion ((Godley et al., 1992),(Kemble et al., 1992)), and the loop to helix transition of HA2 residues 55-81 ((Carr & Kim, 1993),(Bullough et al., 1994)) appears to be necessary as well (Qiao et al, in prep., Ch. 4). The recent developments prompted a new round of structure-based inhibitor searching targeted to two sites surrounding HA2 55-81, on the interface between the globular heads. As a result of this search, we identified several new inhibitors of HA-mediated membrane fusion. Moreover, one of the new compounds represents a novel class of inhibitors that facilitates rather than impedes the HA conformational change.

Materials and Methods

Viruses and Cells

Madin-Darby Canine Kidney 2 (MDCK2) cells, HA300a^{++} cells, and X-31 virus were grown and maintained as described (Ch. 2). Viruses resistant to diiodofluorescein (C22) were isolated as described (Ch. 2) using a single, high multiplicity of infection (MOI) infection procedure and 1 mM C22, a concentration determined to be non-toxic to cells by trypan blue exclusion (Ausubel, 1994) and ^{35}S-methionine incorporation (Ausubel, 1994).

Protein

Biotinylation and purification of bromelain-cleaved HA (BHA) was performed as described (Ch. 2).

Inhibitors

TBHQ and diiodofluorescein (C22) were purchased from Aldrich. Phenolphthalein monophosphate disodium (S22), Zincon-Na (S23), Eosin B (C13), Bromopyrogallol red (S15), Eosin (S17), 3'-dephospho-coenzyme A (C26), Stilbazo (C29) were purchased from Sigma. Maybridge NRB00384 (S19), NRB08312 (S110), NRB02903 (C19), and DFP0028 (S28) were purchased from Maybridge (UK) via Ryan Scientific (USA).

Infectivity Assays

Plaque assays, ELISA, MTT, and single-cycle infectivity assays were performed as described (Ch. 2).

Virus Genome Sequencing

Isolation of HA RNA, reverse-transcription, PCR, and sequencing of X-31 sequences were performed as described (Ch. 2).

Fusion assay

Fusion between erythrocyte (RBC) ghosts loaded with β-galactosidase and $HA300a^{++}$ cells was performed as described (Ch. 2).

Hemolysis

Inhibition of hemolysis as a function of pH was performed and calculated as described (Bodian et al., 1993). Determination of the pH of 50% hemolysis by influenza viruses was performed as described (Ch. 2).

Proteolytic Assays

Inhibition of the conformational change of BHA as determined by thermolysin digestion was performed as described (Ch. 2). Low pH-treated BHA is cleaved by proteinase K (Stegmann et al., 1987). To assay for this conformational change, biotinylated BHA was treated at low pH and reneutralized as described (Ch. 2) and then incubated with proteinase K (5000:1 BHA:proteinase K, w:w) for 30 minutes at 37°C. Samples were then processed for SDS gels and streptavidin-HRP blotting as described (Ch. 2). Digestion of the HA1 band was used as a qualitative measure of the conformational change.

DOCK

DOCK3.5 was employed as described in the Results section, using crystallographic coordinates for BHA at 2.1Å resolution (Watowich et al., 1994) and user-defined variables as listed in Table I. Spheres for each site description were selected by hand from the SPHGEN output. Approximately 150,000 molecules were screened for their predicted affinities for each of the two sites using a rigid-body minimization step and an AMBER-based potential function for evaluating predicted interactions ((Meng, 1992),(Gschwend, 1996)). The top-scoring 200 molecules from the search to each site were screened using computer graphics (Ferrin et al., 1988). Graphical screening involved evaluation of contacts with charged vs. hydrophobic regions of the sites, well- vs. poorly-conserved regions of the sites, and predicted solubility of the compounds. Using these criteria and based on commercial availability, 25 molecules per site were selected from the original 200 for *in vitro* screening, of which we tested 12 total.

Computer Modeling of HA

HA drawings were produced using the MidasPlus software system from the Computer Graphics Laboratory, University of California, San Francisco (Ferrin et al., 1988). Coordinates of HA used in figures are from entry 5hmg (Weis et al., 1990) in the Brookhaven protein data bank (Bernstein et al., 1977).

Results

Identification of new sites and test compounds

The area chosen for the new structure-based inhibitor search lies near the interface between heads of the HA trimer (on the structure of neutral-pH BHA, Fig. 1 (Weis et al., 1990),(Wilson et al., 1981)). Two neighboring sites, referred to here as sites 2A and 2B, were used for independent searches. Their locations are shown in Figure 1; site 1A, the pocket used in the original search that identified TBHQ, is also shown. Three of each site exist in the trimer. The limits of both pockets are partially defined by residues from HA2 54-81, the region of HA that is believed to undergo a random coil to coiled-coil transition at low pH. The sites also contain many intermonomer and intramonomer interactions, both hydrophobic and polar, that could potentially be stabilized or disrupted by a small

Fig. 1. Locations of new DOCK sites in the neutral pH structure of BHA (coordinates are from the Brookhaven Protein Databank entry 5HMG). Monomers in the BHA trimer are colored white, yellow and green. Dots indicate locations of spheres used in orienting potential ligands computationally for evaluation of predicted interaction with a site. Blue dots, site 2A; red dots, site 2B. Magenta, HA2 55-81. Black area, site 1A.

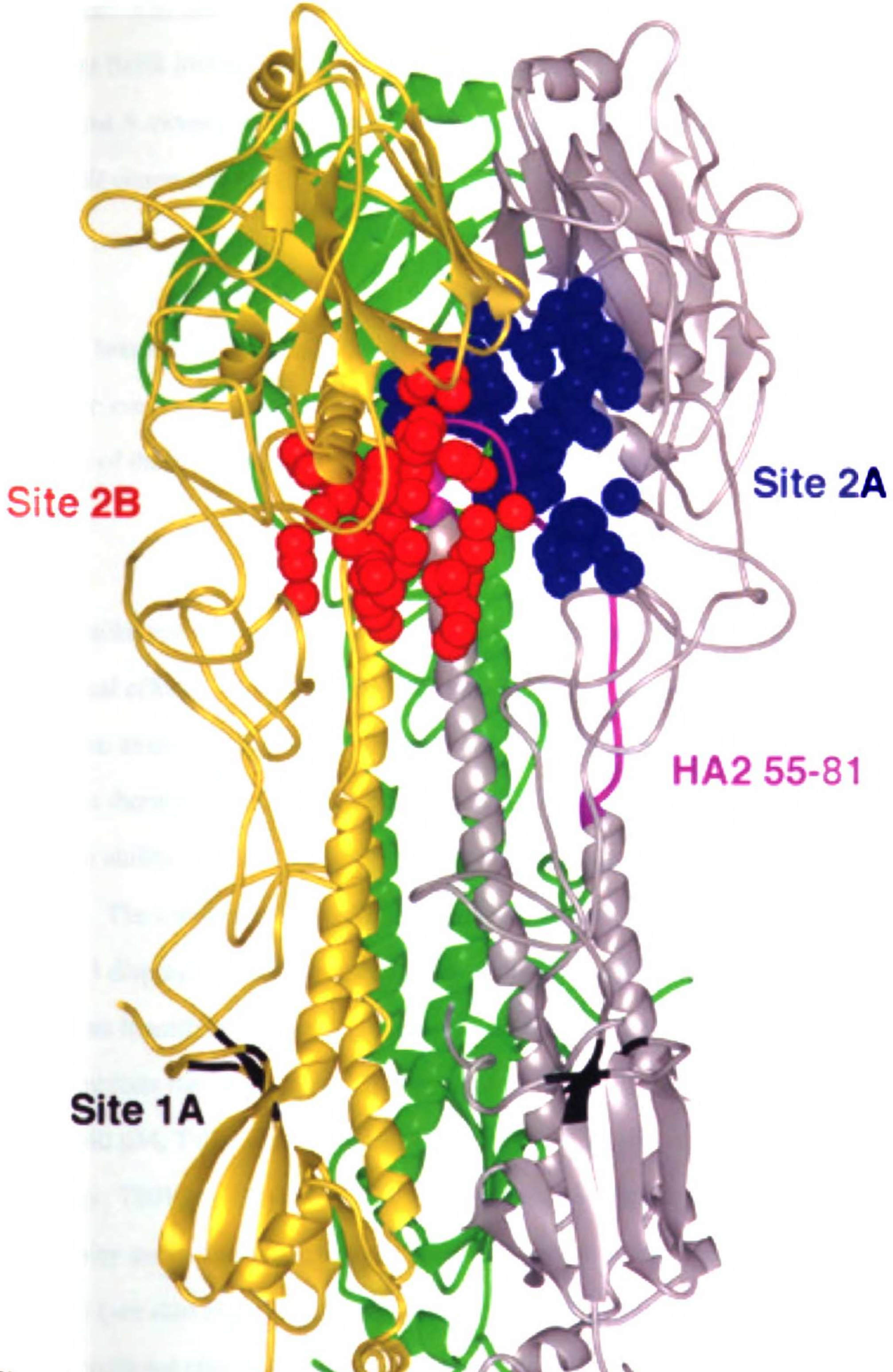
Site 2B
Site 2A
HA2 55-81
Site 1A

Fig. 1

molecule. The sites were also chosen for the low natural variability of their surface residues (98% identity among all influenza viruses of the subtype H3 and 78% among all influenza A viruses for both sites, using data from (Bodian, 1992), Appendix B), their size, and their concave shapes.

Table I lists the parameters used in the DOCK search. Twenty-five molecules per site were selected as described in the Materials and Methods section for *in vitro* screening. Twelve of these compounds were tested; their structures are diagrammed in Fig. 2.

Three initial tests were used to screen potential inhibitors for their biochemical and biological effects. The first assay uses purified BHA and tests the ability of a compound to affect the extent of conversion of BHA to its low-pH form, as assayed by sensitivity to the protease thermolysin (Ch. 2). Compounds that had an effect in this assay were then tested for their ability to inhibit virus infectivity in tissue culture and for cellular toxicity (see below). The corresponding data for the twelve tested compounds are listed in Table II. Figure 3 displays the sensitivity of BHA to thermolysin in the presence of two of the inhibitors identified. As seen in Figure 3A and Table II, phenolphthalein monophosphate (S22) inhibits the conformational change of BHA (IC_{50}< 100 μM) and viral infectivity (IC_{50}=40 μM, Table II). S22 thus behaves quite similarly to our previously identified inhibitor, TBHQ. S19 also inhibits the conformational change, but its potency in the infectivity assay was much higher than in the conformational change assay. As seen in Fig. 3B (see also Figs. 4A and B), however, diiodofluorescein (C22) facilitates the conformational change (EC_{50}= approximately 5 μM) yet inhibits viral infectivity (IC_{50}= 6 μM, Table II). C22 thus defines a new class of agents that appear to inhibit viral infectivity by potentiating the HA conformational change. Two other molecules that facilitate the

Table I: Input parameters for the computer programs SPHGEN, CHEMGRID, and DOCK3.5.

The variables (abbreviated in this table) are defined in the DOCK3.5 User's Manual.

I		II		III		IV		V		VI	
SPHGEN		CHEMGRID		DOCK MATCHING		DOCK SEARCH		DOCK SCORING		DOCK MINIMIZE	
dentag	X	*box*	8, 7.4 Å	*mode*	search	*coloring*	no	*scor_opt*	forcefield	*minimize*	yes
dotlim	0.0	*table*	ambH	*dist_tol*	.8	*rat_min*	0	*interp*	yes	*chk_deg*	no
radmax	5.0	*vdwfil*	amb	*nod_max*	4	*atm_min*	7	*vdw_prm*	amb		
radmin	1.4	*grddiv*	.4	*nod_min*	4	*atm_max*	100		mindock		
srftp	R	*estype*	1	*lig_bin*	.28, .32	*restart*	no	*vdw_max*	1e10		
		esfact	4.5	*lig_ovlp*	1	*num_sav*	200	*elec_scal*	1		
		cutoff	10	*rec_bin*	.28, .32	*nrm_sav*	0	*vdw_scal*	1		
		pcon	2.3	*rec_ovlp*	1	*mol_max*	50,000				
		ccon	2.8	*bmp_mx*	2	*rst_int*	100				
				foc_cyc	0	*init_skip*	0				

Table I

Fig. 2. Structures of compounds selected by DOCK as potential HA inhibitors. The C or S prefix indicates whether the compound came from DOCK output to site 2A or B, respectively.

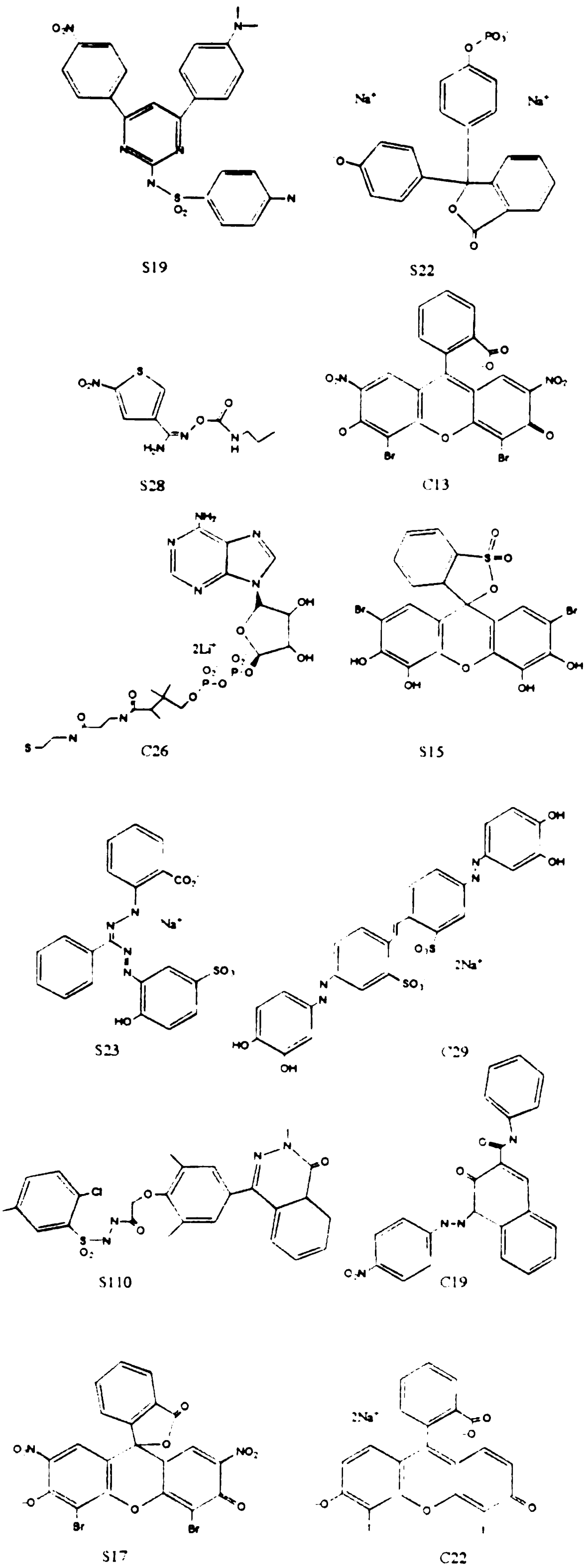

S19 S22

S28 C13

C26 S15

S23 C29

S110 C19

S17 C22

Fig. 2

Table II: Effects of compounds targeted to new DOCK sites.

IC_{50} of infectivity was measured by ELISA, and IC_{50} of cell viability was measured by MTT assay, as described in the Materials and Methods section. DOCK force-field score is described in the DOCK3.5 User's Manual; a more negative number indicates a higher predicted affinity. The effect on BHA conformational change was assayed using the thermolysin assay, as described in the Materials and Methods section.

		IC50		
Name	Effect on conf. Δ	Infectivity	Cell viability	DOCK force-field score
S19	Inhibitor	.8 μM	>> 500 μM	-38.1
S22	Inhibitor	40 μM	>> 100 μM	-43.3
C22	Effector	6 μM	1 mM	-41.9
S23	Effector	> 100 μM	100 μM	-35.6
C29	Effector	ND	<1 μM	-43.0
S28	Weak Inhibitor	>50 μM	>50 μM	-35.7
C13	Weak Inhibitor	>100 μM	>100 μM	-41.1
C26	None	ND	ND	-39.8
S15	None	ND	ND	-35.1
S110	None	ND	ND	-36.7
C19	None	ND	ND	-40.9
S17	None	ND	ND	-34.6

Table II **Effects of compounds targeted to new DOCK sites**

Fig. 3. Effect of S22 and C22 on HA conformational change. Purified, biotinylated BHA was incubated with 100 μM compound in DMSO (lanes 3 and 4) or DMSO alone (lanes 1,2, and 5) (1% DMSO final) and exposed to pH 5 (lanes 2, 4, and 5) or pH 7 (lanes 1 and 3) for 7 minutes before reneutralization. In post controls (lane 5), compound was added after reneutralization. Samples were then analyzed for thermolysin sensitivity as described in the Materials and Methods section.

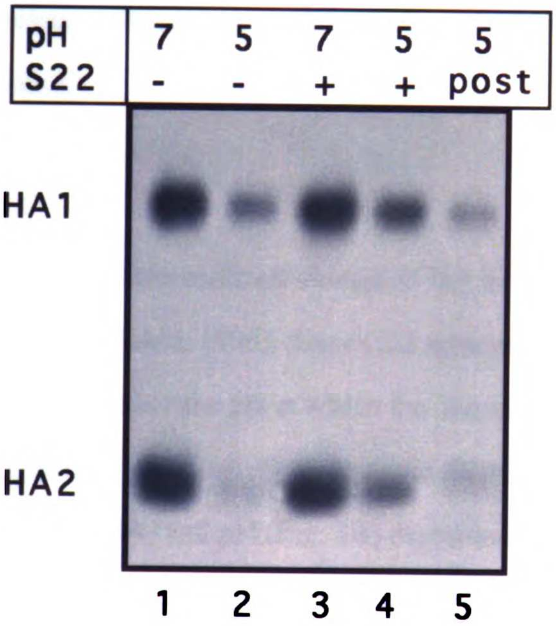
pH
S22
7 5 7 5 5
- - + + post
HA1
HA2
1 2 3 4 5

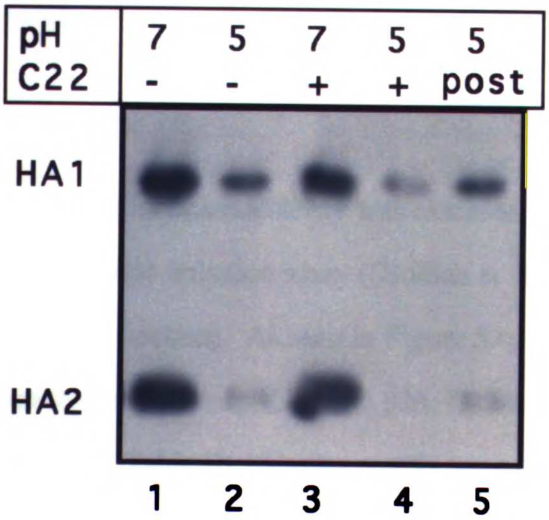
pH
C22
7 5 7 5 5
- - + + post
HA1
HA2
1 2 3 4 5

Fig. 3

conformational change were also identified. One (C29), however, was too toxic to determine its effect on infectivity, while the other (S23) had no measurable effect on infectivity (Table II).

The low pH-induced conformational change of HA is an irreversible event believed to be under kinetic control (Baker, 1994). Since C22 appears to facilitate the conformational change, it might alter either the pH at which the conversion occurs or the time necessary to achieve the conversion (or both). To investigate these possibilities we tested the effects of C22 on the time (Fig. 4A) and pH (Fig. 4B) dependence of the conformational change. As shown in Fig. 4, 100 µM C22 significantly destabilized BHA with respect to both pH and time. Studies examining another measure of the conformational change, the acquisition of proteinase K sensitivity, confirmed the destabilization effect (See Ch. 5). As seen in Fig. 4B, however, C22 did not have any effect on the protease sensitivity of BHA at neutral pH and room temperature.

The effect of C22 on influenza infectivity was examined using both a single-cycle (ELISA) as well as a multiple-cycle infection assay ((Bodian et al., 1993), (Tobita, 1975), see the Materials and Methods section). As seen in Figure 5A, C22 inhibits infectivity in the single-cycle growth assay with an IC_{50} of 6 µM; C22 is not toxic to MDCK2 cells at this concentration (Fig. 5A, Table II). Similar results were obtained using the multiple-cycle assay (IC_{50} approximately 10 µM, data not shown). We next investigated the time window during an infection during which C22 was effective. To this end, C22 was added at various times during a single cycle of infection in MDCK2 cells, and the supernatant was assayed for the amount of virus produced. As shown in Figure 5B, C22 has a significant antiviral effect early in the viral life cycle; the effect continues until 30 minutes

Fig. 4. Effect of C22 on the conformational change of HA: (A) Time and (B) pH dependence. Samples of biotinylated BHA were treated without (filled boxes) or with (open boxes) 100 μM C22, and then (a) incubated at pH 5.2 at room temperature for the indicated time or (b) incubated at the indicated pH for 7 minutes at room temperature. Following reneutralization, samples were analyzed for thermolysin sensitivity as described in the Materials and Methods section.

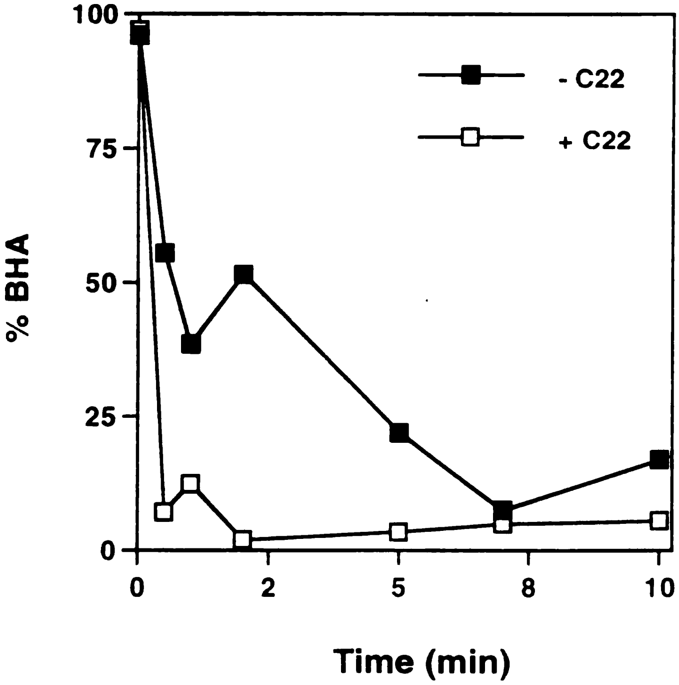

Fig. 4A

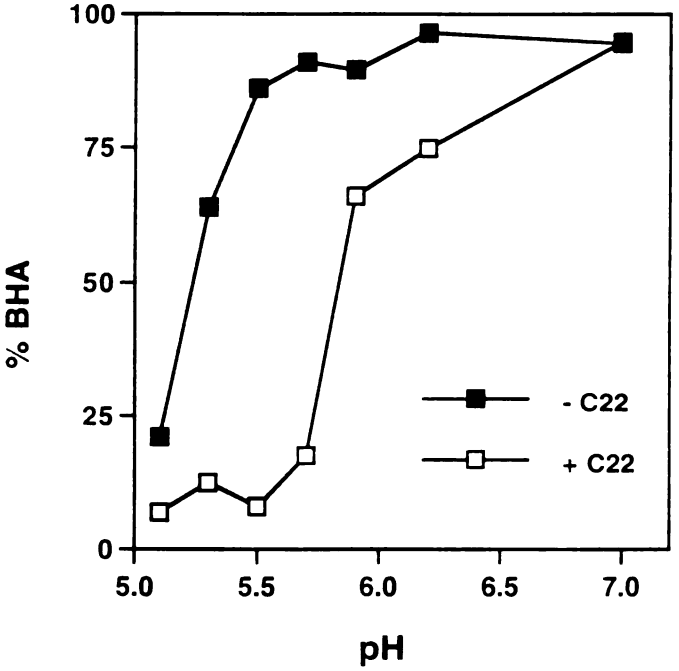

Fig. 4B

Fig. 5. (a) Effect of C22 on infectivity and cell viability. Infectivity was measured for a single cycle using an ELISA, and cell viability was monitored in parallel by assaying for metabolism of MTT, as described in the Materials and Methods section. Open circles, infectivity. Closed circles, cell viability. (b) Effect of C22 when added at various times during a viral infection cycle. Single-cycle infectivity assay was performed as described in the Materials and Methods section. 10 μM C22 was added at the indicated times during a single cycle of influenza infection, and the amount of virus produced was assessed by plaque assay at 15 hours post infection, the time required to complete a single cycle of infection (Gaush, 1968). A control experiment in which C22 was present during viral adsorption in addition to the infection cycle showed no additional inhibition compared to t=0 treatment (data not shown).

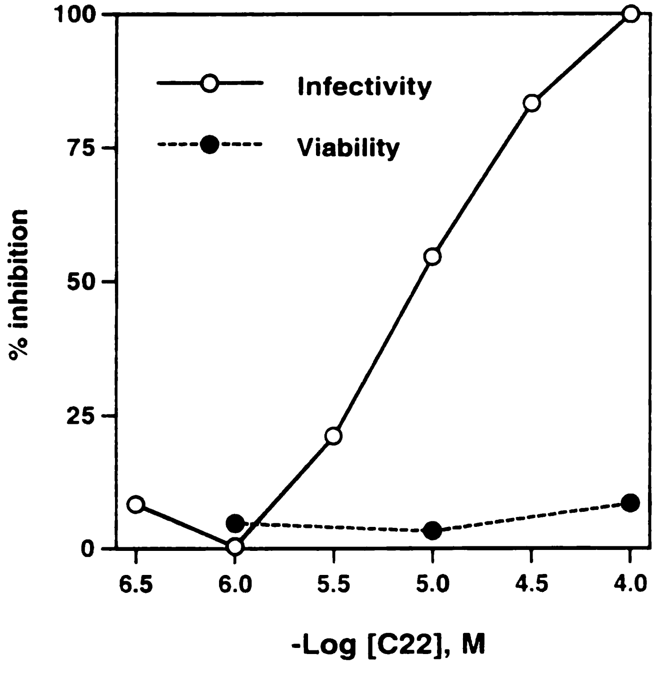
100
75
50
25
0
% inhibition
Infectivity
Viability
6.5
6.0
5.5
5.0
4.5
4.0
-Log [C22], M

Fig. 5A

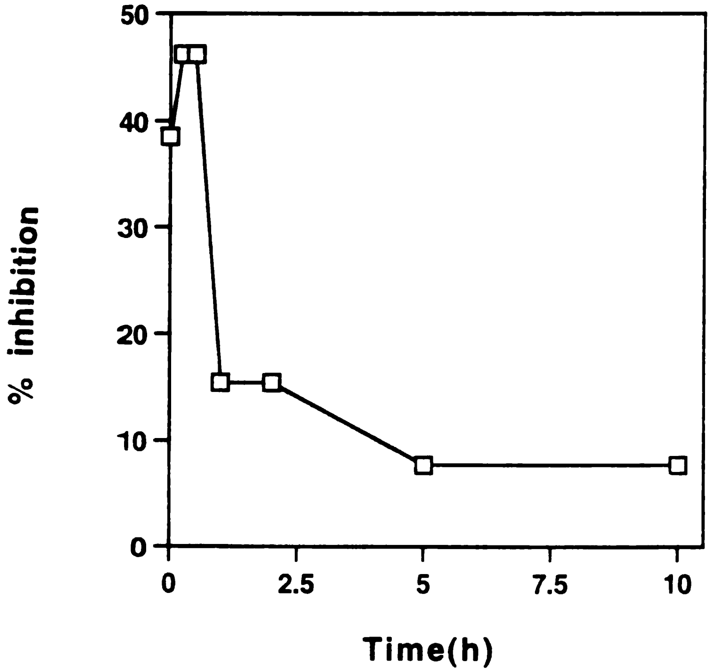

Fig. 5B

post-adsorption but then drops off precipitously at 1 hour. However, a detectable antiviral effect remained at later times; this latter effect was more pronounced at higher concentrations of C22 (data not shown). Another experiment testing hemagglutination showed that viral adsorption (i.e., cell-surface receptor binding) is not affected by 10 μM C22, but that 100 μM C22 inhibits viral adsorption by 50% (data not shown).

That C22 affects the HA conformational change and inhibits infectivity early in the infection cycle suggests that it affects HA-mediated membrane fusion. To test this hypothesis, we examined the effect of C22 on RBC-cell fusion (Ch. 2) and hemolysis (Niles et al., 1990). For the RBC-cell fusion assay, RBCs are preloaded with β-galactosidase and then bound to HA-expressing CHO cells. When the RBC-cell complexes are exposed to pH 5.0, the RBCs will fuse with the CHO cells, delivering β-galactosidase to the CHO cells (Melikyan et al., 1995). As seen in Fig. 6A and Table III, C22 inhibits RBC-cell fusion at 100 μM and 10 μM, in agreement with infectivity and biochemical results. To investigate the effect of C22 on the pH dependence of membrane fusion, we used an hemolysis assay because (1) hemolytic activity of HA has been shown to reflect its fusion activity as well as its conformational change ((Huang et al., 1981), (Doms et al., 1986)), and (2) the hemolysis assay is simple to perform with many samples concurrently and is quantitatively reproducible. As shown in Figure 6B, C22 at 10 μM inhibits hemolysis in the same pH range at which it facilitates the conformational change (Figure 4B); presumably, the effect remains at lower pH values, but the assay is affected by decreasing hemolytic efficiency at pH values approaching and below 5.0 (Bodian et al., 1993).

Fig. 6. Inhibition of fusion and hemolysis by 10 μM C22. (a) Effect of C22 on fusion between CHO cells expressing HA and erythrocyte ghosts containing β-galactosidase. Results are presented in Table III. Assay was performed as described in the Materials and Methods section. Fusion events can be seen as dark patches; cell-cell fusion increases the size of these patches. (b) Effect of C22 on hemolysis. Whole, washed erythrocytes were incubated with (filled boxes) or without (open boxes) 10 μM C22 and virus and treated with the indicated pH for 15 minutes before being analyzed for hemolysis as described in the Materials and Methods section. (c) % difference between the curves in (b), indicating inhibition of hemolysis by C22.

Table III: Effect of C22 on fusion. Column 1: Where indicated, cells were pretreated with trypsin to cleave the inactive precursor HA0 into active HA. Column 2: pH of 2 minute buffer incubation. Column 3: Concentration of C22 present during incubations. Column 4: Number of nuclei in fused areas (blue) per field at 100X magnification. Results are averaged for two assays, one of each of the above types. Column 5: % inhibition by C22 compared to no inhibitor.

HA or HA0	pH	[C22], µM	# fusions/field	% inhibition
HA0	7	0	0	
HA0	5	0	0	
HA	7	0	0	
HA	5	0	20 +/- 2	
HA	5	10	10 +/- 3	49
HA	5	100	1 +/- 1	94
HA0	5	100	0	
HA	7	100	0	

Table III: Inhibition of membrane fusion by C22

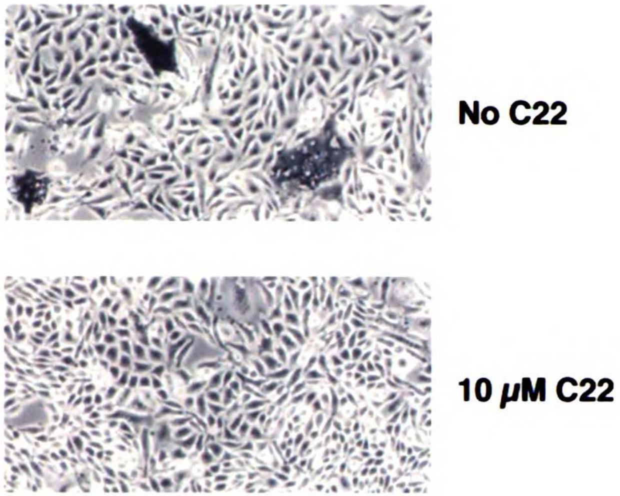
No C22

10 µM C22

Figure 6A

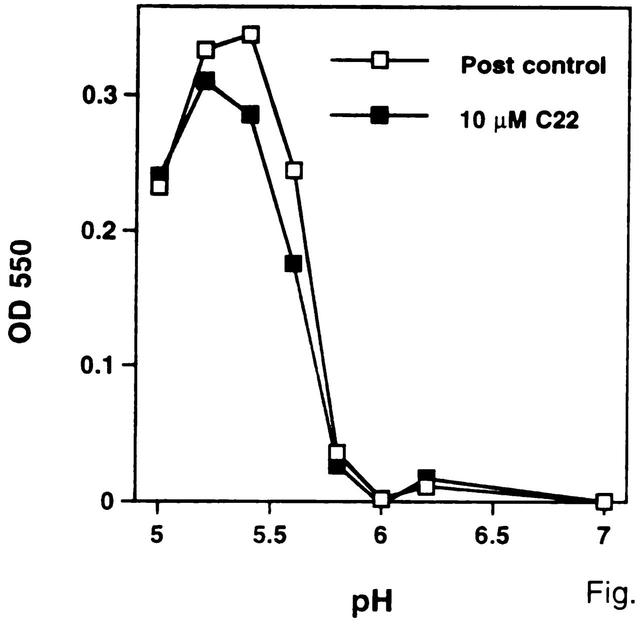

OD 550
0.3
0.2
0.1
0
5
5.5
6
6.5
7
pH
Post control
10 μM C22

Fig. 6B

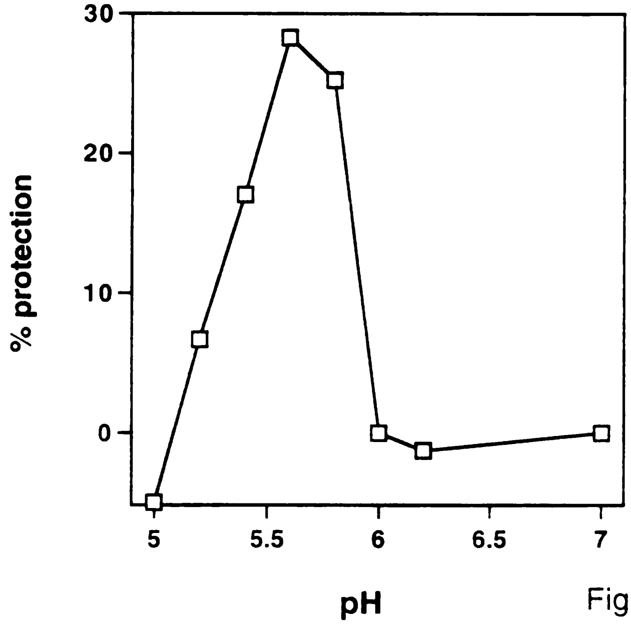

% protection
30
20
10
0
5
5.5
6
6.5
7
pH

Fig. 6C

In order to better characterize the mechanism of antiviral action of C22, we isolated virus variants resistant to C22. Two isolates that are approximately 10-fold resistant were characterized as listed in Table IV. Both resistant mutants lyse RBCs at a lower pH than wild-type virus (Table IV). This finding suggests that both resistant mutants are stabilized with respect to the pH at which their HA is converted to the fusogenic form. Figure 7A shows the locations of the residues mutated in the resistant isolates in the context of the crystal structure of native, wild-type BHA (Weis et al., 1990). The mutation HA1 S219P occurs in the head region, perhaps altering the position of a β-strand that contains intermonomer contacts and allowing new contacts to form. The second mutation, HA1 K27E, was isolated four times independently. Figure 7B shows the area surrounding HA1 K27 in the native structure. This residue lies on the interface between monomers and places a positive charge very close to another positive charge on a neighboring residue (HA2 54 of another HA monomer); the mutation from lysine to glutamate presumably allows an intermonomer salt link to be formed, further stabilizing the interface.

Earlier work identified a virus whose HA is destabilized with respect to the pH of its conformational change as a result of a mutation, HA2 R124G (Ch. 2). Although other mutations are known to destabilize HA (Ch. 2, (Steinhauer et al., 1992)), HA2 R124G was selected for analysis with C22 due to its high resistance to TBHQ (Ch. 2). Figure 7C shows the location of HA2 R124 and the intermonomer salt link presumably removed by the mutation of arginine to glycine. When the mutant virus was tested for sensitivity to C22 using the plaque assay, it proved to be more sensitive to C22 than is wild-type virus by a factor of 2.3 (Table IV).

Fig. 7. HA mutations in C22-resistant isolates. (a) Mutated residues are indicated by magenta, CPK-rendered side-chains of wild-type amino acids. The BHA trimer is displayed as in Fig. 1. Blue space-filling model: DOCK-selected orientation of C22 in site 2A. (b) Close-up of area surrounding HA1 K27. (c) Close-up of area surrounding mutant HA2 R124G.

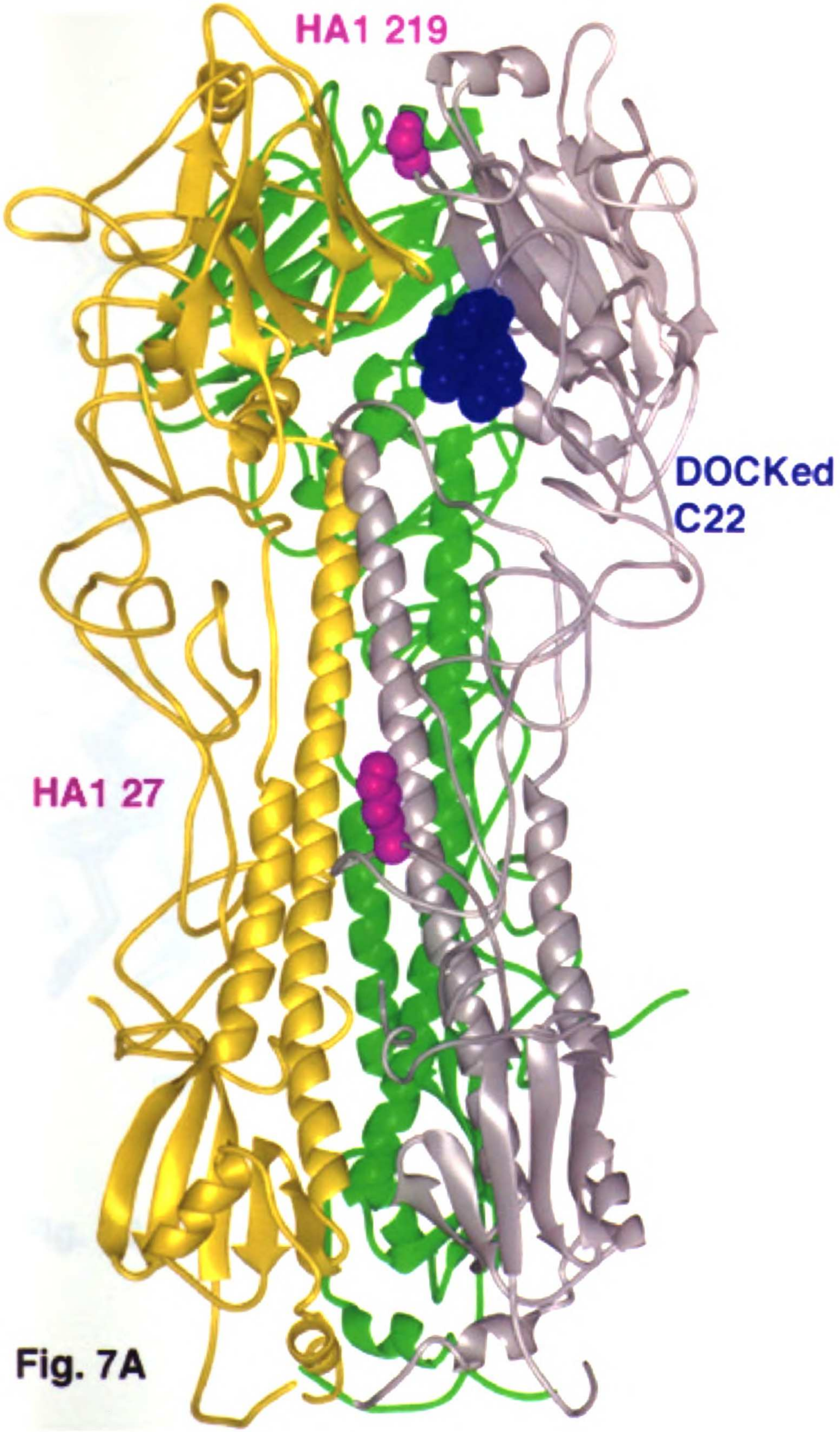
HA1 219
DOCKed
C22
HA1 27

Fig. 7A

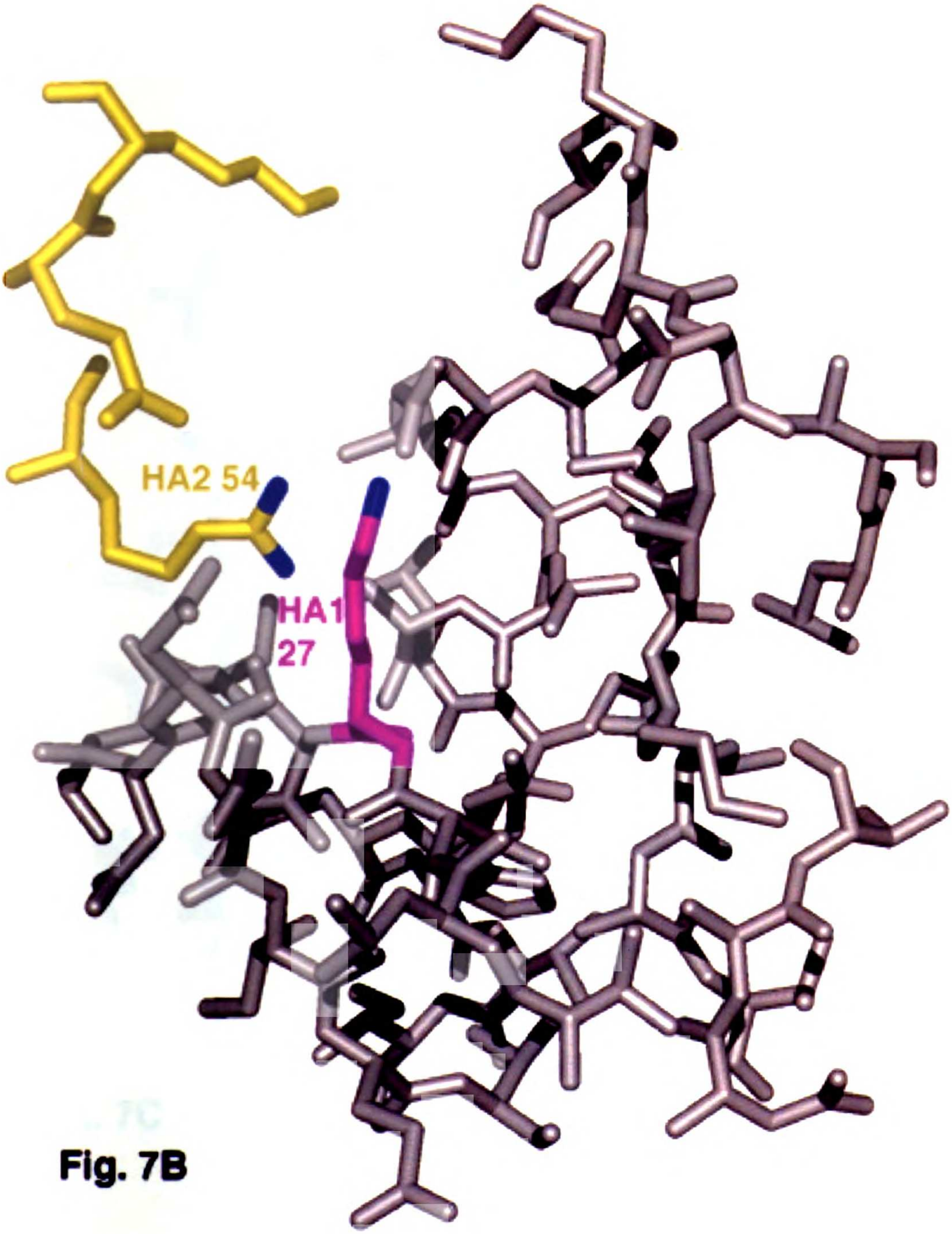
HA2 54
HA1
27

Fig. 7B

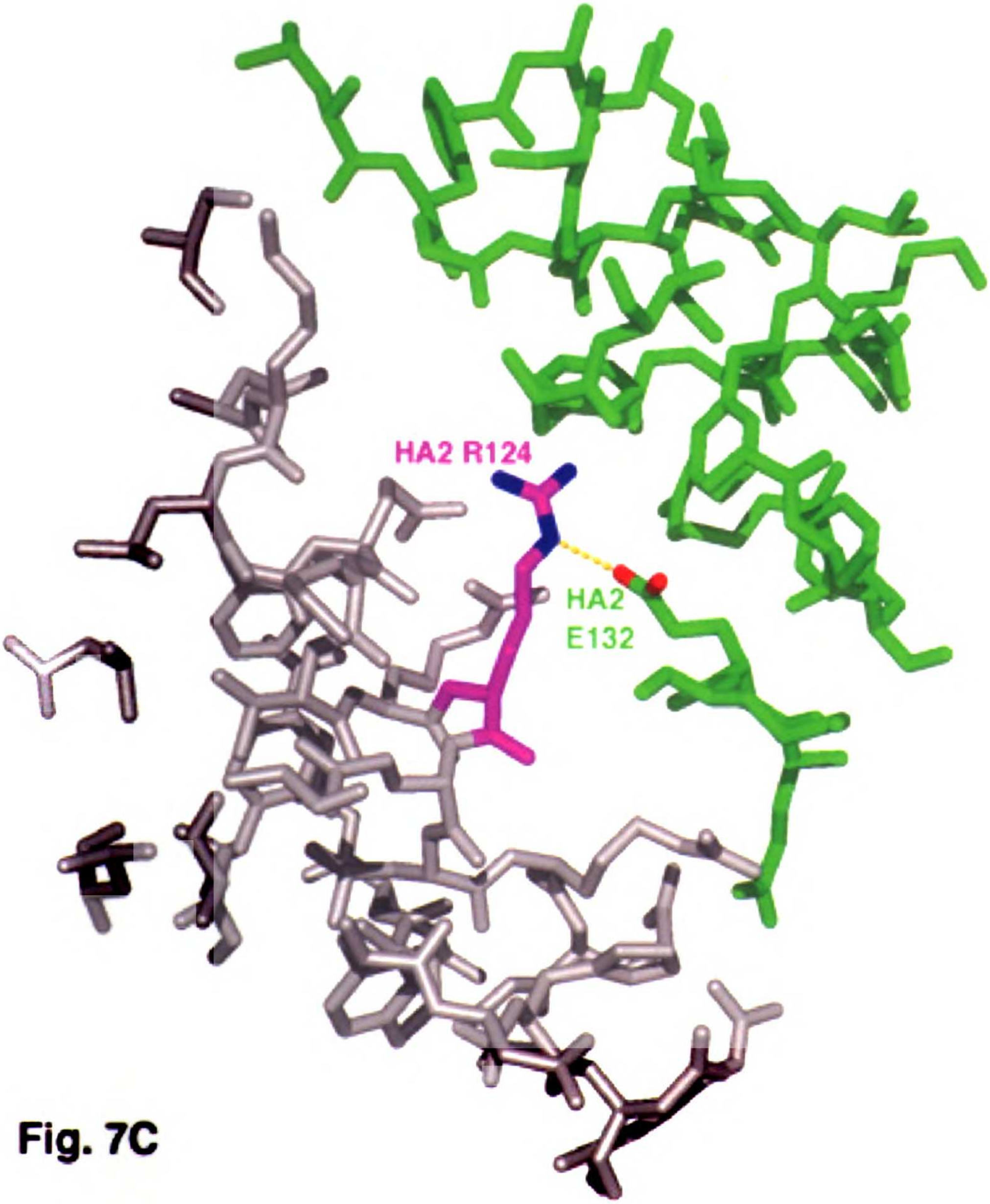
HA2 R124
HA2
E132

Fig. 7C

Table IV: Sensitivity of HA mutants to C22. Column 1: Mutation in HA. Column 2: Method of isolate selection; C22-R indicates that the virus was selected for resistance to C22, TBHQ-R indicates selection for TBHQ resistance. Column 3: IC_{50}s for C22 were measured by plaque assay as described in the Materials and Methods section. Column 4: Shift in pH of hemolysis, measured as described in the Materials and Methods section.

Mutant Residue Number	Selection	Sensitivity to C22 Relative to wt	Δ in pH of hemolysis
HA1 219	C22-R	10-fold lower	-0.3
HA1 27	C22-R	10-fold lower	-0.6
HA2 124	TBHQ-R	2.3-fold higher	+0.25

Table IV: Sensitivity of HA mutants to C22

UCSF

Fig. 8. Reversibility of C22 effect on infectivity. X:31 virus was treated with 10 μM C22. The pH was then lowered to the indicated value for 7 min. at RT and reneutralized. Identical controls (post) were performed in which C22 was added only after reneutralization. Samples were then diluted 100-fold and analyzed for infectivity by ELISA assay as described in the Materials and Methods section. A control experiment showed no inhibition of infectivity by TBHQ when substituted for C22 under these conditions.

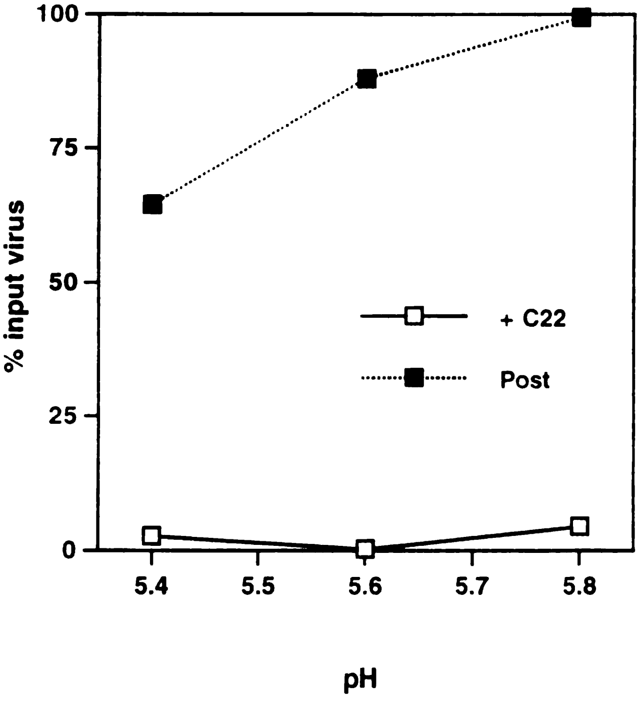

Fig. 8

Since the low pH conformational change in HA is irreversible (White, 1994), if C22 inhibits infectivity by facilitating this change, the inhibition should be irreversible. To examine this possibility, virus was incubated with 10 μM C22 and the pH was lowered to various pH values. The pH values selected have been shown to allow nearly the entire HA population to change conformation in the presence of C22 (5.8, 5.6, 5.4; see Figs. 4B and 6B) while only a portion changes in its absence (Figs. 4B and 6B, (Stegmann et al., 1987)). As seen in Fig. 8, C22 irreversibly inhibits viral infectivity under these conditions.

Discussion

Evaluation of the Method

Since the identification of TBHQ as an inhibitor of the fusion-inducing conformational change in the influenza HA (Bodian et al., 1993), there have been several improvements that encouraged further development of our structure-based inhibitor design strategy: (i) the DOCK program has been improved ((Meng, 1992),(Gschwend, 1996)); (ii) the resolution of the BHA structure increased from 3Å to 2.1Å (Watowich et al., 1994); and (iii) studies have shed insight into the mechanism of fusion peptide exposure, such as the need for motion in the HA1 globular head domains ((Godley et al., 1992),(Kemble et al., 1992)) and a loop to helix transition of HA2 55-81 ((Carr & Kim, 1993),(Bullough et al., 1994), Qiao in prep). We therefore used the refined DOCK in conjunction with the higher resolution BHA structure to perform structure-based inhibitor searches targeting the region of HA that undergoes the loop to helix transition. As a result of this computational analysis, we tested 12 small molecules for their effect on the low pH conformational change and viral infectivity. We consider it significant that, out of the 12 small molecules tested, five have a significant effect on the conformational change at micromolar concentrations; by comparison, 43 molecules were tested before a lead inhibitor (IC$_{50}$=500 μM) was identified in the original search (Bodian et al., 1993). In addition to the improvement in "hit rate," the first generation "hits" found in the new search are more potent than those identified in the earlier work. In fact, the most potent of the new first-generation inhibitors (S19) is more potent than is TBHQ, the best second-generation derivative from the earlier search, and the average potency of the first-generation new inhibitors is about the same as the second generation old ones (both low micromolar IC$_{50}$s). Although certainly not conclusive, our findings suggest that the search using the recent version of DOCK (DOCK3.5, (Meng, 1992), (Gschwend, 1996)) and the improved BHA structure has been more successful at selecting molecules that bind to the sites to which they are targeted than the search using an earlier version of DOCK (DOCK2, (Shoichet, 1991)) and the lower-resolution BHA structure (Bodian et al., 1993). X-ray crystallographic examination of interaction of BHA with the new inhibitors is necessary to clarify this issue.

C22 is an Effector of the Conformational Change in HA

As a consequence of our work, we identified an effector of the low pH-induced conformational change that inhibits influenza virus infectivity. Although this was not a specific goal, the effect of this compound was not wholly unanticipated, since it has been known for some time that if X:31 influenza virus is pretreated at low pH in the absence of a target membrane, it is irreversibly inactivated for fusion (Stegmann et al., 1987). Examination of the DOCK sites analyzed in this search (Fig. 1) reveals many intermonomer contacts that could be either stabilized or destabilized by a small molecule. In addition, the interfaces consist partially of hydrophobic surfaces; an amphipathic molecule could possibly bind to one of these surfaces during the conformational change, lowering the energy barrier of the conversion by shielding the surface from exposure to solvent. As a result of our search we identified three compounds that potentiate the conformational change. It was not clear at the outset, however, that these compounds would inhibit fusion and infectivity. In fact, because C22 does not induce the conformational change at neutral pH but rather likely acts on virus bound to endosomal membranes, it is conceivable that it could lead to increased fusion. One main fact argued against this latter possibility: Influenza viruses bound to membranes display a pH optimum of fusion; below this pH, the efficiency of fusion decreases ((Krumbiegel, 1994), (Doms et al., 1986)). Presumably, the effect of very low pH is similar to the presence of an effector such as C22 in that it decreases the efficiency of fusion through its effect on HA (Fig. 4B).

Our results indicate that C22 destabilizes HA (Figs. 3B, 4A, 4B) and also inhibits hemolysis and fusion (Fig. 6). In fact, the pH range over which C22 inhibits hemolysis most efficiently, pH 5.2-5.8, closely mirrors the range at which it facilitates the conformational change. There are at least three possible explanations for the behavior of C22: (i) Excessively rapid conformational change of HA leads to rapid inactivation, depleting the pool of fusion-active trimers and inhibiting fusion. (ii) (a variant of the first) C22 and/or very low pH (i.e., < 5.0) could cause HA to convert to a fusion-inactive conformation distinct from the low-pH conformation represented by TBHA2. This latter possibility could explain the late effect of C22 in the viral life cycle (Fig. 5B); as HA is being synthesized and processed in the endoplasmic reticulum, C22 may unfold HA, causing the production of defective viruses (this effect would have to be on uncleaved HA, or HA0, since MDCK2 cells do not cleave HA0 into HA1 and HA2 (Tobita, 1975)). Support for this hypothesis comes from the observation that, for HAs that can be cleaved during biosynthesis, altering the pH of vesicles containing newly produced HA with the drug amantadine leads to the production of non-infectious virus (Steinhauer et al., 1991). (iii) The final mechanism supposes that, even though C22 has not been shown to cause conformational changes in HA at neutral pH (Fig. 4B), C22 may allow HA to become inactivated thermally or by other conditions during the course of an infection. This possibility was put forth for viruses with mutations that destabilize their HAs (Daniels et al., 1985). With any of these mechanisms, the effect would be irreversible (unlike that of TBHQ and its relatives (Bodian et al., 1993)). Indeed, C22 is an irreversible inhibitor of viral infectivity (Fig. 8).

Support for the hypothesis that C22 inhibits viral fusion and infectivity by destabilizing HA comes from the location of mutations in viruses resistant to C22: HA1 A219P and HA1 K27E. For both of these mutants, the pH dependence of the conformational change in HA is shifted (0.3 and 0.6 pH units, respectively) in the more acidic direction compared to wild-type HA (Table III). Heretofore, the only known mutation that demonstrated such a stabilizing effect was HA2 K58I (Steinhauer et al., 1991). The mutation at HA1 27 likely involves removal of an intermonomer charge repulsion (Fig. 7B) and formation of a stabilizing salt bridge. The loop on which this residue is found (HA1 14-52) in neutral pH HA has been shown previously to move early during the conformational change (White & Wilson, 1987) and crosses the region of HA2 that undergoes a helix to loop transition at low pH (HA2 106-112, (Bullough et al., 1994)). Hence, this loop could be critical in tethering the trimer in the fusion-inactive conformation. Interestingly, the putative salt bridge is formed with HA2 54 which has been predicted to interact with TBHQ, a stabilizing inhibitor (Ch. 2). The relatively higher sensitivity of the isolate HA2 R124G, which has a destabilized HA, to C22 as compared to wild-type offers more support of the proposed mechanism of C22. Crystallographic analysis of the C22-resistant mutants could shed more light on the control of the HA conformational change.

Premature Triggering of the Fusion-inducing Conformational Change

Premature triggering of the conformational change in HA from X:31 influenza virus is irreversible ((Stegmann et al., 1987), Fig. 8). Hence, irreversible facilitators of the conformational change, such as C22, offer a distinct advantage over reversible inhibitors of the conformational change, such as TBHQ and S22. Although C22 itself does not appear to be able to trigger the conformational change in HA maintained at neutral pH, it may be possible to identify small molecules that do. A conformational change facilitator that functions at neutral pHwould offer the additional advantage of acting outside the cell, a pharmacologically better site for inhibition than in the endocytic compartment, where C22 appears to act. In the case of X:31 influenza, it may be possible to design a variant of C22 that would have this feature.

Currently, only two closely related antiinfluenza drugs are approved for clinical use in the United States: amantadine and rimantidine. Both act by inhibiting a viral ion channel, cause undesirable side effects (Wintermeyer, 1995), and are plagued by clinical resistance ((Houck, 1995), (Wintermeyer, 1995)). A promising new drug, 4-guanidino-Neu5Ac2en (4-GuDANA), was designed to inhibit the viral enzyme neuraminidase (Woods, 1993), and it is currently being evaluated for clinical use, but resistance has already been encountered in laboratory settings (Staschke, 1995). Drugs that inhibit HA-mediated membrane fusion would thus be a welcome addition to the antiinfluenza armament.

It may also be possible to discover or design facilitators of the conformational changes in the fusion proteins of other enveloped viruses such as rabies, HIV, and Ebola. Peptides have already been identified that specifically inhibit fusion of HIV and paramyxoviruses; these peptides are composed of sequences from regions of HIV env and the paramyxovirus F proteins that are believed to be analogous to HA2 55-81 ((Wild et al., 1994), (Lambert, 1996)). It remains to be seen exactly how these peptides inhibit fusion, but it is possible that they prematurely trigger a conformational change. Work with the envelope glycoprotein of another retrovirus, avian sarcoma and leukosis virus, has shown that binding of soluble cell receptor to env renders the viral protein sensitive to thermolysin (Gilbert et al., 1995) in a manner reminiscent of the effect of low pH on HA; this soluble receptor has also been shown to inhibit viral entry into cells (Connally, 1994). Results such as these suggest that the strategy of prematurely triggering viral fusion proteins could be applied to other enveloped viruses.

References

Ausubel, F.M. et al, eds. (1994) *Current Protocols in Molecular Biology*, Vol. 2, Wiley, Brooklyn, NY.

Baker, D., Agard, DA. (1994) *Structure 2*, 907-910.

Bernstein, F. C., Koetzle, T. F., Williams, G. J. B., Meyer, J., E.F., Brice, M. C., Rodgers, J. R., Kennard, O., Shimanouchi, T., & Tasumi, M. (1977) *J. Mol. Biol. 112*, 535-542.

Bodian, D. (1992) *Ph.D. Thesis, University of California, San Francisco.*

Bodian, D. L., Yamasaki, R. B., Buswell, R. L., Stearns, J. F., White, J. M., & Kuntz, I. D. (1993) *Biochemistry 32*, 2967-2978.

Bullough, P. A., Hughson, F. M., Skehel, J. J., & Wiley, D. C. (1994) *Nature 371*, 37-43.

Carr, C. M., & Kim, P. S. (1993) *Cell 73*, 823-832.

Connally, L, Zingler, K; Young, JA. (1994) *Journal of Virology 68*, 2760-2764.

Daniels, R. S., Downie, J. C., Hay, A. J., Knossow, M., Skehel, J. J., Wang, M. L., & Wiley, D. C. (1985) *Cell 40*, 431-439.

Doms, R. W., Gething, M.-J., Henneberry, J., White, J., & Helenius, A. (1986) *J. Virol. 57*, 603-613.

Ferrin, T. E., Huang, C. C., Jarvis, L. E., & Langridge, R. (1988) *J. Mol. Graphics 6*, 13-27.

Gaush, C, Smith, TF. (1968) *Applied Microbiology 16*, 588-594.

Gilbert, J. M., Hernandez, L. D., Balliet, J. W., Bates, P., & White, J. M. (1995) *J. Virol. 69*, 7410-7415.

Godley, L., Pfeifer, J., Steinhauer, D., Ely, B., Shaw, G., Kaufmann, R., Suchanek, E., Pabo, C., Skehel, J. J., Wiley, D. C., & Wharton, S. (1992) *Cell 68*, 635-645.

Gschwend, D. K., Kuntz, ID. (1996) *Journal of Computer-aided Molecular Design 10*, 123-132.

Houck, P, Hemphill, M; LaCroix, S; Hirsch, D; Cox, N. (1995) *Archives of Internal Medicine 155*, 533-7.

Huang, R. T. C., Rott, R., & Klenk, H.-D. (1981) *Virology 110*, 243-247.

Kemble, G. W., Bodian, D. L., Rosé, J., Wilson, I. A., & White, J. M. (1992) *J. Virol. 66*, 4940-4950.

Krumbiegel, M, Hermann, A; Blumenthal, R. (1994) *Biophysical Journal 67*, 2355-60.

Lambert, D; Barney, S; Lambert, AL; Guthrie, K; Medinas, R; Davis, DE; Bucy, T; Erickson, J; Merutka, G; Pettesay, SR Jr. (1996) *PNAS 93*, 2186-2191.

Melikyan, G. B., White, J. M., & Cohen, F. S. (1995) *J. Cell Biol. 131*, 679-691.

Meng, E; Shoichet, BK; Kuntz, ID. (1992) *Journal of Computational Chemistry 13*, 505-524.

Niles, W. D., Peeples, M. E., & Cohen, F. S. (1990) *Virology 174*, 593-598.

Shoichet, B, Kuntz, ID. (1991) *Journal of Molecular Biology 221*, 327-346.

Staschke, K, Colacino, JM; Baxter, AJ; Air, GM; Bansal, A; Hornback, WJ; Munroe, JE, and Laver, WG. (1995) *Virology 214*, 642-646.

Stegmann, T., Booy, F. P., & Wilschut, J. (1987) *J. Biol. Chem. 262*, 17744-17749.

Steinhauer, D. A., Sauter, N. K., Skehel, J. J., & Wiley, D. C. (1992) *Receptor binding and cell entry by influenza viruses*, Vol. 3, Saunders Scientific Publications, Academic Press, London, U.K.

Steinhauer, D. A., Wharton, S. A., Skehel, J. J., Wiley, D. C., & Hay, A. J. (1991) *Proc. Natl. Acad. Sci. USA 88*, 11525-11529.

Tobita, K, Sugiura, A, Enomoto, C, Furuyama, M. (1975) *Med. Microbiol. Immunol. 162*, 9-14.

Watowich, S. J., Skehel, J. J., & Wiley, D. C. (1994) *Structure 2*, 719-731.

Weis, W. I., Bruenger, A. T., Skehel, J. J., & Wiley, D. C. (1990) *J. Mol. Biol. 212*, 737-761.

Wharton, S. A., Calder, L. J., Ruigrok, R. W. H., Skehel, J. J., Steinhauer, D. A., & Wiley, D. C. (1995) *EMBO J. 14*, 240-246.

White, J. M. (1994) in *Cellular Receptors for Animal Viruses* (Wimmer, E., Ed.) pp 281-301, Cold Spring Harbor Laboratory Press, Cold Spring Harbor.

White, J. M., & Wilson, I. A. (1987) *J. Cell Biol. 105*, 2887-2896.

Wild, C. T., Shugars, D. C., Greenwell, T. K., McDanal, C. B., & Matthews, T. J. (1994) *Proc Natl Acad Sci U S A 91*, 9770-9774.

Wilson, I. A., Skehel, J. J., & Wiley, D. C. (1981) *Nature 289*, 366-372.

Wintermeyer, S, Nahata, MC. (1995) *Annals of Pharmacotherapy 29*, 299-310.

Woods, J; Bethell, RC; Coates, JAV; Healy, N; Hiscox, SA; Pearson, BA; Ryan, DM; Ticehurst, J; Tilling, J; Walcott, SM; Penn, CR. (1993) *Antimicrobial Agents and Chemotherapy 37*, 1473-1479.

Chapter 4:

A Specific Proline Substitution in the Coiled-Coil Region of the Influenza Hemagglutinin Impairs its Membrane Fusion Activity

Note: The work in this chapter has been performed by Sandra Pelletier, Hui Qiao, Luke Hoffman, and Jill Hacker and is being prepared as a manuscript for publication.

Introduction

A spring-loaded conformational change has been proposed as a unifying mechanism for the membrane fusion proteins of orthomyxo-, paramyxo-, retro-, and coronaviruses, and a similar mechanism may apply to certain cellular fusion proteins as well ((Rothman, 1996), (Hernandez et al., 1996)). According to the model, the spring-loaded conformational change occurs in the fusion protein in response to a specific fusion trigger (for example, low endosomal pH in orthomyxoviruses), and involves the formation of an extended alpha-helical coiled-coil thus propelling the previously buried fusion peptide upwards toward the target bilayer. Interaction of the fusion peptide with the target bilayer initiates fusion ((White, 1995), (Hernandez et al., 1996)).

The hemagglutinin (HA) of influenza virus is the most extensively characterized membrane fusion protein (for reviews, see (Hernandez et al., 1996), (White, 1996)). In response to low pH, HA undergoes a series of conformational changes, its fusion peptides are exposed, and it binds hydrophobically to target membranes, initiating the cascade of events that lead to membrane merger. In the case of HA, high resolution structural data indicate that a region of the fusogenic subunit, HA2 residues 55-76, is converted from a loop at neutral pH to an extended trimeric alpha-helical coiled-coil in low pH-treated HA (Bullough et al., 1994). This dramatic rearrangement provides a compelling mechanism for exposing and repositioning the fusion peptide at the target membrane surface. Prior to the solution of the x-ray structure of TBHA2, a fragment of low pH-treated HA, residues HA2 55-76, had been predicted to form a coiled-coil

((Ward & Dopheide, 1980), (Carr & Kim, 1993)). In addition, synthetic peptides encompassing this region (HA2 residues 54-89 and HA2 residues 38-89) had been shown to form a trimeric alpha-helical coiled-coil when assayed at low pH at 0°C; the longer synthetic peptide was shown to form a stable trimeric coiled-coil at physiological temperatures both at neutral and low pH (Carr & Kim, 1993). Furthermore, recent experiments have shown that a protein construct encoding HA2 residues 38-175 expressed in E. coli exists as a thermostable trimeric coiled-coil (Chen et al., 1995). These observations support the notion that the low pH extended coiled-coil conformation of HA is its most stable conformation.

Collectively, the recent studies on HA indicate that the neutral pH trimer, the form that sits on the virus surface, is in a metastable conformation that is converted to its most stable conformation only upon exposure to low pH or removal of stabilizing interactions in the intact protein. Despite the certainty of this fact, it is still not known whether the low pH extended coiled-coil conformation is required for fusion and, if so, for what stage of the fusion reaction.

We have recently proposed a model in which there are (at least) two intermediates between the neutral pH HA trimer and its final low pH form (Hernandez et al., 1996). We have further proposed that each intermediate facilitates distinct steps in the fusion process. The studies presented here focus on the first of these intermediates, the conversion of HA2 residues 55-76, designated as segment B (Bullough et al., 1994), from a loop to a helix. This conversion generates a long extended coiled-coil of three alpha-helices, and is required for interaction of the fusion peptide with the target membrane, an essential prelude to membrane merger. Here we show that a specific mutation designed to impede the loop to helix transition of HA2 residues 55-76 does, indeed, impair the fusion activity of HA. We

further show that this mutation impairs fusion by preventing a very early stage of the fusion reaction, mixing of outer leaflet lipids.

Materials and Methods

Computations

Calculations of coiled-coil stability of HA2 54-81 were performed using the computer program COILS2 (Lupas et al., 1991) as described elsewhere (Carr & Kim, 1993). The predicted stability values on a random scale (Carr & Kim, 1993) are listed in Table I.

Internal energy of HA2 54-81, either wild type or with substitutions, was computed using the Measure function within the Biopolymer module of InsightII, a molecular mechanics and modeling package (Biosym). Dihedral angles of wild type residues within this region were determined using this same program, and these angles were mapped onto the plots of allowable such angles using the method of Ramachandran (Ramachandran, 1968) to confirm the viability of planned substitutions.

Mutagenesis

Mutant HAs were generated using the Kunkel method (Kunkel et al., 1987) on single stranded preparations of the cDNA for wt HA (X:31 strain) which has been cloned in to the plasmid pSM. The oligonucleotides (Ch. 2) for mutagenesis were designed to encode

the altered amino acid as well as an additional restriction enzyme site for rapid detection of mutants. Plasmids were sequenced to confirm the desired mutation as well as to check that second site mutations were not introduced.

Expression of wt and mutant HAs

Cos 7 cells were maintained in DMEM (GIBCO BRL, Gaithersburg, MD) plus 10% supplemented Calf Serum (SCS) (Hyclone), 50,000U penicillin and 50,000 mg streptomycin (GIBCO BRL, Gaithersburg, MD), and an additional 146 mg glutamine (GIBCO BRL, Gaithersburg, MD), and transiently transfected using the DEAE Dextran method when they were 60-80% confluent and analyzed ~48 hours post-transfection. Unless stated, 1.25mg of plasmid DNA was added per 6cm plate (2.5mg per 10cm plate). Unless stated, all cells were treated 16 hours before analysis with 0.25mM deoxymannojirimycin (dMM) (CalBiochem, San Diego, Ca) .

Metabolic Labeling

Cells expressing wt and mutant HAs were metabolically labelled with ^{35}S-Translabel (ICN) as described (Kemble et al., 1993). Briefly, 24 hours post transfection cells were incubated with cys-/met- MEM media (GIBCO BRL, Gaithersburg, MD) for 45-90 minutes at 37°C. Media on each 10 cm plate was then replaced with 5 mls cys-/met- MEM containing 200mCi ^{35}S translabel and 2% SCS and the cells were incubated in a CO_2 incubator at 37°C for 14-18 hours.

Trypsin Treatment of Cells

As indicated, cells expressing wt- or mutant HAs were washed 2 times with RPMI media and incubated for 6 minutes at room temperature with RPMI containing either TPCK-trypsin (5mg/ml) or, as negative controls, either TPCK-chymotrypsin (5mg/ml) or soybean trypsin inhibitor (STI) (50mg/ml) (all reagents obtained from Sigma Chemical Co., St. Louis, MO). Trypsin-treated cells were then incubated for 10 min. with RPMI containing STI (50mg/ml) to quench the trypsinization reaction.

Immunoprecipitation

Cells expressing wt- or mutant HAs were washed, lysed in a cell lysis buffer containing NP-40 and protease inhibitors, and immunoprecipitated essentially as described (Kemble et al., 1993). Modifications were that lysis was conducted at room temperature for 15 min. and that the amount of the site A monoclonal antibody (gift of Dr. J. Skehel) was decreased to 0.1-0.3 mg/ml.

Sucrose Gradient Analysis of Trimer Formation

Cells expressing wt and mutant HAs were treated with trypsin and lysed as described above. Cleaved cell lysates were then loaded onto continuous gradients of 3-30% sucrose (w/v) in 0.1% NP40, MES-Saline (30 mM MES, 100mM NaCl, pH 7) and centrifuged at 35,000 rpm for 15 hrs. at 4^{o}C in an SW-55 rotor. A total of 12 fractions were collected from the bottom of each tube. Each fraction was incubated with concavanalin A agarose (Vector Laboratories, Inc., AL-1003) to precipitate glycoproteins, analyzed by SDS-PAGE, and then Western blotted as described below.

Proteinase K Digestion

Cells expressing wt and mutant HAs were treated with trypsin, incubated in MES-Saline at different pH values for 15 min at 37°C, reneutralized in MES-Saline pH 7, lysed in NP40-containing lysis buffer without protease inhibitors, and then digested with 0.2mg/ml proteinase K in the presence of 2mM $CaCl_2$ for 30min at 37°C. The digestion was stopped by adding 10mg BSA, 1mM PMSF and proteinase inhibitors (as per (Kemble et al., 1992)). Samples were then immunoprecipitated with the site A monoclonal antibody and analyzed by either PhosporImager analysis or Western blotting.

Reactivity with C-HA1 Antibody

The C-HA1 antibody is an anti-peptide antibody against the C-terminal residues of HA1. The C-HA1 antibody reacts preferentially with low pH treated HA (White & Wilson, 1987) and efficiently precipitates low pH-treated HA from crude cell lysates (Qiao and White, unpublished results). Immunoprecipitations with the C-HA1 antibody were conducted as follows: Plates of metabolically labeled cells were treated with trypsin, incubated at various pH values in MES - Saline buffer for 15 min. at room temperature, and then reneutralized with MES-Saline buffer pH 7. Cells were then lysed with the NP40-lysis buffer containing protease inhibitors (Kemble et al., 1992) and immunoprecipitated with the C-HA1 antibody for 1 hr at RT. Immune complexes were then bound to protein A agarose (Boehringer Mannheim GmbH, Mannheim, Germany) for 1 hour and washed extensively as described (Kemble et al., 1992). Samples were then analyzed by SDS-PAGE and PhosphorImager analysis.

Electrophoresis and Western blot analysis

Samples were dissolved in SDS sample buffer, and resolved by SDS-PAGE on 12% gels, transfered to nitrocellulose, and immunoblotted first with an anti-HA polyclonal antibody

(Generous gift of Dr. Skehel) and then with HRP conjugated anti-rabbit IgG (Amersham Corp., Arlington Heights, IL). Detection was by enhanced chemiluminescence essentially as described in (Kemble et al., 1994).

Phosphorimager Analysis

Dried gels of ^{35}S-labeled samples were exposed to film and scanned into a PhosphorImager workstation using ImageQuant. HA band intensities were determined by summing the pixels in a constant volume rectangle.

Red Blood Cell Binding and Lipid and Content Mixing Assays

Red blood cells (RBCs) were labeled with octadecylrhodamine (R18) or calcein AM (Molecular Probes, Inc.; Eugene, OR) and then bound to cells expressing wt and mutant HAs and exposed to low pH (to induce fusion) essentially as described (Kemble et al., 1993): Monolayers of cells expressing wt or mutant HAs were washed 2 times with RPMI media and incubated with RPMI containing 0.2mg/ml neuraminidase (Sigma; N-2876) for 10 min. at room temperature (to enhance RBC binding) and then treated with trypsin to cleave HA0 to HA1 and HA2 as described above. RBCs labeled with R18 or calcein AM were then bound to the HA-expressing cells for 20 minutes at room temperature and the unbound RBCs removed by repeated washing. Cell monolayers were then incubated at 37°C with pH 5 buffer (10mM MES, 10mM HEPES, 120mm $NaCl_2$, 10mm succinate, and 2mg/ml glucose) for 2 minutes (or 10 minutes where indicated), neutralized in the same buffer at pH 7, and observed with a fluorescence microscope.

Results

In the present study we asked two questions. First, is the spring-loaded conformational change in the influenza virus (the loop to helix transition of HA2 residues 55-76) required for fusion, and if so for what phase of the fusion reaction: hemifusion, the mixing of the outer leaflet lipids, or full fusion, the mixing of aqueous contents, or rather is it a post fusion conformation resulting in inactivation? We addressed this question by introducing nine site-specific mutations into this region; we assess their effects on the structure and cell surface expression of HA, on its ability to undergo low pH-induced conformational changes and on its ability to mediate membrane fusion--both outer leaflet lipid mixing as well as content mixing.

Design of Site-Specific Mutations

Mutational analysis focused on the region HA2 54-81, the segment of HA predicted by previous computations (Carr & Kim, 1993) to convert from an unstructured, random coil to a coiled-coil during the low-pH HA conformational change. More recent crystallographic analysis of a fragment of HA in its low-pH form supports this prediction and better defined the residues involved in stabilizing the final coiled-coil (Fig. 1B, (Bullough et al., 1994)).

The choice of residues to mutate within this segment was based on several criteria as outlined in Table I. Residues were selected that are not absolutely conserved among naturally-occurring influenza viruses (Table I), indicating that the protein's native structure would not be disrupted by mutations at these locations. Residues known to form salt bridges in the neutral form of the protein were deemed unsuitable, since loss of these types of contacts are already known to affect the pH of fusion by facilitating the conformational change ((Daniels et al., 1985), (Weis et al., 1990)). One residue was chosen to represent each of three general locations within the HA2 54-81 segment: N-terminal (HA2 55),

central (HA2 71), C-terminal (HA2 80, Table I and Figs. 1a-c). The final selection criterion involved the location of the chosen residue in the coiled-coil in the final low-pH conformation; two residues selected lie in "d" positions (HA2 55 and 80, Fig. 1c), critical for coiled-coil formation (Bullough et al., 1994), while the third (HA2 71) was chosen for its location at a residue not responsible for such stabilization, a "b" residue (Bullough et al., 1994).

In selecting the residues to substitute into each of these sites, the abundance of various amino acids within naturally-occurring coiled-coils was considered to represent the ability of those residues to stabilize or destabilize this type of structure ((Lupas et al., 1991), (O'Neil, 1990)). Alanine was chosen due to its high abundance in coiled-coils, while glycine was chosen for its relatively low abundance and proline for its virtual lack of existence in parallel coiled-coils such as that seen in TBHA2 (Table I, (Lupas et al., 1991)). These assumptions were supported by calculations of the relative stability of resulting coiled-coils using the same methods employed by Kim et al (Carr & Kim, 1993) to predict coiled-coil formation by HA2 54-81 as described in the Materials and Methods section (Table I). In addition, the ability of each location to accomodate mutant residues in the neutral-pH form of BHA was considered as follows: The dihedral angles of the wild-type residue at each location in this native crystal structure were determined; as indicated in Table I, these angles were determined to be acceptable also for alanine, glycine, and proline (as described in the Materials and Methods section). Then, each substitution was made isomorphously in the HA2 54-81 region native structure (Watowich et al., 1994) computationally and the internal energy of the segment was calculated as described in the Materials and Methods section. As listed in Table I, all substitutions but one were calculated to not significantly change the internal energy of this region. Although a proline substitution at HA2 80 gave a large change in internal energy due to a predicted close approach between hydrogen atoms, cell-

Fig. 1 HA2 55-81 in pre- and post- fusion forms

(a) All of the residues visible in the TBHA2 structure are shown for neutral pH BHA. Black region, HA2 55-81. Wild type sidechains for residues mutated in this work are displayed and labeled. (b) TBHA2, colored and labeled as in (a). (c) Blow-up of HA2 54-81 in the TBHA2 structure.

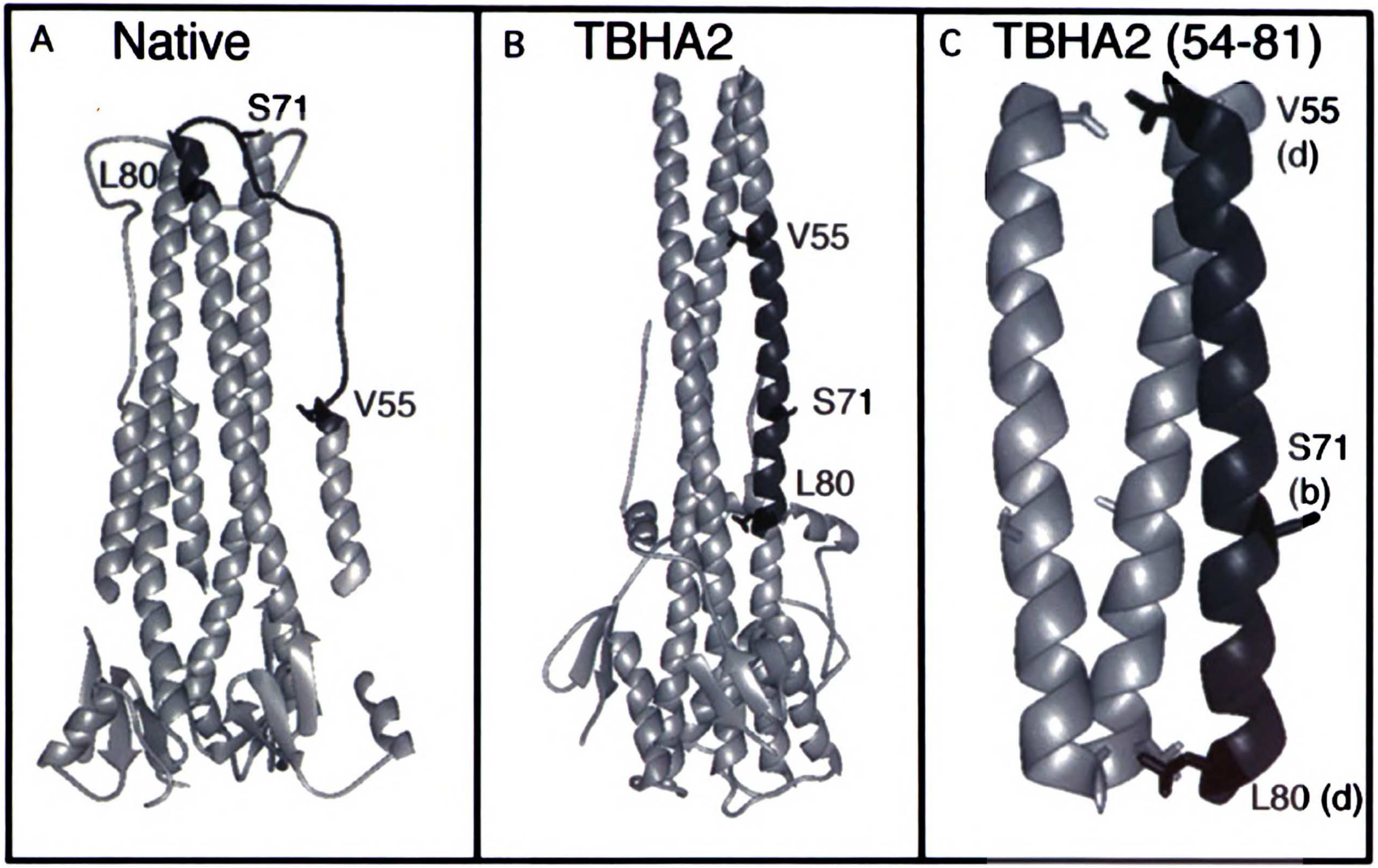
A
Native
S71
L80
V55
B
TBHA2
V55
S71
L80
C
TBHA2 (54-81)
V55
(d)
S71
(b)
L80 (d)

Fig. 1

UCSF LIBRARY

Table I. Mutated residues

Top row: Numbers of residues in HA2 mutated. Second row: Amino acid of those residues in X:31 HA, the protein mutated for these studies (Carr, 1992). Third row: Amino acids of these residues in naturally-occurring variants of influenza HA. Fourth row: Location of these residues within the HA2 54-81 region that undergo a loop to helix transformation at low pH (Carr, 1992). Fifth row: Letter indicating position of the residue in the low-pH coiled-coil (Bullough, 1994). Seventh row: % difference in Amber force-field score between wt X:31 HA2 54-81 and the indicated mutant isomorphously replaced in the neutral-pH, crystallographic conformation as predicted by InsightII (Biosym) using the coordinates of neutral-pH BHA at 2.1Å resolution (Watowich, 1994) with protons added using the program addprh. Eighth row: Indication of whether torsional angles of the wt residue in the neutral structure lie within allowed regions of the mutant residues' Ramachandran plots (see text). Ninth row: Score of HA2 54-81 with indicated mutation using the method of (Carr, 1992); the wt sequence has a score of 1.62. Tenth row: Occurrence of indicated amino acids within coiled-coils (see text).

Residue # in HA2	55			71			80		
Amino acid in wild-type, X31 HA	V			S			L		
Natural variants	I,L			D,E.G,N,T			V		
Location within B helix	N-terminal			Central			C-terminal		
Letter position in low-pH coiled-coil	d			b			d		
Mutants	Alanine	Glycine	Proline	Alanine	Glycine	Proline	Alanine	Glycine	Proline
Change in Amber force field score	< 1%	<1%	<1%	<1%	<1%	<1%	<1%	<1%	>100%
ϕ, ψ angles acceptable?	yes	yes	yes	yes	yes	yes	yes	yes	yes
COILS2 score for HA2 54-81	1.68	1.56	1.41	1.66	1.55	1.51	1.63	1.46	1.32
Occurrence within parallel coiled-coils	Common	Common	Rare						

Table I

expressed HA with this mutation was subsequently found to be processed normally and expressed on the cell surface (See below).

The low-pH conformational change is believed to represent a two-state system under kinetic control (Baker, 1994); therefore, a mutation that affects the height of the energy barrier between the two states would be predicted to change the kinetics of fusion. Since coiled-coil formation is believed to be involved in this transition ((Carr & Kim, 1993), (Bullough et al., 1994)), the mutations described above would be predicted to affect the rate of fusion. If the mutations also abrogate the formation of the final, fusogenic state, the overall extent of fusion would also be expected to be affected. We predicted that, since prolines destabilize coiled-coils, all three proline mutations (and especially those at "d" residues) would inhibit both the rate and extent of fusion (Table I).

HA Processing and Cell Surface Expression

As the first phase of our analysis, we assessed the synthesis, glycosylation, and cell surface expression of mutant HAs. HA is synthesized, core glycosylated and trimerized in the endoplasmic reticulum. It is then transported through the Golgi complex where the seven N-linked carbohydrates are trimmed and further modified (Wiley & Skehel, 1987). Five of the seven N-linked carbohydrates are fully processed to complex structures (those at HA1 residues 8, 22, 38, 285, and at HA2 residue 154) whereas the other two, at HA1 residues 81 and 165, remain in the high mannose form. After transit through the Golgi complex, HA is transported to the cell surface where it has a long residence time. In specialized tissues (e.g. Clara cells of the lung) HAs of subtype A influenza viruses are proteolytically processed from HA0 to a fusion-competent form consisting of two disulfide-bonded subunits, HA1 and HA2. In all other tissues, and all established cell

lines, HA remains at the cell surface in its fusion-inactive form, but can be cleaved to HA1-S-S-HA2 by the addition of low amounts of trypsin.

In the first set of experiments, wild-type (wt) and mutant HAs were expressed in Cos 7 cells. Immunofluorescence assays, red blood cell binding, and green fluorescent protein co-transformations confirmed that an approximately equal number of cells were being transfected with the wt and mutant DNAs (data not shown). The resulting glycoproteins in total cell lysates were separated by sodium dodecylsulfate polyacrylamide gel electrophoresis (SDS-PAGE). The migration of the HA0 species was analyzed by Western blot analysis.

Because recent experience with glycosyl-phosphatidyl-inositol (GPI)-anchored HA indicated that certain HA mutants acquire excess terminal carbohydrate at sites in HA1 that normally remain in the high mannose form, we performed this analysis on cells that were grown in the absence or presence of deoxymannojirimicin (dMM) (Kemble et al., 1993), a terminal glycosidase inhibitor; previous work has shown that wt-HA behaves the same in binding, fusion and infectivity assays whether grown in the absence or presence of dMM. As seen in Fig. 2, when produced in the absence of dMM, the HA0s from the mutants V55A, S71A, S71G, and S71P all co-migrated with wt - HA0, whereas the HA0s from all of the other mutants (L80A, V55G, L80G, V55P, and L80P) ran abberantly as multiple higher molecular weight species. When grown in the presence of dMM, however, all mutant HA0s co-migrated with wt-HA0. These findings suggest that specific substitutions within the B loop region of HA2 (glycine and proline substitutions at position 55, as well as alanine, glycine, and proline substitutions at position 80) affect the initial folding of the HA such that it is aberrantly glycosylated. Reminiscent of the behavior and in view of the analysis of GPI-anchored HA, the most likely explanation for the aberration is that the head domains of specific HA mutants are not packed exactly as in wt HA such that the N-linked

Fig. 2 Migration of wt and mutant HA0s on SDS gels

Cos 7 cells were transfected with plasmids encoding wt and mutant HAs and grown in the absence (-) or presence (+) of 0.25 mM dMM. Cell lysates were prepared and glycoproteins precipitated with concavanalin A agarose. Gel samples were then prepared in sample buffer containing 100 mM DTT and separated by 10% SDS-PAGE. The gel was then analyzed by western blotting with a rabbit anti-HA antiserum (Kemble and White, 1993) as described in the Methods section. The antiserum reacts with HA0 and HA1.

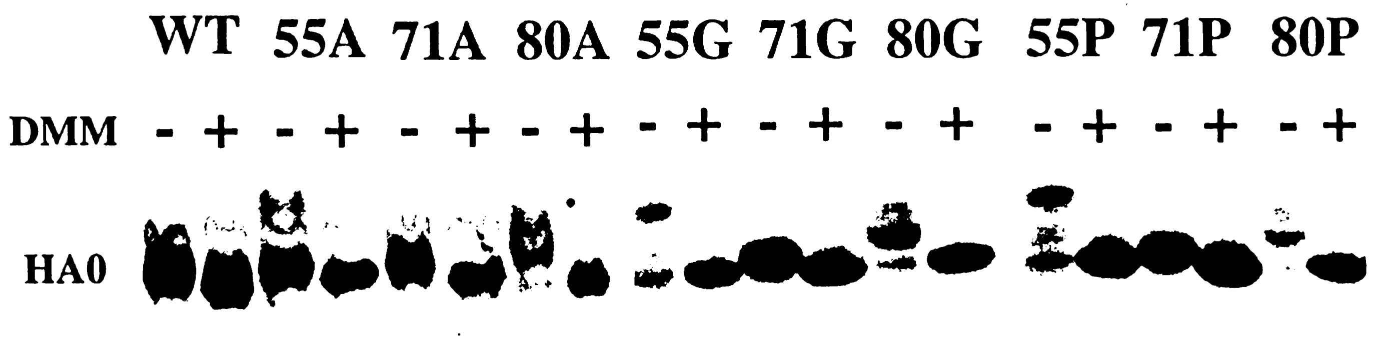
WT 55A 71A 80A 55G 71G 80G 55P 71P 80P
DMM - + - + - + - + - + - + - + - + - + - +
HA0

Fig. 2

carbohydrate addition sites at HA1 positions 81 and 165 are subject to excess terminal glycosylation. In view of these findings and the fact that wt HA behaves the same if grown in the presence or absence of dMM, all subsequent analyses were performed with HAs produced in the presence of dMM.

We next assessed whether the mutant HA0s were delivered to the cell surface and whether they could be proteolytically processed by the addition of trypsin. Cells expressing wt and mutant HA0s, grown in the presence of dMM, were treated with either soy bean trypsin inhibitor (STI) or chymotrypsin as negative controls or with trypsin. Cell lysates were prepared and cleavage of the HA0 protein was analyzed by Western blot analysis. As shown in Fig. 3, all of the mutant HA0s were expressed at approximately comparable levels and, as evidenced by the appearance of a co-migrating HA1 band, were accessible for proper proteolytic cleavage by trypsin. For L80A, V55G, L80G, and V55P, however, the intensity of the HA1 band was diminished. These results suggest that all of the mutant HA0s are transported to the cell surface in a form that can be cleaved to HA1 and HA2, but that the quantity and/or quality of specific mutant HAs was compromised by the amino acid substitution. This latter observation suggests that these mutant HA0s were either less efficiently delivered to the cell surface, less efficiently cleaved from HA0 to HA1 and HA2 or that the resultant HA1 species were more sensitive to general proteolysis. Therefore, in cases where an apparent fusion defect was observed (see below), great care was taken to normalize for cell surface levels of HA1 and HA2.

We next assessed whether the proline-substituted HAs, those mutants which were considered most likely to be impaired in their ability to fuse ((Lupas et al., 1991), (Carr & Kim, 1993)), can form trimers at the cell surface. For this analysis, cells expressing V55P, S71P, or L80P HA0 were treated with trypsin to cleave HA0 to HA1 and HA2. The cell lysates were then subjected to sucrose gradient centrifugation analysis. Samples

Fig. 3 Proteolytic processing of wt and mutant HA0s

Cells transfected with plasmids encoding wt and mutant HAs were grown in the presence of dMM and treated with either 5 μg/mL chymotrypsin (C) or trypsin (T) for 6 min at RT. Cell lysates were prepared and analyzed for HA protein as described in the legend to Fig. 2.

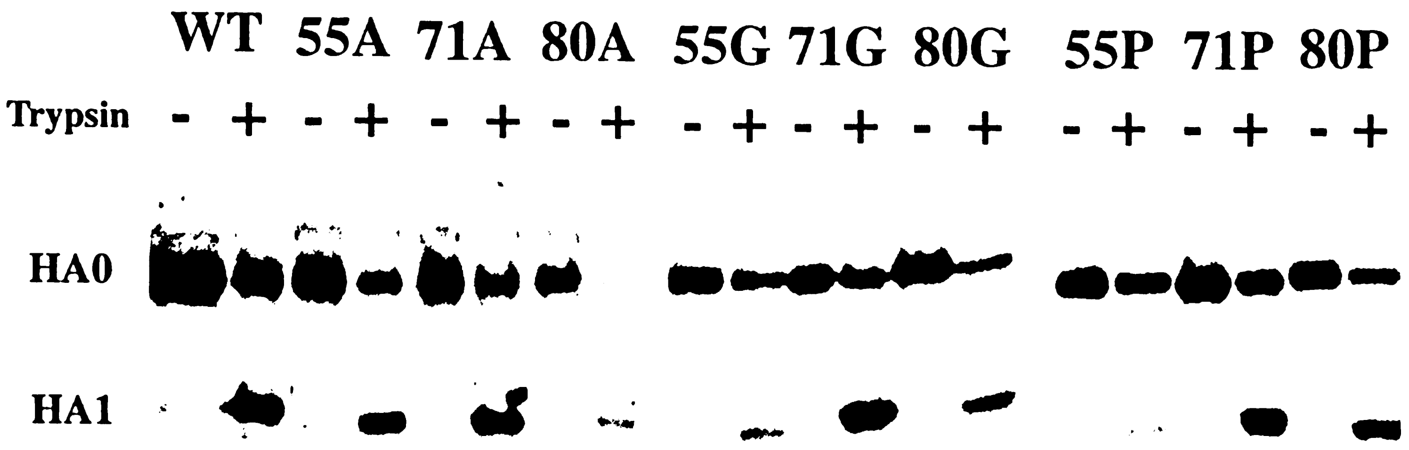
WT
55A
71A
80A
55G
71G
80G
55P
71P
80P
Trypsin
- + - + - + - + - + - + - + - + - + - +
HA0
HA1

Fig. 3

from the gradient fractions were prepared and analyzed by Western blotting. As seen in Fig. 4, all of the proline-substituted HAs approximately co-migrated with wt HA in fractions 6-8 of the gradient indicating that they formed 9S trimers that were stable to sucrose density centrifugation in the presence of a non-ionic detergent. All of the alanine-substituted mutants behaved the same (data not shown).

Collectively, the results presented in Figs. 2-4 (see also Table I, rows 1-3) indicate that: (i) the introduction of certain mutations into the B loop region of HA2 affect the glycosylation pattern of HA, likely by affecting the packing of the globular head domains (Fig. 1); (ii) in some cases, notably V55P, the mutations appear to affect either the efficiency of transport of HA to the cell surface or its susceptibility to trypsin or cellular proteases; (iii) nonetheless, all of the mutant HAs are expressed at the cell surface and can be cleaved to HA1 and HA2; furthermore, both types of mutations, the potential facilitators, Ala, and the more disruptive of the potentially inhibiting mutations, Pro, form stable trimers.

Conformational Changes

We next assessed the ability of the mutant HAs to undergo low pH dependent conformational changes. These conformational changes in wt HA have historically been correlated with sensitivities to various antibodies and proteases. In the first set of experiments we tested the proteinase K sensitivity of each mutant and compared it with wt-HA which becomes sensitive to proteinase K when exposed to low pH during the first stage of the conformational change (Puri et al., 1990). Cells expressing wt or mutant HA0s were metabolically labeled with ^{35}S-Translabel, trypsinized to HA1 and HA2, and treated at the indicated pH values. The cell lysates were then treated with proteinase K, immunoprecipitated and an SDS-PAGE gel of the HA proteins was analyzed for the presence of ^{35}S-labeled HA1 and HA2 by PhosphorImager analysis. The amount of HA

Fig. 4 Sucrose gradient sedimentation analysis of wt and pro-substituted HAs

Cells transfected with plasmids encoding wt and pro-substituted HAs were treated with 5 µg/mL trypsin, lysed in an NP-40 lysis buffer (pH 7.5), and analyzed in 3-30% continuous sucrose gradients (pH 7.5). The gradients were fractionated and samples precipitated with concavanalin A agarose, resolved by 10% SDS-PAGE, and analyzed for HA protein as described in the methods section. Fraction 1 is the bottom of the gradient.

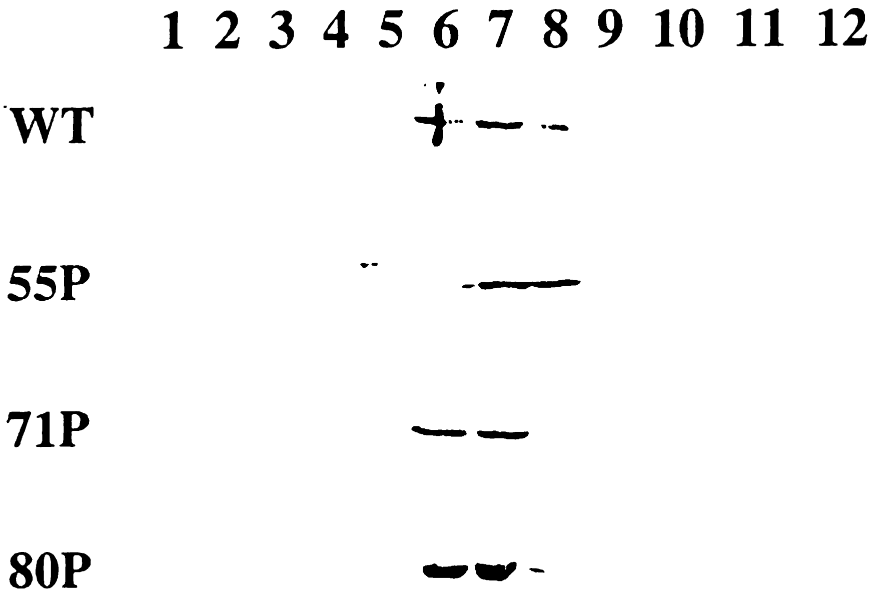
1 2 3 4 5 6 7 8 9 10 11 12
WT
55P
71P
80P

Fig. 4

in each sample was calculated as described in the Methods section and expressed as percent sensitivity to proteinase K. As seen in Fig. 5a, all of the alanine-substituted mutants showed a pH-dependence of proteinase K sensitivity essentially identical to that of wt HA with the exception that the pH dependence of L80A was approximately 0.7 units higher than wt. All of the gly and pro mutants were analyzed by western blot analysis (Fig. 5b). The substitutions at position 71 behaved identically to wt - HA. In contrast, the mutants with glycine or proline at positions 55 or 80 (V55G, L80G, V55P and L80P) were completely sensitive to proteinase K over the entire pH range examined. To our knowledge, V55G, V55P, L80G and L80P are the first mutant HAs that have been found to be sensitive to proteinase K at pH 7.

As a second test of the ability of the mutant HAs to change conformation at low pH we analyzed the ability of HA protein pre-treated at defined pHs to react with an antibody against the C-terminus of HA1 (C-HA1). This antibody efficiently detects low pH treated wt HA in crude cell lysates and HA acquires reactivity to this antibody with a time course and pH dependence very similar to an antibody against the fusion peptide. Cells expressing mutant HAs were metabolically labeled, trypsinized, incubated at different pH values. Cell lysates were immunoprecipitated with C-HA1 and the intensities of the HA1 and HA2 bands on SDS-PAGE gels were quantitated by PhosphorImager analysis.

As seen in Fig. 6a, and mirroring their behavior in the proteinase K assay (Fig. 5a), the alanine mutants acquired reactivity with the C-HA1 antibody with the same pH dependence as wt-HA (V55A, S71A) or with an approximately 0.7 unit shifted pH dependence (L80A). S71P also behaved like wt-HA (Fig. 6b). V55P showed approximately 50% reactivity with C-HA1 at pH 7 and an approximately 0.7 pH unit shifted and much a less well defined pH profile for antibody reactivity. L80P was fully reactive with the C-HA1 antibody over the entire pH range.

Fig. 5 Proteinase K sensitivity of wt and mutant HAs

(a) Cells transfected with plasmids encoding wt and ala-substituted HAs were metabolically labeled with ^{35}S TransLabel, treated with 5 μg/mL trypsin and then incubated at the indicated pH for 15 min at 37^{o}C, reneutralized, and lysed in an NP-40 cell lysis buffer. Cleaved cell lysates were then digested with proteinase K. The proteins were immunoprecipitated with site A mAb and resolved by SDS-PAGE and subjected to PhosphorImager analysis. (b) Cells were transfected with plasmids encoding wt, pro-, and gly-substituted HAs. Cleaved cells lysates were then digested with proteinase K, the proteins precipitated with concavanalin A agarose, reduced, subjected to 10% SDS-PAGE and detected with anti-HA antiserum.

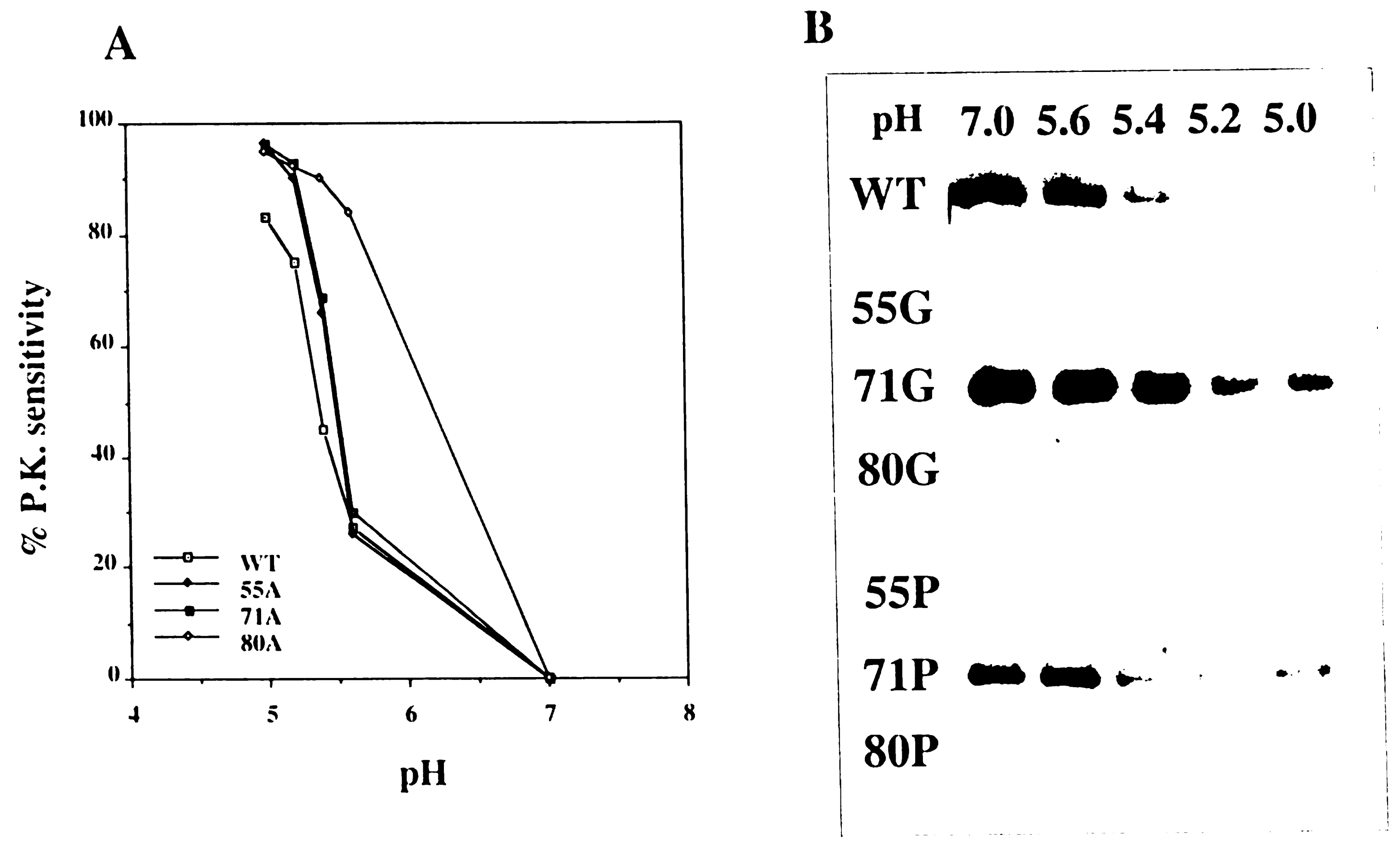
A
% P.K. sensitivity
100
80
60
40
20
0
4
5
6
7
8
pH
WT
55A
71A
80A
B
pH
7.0
5.6
5.4
5.2
5.0
WT
55G
71G
80G
55P
71P
80P

Fig. 5

Fig. 6 Reactivity of wt, ala-, and pro-substituted HAs with the C-HA1 antibody

Cells transfected with plasmids encoding ala- and pro-substituted HAs were metabolically labeled, treated with 5 μg/mL trypsin, incubated at different pH values for 15 min at 37°C, reneutralized and lysed in an NP-40 cell lysis buffer. Cleaved cell lysates were immunoprecipitated with the C-HA1 mAb and subjected to 12% SDS-PAGE gel and PhosphorImager analysis. (a) Reactivity of ala-substituted HAs. B. Reactivity of pro-substituted HAs. % HA ppt. represents total HA precipitated by C-HA1 mAb when total HA precipitated at pH 5 is considered as 100%. The C-HA1 antibody was used instead of an anti-fusion peptide antibody because HA acquires reactivity to the two antibodies under very similar pH, time, and temperature conditions (White and Wilson, 1987) and C-HA1 antibody, but not the fusion peptide antibody, efficiently precipitates low pH-treated HA from total cell lysates (Qiao and White, unpublished results).

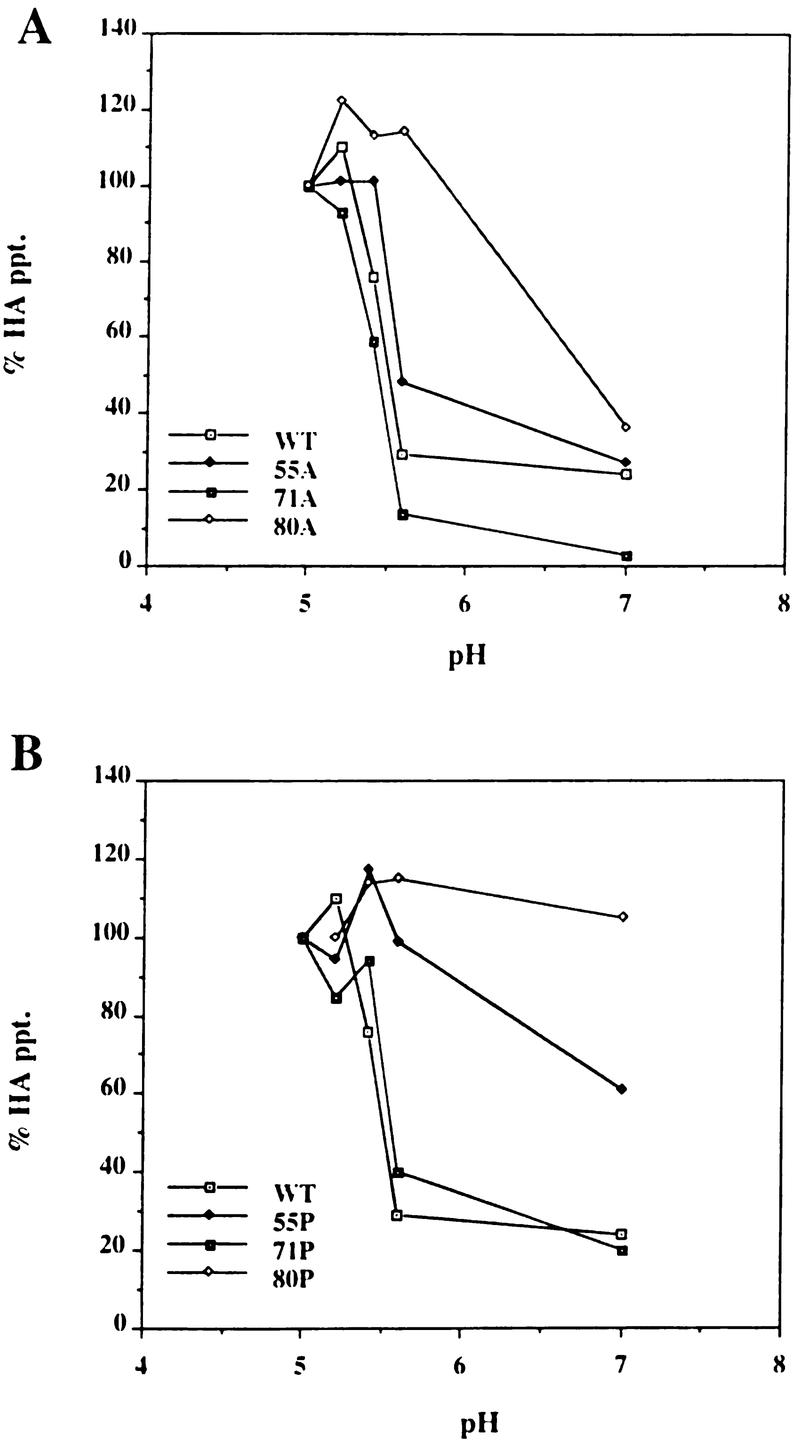
A
% HA ppt.
140
120
100
80
60
40
20
0
4
5
6
7
8
pH
WT
55A
71A
80A
B
% HA ppt.
140
120
100
80
60
40
20
0
4
5
6
7
8
pH
WT
55P
71P
80P

Fig. 6

Collectively, the results presented in figs. 5 and 6 suggest that all of the alanine mutants, as well as all of the mutants with substitutions at position 71, changed conformation at low pH with either an identical or in one case (L80A) an +0.7 unit shifted pH dependence compared to wt-HA. The remaining mutants (55 and 80, gly and pro) were in a conformation recognized by these assays in significant amounts at neutral pH.

Fusion Activity

Having confirmed that the mutant HA0s could be expressed at the cell surface as stable trimers that could be cleaved to HA1-S-S-HA2, and having demonstrated either using proteinase K sensitivity and/or C-HA1 antibody reactivity that the mutant HAs change conformation at low pH, we next tested the ability of cells expressing wt or mutant HAs to fuse with red blood cells (RBCs). We assayed two different aspects of the fusion reaction: hemifusion, mixing of outer leaflet lipids, and full fusion, the transfer of small aqueous contents. We tested the ability of the mutants to induce hemifusion using RBCs labeled with the fluorescent lipid probe octodecylrhodamine (R18). HA0 expressing cells were treated with neuraminidase to optimize RBC binding and then with trypsin to cleave HA0 to HA1 and HA2; cells treated with chymotrypsin or STI served as negative controls. R18-labeled RBCs were allowed to bind and the RBC-cell complexes were then incubated at pH 5 for 2 min. at 37°C and then reneutralized and observed with a fluorescence microscope (Fig. 7).

Like those expressing wt-HA, all of the cells expressing mutant HAs were able to support RBC binding, but none induced transfer of R18 either at neutral or low pH if they hadn't been pre-treated with trypsin and none of the trypsin treated cells induced R18-transfer at

Fig. 7 Fusion activity of pro-substituted HAs: Lipid mixing

Cells transfected with plasmids encoding wt and pro-substituted HAs were treated with neuraminidase (0.2 mg/mL) and either 5 µg/mL trypsin or chymotrypsin (HA0 control, not shown) for 6 min at RT. R18-labeled RBCs (0.05%) were bound to the cells for 25 min. at RT. After unbound RBCs were removed, the cells were incubated in fusion buffer (pH 5) for 2 min at 37°C, reneutralized, and observed with fluorescence microscopy.

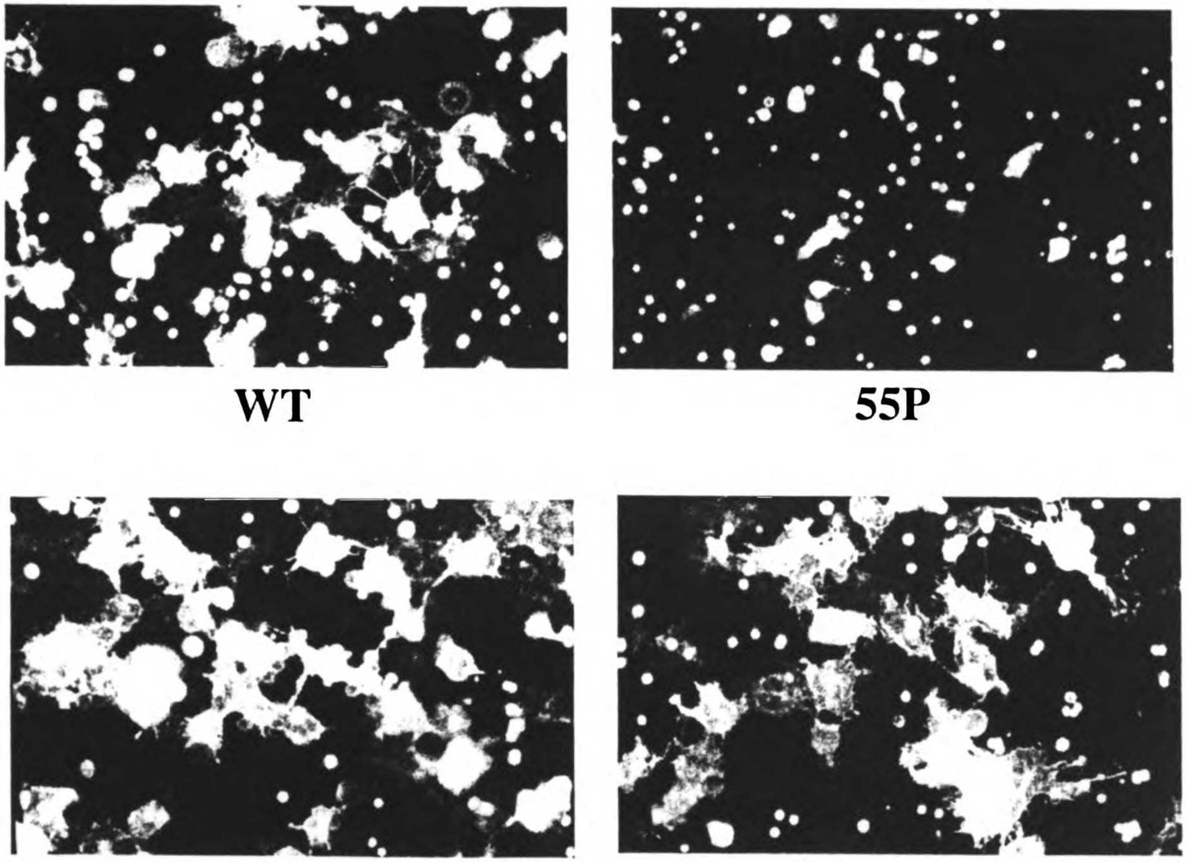

WT

55P

71P

80P

Fig. 7

UCSF LIBRARY

Fig. 8 Fusion activity of pro-substituted HAs: Content mixing

Cells transfected with plasmids encoding wt and pro-substituted HAs were prepared for fusion, incubated with calcein AM-labeled RBCs, and inspected by fluorescence microscopy as described in the legend to Fig. 7 and in the Materials and Methods section.

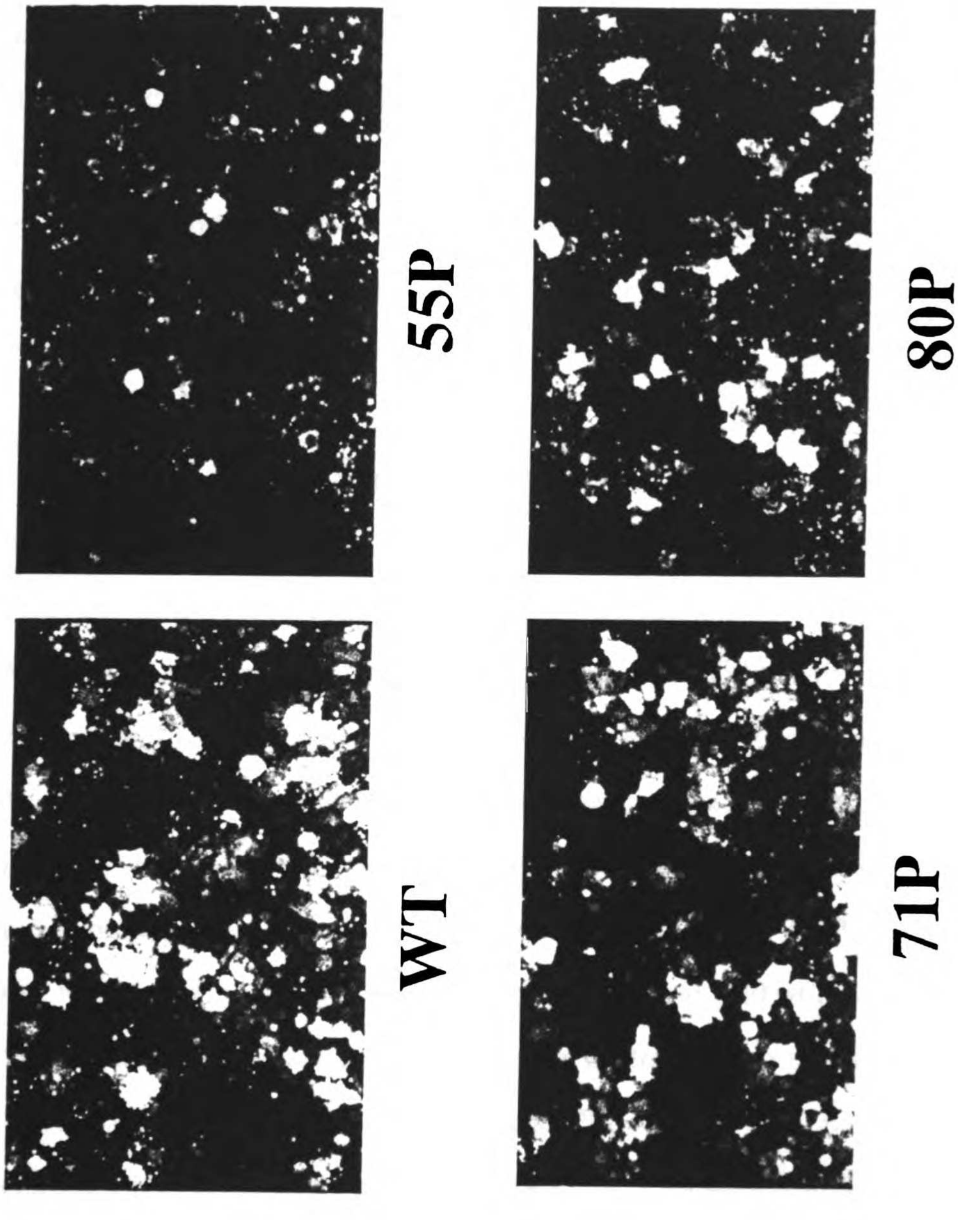
55P
WT
80P
71P

Fig. 8

neutral pH (data not shown). Cells expressing wt and mutant HAs when trypsinized and pre-treated at pH 5 induced transfer of R18 from labeled-RBCs. For all of the mutants except V55P, the extent of R18 transfer appeared equal to or greater than that seen with wt-HA (Fig. 7). Therefore, of the 9 mutants analyzed, only V55P HA appeared to be impaired in its ability to mediate the transfer of outer leaflet lipids. Our preliminary observations of V55P also indicated that although its ability to mediate hemifusion was significantly impaired, it was not totally abolished.

To explore further the ability of V55P to mediate outer leaflet lipid transfer we next conducted a quantitative analysis of its level of cell surface expression and its ability to mediate transfer of R18 relative to wt-HA.

To test if the impaired fusion capability of V55P-HA was a quantitative effect due to its significantly diminished formation of the activatable HA1-S-S-HA2 species from HA0 in the presence of trypsin (Fig. 3), cells expressing different amounts of V55P-HA and wt-HA DNA were assayed in parallel for surface expression, cleavability with trypsin and fusion activity. Cells for quantitation were metabolically labeled, prepared as described previously and the intensities of the HA bands were quantitated and analyzed with a PhosphorImager. Fusion activity was assayed after incubation at low pH for both 2 min. and 10 min. Comparison of fusion activity reveals that although 1X V55P, when trypsinized, forms an amount of HA1 between that of 1/10 and 1/20 wt HA (Figs. 9A and 9B), its fusion after both 2 minute and 10 minute low pH treatment is much less extensive than with these wt expression levels (Figs. 10A and 10B, respectively). A similar result occurs with 5X V55P; the quantity of HA1 for 5X V55P is between that of 1/10 and 1X wt-HA and yet its fusion is even less than that of 1/20 wt-HA. When normalized for expression, V55P fusion activity is approximately 20% that of wt at 2 min. and

Fig. 9 Cell surface expression of wt and V55P HA

Cells transfected with the indicated amounts of plasmid encoding with wt or V55P HA (1x=1.25 μg) were metabolically labeled, treated with either 5 μg/mL chymotrypsin (C) or trypsin (T), lysed with an NP-40 lysis buffer, and immunoprecipitated with the site A mAb. Samples were then resolved by 12.5% SDS-PAGE and analyzed with a PhosphorImager. (a) Gel scan. (b) Quantitation of the band intensities.

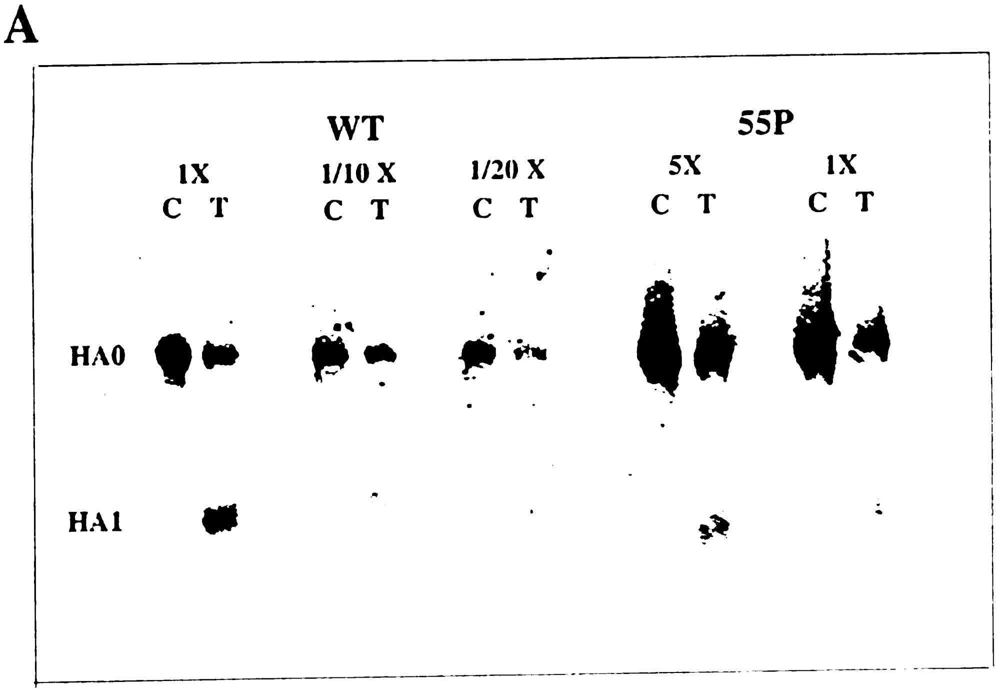
A
WT
55P
1X
1/10 X
1/20 X
5X
1X
C T
C T
C T
C T
C T
HA0
HA1

Fig. 9

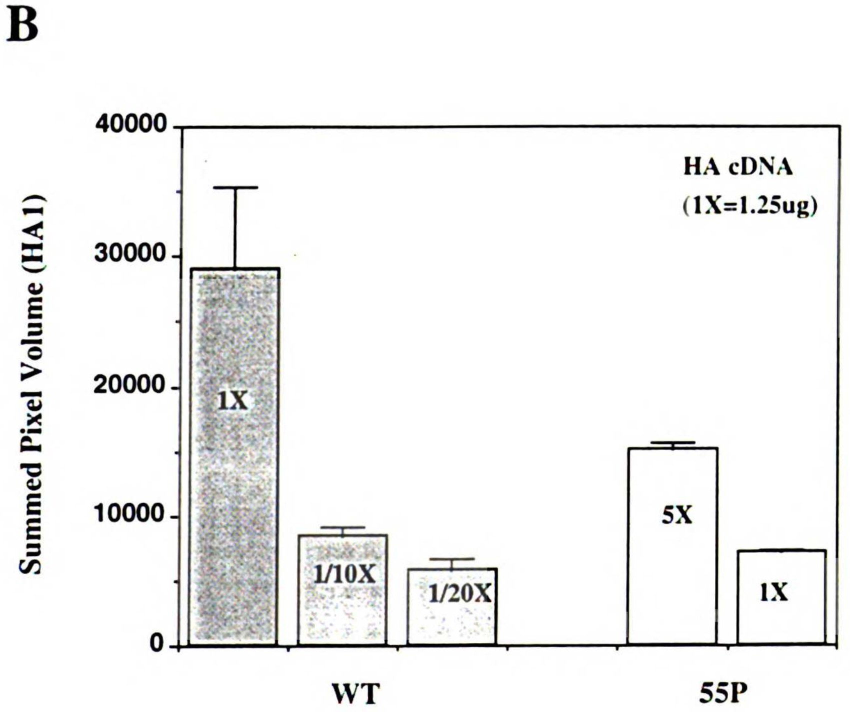
B
HA cDNA
(1X=1.25ug)
Summed Pixel Volume (HA1)
40000
30000
20000
10000
0
1X
1/10X
1/20X
5X
1X
WT
55P

Fig. 9

Fig. 10 Normalized fusion activity of wt and V55P HA

Parallel cultures of the cells analyzed in Fig. 9, expressing different amounts of wt and V55P HA at their surface, were subjected to the fusion assay described in Fig. 7. The number of fused cells per field were counted. The graph represents the average value from 5 different fields. (a) Cells treated with pH 5 fusion buffer for 2 min. at 37°C. (b) Cells treated with pH 5 fusion buffer for 10 min. at 37°C.

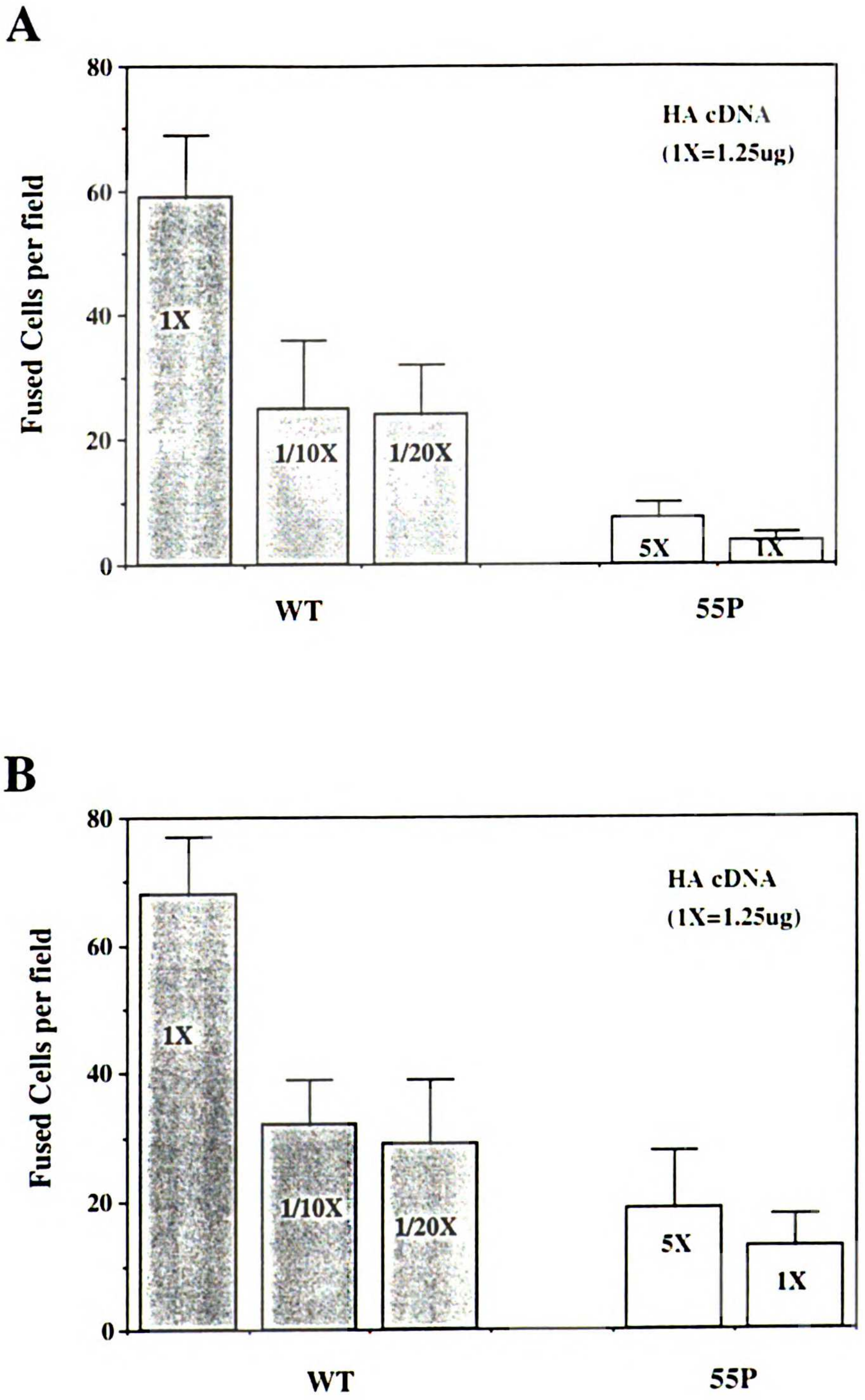
A
80
60
40
20
0
Fused Cells per field
HA cDNA
(1X=1.25ug)
1X
1/10X
1/20X
5X
1X
WT
55P
B
80
60
40
20
0
Fused Cells per field
HA cDNA
(1X=1.25ug)
1X
1/10X
1/20X
5X
1X
WT
55P

Fig. 10

Fig. 11 Fusion activity of wt and V55P/S71P HA

(a) Cells transfected with the indicated amounts of plasmids encoding wt and V55P/S71P were analyzed for fusion as described in the legend to Fig. 7 with the exception that the concentration of trypsin (T) or chymotrypsin (C) was 10 μg/mL. (b) Parallel cultures of the cells analyzed in (a) were treated with 10 μg/mL trypsin for 6 min. at RT, lysed and precipitated with concavanalin A agarose. Gel samples were prepared in sample buffer containing 100 mM DTT and separated by 8% SDS-PAGE. The gel was then analyzed by western blotting with the C-HA1 mAb.

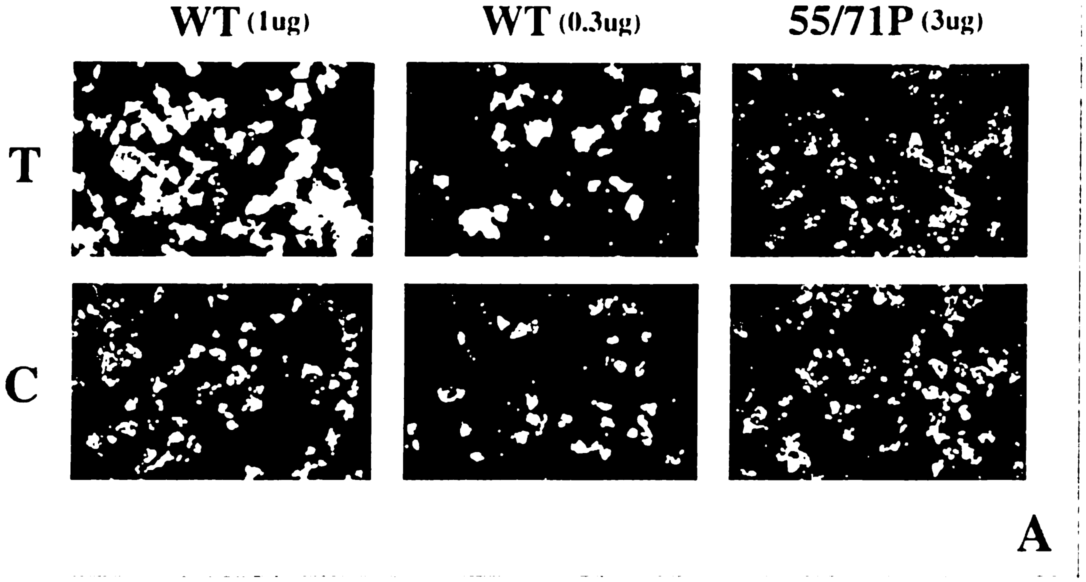
WT (1ug)
WT (0.3ug)
55/71P (3ug)
T
C
A

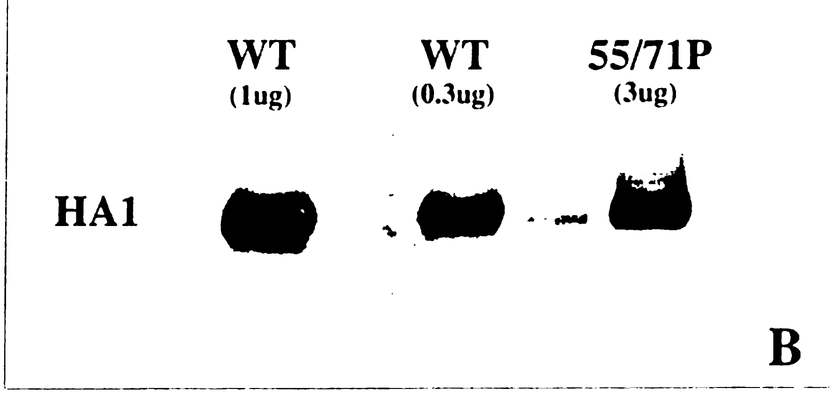
WT
(1ug)
WT
(0.3ug)
55/71P
(3ug)
HA1
B

approximately 50% wt at 10 minutes. Thus, V55P HA is, in fact, qualitatively impaired in fusion. We also tested the transfer of content from RBCs loaded with a small (MW 994.87) fluorescent content probe, calcein AM, into mutant HA expressing cells. The fusion protocol was identical to that described for the outer leaflet mixing assay. The results for content mixing (Fig. 8) paralleled those of lipid mixing, such that only V55P was impaired. This indicates that the remaining mutants facilitate transfer of a small MW molecule into low pH treated mutant HA expressing cells as well as wt-HA. Again, although V55P was impaired in its ability to form a pore capable of transferring a small fluorescent probe, pore formation was not completely eliminated.

Discussion

The results presented above represent a work in progress. The finding that a proline mutation (V55P) affects the kinetics of fusion supports the hypothesis that coiled-coil formation is a critical part of the low pH conformational change in HA that leads to fusion. However, glycine and some proline mutations do not affect the kinetics of fusion; this result was quite unexpected. Preliminary fluorimetry experiments (S. Pelletier, personal communication) have confirmed the decreased rate and extent of fusion by V55P compared to wt HA when normalized for expression level.

Analysis of the double-mutant V55P, S71P is underway. Preliminary experiments (Qiao, H. and Pelletier, S., Fig. 11) suggest that the HA with these mutations is expressed on the cell surface and can be cleaved efficiently to HA1 and HA2 but cannot trigger fusion. Analysis of the conformational changes permitted in this mutant could shed new light on which changes lead to the various steps of fusion.

References

Baker, D, Agard, DA. (1994) *Structure 2*, 907-910.

Bullough, P. A., Hughson, F. M., Skehel, J. J., & Wiley, D. C. (1994) *Nature 371*, 37-43.

Carr, C. M., & Kim, P. S. (1993) *Cell 73*, 823-832.

Chen, J., Wharton, S. A., Weissenhorn, W., Calder, L. J., Hughson, F. M., Skehel, J. J., & Wiley, D. C. (1995) *Proc. Nat'l. Acad. Sci. USA 92*, 12205-12209.

Daniels, R. S., Downie, J. C., Hay, A. J., Knossow, M., Skehel, J. J., Wang, M. L., & Wiley, D. C. (1985) *Cell 40*, 431-439.

Hernandez, L. D., Hoffman, L. R., Wolfsberg, T. G., & White, J. M. (1996) *Ann. Rev. Cell Devel. Biol. 12*, in press.

Kemble, G. W., Bodian, D. L., Rosé, J., Wilson, I. A., & White, J. M. (1992) *J. Virol. 66*, 4940-4950.

Kemble, G. W., Danieli, T., & White, J. M. (1994) *Cell 76*, 383-391.

Kemble, G. W., Henis, Y., & White, J. M. (1993) *J. Cell Biol. 122*, 1253-1265.

Kunkel, T. A., Roberts, J. D., & Zakour, R. A. (1987) in *Methods in enzymology* (Wu, R., Ed.) pp 367-382, Academic Press, Inc.

Lupas, A., Van Dyke, M., & Stock, J. (1991) *Science 252*, 1162-1164.

O'Neil, K.T., DeGrado, WF. (1990) *Science 250*, 646-651.

Puri, A., Booy, F. P., Doms, R. W., White, J. M., & Blumenthal, R. (1990) *J. Virol. 64*, 3824-3832.

Ramachandran, G.N., Sasisekharan, V. (1968) *Advances in Protein Chemistry 23*, 283-438.

Rothman, J. E. (1996) *Prot. Sci. 5*, 185-194.

Ward, C. W., & Dopheide, T. A. (1980) *Aust. J. Biol. Sci. 33*, 449-455.

Watowich, S. J., Skehel, J. J., & Wiley, D. C. (1994) *Structure 2*, 719-731.

Weis, W. I., Cusack, S. C., Brown, J. H., Daniels, R. W., Skehel, J. J., & Wiley, D. C. (1990) *EMBO J. 9*, 17-24.

White, J.M.,Hoffman, LR; Arevalo, JH; Wilson, IA. (1996) in *Structural Biology of Viruses*, (W. Chu, R. Burnatt, R. Garcea, Eds.) Oxford University Press. In press.

White, J. M. (1995) *CSHSQB 60*, 581-588.

White, J. M., & Wilson, I. A. (1987) *J. Cell Biol. 105*, 2887-2896.

Wiley, D. C., & Skehel, J. J. (1987) *Annu. Rev. Biochem. 56*, 365-394.

Chapter 5:

Recent developments in elucidating the mechanism of action of HA inhibitors: Further general conclusions regarding HA structure and function

Introduction

The results described in the last three chapters indicate that the influenza hemagglutinin operates as a tightly-controlled, spring-activated system. According to current models (Hernandez et al., 1996), in its neutral-pH conformation, HA serves to bind the virus to the host cell and to hide the fusion machinery. A large number of intermonomer and intramonomer interactions serve to maintain this inactive conformation. Upon exposure to a critical pH, however, the protein is converted to at least one new conformation in which the fusion machinery (especially the fusion peptide) is exposed, and only a limited window of time exists for this new conformation to interact with target membrane before the protein becomes inactivated by chaotic aggregation or insertion of the fusion peptide into the viral membrane ((Weber et al., 1994), (Wharton et al., 1995), (Gutman et al., 1993), (Stegmann et al., 1987)). TBHQ clearly inhibits the conversion to the active conformation, but it is not clear whether the inhibited state is the neutral-pH form of HA or some intermediate along the pathway of the conformational change. C22, on the other hand, could either speed up conversion to the active conformation (and therefore speed up inactivation), or it could force HA to convert to a completely different inactive conformation. Since it has been suggested that HA represents a two-state system in which a single metastable state under kinetic control converts to a final, stable (fusion-active) state (Baker, 1994), it is of interest to explore the conformation(s) of TBHQ- and C22-treated BHA. In addition, since S22 and TBHQ act via similar mechanisms (i.e., stabilization of an inactive form of HA), it is possible that the two molecules act synergistically to inhibit infectivity. Conversely, TBHQ and C22 should inhibit each other's activity. In this chapter I present preliminary data that bear on these questions.

Results

Proteolytic studies

Assays in previous chapters have focused on the sensitivity of low pH-treated BHA to thermolysin. Two other proteases, proteinase K and trypsin, have been used previously to detect conformational changes in BHA ((Skehel et al., 1982), (Doms et al., 1985)). Figure 1 shows the sensitivity of BHA treated with 100 μM TBHQ or C22 to proteinase K.

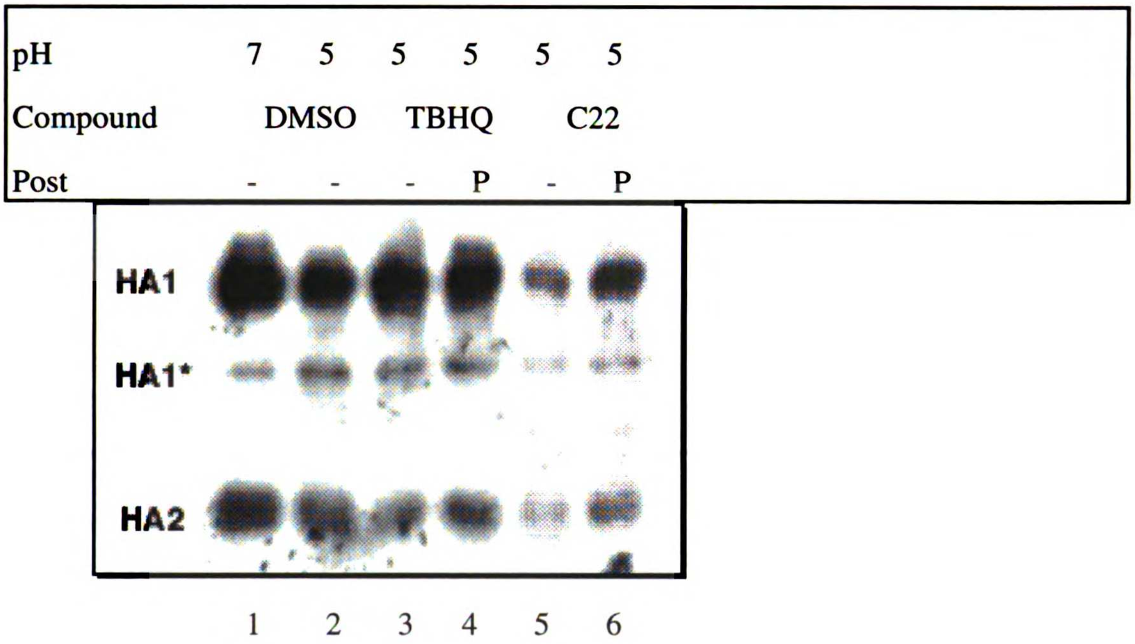

Fig. 1 Effect of 100 μM TBHQ and C22 on acquisition of proteinase K sensitivity of BHA at low pH. BHA was incubated with TBHQ (lane 3), C22 (lane 5) or DMSO (lanes 1 and 2), exposed to low pH (lanes 2-6), and reneutralized as in the thermolysin assay. Compounds were then added to post controls (lanes 4 and 6). The samples were then treated with proteinase K and examined by SDS-PAGE as described in the Materials and Methods section. Top bands, HA1; middle bands, cleavage product of HA1 (HA1*); bottom bands, HA2.

As shown in lanes 3 and 4, TBHQ does not significantly affect the extent of proteinase K digestion upon exposure to low pH under the conditions used. (Other concentrations of proteinase K were also tried in this assay; HA was either digested too much or too little in these other experiments. A lower ratio of protease/BHA was used in this assay than in (Kemble et al., 1992).). C22, on the other hand, increases the conversion of BHA to a proteinase-K sensitive form, as shown in lanes 5; in fact, both HA1 and HA2 became more sensitive to proteolysis in the presence of this inhibitor.

Figure 2 shows the results of a similar assay using trypsin.

pH	7	5	5	5	5	5
Compound	DMSO		TBHQ		C22	
Post	-	-	-	P	-	P

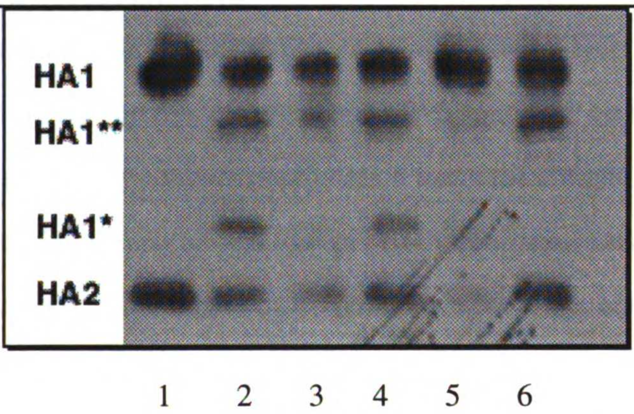

Fig. 2 Effect of 100 μM TBHQ and C22 on acquisition of trypsin sensitivity by BHA at low pH. Experiment was conducted and results are displayed as in Fig. 1, except that trypsin was used instead of proteinase K as described in Materials and Methods. Top bands, HA1; middle 2 bands, trypsin cleavage products of HA1 (HA1* and HA1**); bottom bands, HA2.

In this experiment, TBHQ clearly inhibits one cleavage (lane 3): the one generating the lighter cleavage product. Earlier work (Skehel et al., 1982) has shown that the heavier product is HA1 28-328 (HA1**), and two lighter products are HA1 28-224 (HA1*) and HA1 225-328 (this last product was not visible on our gels, possibly because it does not contain biotin label). Thus, cleavage at HA1 27 is apparently not inhibited by TBHQ, while that at HA1 225 is. Somewhat surprisingly, C22 appears to inhibit cleavage of HA1 altogether, while digestion of HA2 was observed with both inhibitors (this HA2 digestion by trypsin has not been observed in significant amounts before (Skehel et al., 1982)).

Immunoprecipitations

Several conformation-specific antibodies were used to study the conformation of BHA in its various, inhibited forms. TBHQ was shown previously (Bodian et al., 1993) to inhibit fusion peptide exposure using an antibody to this region. As illustrated in the following figures, the effects of TBHQ and C22 on head separation were further examined by immunoprecipitation using the antibodies N2 and interface which are specific for neutral and low-pH BHA conformations, respectively. As a control, site A antibody, which exhibits no preference for either conformation of HA, was used in parallel immunoprecipitations. Experiments were conducted as described (Kemble et al., 1992) except that pure, biotinylated BHA was used in the concentrations used in the thermolysin assay.

Fig. 3 shows the effects of TBHQ on site A and N2 binding after low pH treatment of BHA.

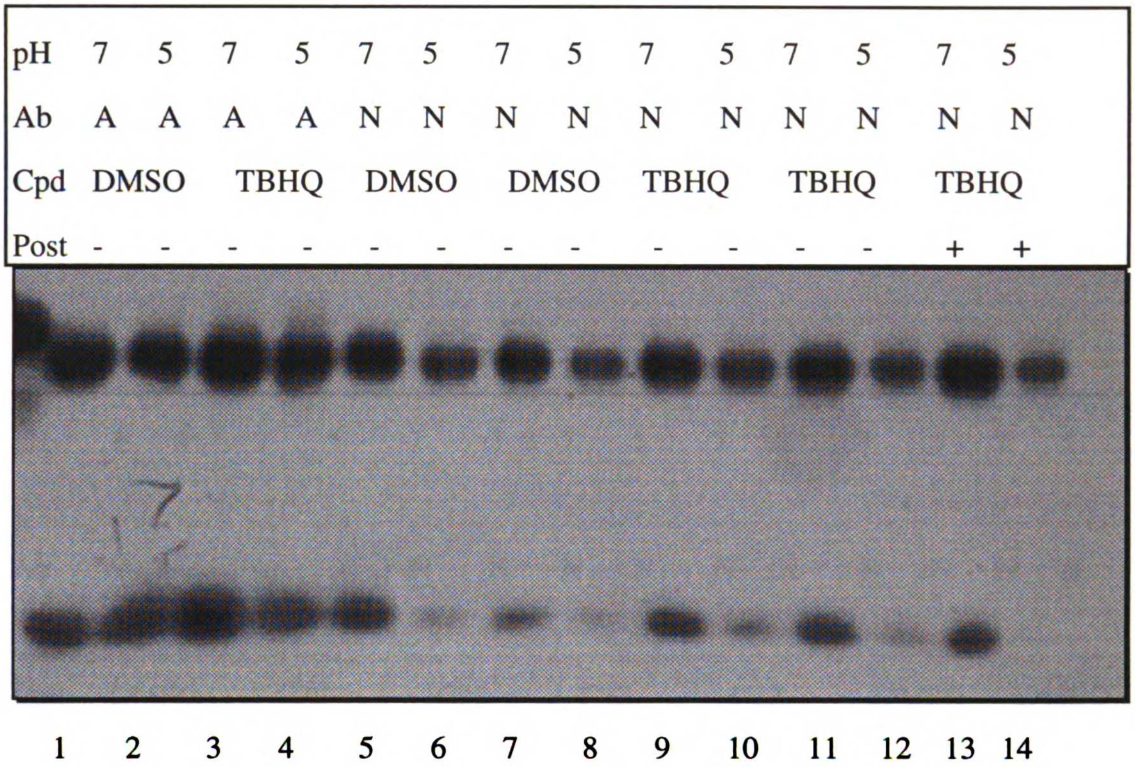
pH 7 5 7 5 7 5 7 5 7 5 7 5 7 5
Ab A A A A N N N N N N N N N N
Cpd DMSO TBHQ DMSO DMSO TBHQ TBHQ TBHQ
Post - - - - - - - - - - - - + +
1 2 3 4 5 6 7 8 9 10 11 12 13 14

Fig. 3 Effect of 100 μM TBHQ on binding by Site A and N2 antibodies. Biotinylated BHA samples were treated in a manner identical to that for proteolytic assays, except that 0.1% NP-40 was added to the buffer to inhibit HA aggregation, and 11 μL of γ-bind beads prebound with either site A (lanes 1-4) or N2 antibody (lanes 5-14) and washed, 3x with PBS, were added instead of protease. Samples were incubated at 4°C overnight with shaking and then washed 1x with MSSH-0.1% NP40 and 2x with 0.5 M NaCl, 10 mM Tris-HCl, pH 8. Beads were then resuspended in 40 μL 2X sample buffer and subjected to SDS-PAGE and analysis for biotinylated protein as described for the thermolysin assay.

Fig. 3 shows that, while neither low pH nor TBHQ inhibit site A binding, the extent of N2 binding to BHA after low pH treatment is increased if TBHQ is present, suggesting that the globular heads do not significantly separate (Kemble et al., 1992). This result is not as impressive as inhibition of thermolysin digestion, however.

As seen in Fig. 4, the effect of C22 on binding of BHA by these same two antibodies was investigated.

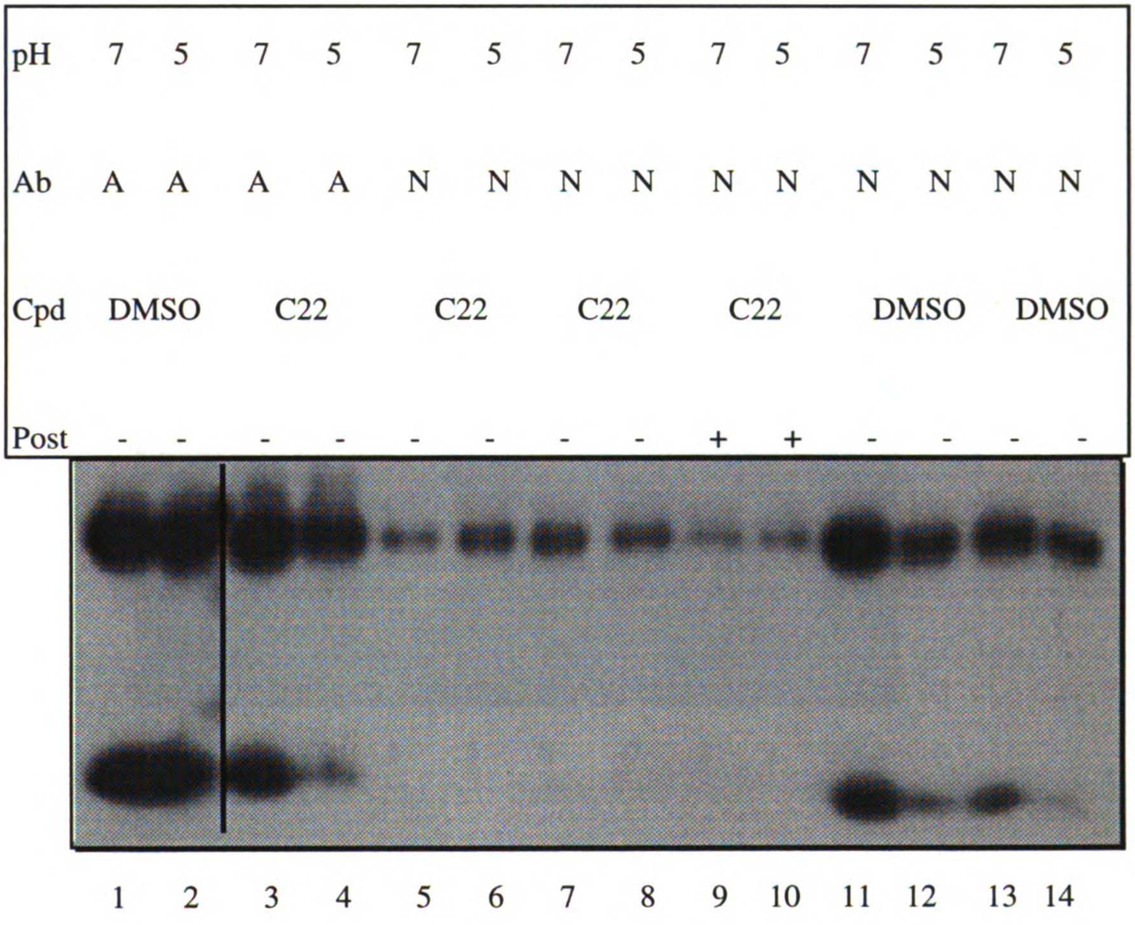
pH 7 5 7 5 7 5 7 5 7 5 7 5 7 5
Ab A A A A N N N N N N N N N N
Cpd DMSO C22 C22 C22 C22 DMSO DMSO
Post - - - - - - - - + + - - - -
1 2 3 4 5 6 7 8 9 10 11 12 13 14

Fig. 4 Effect of C22 on binding to BHA of Site A and N2 antibodies. Experiment was performed as in Fig. 3 except that 100 μM C22 was used instead of TBHQ.

As shown in Figure 4, C22 at low pH renders BHA less susceptible to binding by Site A antibody. In contrast to the Site A result, binding of N2 antibody at both neutral and low pH appears to be inhibited by the presence of C22, possibly because binding of C22 to the antibody itself or because C22 changes the conformation of the N2 epitope.

The experiment shown in Figure 5 investigated the effect of TBHQ on binding of interface antibody (12CA5), which binds specifically to the low-pH form of BHA (White & Wilson, 1987).

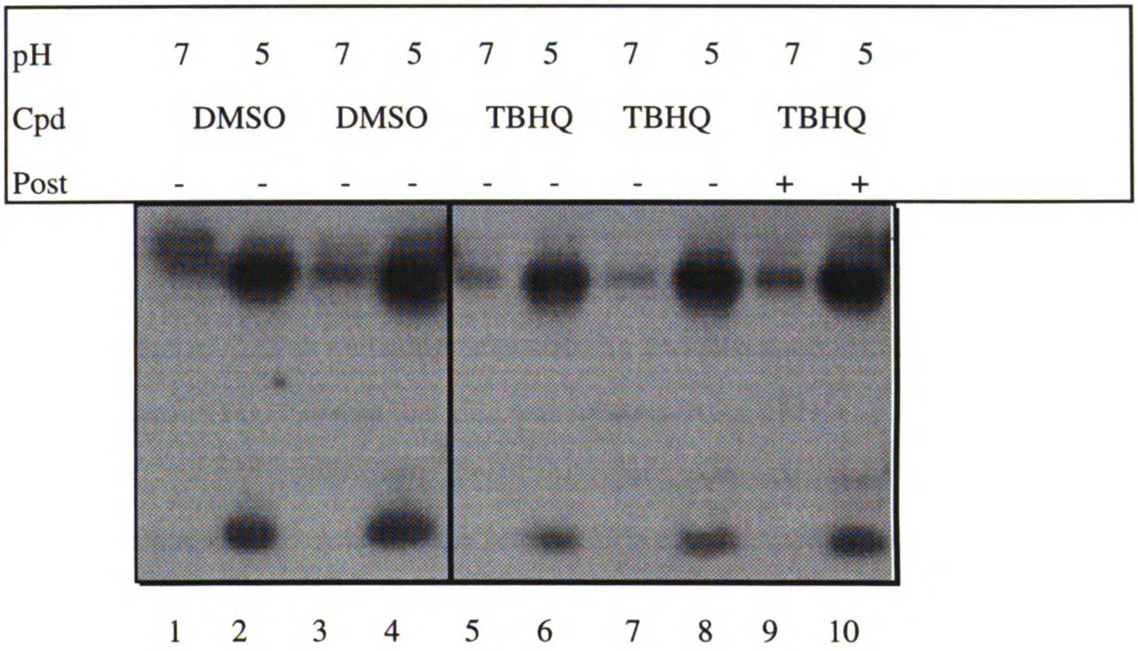

Fig. 5 Effect of TBHQ on interface antibody binding to BHA. Experiment was performed as in Fig. 3 except that interface antibody was used instead of N2 or Site A.

Pretreatment of BHA with TBHQ apparently decreases the extent of interface antibody binding upon exposure to low pH, as shown in lanes 6 and 8 vs. 2, 4 and 10; this effect is subtle but the result has been repeated several times and confirmed by densitometry (65% difference between HA2 bands of pH 7 and 5 without TBHQ vs. 23% difference with 100 μM TBHQ, data not shown). The effect of C22 on binding by this antibody is shown in Fig. 6.

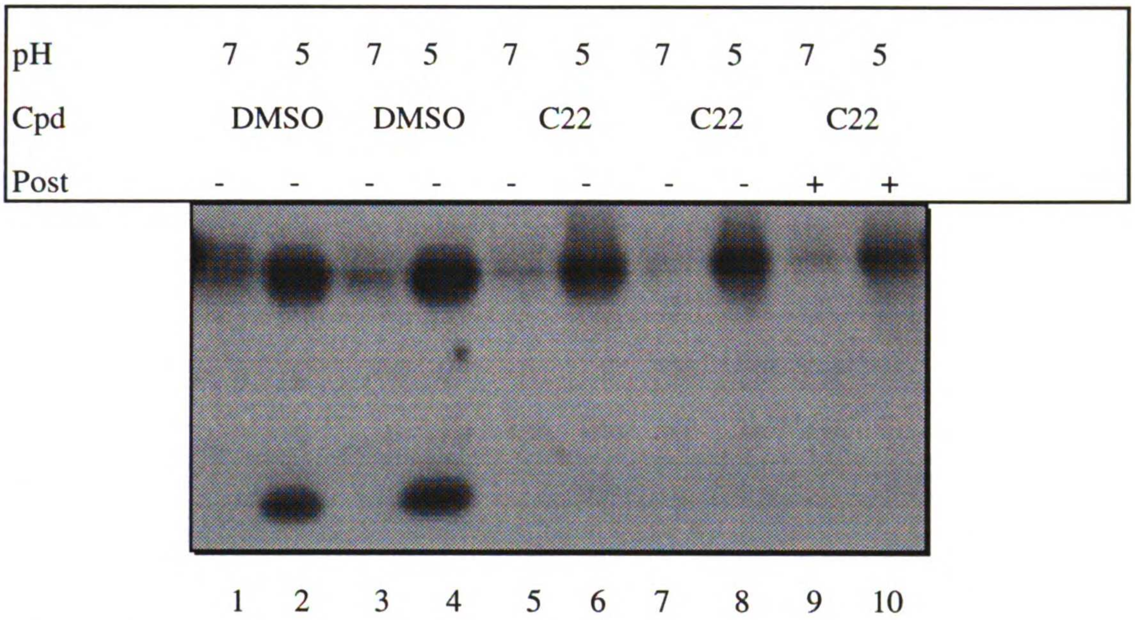

Fig. 6 Effect of C22 on immunoprecipitation by interface antibody. Experiment was conducted as in Fig. 5 except that C22 was substituted for TBHQ.

This experiment is inconclusive; the low-pH form of BHA recognized by interface antibody runs as a smear on the gel in the presence of C22, and HA2 appears not to be present. C22 may be reducing or crosslinking portions of the protein to itself and/or the antibody; the effect does not require C22 to be present during the low-pH treatment, however. More likely are the possibilities that C22 causes SDS gels to run differently than in its absence or that HA2 is being digested by a contaminating protease such as bromelain.

S22 and TBHQ were mixed together in ratios of 1:0, 1:10, 1:2, and 1:1; 100 μM of S22 was added to each of 5 samples and the concentration of TBHQ was increased from 0 to 10 µM, 50 µM, and then 100 µM, and the same was done with the compounds reversed. These mixes were analyzed for inhibition of the BHA conformational change by thermolysin assay and for inhibition of virus infectivity and cell toxicity by the EIA and MTT assays, respectively. The mixture of the two compounds produced solutions with a yellow color, while each compound alone produced uncolored solutions; the two molecules react, therefore, but the analysis was continued. The results are shown in Fig. 7:

pH	7	5	7	5	7	5	5	5	5	5	5
[TBHQ], µM	0	0	100	100	0	0	100	100	100	50	10
[S22], µM	0	0	0	0	100	100	10	50	100	100	100

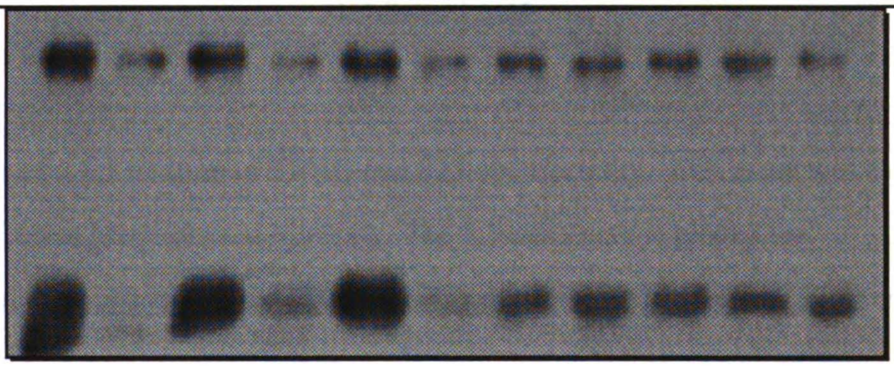

Fig. 7 Effect of mixtures of S22 and TBHQ on the conformational change of BHA. TBHQ and S22 were mixed together and incubated with BHA as described in the text, then analyzed for inhibition of the BHA conformational change by thermolysin assay as described in Materials and Methods.

Figure 8 shows the effects on infectivity of TBHQ, S22, and a 1:1 mixture of the two on infectivity as assayed by EIA. None of these concentrations of compounds were toxic to

MDCK cells as assessed by MTT assay.

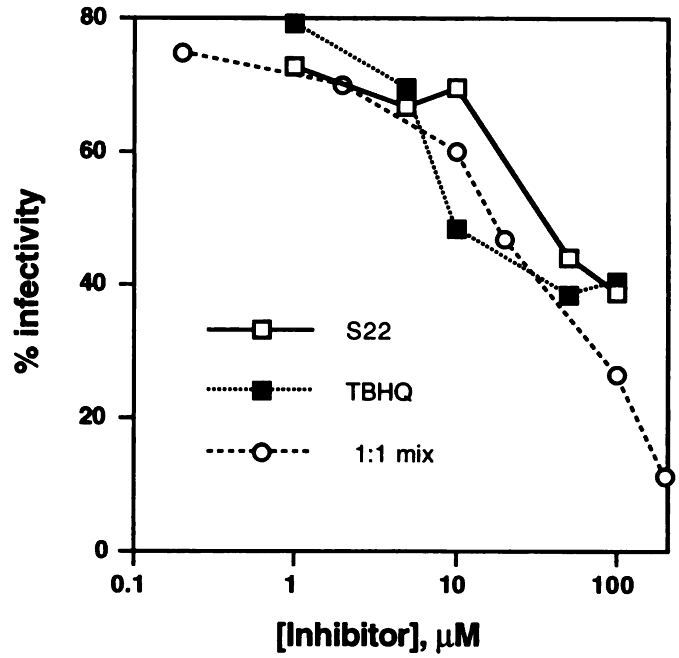

Fig. 8 Effect of a 1:1 mixture of TBHQ and S22 on infectivity. EIA assay was carried out as described in Materials and Methods. The 1:1 mix curve is plotted for concentration of total inhibitor; i.e., 20 µM mix contained 10 µM each of TBHQ and S22.

At high inhibitor concentrations, the mix of two inhibitors appears to synergize in inhibiting infectivity; at lower concentrations, the effect is not detectably present. The observable reaction between the two molecules is a confounding variable in this experiment. Similar results were obtained with a mix of S22 and TBP: The mixture of the two did not generate a color, however, the mixture was less toxic to cells than TBP alone (at the same concentration of TBP in each case), perhaps indicating that a reaction between the two compounds occurred. In addition, the mixture did not have significantly higher potency than TBP alone (not shown).

In Figures 9 and 10 the results of analyses similar to that shown in Figures 7 and 8 except with TBHQ and C22 are presented.

pH	7	5	7	5	7	5	5	5	5	5	5
[TBHQ], µM	0	0	100	100	0	0	100	100	100	50	10
[C22], µM	0	0	0	0	100	100	10	50	100	100	100

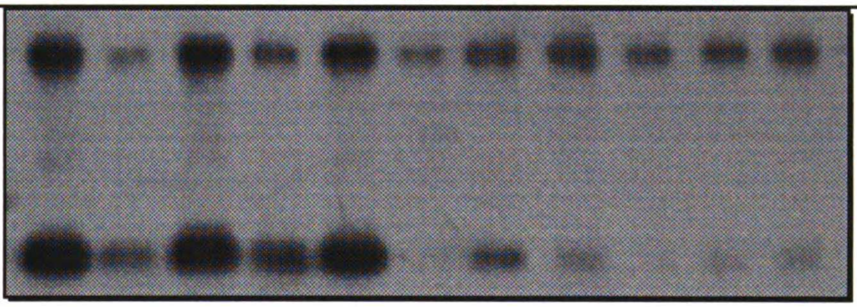

Fig. 9 Effect of mixtures of TBHQ and C22 on the BHA conformational change. Experiment was conducted as in Fig. 7, except that C22 was used instead of S22.

C22 at 10 µM appears to abrogate the effect of 100 µM TBHQ.

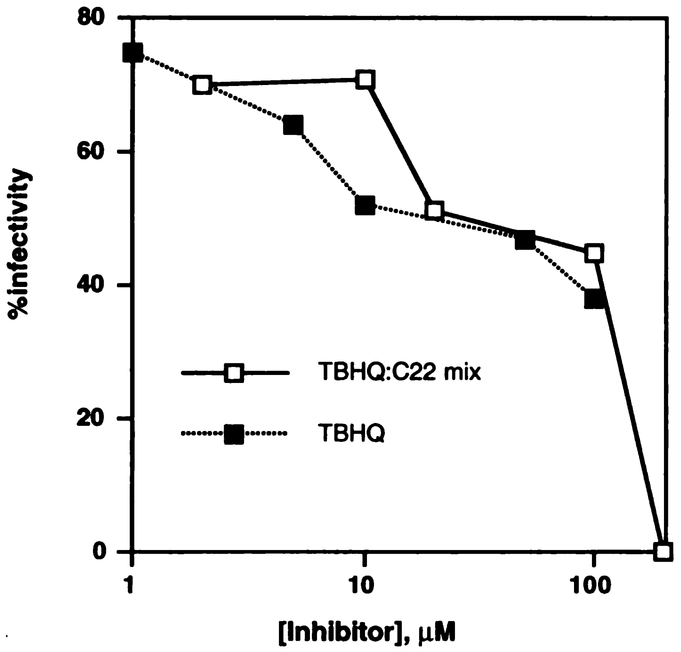

Fig. 10 Effect of a 1:1 mix of TBHQ and C22 vs. TBHQ alone in the EIA assay. Experiment was performed as in Fig. 7 except a mixture of TBHQ and C22 was used instead of TBHQ and S22. None of the treatments was detectably toxic to cells by the MTT assay.

As shown in Fig. 10, it appears that C22 and TBHQ, at concentrations below 200 μM, are not as potent together as is TBHQ alone, suggesting that the effect of one diminishes the other; the results are not striking, however. C22 was not used alone in this assay, but it has been shown in previous chapters to have an IC_{50} of 6 μM by infectivity.

Discussion

These results, taken together with thermolysin assay results and others presented in earlier chapters, are suggestive but not conclusive. The effect of each compound in each assay must be considered separately. TBHQ will be considered first.

TBHQ appears to inhibit almost all movement of BHA when bound at low pH. Fusion peptide exposure is inhibited, as demonstrated by thermolysin digestion and fusion peptide antibody binding (Bodian et al., 1993). In addition, inhibition of trypsin cleavage at HA1 225 and of binding by N2 and interface antibody are inhibited by the presence of the compound during low pH treatment of BHA, suggesting that even small movements in the globular HA1 heads are inhibited by the presence of the compound. However, the ability of trypsin to cleave at HA1 27 in the inhibitor's presence suggests that the short loop of HA1 containing this residue (this epitope was referred to in earlier reports as "loop", (White & Wilson, 1987) moves; earlier work (White & Wilson, 1987) has shown this epitope to move very early upon treatment at low pH, and a C22-resistant virus contains a mutation at this amino acid, further suggesting a functional importance of the region. Quite possibly, the region serves as a "safety latch;" its movement occurs early and is necessary for the conformational change of BHA, yet the movement does not itself lead to the rest of the conformational change.

The observation that TBHQ's effects on both thermolysin sensitivity and infectivity are not significantly modulated by S22 may signify that the two molecules act at the same site; alternatively, the binding of one may (perhaps allosterically) otherwise abrogate the binding of the other (competitive inhibition). In the case of TBHQ and C22, the effect of one compound appears to inhibit that of the other; by thermolysin assay, as shown in Fig. 8, 10 μM C22 obviates the stabilizing effect of 100 μM TBHQ. This effect could also be competitive, or the two molecules could bind at the same time. More information is necessary to clarify this issue.

The effects of C22 alone on the conformation of BHA are difficult to interpret as well. Its presence inhibits binding of N2 antibody even at neutral pH, possibly signifying that C22 binds to the N2 epitope, changes the conformation of this epitope, or it may bind to N2 antibody. The DOCK site (site 2A) for which C22 was selected is close to the N2 epitope (known as site B (White & Wilson, 1987)), and C22 binding at neutral pH could cause motion in this nearby epitope that alters its structure. At low pH, C22 allows recognition by interface antibody, although only HA1 is visible on the gel, and it appears as a smear. As mentioned above, HA1 and HA2 could be dissociated by C22 at low pH, but the results with site A do not support this possibility. As shown in Figure 4, site A at low pH in the presence of C22 does not recognize BHA as well as in its absence, HA1 appears as a smear, but HA2 is visible on the gel. This observation also suggests that the structure of HA1 has been significantly altered by C22 at low pH, a hypothesis supported by the results shown in Figures 1 and 2 illustrating that C22 alters the trypsin and proteinase K cleavage pattern of BHA at low pH. Finally, the Post control of C22 in the trypsin assay shown in Figure 2 suggest that C22 inhibits trypsin cleavage at HA1 27; this could be due to aggregation, binding to this area in low-pH BHA by C22, or causing BHA to assume a conformation not seen before (which is inactive, as determined by infectivity and fusion assays in previous chapters).

A possible site of action of TBHQ and its relatives, as shown in previous chapters, is the pocket surrounded by HA2 54 and 58. Those sites bound by S22 and C22 remain to be determined; crystallography continues to offer the most hope for this issue. However, as with TBHQ, it is not necessary that either molecule acts by binding to the neutral-pH conformation of BHA. For example, C22 may bind to an intermediate along the pathway of the conformational change, either lowering the energy barrier to further changes or shunting the molecule along a different pathway to a new, inactive conformation. As described in the last paragraph, the possibility of a new HA conformation induced by C22 is supported by the results presented in this chapter. If

C22 does not act by binding to neutral-pH BHA, crystal soaks with BHA and C22 at neutral pH might generate no useful data.

References

Baker, D, Agard, DA. (1994) *Structure 2*, 907-910.

Bodian, D. L., Yamasaki, R. B., Buswell, R. L., Stearns, J. F., White, J. M., & Kuntz, I. D. (1993) *Biochemistry 32*, 2967-2978.

Doms, R. W., Helenius, A., & White, J. (1985) *J. Biol. Chem. 260*, 2973-2981.

Gutman, O., Danieli, T., White, J. M., & Henis, Y. I. (1993) *Biochem. 32*, 101-106.

Hernandez, L. D., Hoffman, L. R., Wolfsberg, T. G., & White, J. M. (1996) *Ann. Rev. Cell Devel. Biol. 12*, in press.

Kemble, G. W., Bodian, D. L., Rosé, J., Wilson, I. A., & White, J. M. (1992) *J. Virol. 66*, 4940-4950.

Skehel, J. J., Bayley, P. M., Brown, E. B., Martin, S. R., Waterfield, M. D., White, J. M., Wilson, I. A., & Wiley, D. C. J. (1982) *Proc. Natl. Acad. Sci. USA 79*, 968-972.

Stegmann, T., Booy, F. P., & Wilschut, J. (1987) *J. Biol. Chem. 262*, 17744-17749.

Weber, T., Paesold, G., Mischler, R., Semenza, G., & Brunner, J. (1994) *J. Biol. Chem. 269*, 18353-18358.

Wharton, S. A., Calder, L. J., Ruigrok, R. W. H., Skehel, J. J., Steinhauer, D. A., & Wiley, D. C. (1995) *EMBO J. 14*, 240-246.

White, J. M., & Wilson, I. A. (1987) *J. Cell Biol. 105*, 2887-2896.

Addendum: New DOCK run to the proposed TBHQ crystallographic site

Introduction

TBHQ was designed to inhibit fusion peptide exposure by binding directly to the residues of the fusion peptide itself. However, the evidence presented in previous chapters suggests that TBHQ binds to a site including HA2 54, 55 and 58; all these residues have been implicated as being important in stabilizing HA by mutational data (Chs. 2, 3 and 4). This site has until now been unexplored as a pocket for inhibitor design (although it has been suggested previously (Steinhauer et al., 1992)), and the abovementioned data suggest that a new DOCK search employing the area could identify new families of inhibitors. Indeed, the mutant data mentioned above indicate that, even if the pocket proves not to be the site of TBHQ action, a molecule that does bind there could have an effect on fusion and infectivity by influenza. To this end, a fresh round of structure-based inhibitor design employing this pocket in the 2.1Å structure of BHA, DOCK3.5, and the ACD was begun. Only compounds with an absolute value of formal charge less than or equal to 2 were DOCKed.

Results

The sphere files and CHEMGRID maps used for this run are identical to those employed in the runs described in the TBHQ and TBP work. A sample INDOCK file from the new search runs is shown below:

```
DOCK 3.5 parameter
#########################################################################################
################### DOCK 3.5 INPUT PARAMETER FILE #################################
#########################################################################################
#
#########################################################################################
#                                                              INPUT
#
mode                search
```

```
receptor_sphere_file     1175ang.sph
cluster_numbers         1
ligand_type           coordinates
ligand_atom_file        /marco/db/db35.95.1/acd/acd.0.l.db35
#
###############################################################################
#                                                            OUTPUT
#
output_file_prefix     117sitel.out
output_hydrogens        yes
#
###############################################################################
#                                                            MATCHING
#
distance_tolerance      .8
nodes_maximum            4
nodes_minimum            4
ligand_binsize        0.32
ligand_overlap        0.1
receptor_binsize       0.32
receptor_overlap       0.1
bump_maximum             2
focus_cycles          0
#
###############################################################################
#                                                            COLORING
#
#chemical_matching
#case_sensitive   no
#
###############################################################################
#                                                            SINGLE MODE
#
rmsd_override          0.0
contact_minimum         0.0
energy_maximum           0.0
#
###############################################################################
#                                                            SEARCH MODE
#
ratio_minimum          0.0
atom_minimum            1
atom_maximum             60
restart            no
number_save            200
normalize_save         0
molecules_maximum          180000
restart_interval     100
initial_skip       0
#
###############################################################################
#                                                            SCORING
#
scoring_option        forcefield
distmap_file          117site.map
delphi_file          <map_name>
chemgrid_file_prefix    117site
interpolate         yes
vdw_parameter_file      /bert/dock/parms/vdw.parms.amb.mindock
vdw_maximum             1.0e10
electrostatic_scale    1.0
vdw_scale            1.0
#
###############################################################################
```

```
#                                                    MINIMIZATION
#
minimize                   yes
check_degeneracy            no
degeneracy_wobble           0
degenerate_save_interval    25
check_degenerate_children   no
simplex_iterations          100
simplex_convergence         0.2
simplex_restart             1.0
simplex_initial_translation 1.0
simplex_initial_rotation    0.5
#
#
#########################################################################################
#########################################################################################
#########################################################################################
```

Preliminary exploration of this site using DOCK without minimization was performed by Brian Young (data not shown). The results of the full run with minimization are tabulated; the top 100 compounds selected by graphical screening are supplied in Appendix C. Screening involved selection of molecules that appear water-soluble and are not highly charged; compounds that maintain the same contacts made by TBHQ in the DOCK prediction (see previous chapters) were favored.

References

Steinhauer, D. A., Sauter, N. K., Skehel, J. J., & Wiley, D. C. (1992) *Receptor binding and cell entry by influenza viruses*, Vol. 3, Saunders Scientific Publications, Academic Press, London, U.K.

Chapter 6

Perspectives on HA function

In terms of design of inhibitors of viral infectivity, one main conclusion that can be drawn from the work presented in this thesis: The strategy of inhibiting membrane fusion by noncovalent modification and/or alteration of the BHA conformational change pathway is valid and effective, and this strategy can be realized by at least two methods: inhibiting or facilitating the conformational change. The application of this strategy to other disease-causing viruses is a tantalizing possibility. With regard to the biochemistry of membrane fusion, a new concept of the role of HA in regulating fusion has emerged from this thesis. The protein appears to function not only as a sheath for the fusion peptide, but also as an exquisitely tuned timing device for exposing and positioning the fusion peptide near target membranes. A molecule such as TBHQ that inhibits exposure of the fusion machinery fits the paradigm of a crude system with a metastable state that converts to a more stable one, but C22 does not fit as easily. It inhibits fusion by altering the timing in the direction opposite of TBHQ, suggesting that the conformational change must not proceed too quickly. In the context of an infection, it appears that HA operates in a finely-tuned fashion as well; data presented in this thesis suggest that C22 inhibits infectivity by destabilizing HA. TBHQ, on the other hand, could be stabilizing HA until it reaches a vesicular compartment in which the protein is degraded (Bodian, 1992).

In light of this and other observations, this project had an unanticipated benefit. The original goal was to design and characterize inhibitors of HA function to make better inhibitors; in doing so, however, a wealth of new information about the fusion-inducing conformational change was generated. In retrospect, this analysis was akin to a simple mutagenetic analysis of protein function; a system was perturbed and the behavior of the system was observed. However, instead of changing amino acids, a small molecule was introduced as the perturbation.

The concept of using small molecules to study a biological system is not new; drugs and analogs of natural ligands have been used to study macromolecular structure and function since the early days of biochemistry. However, the idea of designing a ligand to fit a particular structure as a probe of the receptor is not common because structure-based design is relatively young; we await further crystallographic analysis of the HA inhibitors to validate this method of biochemical investigation.

References

Bodian, D. (1992) *Ph.D. Thesis, University of California, San Francisco.*

Chapter 7:

Preliminary structure-based searches for ASV/HIV integrase inhibitors

Note: The work in this chapter has been performed by Luke Hoffman, Malin Young, Donna Hendrix, Keith Burdick, and George Robles

Introduction

The defining property of a retrovirus is its ability to reverse transcribe its RNA genome into a DNA copy upon infection of a host cell. This copy is then covalently integrated into the host genome by a complicated mechanism involving the viral enzyme integrase ((Engelman, 1991),(Engelman, 1995)). The integrated viral genome is then transcribed to produce both viral genome RNA and mRNA coding for viral proteins; since the integration is irreversible, the infection is permanent beyond this point and the viral DNA will be passed on to all progeny cells of the infected parent (Katz, 1994). In addition, available evidence suggests that integration is necessary for production of progeny virions (Englund, 1995). Thus, integration and events prior to this step are practical targets for antiretroviral intervention.

Reverse transcription was the first target of clinical antiretroviral therapy; the drugs AZT and DDI, for example, are potent inhibitors of HIV-1 reverse transcriptase (Katz, 1994). Clinical resistance to these drugs as the single class presents a concern for their use (Katz, 1994). Furthermore, recent reports have shown that combination therapy in which anti-RT drugs are used in conjunction with drugs that inhibit another retroviral enzyme (Katz, 1994) is more effective than a regimen employing either class of drug alone (Carpenter, 1996). Thus, inhibitors of other retroviral enzymes would be useful in designing more potent treatments for HIV infection. Recently, the catalytic domains of INs from two retroviruses, HIV-1 and avian sarcoma virus (ASV), were crystallized and their structures solved as shown in Fig. 1 ((Dyda, 1994),(Bujacz, 1995)), enabling the structure-based design of inhibitors of retroviral integration.

The structures reveal that the proteins exist as homodimers of mixed α/β monomers; portions of each are disordered and not present in the models shown in Fig. 1

((Dyda, 1994),(Bujacz, 1995)). Examination of the solvent-accessible surfaces of the two models (not shown) reveals several invaginations with geometric and chemical properties that we found interesting for inhibitor design.

Using these two crystallographic structures of IN core regions, we have undertaken efforts to identify and develop inhibitors of IN activity. Potential inhibitors were selected using DOCK3.5, a structure-based searching program, and three putative sites on the ASV IN central domain. We searched the Available Chemical Directory (Molecular Design Limited, Information Systems, San Leandro, CA) as well as carrying out similarity searches of known integrase inhibitors. Compounds selected by this method were then tested *in vitro* (using *att*-site oligonucleotide assays, (Hickman, 1994) to independently score for inhibition of two HIV-1 IN activities of recombinant HIV-1 IN shown to be relevant to integration in vivo (3' processing and strand transfer, reviewed in (Katz, 1994)). The concentration at which each compound inhibited these activities 50% (IC_{50}) was determined when possible, and a number of promising lead compounds have been identified.

Results

The structures of the catalytic domains of these two analogous integrases are diagrammed in Fig. 1. The proteins are homodimers of the catalytic domains alone. A brief examination of this figure shows that, despite only moderate sequence identity between the two proteins, they are similar in structure, but several key differences are visible. For example, divalent cation (Mn^{2+}), known to be critical for integrase function (Bujacz, 1995), is ordered and visible in the ASV structure, whereas no such ion is

Fig. 1

X-ray crystallographic structures of the dimeric catalytic domains of ASV IN (left) and HIV-1 IN ((Bujacz, 1995),(Dyda, 1994)). Each monomer is colored differently in the respective structures; red dotted spheres in the ASV IN indicate the locations of Mn^{2+} binding to the enzyme.

Integrase Catalytic Domain Structures

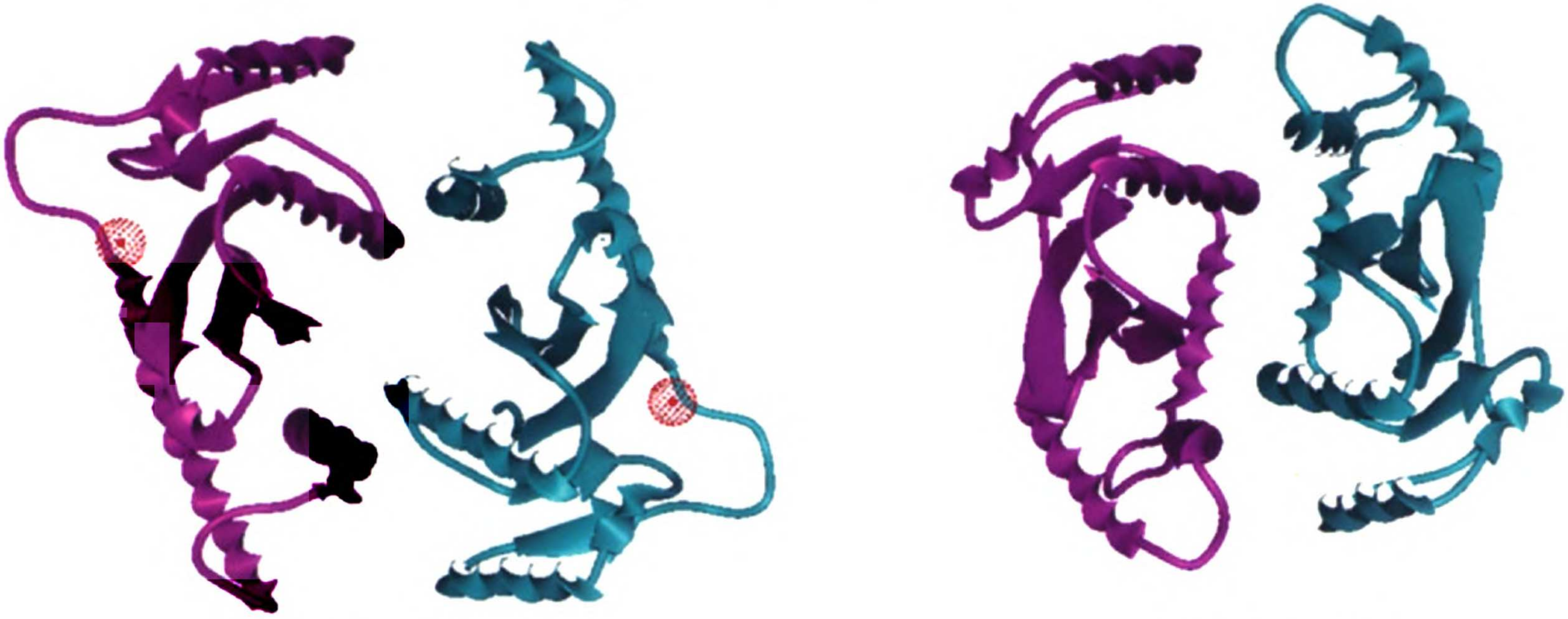

Fig. 1 ASV IN

HIV-1 IN

present in the HIV IN model. Other differences not visible in the figure include the higher overall resolution of the ASV structure (1.7 vs 2.5 Å for HIV-1 IN, (Bujacz, 1995),(Dyda, 1994)) and the fact that one of three "catalytic" residues in the proteins' active sites lies on a chain that is completely disordered in the HIV-1 structure, while all three such residues are present and ordered in the ASV-1 structure. For these reasons, the ASV structure was used for DOCKing with the hope that the similarities between that protein and HIV-1 IN would allow the generalization of the DOCK results to the latter protein.

DOCK3.5 was run using minimization on three sites. The first site, known as the active site (Fig. 2a, (Bujacz, 1995)), is the location of divalent cation binding and contains the three acidic residues known to be critical for IN function. The second site, referred to here as the dimer site (Fig. 2b), lies on the interface between dimers. The dimer site is a positively-charged cleft with an ordered distribution of solvent molecules in the ASV structure (Bujacz, 1995); these properties have led some authors to suggest that the region binds DNA (Bujacz, 1995). In addition, a mutation that affects dimerization of the protein, S85G, also affects integrase activity, suggesting a causal relationship between the two activities (Katz, 1992). This evidence that the dimer interface plays a role in IN activity suggests that a molecule that binds to the area could affect integration. The third site, the HEPES site (Fig. 2c), was chosen for DOCKing because of the observation by the authors who solved the ASV-IN crystal structure that a buffer constituent, HEPES, binds in a well-ordered fashion to this area (Fig. 2d, (Bujacz, 1995)). They also noted a chemical similarity between HEPES and nucleotide (A. Wlodawer, pers. comm.), suggesting a functional importance for this location.

Each DOCK run used the ASV-IN catalytic domain structure with all solvent molecules, HEPES, and divalent cation removed, using the Available Chemicals Directory (ACD) and Concord-generated molecular structures (Molecular Design Limited, San Leandro, CA). The database was divided into three groups of molecules that differ by

Fig. 2

Locations of the three sites chosen for DOCKing on the surface of the ASV IN crystal structure. Each site is represented by dots; these denote the locations of sphere centers onto which potential ligand atoms are mapped when evaluating these compounds for computed interaction with the protein computationally. (a) Location of the "active site." (b) The "dimer site." (c) The "HEPES" site. (d) HEPES bound to ASV IN as in models of crystallographic analysis of the crystals of the protein grown in the presence of the buffer. (e) All of the sites displayed concurrently on a dimer.

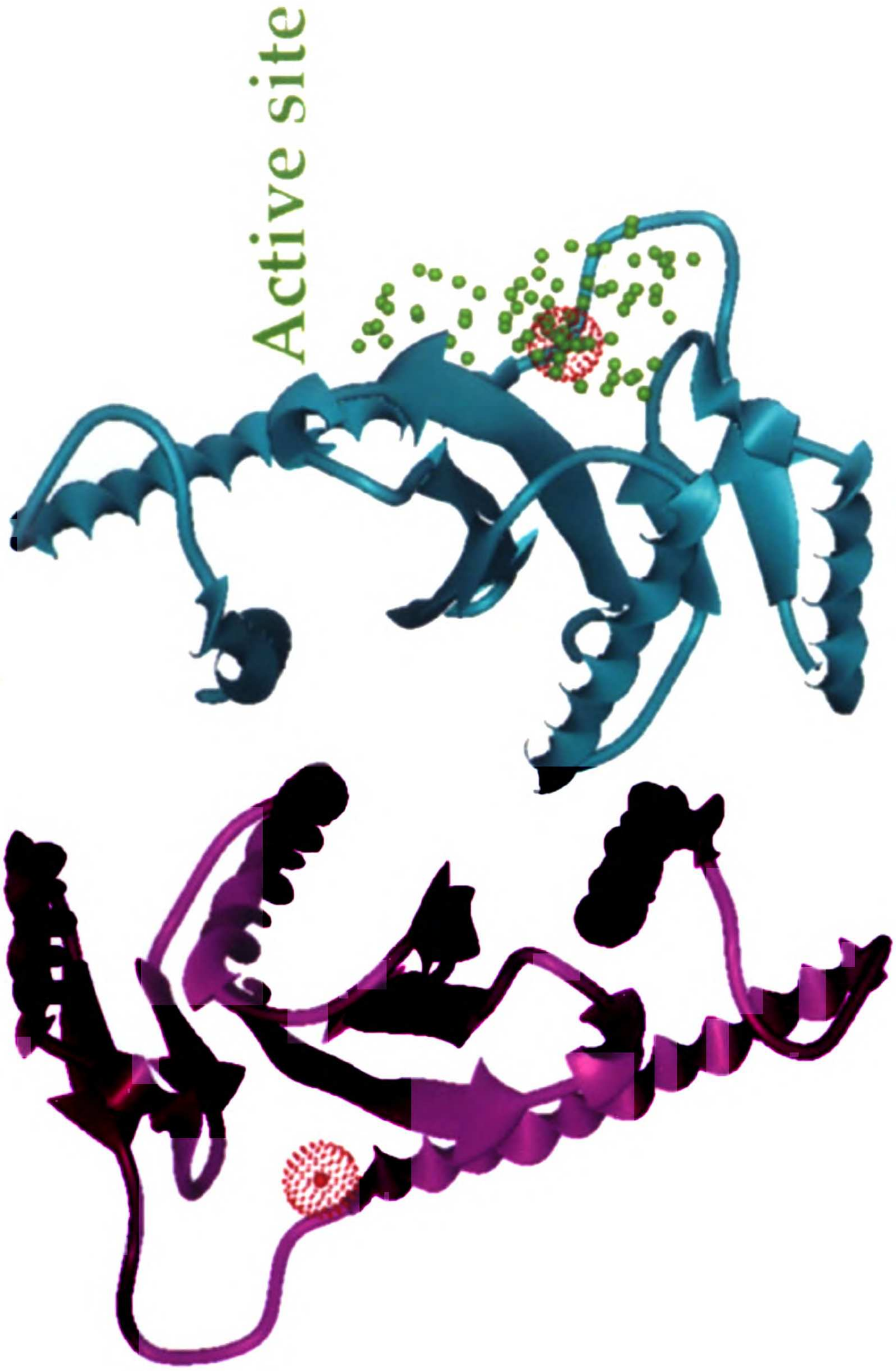
Active site

Fig. 2A

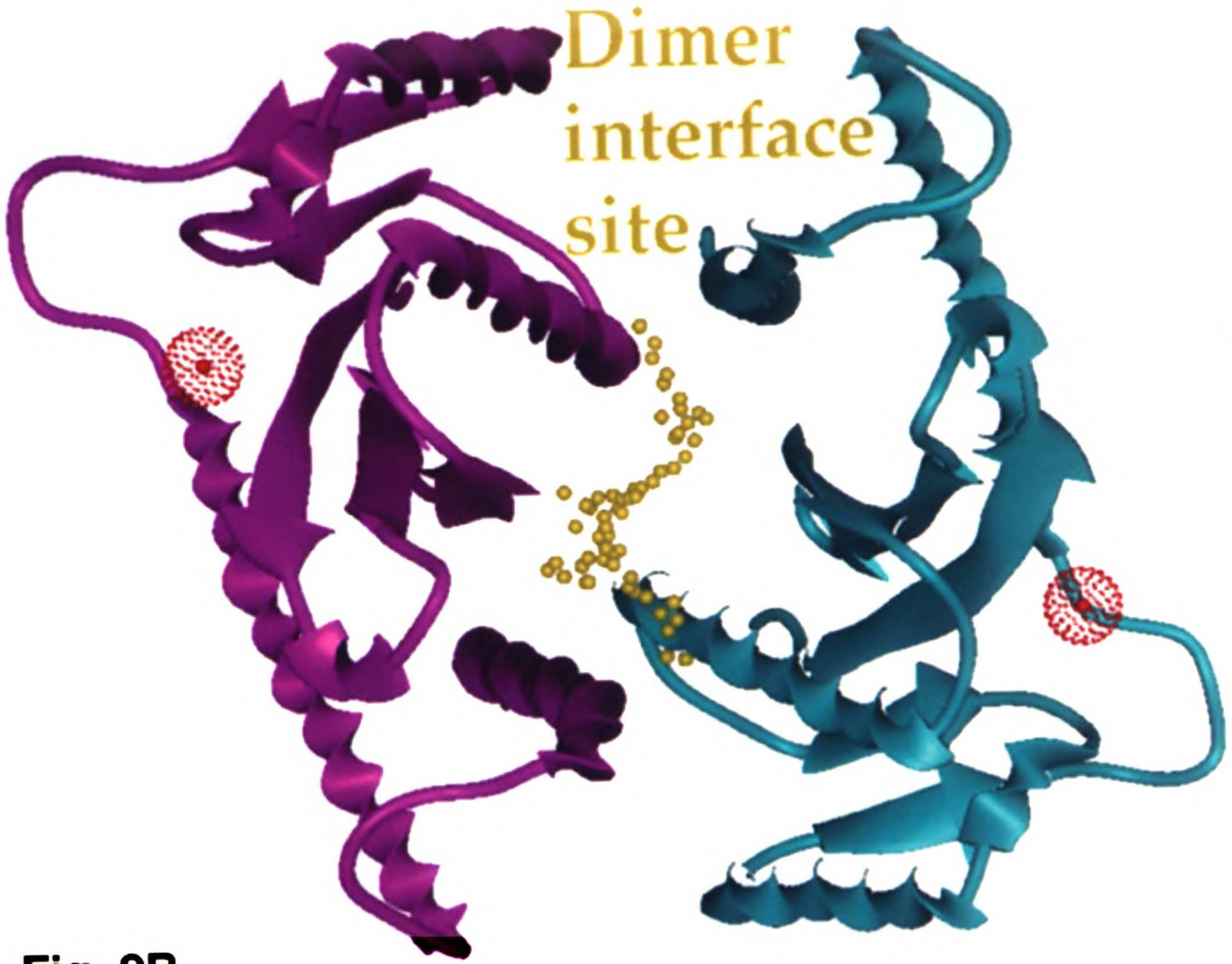
Dimer
interface
site

Fig. 2B

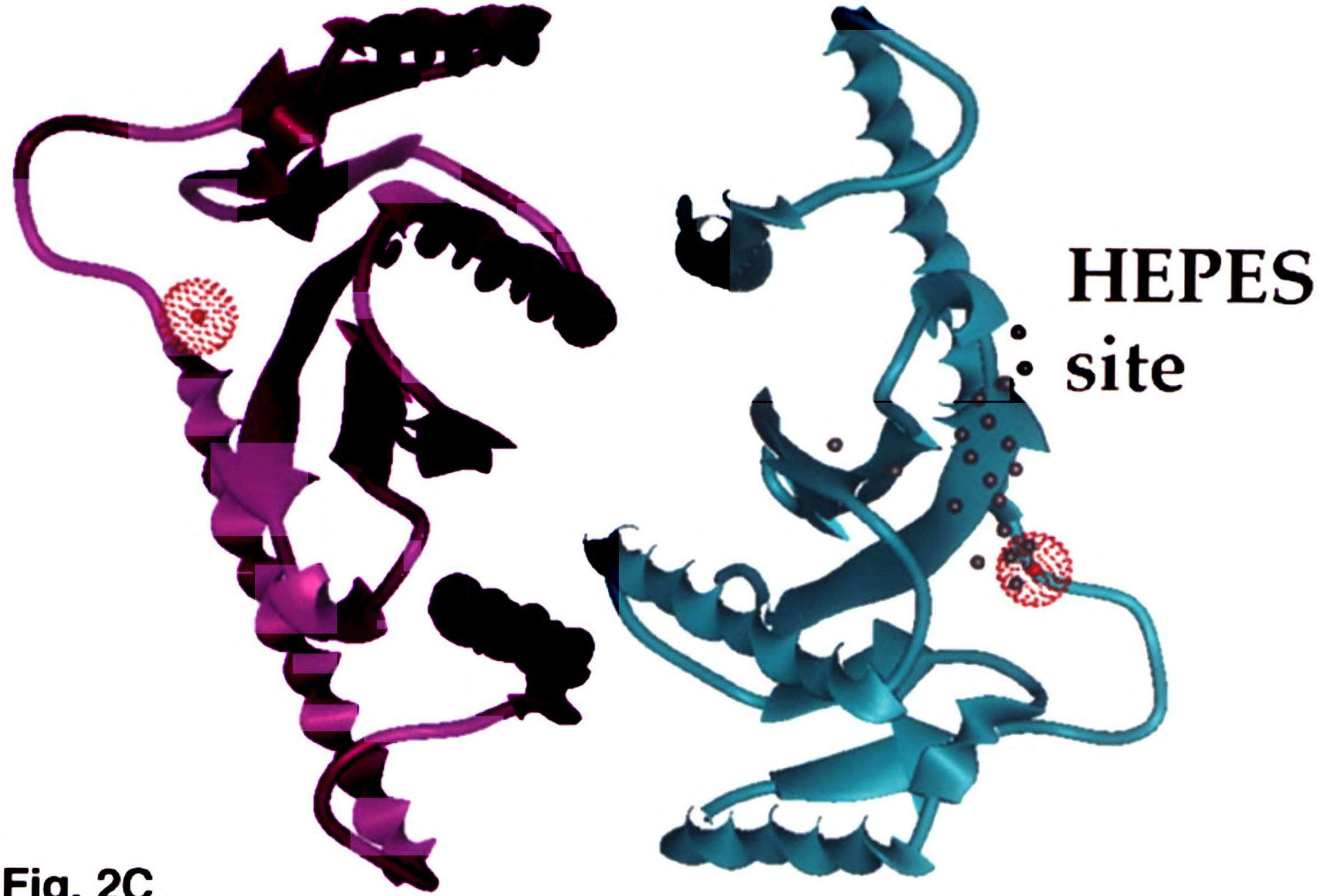

Fig. 2C

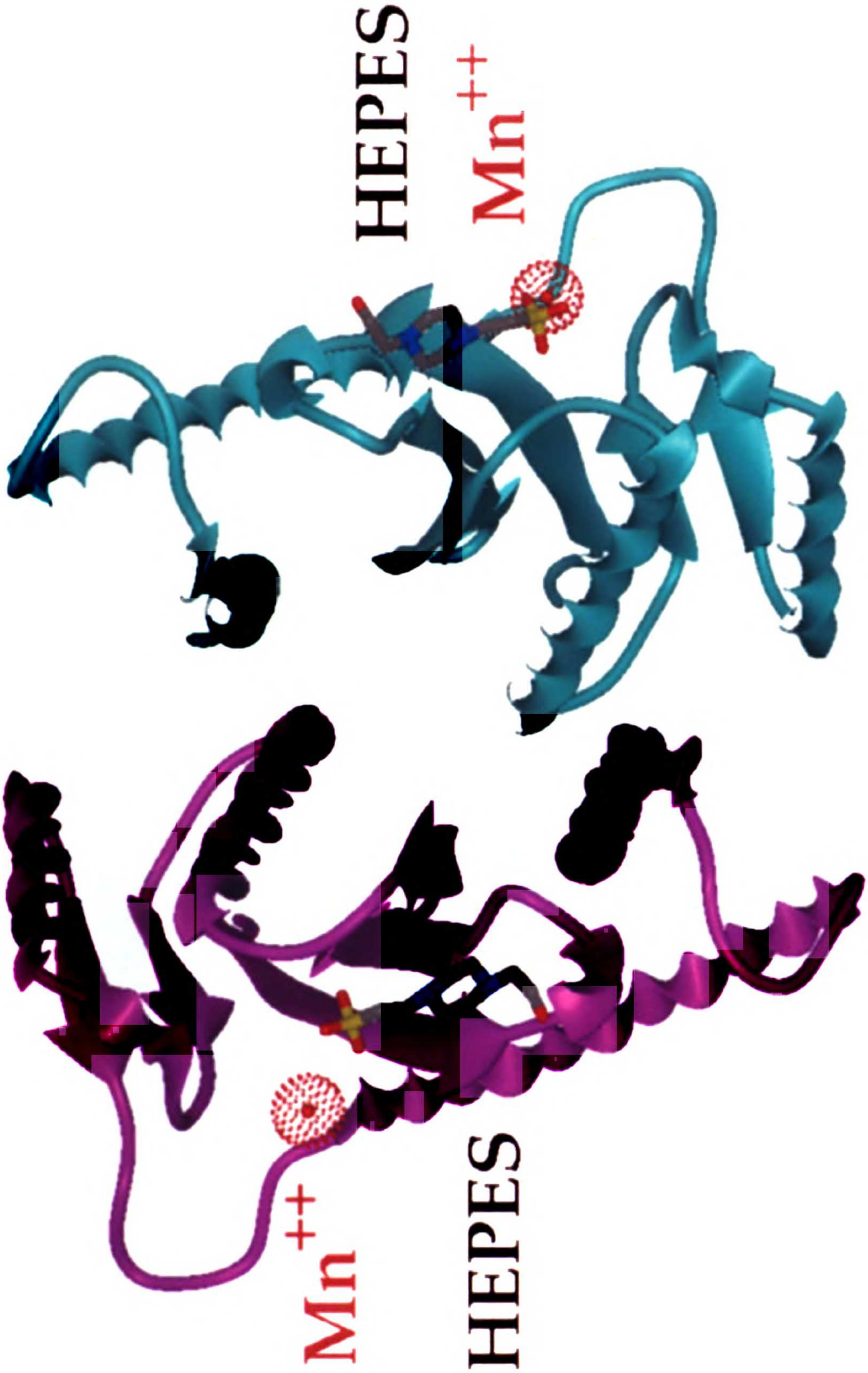
HEPES
Mn++
HEPES
Mn++

Fig. 2D

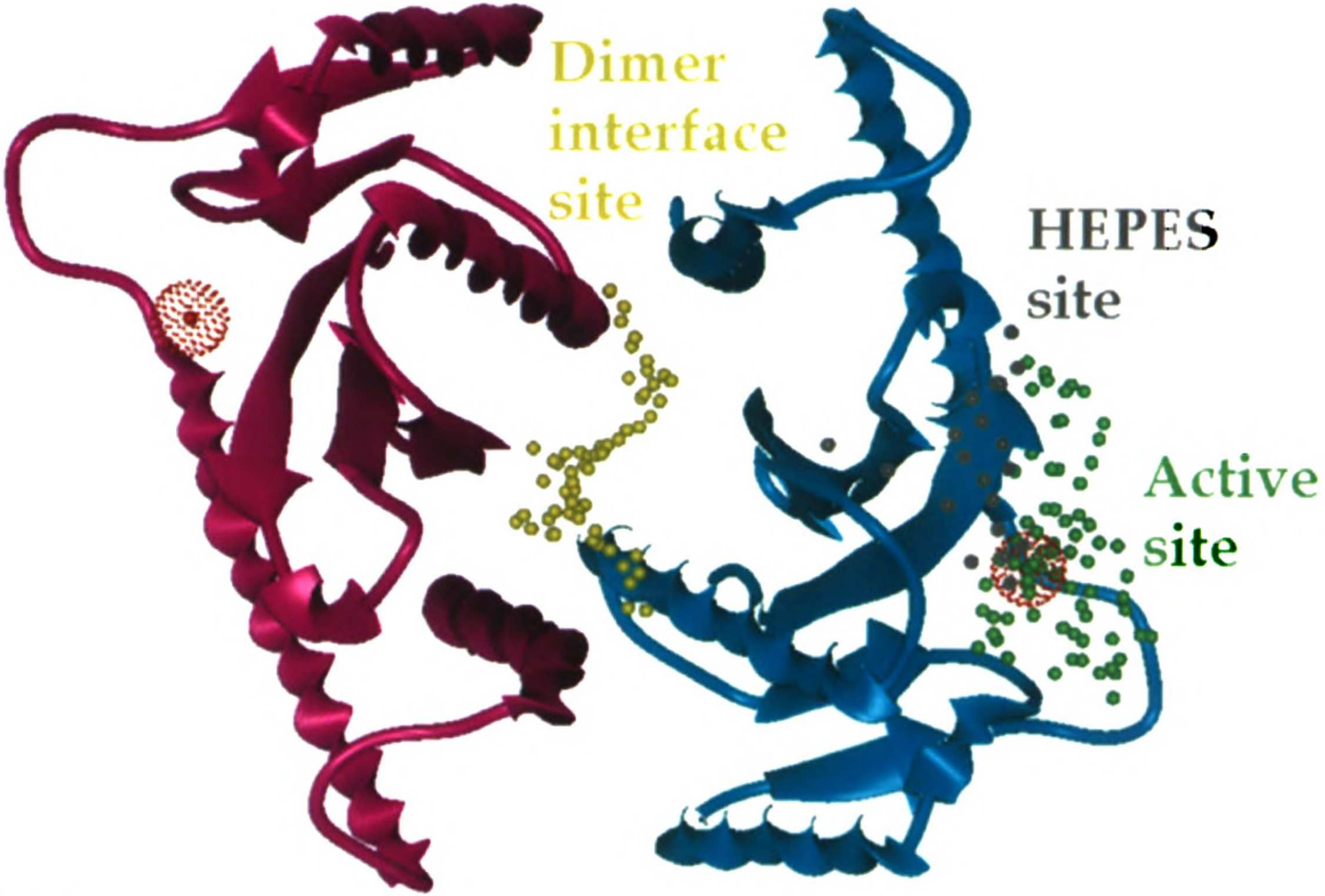
Dimer interface site
HEPES site
Active site

Fig. 2E

charge; one group had a range of absolute value of formal charge of 0-1, another 1-2, and the third >2. Output from runs to each group was considered separately and screened visually for: (1) Solubility in aqueous solvents, (2) predicted interaction with important regions of the sites, and (3) reasonable chemistry. Approximately 30 compounds from each run were selected for testing in *in vitro* assays. The compounds' structures and DOCK scores were sent for analysis to a collaborating laboratory (that of Alexander Wlodawer, NCI) that uses various forms of ASV IN. In the meantime, a laboratory on campus (that of Andy Leavitt, Department of Laboratory Medicine) has started testing the DOCK output in a series of in vitro assays using full-length HIV-1 IN.

Since DOCK was run against the structure of ASV IN and is being tested against HIV-1 IN, we sought to improve the likelihood of finding novel inhibitors by searching the ACD for molecules that bear a structural resemblance to known HIV-1 IN inhibitors (Fesen, 1993). Two computer program were used to perform this similarity searching: FPRINTS, an algorithm that searches for molecules that are similar in shape to a seed compound written by Malin Young, and Daylight, whose similarity searching function finds molecules in which the connectivity between constituent atoms is similar to the seed compound. The results of a hypothetical similarity search against a seed compound by each of these programs is given in Fig. 3 to illustrate their differences. These similarity searching methods were used to identify molecules similar to 5-hydroxynaphthoquinone, an IN inhibitor identified several years ago (Fesen, 1993). It was coincidentally found that this inhibitor is structurally similar to a family of compounds currently under evaluation for inhibition of influenza virus (Bodian et al., 1993). Since these compounds had already been purchased and were conveniently on the shelves on campus, they were included in the list of potential inhibitors to test against HIV-1 IN. These compounds have also been modeled into the active site using DOCK, given the possibility that this area could be their site of inhibitor action.

Fig. 3

A hypothetical similarity search to a seed molecule and its products. Fprints (Malin Young, pers. comm.) searches for molecules similar to the seed compound in shape, while the Daylight similarity searching function does so on the basis of connectivity.

Similarity Search Types

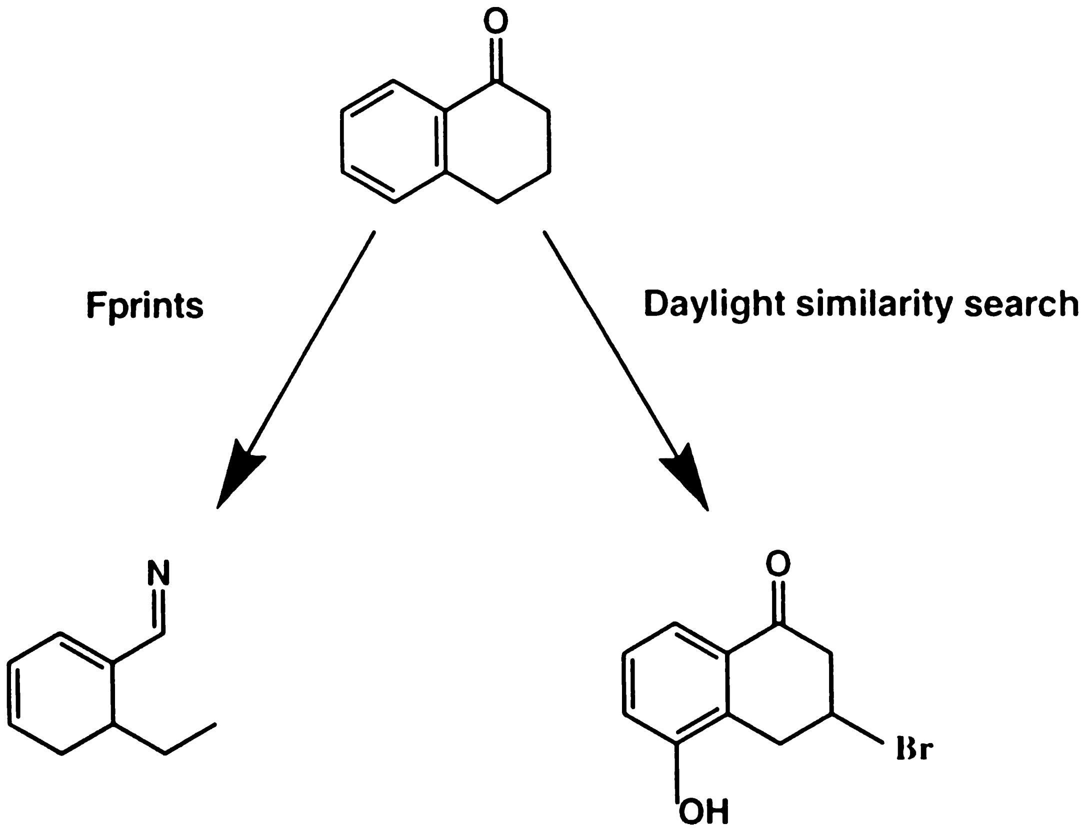
Fprints
Daylight similarity search
O
N
O
Br
OH

Fig. 3

Another coincidence led to the testing of compounds that had already been purchased: It was noticed that a series of compounds predicted by DOCK3.5 to bind to the ASV IN dimer site are similar to carbonyl J, a molecule that had already been found to inhibit HIV-1 RT by another laboratory on campus (that of George Kenyon, Dept. of Pharmaceutical Chemistry). The Kenyon group had already begun synthesizing and testing molecules similar to this compound, and they had also purchased molecules that are fragments of carbonyl J for testing. Since carbonyl J was found to inhibit HIV-1 IN (Andy Leavitt, pers. comm.), these fragments and similar compounds were also tested for inhibition of integrase activity.

Finally, promising compounds identified via any of the above methods that display inhibitory activity *in vitro* (see below) were subjected to similarity searching as described above, and new compounds to test were selected.

The Leavitt lab has tested output from each of the aforementioned search methods using *att* site-directed oligonucleotide assays ((Engelman, 1991) data not shown). The results of this testing so far are listed in Table I.

Table I: **Results to Date**

HIV-1 IN

DOCK:

- 29 molecules tested, active site
- Best IC_{50} = 83 µM
- 14 molecules tested, interface
- Best IC_{50} = 4 µM

Similarity:

- 46 molecules tested, modeled into active site
- Best IC_{50}= 10 μM
- Three generations of similarity tested

RT inhibitors:

- 22 molecules tested
- Best IC_{50}= 6.3 μM

Discussion and Future Directions

At this point, novel inhibitors of HIV-1 IN have been identified by all methods used. The most promising of these new compounds have come from the RT inhibitors, which were identified as similar to a DOCK output, and from a DOCK run to the dimer site.

Chemical cross-linking studies (Yves Pommier, pers. comm.) have suggested that several known inhibitors bind to the interface region of HIV-1 IN. Two of these compounds are nucleotide-based, and the third is a phenolic compound of the type used for our similarity searches (see "similarity" in Table I). The deep cleft and positive charge of the dimer region of the protein may serve to bind many different types of molecules; this possibility would predict that the DOCK runs to the dimer site would be the most successful of our DOCK searches. Crystallographic analysis could lead to the dentification of the actual binding sites of the inhibitors and the resolution of these issues.

At this point, the results of the DOCK runs to the HEPES site of ASV IN have not een tested in *in vitro* HIV-1 IN assays. HEPES itself does not appear to inhibit integrase ctivity (Alex Wlodawer, pers. comm.). The output of this search may be tested against

ASV IN, but we believe the probability of identifying new HIV-1 IN inhibitors from this list of compounds to be low.

The promising inhibitors listed in Table I will be tested further by the Leavitt lab for inhibition of in vivo integrase activity in a cell culture-based assay and for toxicity to those cells. In addition, inhibition and dissociation constants for each of the inhibitors will be pursued. Similarity searching will continue to be performed for each promising compound to identify new leads and elucidate the molecular determinants of each inhibitor family's activity.

References

Bodian, D. L., Yamasaki, R. B., Buswell, R. L., Stearns, J. F., White, J. M., & Kuntz, I. D. (1993) *Biochemistry 32*, 2967-2978.

Bujacz, G, Jaskolsky, M; Alexandratos, J; Wlodawer, A; Merkel, G; Katz, RA; Skalka, AM. (1995) *Journal of Molecular Biology 253*, 333-46.

Carpenter, C, Fischl, MA; Hammer, SM; Hirsch, MS; Jacobsen, DM; Katzenstein, DA; Montaner, JS; Richman, DD; Saag, MS; Schooley, RT et al. (1996) *JAMA 276*, 146-54.

Dyda, F; Hickman, AB; Jenkins, TM; Engelman, A; Craigie, R; Davies, DR. (1994) *Science 266*, 1981-86.

Engelman, A, Englund, G; Orenstein, JM; Martin, MA; Craigie, R. (1995) *Journal of Virology 69*, 2729-36.

Engelman, A, Mizuuchi, K; Craigie, R. (1991) *Cell 67*, 1211-1221.

Englund, G, Theodore, TS; Freed, EO; Engleman, A; Martin, MA. (1995) *Journal of Virology 69*, 3216-9.

Fesen, M, Kohn, KW; Leteurtre, F; Pommier, Y. (1993) *PNAS 90*, 2399-2403.

Hickman, A, Palmer, I; Engelman, A; Craigie, R; Wingfield, P. (1994) *Journal of Biological Chemistry 269*, 29279-87.

Katz, R, Mack, JP; Merkel, G; Kulkosky, J; Ge, Z; Leis, J; Skalka, AM. (1992) *PNAS 89*, 6741-5.

Katz, R, Skalka, AM. (1994) *Annu. Rev. Biochem. 63*, 133-73.

Appendices:

Appendix A: Sample computer files used in this work

Appendix B: Protocols for methods developed during this project

Appendix C: 100 top compounds from a DOCK-based search to the alternate candidate TBHQ-binding site

Appendix A

Sample computer files used in this work

Spheres: Site 1A

```
DOCK 3.5 receptor_spheres
cluster     1   number of spheres in cluster    12
   20  47.87177  -3.46472  31.37354   1.602   15 0  0
  176  38.15245  -3.92949  38.82715   3.438  309 0  0
  235  46.78054  -2.62316  30.49780   1.698  591 0  0
  238  45.11676  -4.19949  29.17647   1.694  591 0  0
  240  44.81821  -5.56348  31.31993   3.024  595 0  0
  241  44.51693  -7.60792  30.27141   2.785  590 0  0
  245  42.48576  -4.49396  32.68764   2.230  254 0  0
  247  42.94839  -3.00336  32.13933   1.704  254 0  0
  252  44.58435  -1.85532  31.84589   1.655  247 0  0
  253  39.84719  -3.73898  35.32500   1.987  177 0  0
  255  45.55906  -3.14954  31.32295   2.333  235 0  0
  591  46.46193  -3.10130  31.07494   2.036   20 0  0
```

Spheres: Alternate Candidate Site

```
DOCK 3.5 receptor_spheres
cluster     1   number of spheres in cluster  44
  70  24.61642  19.87480  15.19369   2.335 2691 0  0
  91  33.29370  19.76036  12.95232   2.233 2641 0  0
 103  33.55648  18.53900  13.76532   1.603 2646 0  0
 104  34.83367  19.76937  11.80278   1.663 3213 0  0
 613  23.37243  27.06266  10.45598   1.898 2747 0  0
 620  25.98878  25.33674  15.50249   1.794 2720 0  0
1247  26.54187  26.16287  14.94806   1.648 2720 0  0
1258  31.12866  23.61165  13.13831   1.568 1310 0  0
1301  27.05003  24.93514  15.31842   1.517 2720 0  0
1302  31.54646  21.62107  12.20600   2.666 1259 0  0
1303  25.15565  21.67307  14.77051   2.366 2705 0  0
1312  32.43145  21.01337  14.96115   1.401 1370 0  0
1313  31.07674  22.52641  12.52822   2.073 1259 0  0
1315  32.32785  22.63814  12.87646   1.998 1259 0  0
1318  32.75126  20.56565  12.96068   2.556 2641 0  0
1323  32.18943  22.17537  13.62425   1.776 1302 0  0
1325  32.02711  23.99327  13.63174   1.401 1310 0  0
1370  32.81160  19.77500  13.54342   2.071 2641 0  0
1961  29.30400  24.10095   7.18280   1.868 2191 0  0
1968  26.46761  21.92250   6.09893   1.750 2714 0  0
1979  30.42982  24.71623   7.58096   1.855 1271 0  0
1991  31.63043  24.60221   7.65611   1.442 1271 0  0
2191  29.67285  24.48058   6.94657   1.805 1979 0  0
```

```
2192 25.51684 24.47106  4.93346  1.743 1964 0  0
2634 31.70998 20.47750 14.41459  1.608 1302 0  0
2636 29.49930 20.55669 13.47900  1.599 1313 0  0
2637 30.97327 21.44847 12.06550  2.626 2719 0  0
2638 30.24824 21.35534 11.77421  2.100 2719 0  0
2641 32.48800 20.96298 12.30000  2.703 1318 0  0
2642 33.96737 18.21919 11.34060  1.540 3213 0  0
2656 33.00731 19.11096 11.08194  1.497 2630 0  0
2658 30.45350 22.79645  8.43841  2.046 1271 0  0
2660 30.74928 21.90875 10.80904  2.185 1271 0  0
2663 31.25311 22.81436  6.47063  1.400 1980 0  0
2690 28.79594 20.77494 12.44885  1.709 2719 0  0
2691 23.76289 18.10660 15.86238  2.695   69 0  0
2693 29.22883 20.83416 12.67327  1.912 2719 0  0
2705 24.23981 21.04088 15.14949  3.050   70 0  0
2707 26.51716 21.19438 14.14378  1.960 1303 0  0
2718 29.67608 22.69294  8.69931  1.965 2658 0  0
2719 30.07004 22.10262 10.16864  2.115 2660 0  0
2720 23.96823 23.66481 15.44918  2.668  629 0  0
3148 31.60856 22.20041  9.42725  1.696 2660 0  0
3157 33.23434 22.76699 11.06240  1.419 1259 0  0
END
```

Sphere file for Site 2A

```
cluster     1   number of spheres in cluster  88
  217   5.88118  55.81165  26.97523   1.400   206 0  0
  309   7.35546  49.72410  25.60130   3.351   206 0  0
  316   5.15119  52.95730  27.52443   1.736   206 0  0
  317   1.64331  50.39646  24.17032   4.897 2924 0  0
  318  -0.39908  52.52329  24.74146   4.807 2795 0  0
  324   4.95860  54.68575  27.44234   1.840   206 0  0
  325   0.36558  54.25681  24.30173   4.073 2802 0  0
  326   2.67273  54.27213  23.66198   3.603 2802 0  0
  348   6.29344  57.81026  22.32480   1.616   369 0  0
  349   3.73115  59.17030  22.88774   1.433   352 0  0
  351   7.66640  56.80775  25.37500   1.599   370 0  0
  352   2.07267  57.41787  22.13522   2.508 2801 0  0
  353   6.59013  57.38583  17.79641   2.455   367 0  0
  354   5.56939  58.11674  15.08758   2.109 2806 0  0
  355   6.29377  59.69616  12.76561   2.500 2810 0  0
  365  17.06533  61.73911   7.81357   4.512 4415 0  0
  366  11.94041  55.48748  14.93947   1.989   373 0  0
  367   9.61157  54.71347  14.59042   3.121 1593 0  0
  368   6.69604  55.92540  18.83932   2.421 2803 0  0
  369   6.80799  52.73788  21.71505   3.070 2803 0  0
  370   6.00029  52.54526  22.70500   3.675 2803 0  0
  372  12.93792  52.44028  20.13116   1.886 1011 0  0
  373  11.25959  51.23898  18.64669   2.766 1011 0  0
  374  16.23558  52.47633  19.95735   1.698 1562 0  0
```

377	19.26742	57.49700	12.28928	1.816	5654	0	0
384	11.03739	52.64020	24.58016	1.603	302	0	0
385	15.12402	52.49306	20.23526	1.586	372	0	0
389	18.17246	52.43018	18.62126	1.798	1562	0	0
829	-3.65503	56.30823	23.78926	1.572	2797	0	0
834	0.28894	56.72876	23.35648	2.693	2800	0	0
1008	7.63172	50.68752	24.08700	3.504	206	0	0
1009	9.15696	50.10461	21.85921	2.274	1583	0	0
1011	9.36338	50.84302	20.82605	2.426	1583	0	0
1557	20.07628	50.48112	16.43883	2.043	5647	0	0
1562	17.28470	51.31499	17.44823	1.988	5647	0	0
1577	12.11101	49.05404	18.88984	2.152	1011	0	0
1578	11.08076	49.51357	17.60589	2.392	1586	0	0
1580	14.91291	50.14590	17.08445	1.866	1562	0	0
1586	6.23767	51.69096	23.19938	3.998	206	0	0
1591	9.90674	54.31080	9.00552	3.336	2402	0	0
1592	7.71735	51.81020	13.18125	1.758	1585	0	0
1624	19.10852	50.40836	16.71655	1.942	1562	0	0
2415	13.66027	52.26366	6.24560	1.921	1607	0	0
2797	-3.06894	52.12131	26.63833	4.621	319	0	0
2800	-0.12887	55.60412	23.75304	3.269	834	0	0
2801	1.50784	58.50351	20.43298	1.554	352	0	0
2802	1.95845	52.75659	24.36493	4.345	318	0	0
2803	8.26630	55.74633	13.77634	3.884	363	0	0
2804	4.24712	58.14900	19.66577	1.642	353	0	0
2806	7.82456	56.41900	12.36260	4.140	361	0	0
2914	4.05346	52.77216	11.33657	3.121	2803	0	0

3626	20.21324	61.06428	8.40000	3.494	4415	0	0
3630	15.71528	57.57428	4.44100	4.183	2401	0	0
5640	19.85330	60.75134	10.62579	3.204	365	0	0
5644	19.94523	58.74217	11.70809	2.400	5654	0	0
5646	18.68261	52.58855	17.91261	1.927	389	0	0
5647	19.79861	51.38618	17.19441	1.851	5661	0	0
5648	15.83016	55.37026	10.32976	2.438	1607	0	0
5649	12.91437	55.68763	12.19292	2.536	363	0	0
5651	20.64613	50.24292	14.99147	1.495	1624	0	0
5652	20.36708	57.72255	12.82900	1.741	5644	0	0
5653	21.23884	59.07661	10.41400	2.295	5642	0	0
5654	19.53679	60.24860	8.22467	3.863	4416	0	0
996	20.74088	48.69801	23.74632	2.026	1564	0	0
1001	18.60255	46.66452	24.29990	2.075	1130	0	0
1003	21.45867	46.89717	26.83503	1.586	1001	0	0
1005	16.46297	46.59092	24.66165	1.913	1563	0	0
1006	10.63607	41.83641	26.85100	3.226	1574	0	0
1010	15.56551	45.28675	23.88935	1.910	1131	0	0
1013	12.49504	42.64939	25.98068	2.047	1574	0	0
1014	10.21577	44.83200	29.19559	1.800	310	0	0
1018	10.41845	37.00219	31.38409	3.810	1297	0	0
1019	6.70510	38.66445	26.94182	4.788	1297	0	0
1065	12.58659	38.23924	29.93040	2.180	1297	0	0
1067	12.13192	37.50500	30.41531	2.500	1297	0	0
1130	21.44791	46.43940	23.85548	2.411	1560	0	0
1131	14.08856	42.58736	25.56125	1.966	1013	0	0
1132	22.83750	43.62261	23.32877	1.612	1569	0	0

1555	21.61114	47.38070	23.81297	2.462	996	0	0
1556	21.43622	48.51200	23.35564	2.144	996	0	0
1561	19.05927	45.90079	23.01382	2.009	1130	0	0
1563	17.43519	45.88828	24.24907	2.009	1130	0	0
1564	19.41485	47.92203	23.93466	1.635	1001	0	0
1568	19.69065	44.57420	22.25301	1.519	1130	0	0
1569	20.89548	44.39875	22.53167	1.592	1130	0	0
1575	13.41655	39.91142	25.85854	1.690	1297	0	0
1576	11.32778	45.42991	22.00224	1.962	1007	0	0
1582	8.78846	42.48234	21.67247	2.843	1574	0	0

Sphere file: Site 2B

```
cluster    1   number of spheres in cluster  71
 1585   4.31065  50.92066  12.04463   2.426 2915 0  0
 1590   5.94703  51.32127   9.19923   1.906 2908 0  0
 1591   9.90674  54.31080   9.00552   3.336 2402 0  0
 1592   7.71735  51.81020  13.18125   1.758 1585 0  0
 1594  13.12522  50.30847   7.88893   1.472 1605 0  0
 1595   7.65849  51.65902   8.28146   1.903 2909 0  0
 1597  14.21234  46.13885   2.44299   1.529 2426 0  0
 1598  15.72932  45.33480   2.43716   2.168 3590 0  0
 1600  16.70441  47.07174   0.55971   1.790 3590 0  0
 1606  13.05216  51.78672   9.16000   1.795 1591 0  0
 2411  13.30501  46.38818  -2.14349   1.427 2423 0  0
 2415  13.66027  52.26366   6.24560   1.921 1607 0  0
 2424  13.68745  45.53233  -1.23403   1.732 3590 0  0
 2426  14.80918  45.98960   1.45331   2.058 3590 0  0
 2916   3.80567  48.65081  12.87229   1.727 1585 0  0
 3156  20.45004  35.28234   0.46918   1.514 3596 0  0
 3574  15.16311  41.46481   1.33495   1.547 3592 0  0
 3577  17.76691  36.97719  -0.00755   2.227 3154 0  0
 3580  15.19335  43.38309   2.70801   1.716 1616 0  0
 3582  17.44451  45.31110   3.04277   1.831 3649 0  0
 3583  18.06342  45.48820   4.32716   1.638 1616 0  0
 3586  16.24501  38.22182  -0.48480   2.442 3030 0  0
 3592  12.89124  44.26039  -0.26572   1.715 2426 0  0
 3596  18.51409  37.82429  -0.43017   2.032 3154 0  0
```

3648	18.01713	45.45221	2.01648	1.565	3587	0	0
3649	17.42593	45.31092	3.01200	1.842	3582	0	0
1125	17.82073	34.59936	16.23846	2.991	1650	0	0
1126	16.86587	36.10180	14.94963	2.935	1650	0	0
1571	15.41971	39.20937	15.80656	2.051	1628	0	0
1572	12.82904	38.37640	16.94673	3.058	1628	0	0
1573	8.76685	40.26736	20.43355	3.286	1583	0	0
1584	4.43815	40.70070	17.21600	4.265	3016	0	0
1588	9.95264	43.86926	10.02524	1.831	1613	0	0
1589	8.63799	40.15551	10.78500	2.638	3016	0	0
1596	11.08846	44.43462	9.28672	1.887	1613	0	0
1616	10.73216	41.15474	8.55624	2.389	2439	0	0
1617	16.99509	40.23407	7.32977	1.515	3579	0	0
1627	15.36735	36.18774	13.93029	3.640	1650	0	0
1628	14.47081	36.06906	15.17225	4.018	1126	0	0
1634	21.08692	35.28123	7.68835	1.602	3561	0	0
1643	18.31833	39.21426	15.39700	1.751	1126	0	0
1644	18.70812	37.99396	15.26913	2.033	1126	0	0
1649	16.95932	37.41179	14.56974	2.718	1126	0	0
1650	17.04609	32.16406	16.58147	4.115	1163	0	0
1651	16.58286	35.61649	9.02219	2.477	3575	0	0
1655	23.26760	35.68230	8.20071	1.400	3678	0	0
1664	19.86872	32.58500	15.54683	2.139	1650	0	0
1665	18.92490	33.41874	16.16136	2.575	1650	0	0
2429	10.18769	42.84106	6.75236	1.936	1616	0	0
2431	6.03158	41.16309	7.95230	2.217	1589	0	0
2439	9.64355	40.30574	9.84027	2.708	1629	0	0

2440	6.68490	38.64561	8.22633	1.592	3015	0	0
2666	-0.93525	39.90945	12.50034	1.733	3009	0	0
2667	2.09071	40.18092	15.22165	3.020	3016	0	0
2668	2.67877	40.43974	15.95967	3.421	3016	0	0
3007	2.50752	41.37317	11.96135	2.228	3016	0	0
3008	2.54406	44.04148	11.49111	1.500	2668	0	0
3009	1.88551	40.55610	11.58764	1.909	3016	0	0
3014	6.30844	39.77610	8.17000	1.795	2439	0	0
3016	5.81307	36.27657	18.12075	4.827	1302	0	0
3019	11.34511	36.35163	11.37075	3.612	1629	0	0
3020	10.81806	32.17025	9.31131	1.971	3565	0	0
3025	10.41232	35.39824	6.10403	1.472	3019	0	0
3560	15.06305	33.78853	9.50939	2.947	3565	0	0
3563	14.75081	34.76659	7.40296	1.667	3575	0	0
3564	11.99508	34.99063	8.42163	2.336	3019	0	0
3565	11.33239	33.37655	8.75677	1.778	3019	0	0
3571	11.60838	35.42894	7.70828	1.954	3019	0	0
3572	13.57422	40.07400	8.45527	2.191	1627	0	0
3575	13.59760	36.15355	10.55832	3.647	1627	0	0
3576	19.49380	35.43438	7.30021	1.401	3560	0	0

Box: Site 1A

```
HEADER    CORNERS OF BOX
REMARK    CENTER (X Y Z)   46.407  -2.462  31.318
REMARK    DIMENSIONS (X Y Z)   24.997  24.301  22.737
ATOM      1  DUA BOX   1      33.909 -14.612  19.949
ATOM      2  DUB BOX   1      58.905 -14.612  19.949
ATOM      3  DUC BOX   1      58.905 -14.612  42.686
ATOM      4  DUD BOX   1      33.909 -14.612  42.686
ATOM      5  DUE BOX   1      33.909   9.689  19.949
ATOM      6  DUF BOX   1      58.905   9.689  19.949
ATOM      7  DUG BOX   1      58.905   9.689  42.686
ATOM      8  DUH BOX   1      33.909   9.689  42.686
CONECT    1    2    4    5
CONECT    2    1    3    6
CONECT    3    2    4    7
CONECT    4    1    3    8
CONECT    5    1    6    8
CONECT    6    2    5    7
CONECT    7    3    6    8
CONECT    8    4    5    7
```

Box: Alt. Cand. Site

```
HEADER    CORNERS OF BOX
REMARK    CENTER (X Y Z)   29.103  22.585  10.398
REMARK    DIMENSIONS (X Y Z)   17.461  14.956  16.929
ATOM      1  DUA BOX    1      20.372  15.107   1.933
ATOM      2  DUB BOX    1      37.834  15.107   1.933
ATOM      3  DUC BOX    1      37.834  15.107  18.862
ATOM      4  DUD BOX    1      20.372  15.107  18.862
ATOM      5  DUE BOX    1      20.372  30.063   1.933
ATOM      6  DUF BOX    1      37.834  30.063   1.933
ATOM      7  DUG BOX    1      37.834  30.063  18.862
ATOM      8  DUH BOX    1      20.372  30.063  18.862
CONECT    1    2    4    5
CONECT    2    1    3    6
CONECT    3    2    4    7
CONECT    4    1    3    8
CONECT    5    1    6    8
CONECT    6    2    5    7
CONECT    7    3    6    8
CONECT    8    4    5    7
```

Box: Site 2A

```
HEADER    CORNERS OF BOX
REMARK    CENTER (X Y Z)   9.591  49.371  17.913
REMARK    DIMENSIONS (X Y Z)   41.293  39.537  41.743
ATOM      1  DUA BOX    1    -11.055  29.602  -2.959
ATOM      2  DUB BOX    1     30.237  29.602  -2.959
ATOM      3  DUC BOX    1     30.237  29.602  38.784
ATOM      4  DUD BOX    1    -11.055  29.602  38.784
ATOM      5  DUE BOX    1    -11.055  69.139  -2.959
ATOM      6  DUF BOX    1     30.237  69.139  -2.959
ATOM      7  DUG BOX    1     30.237  69.139  38.784
ATOM      8  DUH BOX    1    -11.055  69.139  38.784
CONECT    1    2    4    5
CONECT    2    1    3    6
CONECT    3    2    4    7
CONECT    4    1    3    8
CONECT    5    1    6    8
CONECT    6    2    5    7
CONECT    7    3    6    8
CONECT    8    4    5    7
```

Box: Site 2B

```
HEADER    CORNERS OF BOX
REMARK    CENTER (X Y Z)   11.166  43.237   9.145
REMARK    DIMENSIONS (X Y Z)   40.203  38.147  38.577
ATOM      1  DUA BOX   1      -8.935  24.164 -10.143
ATOM      2  DUB BOX   1      31.268  24.164 -10.143
ATOM      3  DUC BOX   1      31.268  24.164  28.434
ATOM      4  DUD BOX   1      -8.935  24.164  28.434
ATOM      5  DUE BOX   1      -8.935  62.311 -10.143
ATOM      6  DUF BOX   1      31.268  62.311 -10.143
ATOM      7  DUG BOX   1      31.268  62.311  28.434
ATOM      8  DUH BOX   1      -8.935  62.311  28.434
CONECT    1    2    4    5
CONECT    2    1    3    6
CONECT    3    2    4    7
CONECT    4    1    3    8
CONECT    5    1    6    8
CONECT    6    2    5    7
CONECT    7    3    6    8
CONECT    8    4    5    7
```

INCHEM: Site 1A

```
stanh.nocarb.pdb
/bert/dock/parms/prot.table.ambcrg.pdbH
/bert/dock/parms/vdw.parms.amb.mindock
site1a.box
.3
1
4.5
10
2.3 2.8
site1a
```

INCHEM: Alternate Candidate Site

```
stanh.nocarb.pdb
/bert/dock/parms/prot.table.ambcrg.pdbH
/bert/dock/parms/vdw.parms.amb.mindock
117site.box
.3
1
4.5
10
2.3 2.8
117site
```

INCHEM: Site 2A

```
stanh.nocarb.pdb
/amd/einstein/bert/dock/parms/prot.table.ambcrg.pdbH
vdw.parms.amb.mindock
crysite65.box
.4
1
4.5
10
2.3 2.8
crysite
```

INCHEM: Site 2B

```
stanh.pdb
/amd/einstein/bert/dock/parms/prot.table.ambcrg.pdbH
/amd/einstein/bert/dock/parms/vdw.parms.amb
secsite8.box
.4
1
4.5
10
2.3 2.8
secsite
```

INDOCK: Site 1A

```
DOCK 3.5 parameter
################################################################################
################# DOCK 3.5 INPUT PARAMETER FILE ##############################
################################################################################
#
################################################################################
#                                                               INPUT
#
mode                    search
receptor_sphere_file        site1a.sph
cluster_numbers           1
ligand_type              coordinates
ligand_atom_file          117sub.db35
#
################################################################################
#                                                               OUTPUT
#
output_file_prefix         site1a.out
output_hydrogens            yes
#
################################################################################
#                                                               MATCHING
#
distance_tolerance         .8
nodes_maximum               4
nodes_minimum               4
ligand_binsize            0.32
ligand_overlap            0.1
receptor_binsize           0.32
receptor_overlap           0.1
bump_maximum                2
focus_cycles              0
#
################################################################################
#                                                               COLORING
#
#chemical_matching
#case_sensitive       no
#
################################################################################
#                                                               SINGLE MODE
#
rmsd_override              0.0
contact_minimum              0.0
energy_maximum                0.0
#
################################################################################
#                                                               SEARCH MODE
#
ratio_minimum               0.0
atom_minimum                 1
atom_maximum                  100
restart                 no
number_save                 200
normalize_save              0
molecules_maximum                10000
restart_interval          100
initial_skip             0
#
################################################################################
#                                                               SCORING
```

```
#
scoring_option                forcefield
distmap_file                ../chemgrid/site1a.map
delphi_file                 <map_name>
chemgrid_file_prefix            ../chemgrid/site1a
interpolate                 yes
vdw_parameter_file               /bert/dock/parms/vdw.parms.amb.mindock
vdw_maximum                    1.0e10
electrostatic_scale          1.0
vdw_scale                    1.0
#
##########################################################################
#                                                          MINIMIZATION
#
minimize                    yes
check_degeneracy               no
degeneracy_wobble              0
degenerate_save_interval       25
check_degenerate_children      no
simplex_iterations           500
simplex_convergence            0.2
simplex_restart              1.0
simplex_initial_translation  1.0
simplex_initial_rotation     0.5
#
#
##########################################################################
##########################################################################
##########################################################################
```

INDOCK: Search to alternate candidate site

```
DOCK 3.5 parameter
#########################################################################################
################### DOCK 3.5 INPUT PARAMETER FILE #################################
#########################################################################################
#
#########################################################################################
#                                                           INPUT
#
mode                    search
receptor_sphere_file        1175ang.sph
cluster_numbers           1
ligand_type              coordinates
ligand_atom_file            /marco/db/db35.95.1/acd/acd.1.a.db35
#
#########################################################################################
#                                                           OUTPUT
#
output_file_prefix         117site.out
output_hydrogens            yes
#
#########################################################################################
#                                                           MATCHING
#
distance_tolerance          .8
nodes_maximum                4
nodes_minimum                4
ligand_binsize            0.32
ligand_overlap            0.1
receptor_binsize           0.32
receptor_overlap           0.1
bump_maximum                 2
focus_cycles              0
#
#########################################################################################
#                                                           COLORING
#
#chemical_matching
#case_sensitive       no
#
#########################################################################################
#                                                           SINGLE MODE
#
rmsd_override             0.0
contact_minimum              0.0
energy_maximum                0.0
#
#########################################################################################
#                                                           SEARCH MODE
#
ratio_minimum              0.0
atom_minimum                1
atom_maximum                 60
restart                 no
number_save                200
normalize_save             0
molecules_maximum               180000
restart_interval          100
initial_skip              0
#
#########################################################################################
#                                                           SCORING
```

```
#
scoring_option              forcefield
distmap_file               117site.map
delphi_file               <map_name>
chemgrid_file_prefix         117site
interpolate               yes
vdw_parameter_file            /bert/dock/parms/vdw.parms.amb.mindock
vdw_maximum                1.0e10
electrostatic_scale          1.0
vdw_scale                  1.0
#
##########################################################################
#                                                          MINIMIZATION
#
minimize                   yes
check_degeneracy             no
degeneracy_wobble            0
degenerate_save_interval       25
check_degenerate_children      no
simplex_iterations           100
simplex_convergence           0.2
simplex_restart             1.0
simplex_initial_translation   1.0
simplex_initial_rotation      0.5
#
#
##########################################################################
##########################################################################
##########################################################################
```

INDOCK: Search to Site 2A

```
DOCK 3.5 parameter
#####################################################################################
################## DOCK 3.5 INPUT PARAMETER FILE ################################
#####################################################################################
#
#####################################################################################
#                                                                  INPUT
#
mode                    search
receptor_sphere_file        crysite22.sph
cluster_numbers           1
ligand_type               coordinates
ligand_atom_file             /joey/db/dock3db/acd/spnsb.db3
#
#####################################################################################
#                                                                  OUTPUT
#
output_file_prefix          output/crysite22sb.out
output_hydrogens             yes
#
#####################################################################################
#                                                                  MATCHING
#
distance_tolerance          .8
nodes_maximum                4
nodes_minimum                4
ligand_binsize            0.28
ligand_overlap            0.1
receptor_binsize           0.28
receptor_overlap            0.1
bump_maximum                 2
focus_cycles              0
#
#####################################################################################
#                                                                  COLORING
#
#chemical_matching
#case_sensitive        no
#
#####################################################################################
#                                                                  SINGLE MODE
#
rmsd_override              0.0
contact_minimum              0.0
energy_maximum                0.0
#
#####################################################################################
#                                                                  SEARCH MODE
#
ratio_minimum               0.0
atom_minimum                  7
atom_maximum                  100
restart                  no
number_save                 200
normalize_save              0
molecules_maximum                50000
restart_interval            100
initial_skip             0
#
#####################################################################################
```

```
#                                                                 SCORING
#
scoring_option          forcefield
distmap_file            distmap/crysite74.map
delphi_file           <map_name>
chemgrid_file_prefix      chemgrid/crysite
interpolate           yes
vdw_parameter_file         vdw.parms.amb.mindock
vdw_maximum                1.0e10
electrostatic_scale      1.0
vdw_scale              1.0
#
#####################################################################################
#                                                                 MINIMIZATION
#
minimize               yes
#check_degeneracy           no
#degeneracy_wobble           0
#degenerate_save_interval     25
#check_degenerate_children     no
#simplex_iterations        500
#simplex_convergence          0.2
#simplex_restart          1.0
#simplex_initial_translation  1.0
#simplex_initial_rotation    0.5
#
#
#####################################################################################
#####################################################################################
####################################################################################
```

INDOCK: Site 2B

```
DOCK 3.5 parameter
################################################################################
################# DOCK 3.5 INPUT PARAMETER FILE ###############################
################################################################################
#
################################################################################
#                                                              INPUT
#
mode                  search
receptor_sphere_file       secsite22.sph
cluster_numbers          1
ligand_type              coordinates
ligand_atom_file           highscoredock/highscore.sec.out.db3
#
################################################################################
#                                                              OUTPUT
#
output_file_prefix         output/highscore.sec.out
output_hydrogens             yes
#
################################################################################
#                                                              MATCHING
#
distance_tolerance          1.0
nodes_maximum                 4
nodes_minimum                 4
ligand_binsize            0.32
ligand_overlap            0.1
receptor_binsize           0.32
receptor_overlap            0.1
bump_maximum                  2
focus_cycles              0
#
################################################################################
#                                                              COLORING
#
#chemical_matching
#case_sensitive       no
#
################################################################################
#                                                              SINGLE MODE
#
rmsd_override             0.0
contact_minimum              0.0
energy_maximum                0.0
#
################################################################################
#                                                              SEARCH MODE
#
ratio_minimum              0.0
atom_minimum                 7
atom_maximum                  100
restart               no
number_save                200
normalize_save             0
molecules_maximum               50000
restart_interval         100
initial_skip           0
#
################################################################################
```

```
#                                                                      SCORING
#
scoring_option              forcefield
distmap_file                distmap/secsite8.map
delphi_file                <map_name>
chemgrid_file_prefix          chemgrid/secsite
interpolate                yes
vdw_parameter_file            vdw.parms.amb.mindock
vdw_maximum                   1.0e10
electrostatic_scale         1.0
vdw_scale                  1.0
#
#########################################################################################
#                                                                      MINIMIZATION
#
minimize                    yes
#check_degeneracy                no
#degeneracy_wobble               0
#degenerate_save_interval        25
#check_degenerate_children       no
#simplex_iterations          500
#simplex_convergence            0.2
#simplex_restart              1.0
#simplex_initial_translation   1.0
#simplex_initial_rotation       0.5
#
#
#########################################################################################
#########################################################################################
########################################################################################
```

Appendix B

Protocols for methods developed or altered in this work:

Equilibrium dialysis

RBC-cell fusion

Hemolysis

^{35}S-Met label incorporation

Intrinsic tryptophan fluorescence

ELISA/MTT

Care of MDCK2 cells

Mutant influenza virus isolation

HA sequencing

Nile red fluorescence

Plaque assay

BHA biotinylation, bromelain cleavage, and purification

Proteolytic assays

Single-cycle time-of-addition inhibition

Equilibrium dialysis protocol

(reference for dialysis equipment: Legler, UF and Benet, LZ (1986) Eur J. Clin. Pharmacol. **30**: 51-55)

1) Wash and dry several equilibrium dialysis setups (borrowed from Les Benet's laboratory). Cut 1 1/2 cm dialysis tubing to make a single layer (use mw cutoff of <25 kD).

3) Wash membrane x7 with deionized water.

4) Equilibrate in MSSH overnight at room temperature.

5) Make a mix of 50 μg/mL BHA in MSSH, and another of compound in MSSH at the desired concentration.

6) Sandwich membrane into dialysis setup; screw closed.

7) Introduce 250 μL protein solution in one side of apparatus using gel-loading tips, 250 μL compound solution on other.

8) Close apparatus with screws.

9) In a control, place buffer with no protein on one side, compound solution on other.

10) Set apparatus upright, and shake gently overnight (10 hours minimum) at room temperature.

11) Make standards of compound concentration to create a standard plot of concentration vs. absorbance (must know λ_{max} of compound); fit a curve or line to the plot.

12) Remove 120 µL from each well of each apparatus. Read absorbance. For samples containing protein, zero on protein solution alone. For samples without protein, zero on buffer.

13) Repeat at various compound concentrations.

14) Can calculate K_d several ways using the dissociation constant equation: For example, use the difference between compound concentration between protein-containing and non-protein containing sides of one apparatus. Or, if absorbance of compound is the same as protein (i.e., λ_{max}= 290), use the difference between compound concentration on the non-protein containing side of the experimental cell and that in the control cell (no protein on either side).

RBC- cell fusion assay protocol

Loading of RBCs

1) Collect 3 mL fresh erythrocytes; wash X3 with PBS with calcium and magnesium, removing the buffy coat in the first wash.

2) Make a 50% suspension of RBCs in PBS

3) Add 300 μL of this to 11.4 mL swelling buffer (6 mL PBS + 5.4 mL H_2O; be precise)

4) Suspend and spin 1000xg for 10 minutes.

5) Aspirate all of supernatant (pink); add 150 μL of hypotonic buffer (10 mM Tris-HCl, 5 mM EGTA, pH 7.5) containing visualization molecule of choice (I've used 35 mg/mL β-galactosidase and 1 mM ethidium bromide.

6) Vortex gently and briefly and incubate on ice for 2 minutes.

7) Add 22 uL 10X Hanks (1.0 mL Hanks V, 0.3 mL 20 mg/mL $NaHCO_3$, 0.1 mL 20 mg/mL glucose, 1 mL Hanks VI; see (Ellens, Doxsey, Glenn, & White, 1989: Meth. Cell Biol. **31**: 155-176) for Hanks buffer recipes.

8) Incubate 1 hour, 37°C, then wash x2 with PBS.

9) Make a 0.05-0.5% suspension of RBCs (I use about 0.1%) and use within 1 day.

Binding and fusion-- if testing inhibitors, they should be present in all steps marked with *.

1) Grow HA-expressing cells to 60% confluence. Wash x2 with PBS.

2) Treat with 5 µg/mL trypsin, 250 ug/mL neuraminidase in PBS or neuraminidase alone, 1 mL per well in 6-well dishes, 10 minutes at room temperature.

3) Aspirate off enzymes, add growth medium to quench. Wash x2 with PBS.

4)* Incubate each well with 1 mL of RBC suspension (#9 above) with rocking every 3-5 minutes at room temperature for 15 minutes

5)* Wash x3 with PBS

6)* Treat with 1 mL low pH buffer (100 mM NaCl, 2.5 mM $CaCl_2$, 20 mM succinate, pH 5) for 2 minutes, room temperature (Treat controls with neutral pH buffer: 110 mM NaCl, 1.5 mM KCl, 2 mM $MgCl_2$, 1 mg/mL glucose, and 20 mM Hepes, pH 7.4)

7)* Aspirate off buffer, add 1 mL neutral pH buffer; incubate for 60 minutes at 37°C.

8) Aspirate, treat with 0.35 mL 20 mg/mL neuraminidase in PBS for 30 minutes at 37°C with agitation to remove unfused, bound RBCs.

9) Wash x3 with PBS.

10) For ethidium bromide, analyze by fluorescent microscopy using a rhodamine filter (ex 510-560 nm).

11) For β-galactosidase, fix cells in 1 mL 0.05% glutaraldehyde in PBS for 10 minutes at room temperature in the fume hood.

12) Rinse once in PBS quickly, then leave a second PBS rinse on for 10 minutes, and wash one last time in PBS quickly.

13) Add 450 μL xgal solution (20 mM $K_3Fe(CN)_6$, 20 mM $K_4Fe(CN)_6 \cdot 3H_20$, 1 mM $MgCl_2$, 1 mg/mL Xgal (from a 20x stock in dimethylformamide)).

14) Incubate at 37°C for a few hours until color is as dark as desired; can be kept indefinitely at 0°C.

Hemolysis assay protocol

1) Wash fresh red blood cells (RBCs) x3 in PBS; for each centrifuge step, spin in a 15 mL conical tube for 10 minutes at 1000 rpm.

2) Make a final solution of 1% RBCs in PBS in MES-S (0.13 M NaCl, 20 mM MES, pH 7.0).

3) Make a solution of virus to make 5-10 μg viral protein per mL MES-S. If using stocks of mutant virus collected in media, do a preliminary experiment with dilutions of stocks at a single pH; a maximum OD_{550} of 0.3-0.5 is a good target.

4) Mix 100 μL virus solution and 350 μL RBC solution; incubate with compound in DMSO if desired at this point to give no more than 0.5% DMSO final. Always run a no virus control to quantify lysis of RBCs as a function of pH. pH values approaching and below 5 lyse RBCs.

5) Warm to 37°C for 5 minutes.

6) Lower pH to desired value for 15 minutes at 37°C.

7) Reneutralize.

8) Spin for 3 minutes at a setting of 11 in an Eppendorf microfuge.

9) Take 150 μL aliquots of supernatant and put into a microtiter plate. Take OD_{550}.

Intrinsic tryptophan fluorescence assay

1) Make a solution of 20-200 μg/mL BHA in MSSH.

2) Measure fluorescence by fluorimetry (zero on MSSH); $\lambda_{excitation}$=288 nm, $\lambda_{emission}$=350 nm. Monitor and record constantly.

3) Add a small amount of buffer (equivalent to the amount of acid to add in (4)) to gauge the effect of dilution.

4) Add 1N HOAc to bring pH to 5.2. Monitor as trace (fluorescence vs. time) falls.

5) When trace has leveled out, add 1N NaOH to reneutralize. Monitor briefly.

6) Analysis of kinetics is possible; extent of conformational change is difficult to quantify by this method. Since many small molecules are fluorescent, use of this assay to analyze inhibition by compounds is also difficult.

^{35}S-Met label incorporation for toxicity

1) Make minimal essential medium with Earle's basic salt solution (MEM-EBSS) with 1X pen/strep lacking cysteine and methionine.

2) Wash MDCK2 cells x2 with PBS.

3) Incubate MDCK2 cells in this medium (1 mL per well in a 6-well plate will suffice) for 30 minutes at 37°C.

4) Remove this medium. Add 500 µL of this medium containing Translabel to give 0.277 mCi/mL final and the inhibitor being studied.

5) Incubate for 2 hours at 37°C.

6) Wash x1 with ice-cold PBS containing Ca/Mg.

7) Add 2.5 mL cold PBS to each well; scrape cells to remove and pipet into Falcon tubes.

8) Centrifuge for 5 minutes at 300Xg. Discard the supernatant.

9) Resuspend the cells in the residual volume. Add to the pellet 0.5 mL of 0.1 mg/mL BSA with 0.02% N_3^-. Place on ice.

10) Add 0.5 mL ice-cold 20% TCA (see Current Protocols). Vortex vigorously, then incubate for 30 minutes on ice.

11) Filter solution on glass filters (Whatman).

12) Wash each filter x2 with ice-cold 10% TCA.

13) Wash x2 with 100% ethanol and air dry each filter 30 minutes at room temperature.

14) Transfer the filters to scintillation vials, add scintillation fluid, and count.

Care of MDCK2 cells protocol

1) Growth medium is minimal essential medium (Eagle's) with Earle's basic salt solution, otherwise known as MEM-EBSS, with 10% FBS (or SCS), 25 mM HEPES (important), and 1x pen/strep. Cells can be adapted to lower serum if desired; I haven't tried plaquing under those conditions, however.

2) Cells should be split between 1:5 to 1:20; I usually go 1:10 or 1:20. They'll grow to be confluent in about 5 or 6 days at these dilutions.

3) Cells contact inhibit laterally, but they try to form tubules (Madin-Darby canine KIDNEY cells) about a day after reaching confluence. These "prototubules" do not affect plaquing.

4) Cells are only slightly less infectable with X:31 influenza if grown for a week.

5) Cells are quite resistant to trypsinization; I use 0.25% trypsin in versene, and it takes about 25-30 minutes to lift them off for splitting.

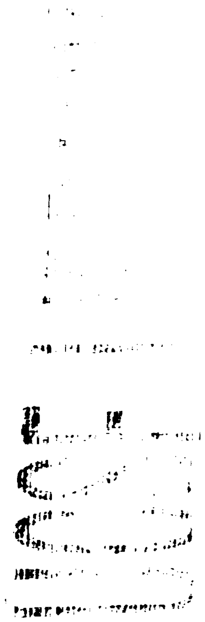

EIA and MTT assay protocols (From Bodian *et al*, *Biochemistry* **1993**. 32:2967-2978).

1) Seed 96-well microtiter tissue culture-treated plates with 35,000 MDCK cells/well (about 1 10-cm plate of 90% confluent cells in 20 mL growth medium; 100 μL per well).

2) Grow 24 hours (standard growth medium).

3) Incubate C22 virus with appropriate concentration of test compound in DMSO or DMSO alone (maximum 1% DMSO final) in MEM-EBSS with 1X pen/strep for 25 minutes, RT.

For each well:

4) Remove medium from cells, infect with 100 μL virus in compound for 15-18 hours in the incubator.

5) Aspirate medium; wash x1 with 50 μL PBS with Ca/Mg.

6) Aspirate; add 100 μL 80% acetone:20% PBS. Allow to fix for 15 minutes, RT. From this point forward, you can simply dump off liquids from the whole plate; cells are fixed.

7) Dump off fixative and air dry for about 1 hour (cells should now be opaque).

8) Wash x4 with PBS containing 0.05% Tween-20.

UCSF [illegible]

9) Add 100 µL EIA diluent (PBS with 1% FBS, 0.1% Tween-20) to block; incubate 30 minutes at RT. Dump.

10) Add 100 µL site A antibody; use lab stocks diluted 1:200 (about 14.5 µg/mL final) in EIA diluent. Incubate 1 hour, 37°C.

11) Wash x4 with PBS containing 0.05% Tween-20.

12) Add 100 µL secondary antibody (F(ab)'-2-goat-amti-mouse Ig(G)-peroxidase from Boehringer Mannheim) diluted 1:6000 in EIA diluent. Incubate 1 hour, 37°C.

13) Wash x4 with PBS containing 0.05% Tween-20.

14) Add 50 µL working solution of TMB. Working solution contains 10 mLs citrate-acetate buffer (4.1 g NaOAc, 500 mL water, pH 5.5 with 1 M HOAc), 1.6 µL H_2O_2 (0.005% final), and 600 µL TMB stock (.3-.5 g 3,3',5,5'-tetramethylbenzidine in 100 mL DMSO; I used 0.5 g). Incubate at RT for 10-15 minutes (will turn blue), then add 50 µL 2M sulfuric acid (turns yellow, quenches reaction).

15) Read OD 410 to 420 (Dale used 410, I used 420) on a microtiter plate reader.

MTT assay:

1) Infect as above, steps 1-5. After wash;

2) Add to each well 25 μL MTT solution (2 mg/mL 3-(4,5-dimethylthiazol-2-yl)-2,5-diphenyltetrazolium bromide in PBS with Ca/Mg) and 50 μL MDCK growth medium.

3) Incubate 4 hours in incubator.

4) Add 80 μL developing solution (96 mL 2-propanol and 4 mL 1 N HOAc); pipet up and down vigorously about 20 times per well (much easier with a multichannel pipet) to break up crystals.

5) Incubate 30 minutes at room temperature.

6) Read OD; I used OD_{550}-OD_{650}, Dale Bodian used OD_{570}. Both work. Standards for 100% viability have no virus or DMSO, and that for 0% viability have no cells.

UCSF [illegible]

Mutant isolation protocol

Two methods were used to isolate mutant viruses; a multiple passage method and a single, high multiplicity of infection (MOI) method.

Multiple passages:

1) Infect a well of MDCK cells in a 6-well plate with virus as in the plaque assay, using 100 and 10 µM inhibitor (TBHQ) in pretreatment only. Overlay as in the plaque assay.

2) Using a sterile filtered, 200 µL pipetman tip and a p200, insert the tip into the agarose overlay, touching the center of the plaque, with the plunger already down. Release the plunger to take up a big of the agarose and some cells.

3) Pipet up and down into a cryovial of 50 µL diluent. This stock of plaque-purified virus will now be used for a second passage, or it can be quick-frozen in liquid nitrogen.

4) Dilute the 50µL virus stock into 2 mL diluent and pretreat the virus with inhibitor. Use 250µL to infect a well in a 6-well plate of MDCK cells and allow to plaque as usual in the presence of inhibitor but with inhibitor in overlay as well. Repeat this process 7 times.

5) Amplify virus by passing as in (4), but overlaying with diluent instead of agarose and omitting trypsin. This will give a virus stock ready to amplify and sequence; collect at 48-72 hours when cytopathic effect is evident.

6) Titer this stock by plaque assay. Use in mutant sequencing protocol.

Single selection:

1) Grow a 1.75 cm plate (such as a single well of a 12-well tissue culture plate) of MDCK cells (about 200,000 cells) to confluence.

2) Determine the highest concentration of inhibitor that displays no toxicity to MDCK cells by MTT assay or trypan blue exclusion.

3) Pretreat a virus solution in diluent with the inhibitor concentration found in (2); virus concentration should be sufficient to give an MOI of 0.5-1 PFU/cell (about 120,000 PFU) in a 75 µL volume.

4) Infect as in the plaque assay. Overlay with 500 µL of diluent (no trypsin).

5) Collect overlay at 15-20 hours.

6) Dilute serially, 10-fold; treat with 5 µg/mL trypsin and inhibitor for 30 minutes, RT.

7) Use these dilutions to infect 6-well dishes of confluent MDCK cells; allow to plaque as in plaque assay.

8) Collect plaques and amplify as in serial passage method.

HA mutant amplification and sequencing protocol

HA amplification and Sequencing Primers

HART2: ATA ATT CTA TTA ATC ATG AAG

Tm = 50 °C Equivalent to nts 15-35 in Genbank accession # J02090

Reverse-transcription primer

HAPCR2: CCT AAT GTT GCC TCT CTG GC

Tm=60°C Complementary to nts 1693-1712, non-coding direction PCR primer

HAPCR3: ACC ATC ATT GCT TTG AGC TAC

Tm = 60°C Equivalent to nts 36-56 PCR and sequencing primer

HASEQ2: GCT CTA TTG GGG GAC CCT CAT GTG G

Tm= 78°C Equivalent to nts 282-306 Sequencing primer

HASEQ3: CT TGG ACT GGG GTC ACT CAG AAT G

Tm= 74°C Equivalent to nts 454-477 Sequencing primer

HASEQ4: GAG AGT CAC AGT CTC TAC CAG GAG

Tm=74°C Equivalent to nts 677-700 Sequencing primer

HASEQ5: GCG CAC TGG GAA AAG CTC AAT AAT G

Tm=74°C Equivalent to nts 857-881 Sequencing primer

HASEQ6: GGC AAC AGG GAT GCG GAA TGT ACC

Tm=76°C Equivalent to nts 1025-1048 Sequencing primer

HASEQ7: GCA GCC ATC GAC CAA ATC AAT GGG

Tm=74°C Equivalent to nts 1191-1214 Sequencing primer

HASEQ8: GCG GAG CTT CTT GTC GCT CTG GAG

Tm=78°C Equivalent to nts 1350-1373 Sequencing primer

HASEQ9: GAC AAC GCT TGC ATA GAG TCA ATC

Tm=70°C Equivalent to nts 1497-1520 Sequencing primer

HASEQ10: CTG GAT CCT GTG GAT TTC CTT TGC C

Tm=72°C Equivalent to nts 1596-1640 Sequencing primer

Virus purification and RNA prep

1) Infect a 10-cm plate of confluent MDCK cells using 1 mL of virus in diluent at a multiplicity of infection (MOI) of 0.1 PFU/cell. Adsorb at 37°C for 1 hour with rocking every 15 minutes. (Remember to pretreat with trypsin to activate virus if needed).

2) Aspirate diluent, replace with 10 mL diluent.

3) Replace in incubator; incubate for 48 hours.

4) Collect diluent. Spin in 15 mL conical tubes for 10 minutes at 2400 rpm to debris clear.

5) Spin down virus; I use an SW41 rotor for 1 hour at 40,000 rpm.

6) Resuspend in 350 µL 1X TSE (20 mM Tris-HCl, 150 mM NaCl, 2 mM EDTA, pH 7). Add it to:

40 µL 10x RSB (0.1 M Tris, 0.1 M KCl, 0.015 $MgCl_2$, pH 7.4)

12 µL 10% SDS

40 µL 5 mg/mL proteinase K

Incubate for 15 minutes at 56°C.

7) Add 8 µL 10X LiCl buffer (5% SDS, 0.1 M acetate buffer (0.4 M acetate pHed to 4.9), 1.4 M LiCl) and 400 µL of phenol saturated with an aqueous buffer (I use the preprepared, equilibrated phenol).

8) Vortex 1 minute. Incubate at 56°C and vortex every 2 minutes for 10-15 minutes total.

9) Centrifuge 5 minutes at top speed in a microfuge.

10) Take the (cloudy) aqueous layer and transfer to a new tube. Repeat extraction with 400 µL phenol. Vortex and spin 1 minute in microfuge.

11) Take the (clear) aqueous layer and transfer to a new tube. Extract with 200 µL phenol and 200 µL chloroform:isoamyl alcohol (24:1). Vortex and spin 1 minute.

12) Remove aqueous layer to a new tube. Precipitate RNA with 2-2.5 volumes of ice-cold 100% EtOH at -20°C overnight or -70°C for 1 hour.

13) Spin down RNA at top speed in a microfuge for 15 minutes at 4°C.

14) Pour off EtOH carefully and wash the pellet with ice-cold 70% EtOH; spin 5 minutes at 4°C. Repeat this step.

15) Pour off the EtOH and dry the RNA in a speed-vac for 5-10 minutes.

16) Resuspend RNA in 10 µL of autoclaved H_2O.

Reverse transcription

1) Mix:
   - 4 µL RNA from above
   - 1.25 µL 0.1 M DTT (comes with SuperScript Reverse Transcriptase, or RT)
   - 1.25 µL HART2, 50 µM
   - 6.25 µL 2mM dNTP mix
   - 5 µL 5x RT buffer (comes with RT)
   - 5 µL autoclaved water
2) Heat up to 90°C for 90 seconds, then plunge into ice for 5-10 minutes.
3) Add 1 µL SuperScript RT and 1.25 µL RNAse inhibitor
4) Incubate at 10 minutes at room temperature, then 1 hour at 37°C.

PCR

1) Mix:
   - 1.5 µL $MgCl_2$
   - 5 µL 10X PCR buffer
   - 2.5 µL 2 mM dNTP mix
   - 1 µL HAPCR2 (50 µM)
   - 1 µL HAPCR3 (50 µM)
   - 34 µL water
   - 5 µL cDNA from above
2) In PCR machine, heat to 97°C for 1 minute
3) Add 0.5 µL Taq polymerase
4) Run program: i. 94° for 1 minute

    ii. 58^o for 30 seconds
    iii. 72^o for 2 minutes 44 seconds (it works...)
    iv. 35 times to i
    v. end

5) Gel-purify PCR product using any PCR purification kit; I use Promega Wizard or Qiex II by Qiagen kits.

Sequencing

1) Follow procedures given with the Promega fmol cycle sequencing kit, using the above primers.

Nile red fluorescence assay

1) Make an approximately 20 μg/mL purified BHA solution in MSSH, pH 7.2; each sample should be about 300 μL for a small fluorimetry cell.

2) Incubate with compound in DMSO or DMSO alone (final 1% DMSO or less) for 25 minutes, room temperature.

3) Add 1 N HOAc to take the pH to 5.2. Incubate for 10 minutes at 37°C. Add 1 N NaOH to reneutralize.

4) Add a solution of nile red (Sigma) in MSSH to give a final concentration of 0.05 μM final.

5) Incubate for 1 hour at 37°C.

6) Read each sample in the fluorimeter; λ_{excite}=550 nm, $\lambda_{emission}$=610 nm. Zero on a sample of neutral red in MSSH without protein.

7) Assay is good for extent of conformational change; I have not tried to modify this protocol for kinetics.

Plaque assay protocol

1) Grow MDCK2 cells to confluence in 6-well tissue culture plates.

2) Wash cells x2 with PBS with Ca^{++}/Mg^{++}.

3) Dilute virus in diluent (Minimal essential medium with Earle's basic salt solution (MEM-EBSS), 25 mM HEPES, 1X pen/strep, 1% FBS); incubate with compound in DMSO to give no more than 1% DMSO final. If necessary, treat with 5 µg/mL trypsin at this step to cleave HA0 to HA1 and HA2.

4) Aspirate PBS from cells; add 0.25 mL virus solution per well. Rock to moisten cells, then place at 37°C.

5) Rock cells again every 5 minutes for 15 minutes, then every 15 minutes until 1 hour total has passed.

6) Aspirate virus, and replace with 2.5 mL of a solution of 0.5% SeaPlaque agarose final, 1X MEM-EBSS (starting with a 2x solution, containing 2x pen/strep, 50 mM HEPES, 5% FBS) and 10 µg/mL trypsin. Compounds in DMSO can be added to this overlay to give no more than 1% DMSO final.

7) Allow agarose to harden for 30 minutes at RT (or more) or 10 minutes at 4°C.

8) Replace cells in incubator.

9) After 36-48 hours, CPE should be visible (dead cells in clumps). Overlay each well with 2.5 mL of a solution of 0.9% SeaPlaque agarose final, 1X MEM-EBSS, 1 mL Sigma cell culture neutral red solution per 50 mL final solution.

10) Harden as before; return to incubator.

11) After 6-24 hours, read plaques by flipping over plates and placing on a light box.

BHA biotinylation, bromelain cleavage, and purification protocols

Biotinylation of virus

1) Suspend 13 mg (by Lowry) of virus in 1 mg/mL NHS-LC-biotin in ice-cold PBS with Ca/Mg, 3 mL final. It's often necessary to sonicate the biotin into solution.

2) Incubate 4°C, 45 minutes.

3) Spin out virus in a TLA100.3 @ 55,000 RPM for 30 minutes.

4) Add 50 mM glycine in ice-cold PBS with Ca/Mg; resuspend pellet, and spin down again.

5) Resuspend in 1 mL 0.1 M Tris, pH 8.

Bromelain cleavage

1) Add bromelain to make a final concentration of 2.5 mg/mL in 0.1 M Tris, pH 8.

2) Add 7.7 μL concentrated β-mercaptoethanol (BME).

3) Incubate at 37°C, overnight.

4) Bring volume up to fill up an ultracentrifuge tube using 0.1 M Tris, pH 8 (for TLA 100.3, 2.8 mL).

5) Spin out virus; I use a TLA100.3 @ 55,000 RPM for 30 minutes.

6) Collect supernatant.

7) Pellet may contain HA; take a 10 µL sample of the pellet resuspended in its residual volume to run on a gel. Freeze the rest in 1 M Tris at -70°C.

Ricin-agarose chromatography

1) Wash 1.5 mL resin slurry of 1.5 mL ricin I conjugated to agarose (Sigma) two times with 0.1 M Tris, pH 8. Centrifuge each time at 400 rpm for 2 minutes in Falcon tubes.

2) Aspirate wash off of resin. Add to the pelleted slurry the supernatant from bromelain cleavage. Add protease inhibitors (optional).

3) Nutate at 4°C overnight.

4) Pour slurry onto a BioRad 2 mL column. Collect flow-through fractions (I collect 1 mL fractions).

5) Wash with 0.1M Tris, pH 8 (I also add azide to all solutions from this point forth). Collect wash fractions.

6) Bump BHA off the column using 0.2 M galactose (.54 grams in 15 mL) in 0.1 M Tris, pH 8. Collect at least 4 fractions.

7) Store the column in 0.2 M galactose at 4°C.

Gel analysis

1) Analyze purity of the fractions by running 10 μL on 12% SDS reducing gels. Include the 10 μL of virus pellet.

2) Analyze for biotinylated protein as with the thermolysin assay.

3) Can analyze for purity using Coomassie staining on a parallel gel.

4) Determine protein concentration using absorbance at λ=280 nm, zeroing on 0.1M Tris, pH 8, with 0.2M galactose or with Lowry or Bradford protein assays. By absorbance, A_{280}/2.16e5 (times the dilution factor) gives the molar concentration of BHA if pure. This value, multiplied by 1.688e5 g/mol, will give the concentration in g/L.

5) The fractions can be used in assays as is or the buffers exchanged by dialysis.

Proteolytic assay protocols

1) Make a solution of 1-5 mg/mL biotinylated BHA in MSSH (10 mM HEPES, 10 mM MES (2-(N-morpholino)ethanesulfonic acid), 10 mM succinate, 0.10 M NaCl, pH 7.2).

2) Incubate 100 µL of protein solution with desired concentration of compound in DMSO to make 0.5-1% DMSO final, 25 minutes, RT.

3) Add 1 M HOAc to take solution to pH 5.2 for 7 minutes, RT.

4) Reneutralize with 1 M NaOH.

5) Add $CaCl_2$ to make 1 mM final and thermolysin (made up fresh in PBS, Ca/Mg free) to give a BHA:protease ratio of 100, w:w.

6) Incubate for 2 hours, 37°C.

7) Quench with 10 mM final EDTA, add 2X sample buffer with 0.2M DTT and 8% SDS. Heat at 95°C for 5 minutes.

8) Run on 12% agarose gels. Transfer to pvdf membrane, blot with streptavidin-HRP.

For trypsin, replace (5)-(7) with:

5) Add trypsin to give a BHA/protease ratio of 1000, w:w. Incubate at RT for 20 minutes.

6) Add 2X sample buffer as in (7) above, continue.

For proteinase K, replace (5)-(7) with:

5) Add $CaCl_2$ to give a final concentration of 10 mM, and add proteinase K to give a BHA/proteinase ratio of 5000, w:w. Incubate at 37°C for 30 minutes.

6) Continue as in 7, above.

Alternative protocol using whole virus:

1) Make a solution of whole virus in MSSH containing 215 μg viral protein (by Lowry) per mL (for lab virus stocks, this is 18 μL virus per mL MSSH).

2) Carry out steps 2-4, above.

3) After reneutralization, spin down samples (bring up volume with MSSH to fill tube) in a TLA 100 rotor, 75,000 rpm, 1.5 hours, 4°C.

4) Aspirate supernatant; resuspend pellet in PBS, pH 7.2, with 1 mM $CaCl_2$ by leaving at 1 hour, RT. Then pipet up and down with a P200 until resuspended.

5) Add 2.7 μL 10 mg/mL thermolysin. Mix.

6) Proceed with steps 6-8, above, but blot with Toots (rabbit antiserum against whole virus), 1:100 as a primary, and HRP-conjugated anti-rabbit as a secondary.

Single-cycle time-of-addition inhibition assay protocol

1) Make a solution of compound in diluent (see plaque assay).

2) Make a solution of virus in cold (4°C) diluent; use about 300 PFU per 6-well dish.

3) Wash MDCK cells (in 6-well tissue culture plates) X2 with cold PBS with Ca/Mg.

4) Add 250 μL virus solution to each well; rock to moisten all cells. Adsorb in cold room, rocking once every 5 minutes for 15 minutes and then every 15 minutes for 1 hour total.

5) Add prewarmed (37°C) diluent. For t=0 treatment, this diluent will contain inhibitor. For others, diluent alone. This overlay does NOT contain trypsin.

6) Remove diluent at various intervals (I used t=0, 15 minutes, 30 minutes, 1 hour, 2 hours, 5 hours, and 10 hours post rewarming) and replace with either fresh diluent or diluent containing compound (do this for all samples at every time point), so that a given sample always is exposed to inhibitor after a given time, representing all of the above times.

7) Remove diluent from each sample at 15 hours post adsorption.

8) Either quick-freeze in vials in liquid nitrogen or plaque now. If freezing, thaw when ready at 37°C as quickly as possible, then place sample on ice.

9) When plaquing, add trypsin to 5 μg/mL final and incubate at RT for 30 minutes. Then dilute by 10-fold dilutions in diluent and titer by plaque assay.

Appendix C

100 compounds selected for testing from running DOCK3.5 to the alternate candidate site

Force-field scores:

MFCD00211222	score = -43.686
MFCD00201890	score = -41.076
MFCD00209412	score = -40.130
MFCD00020348	score = -39.357
MFCD00121308	score = -39.303
MFCD00098455	score = -38.729
MFCD00087796	score = -38.720
MFCD00117257	score = -38.106
MFCD00052469	score = -38.104
MFCD00020470	score = -37.840
MFCD00187753	score = -37.387
MFCD00208419	score = -37.386
MFCD00172529	score = -37.167
MFCD00020404	score = -37.013
MFCD00194471	score = -36.963
MFCD00021752	score = -36.947
MFCD00185902	score = -36.796
MFCD00121607	score = -36.564
MFCD00141168	score = -36.549
MFCD00101255	score = -36.499
MFCD00020452	score = -36.475
MFCD00014360	score = -36.451
MFCD00113329	score = -36.443
MFCD00191414	score = -36.428
MFCD00003135	score = -36.416

MFCD00031396 score = -36.109

MFCD00176994 score = -35.943

MFCD00157479 score = -35.889

MFCD00141193 score = -35.795

MFCD00177986 score = -35.794

MFCD00206668 score = -35.716

MFCD00189397 score = -35.599

MFCD00202912 score = -35.592

MFCD00181699 score = -35.318

MFCD00022646 score = -35.231

MFCD00206327 score = -35.164

MFCD00141190 score = -35.121

MFCD00099499 score = -35.042

MFCD00207881 score = -34.665

MFCD00121315 score = -34.543

MFCD00197239 score = -34.352

MFCD00087249 score = -34.279

MFCD00181440 score = -34.229

MFCD00205753 score = -34.167

MFCD00120879 score = -34.089

MFCD00141743 score = -34.033

MFCD00176025 score = -33.875

MFCD00186452 score = -33.845

MFCD00156816 score = -33.843

MFCD00121606 score = -33.775

MFCD00208021 score = -33.724

MFCD00168494 score = -33.656

MFCD00120174 score = -33.646
MFCD00139612 score = -33.502
MFCD00185326 score = -33.499
MFCD00202220 score = -33.428
MFCD00031316 score = -33.303
MFCD00020144 score = -33.255
MFCD00114469 score = -33.237
MFCD00172388 score = -33.101
MFCD00047160 score = -33.002
MFCD00126660 score = -32.912
MFCD00099937 score = -32.902
MFCD00055975 score = -32.873
MFCD00170637 score = -32.834
MFCD00195065 score = -32.791
MFCD00158209 score = -32.789
MFCD00025810 score = -32.744
MFCD00118032 score = -32.716
MFCD00140856 score = -32.707
MFCD00207533 score = -32.681
MFCD00037927 score = -32.673
MFCD00187050 score = -32.648
MFCD00152507 score = -32.609
MFCD00157695 score = -32.522
MFCD00009928 score = -32.466
MFCD00086876 score = -32.462
MFCD00150092 score = -32.401
MFCD00197455 score = -32.382

MFCD00086081	score = -32.322
MFCD00042557	score = -32.283
MFCD00159245	score = -32.252
MFCD00185246	score = -32.205
MFCD00186412	score = -32.191
MFCD00033564	score = -32.177
MFCD00189168	score = -32.169
MFCD00086611	score = -32.023
MFCD00188125	score = -32.003
MFCD00087389	score = -31.987
MFCD00047844	score = -31.958
MFCD00086875	score = -31.950
MFCD00039804	score = -31.942
MFCD00087434	score = -31.908
MFCD00002320	score = -31.885
MFCD00060320	score = -31.651
MFCD00014078	score = -31.364
MFCD00016762	score = -31.295
MFCD00006832	score = -30.816
MFCD00014537	score = -30.655
MFCD00010691	score = -30.449

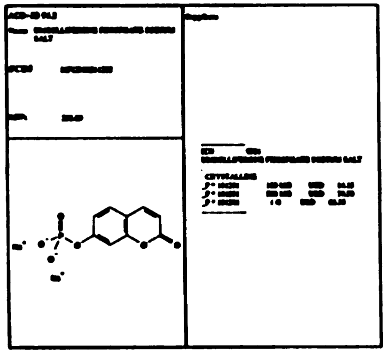

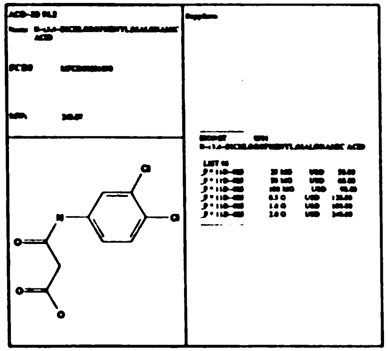

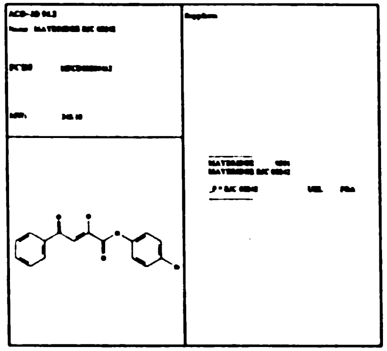

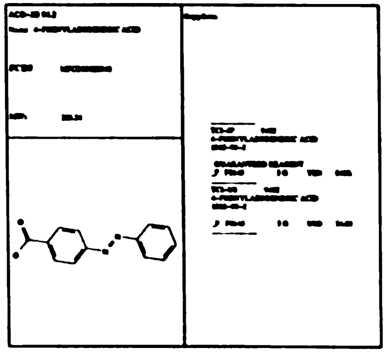

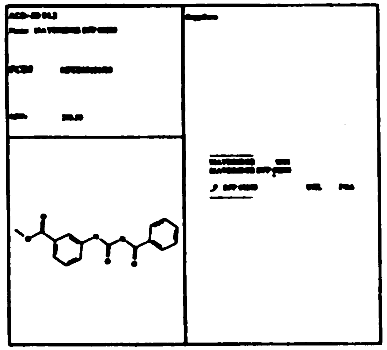

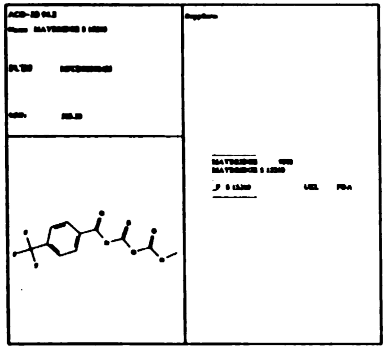

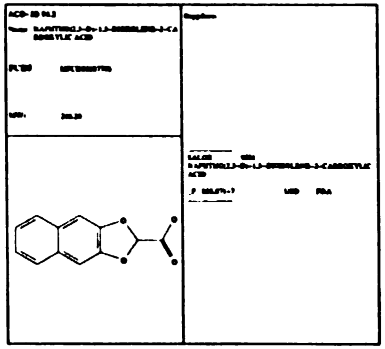

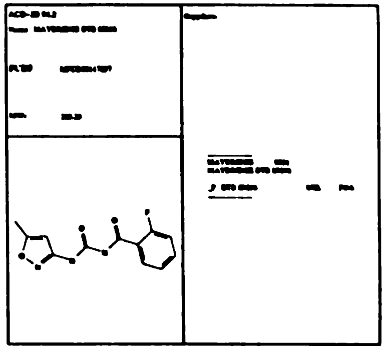

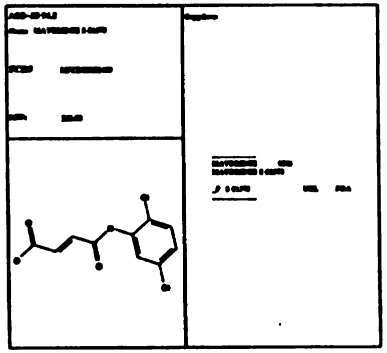

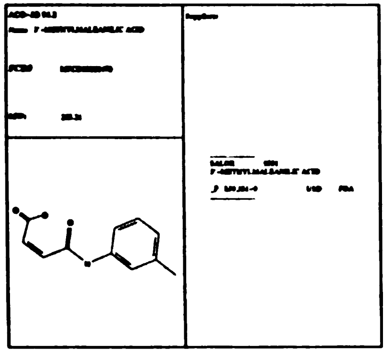

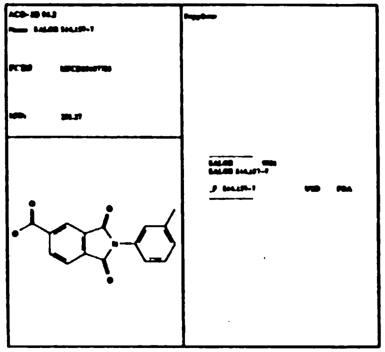

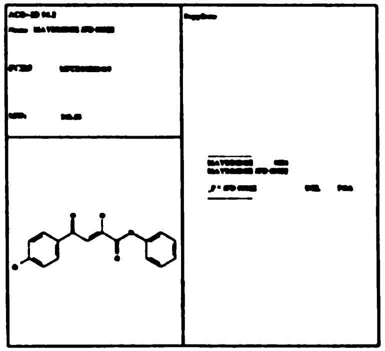

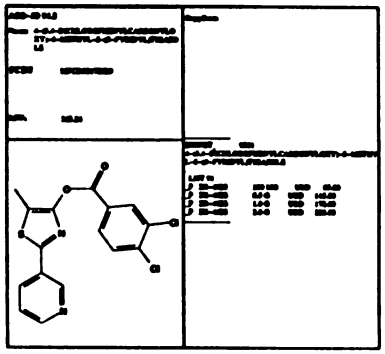

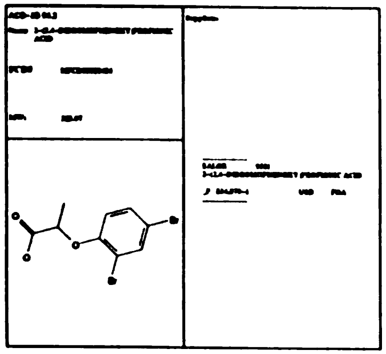

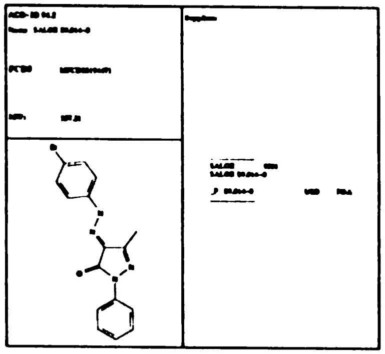

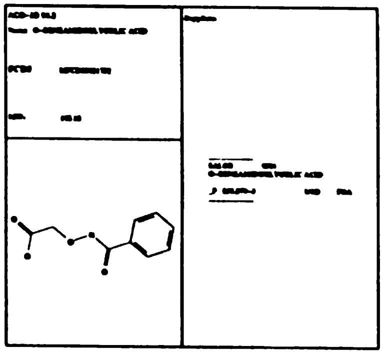

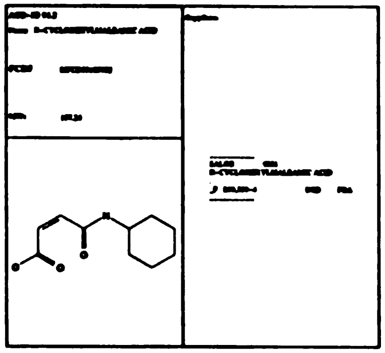

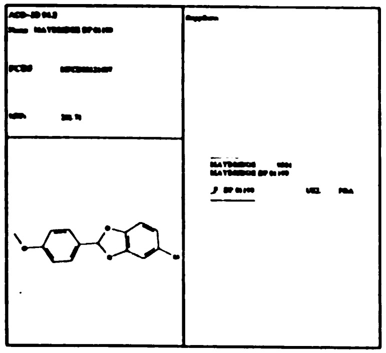

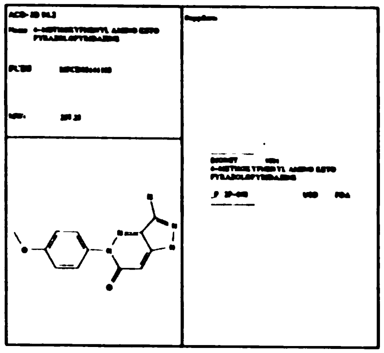

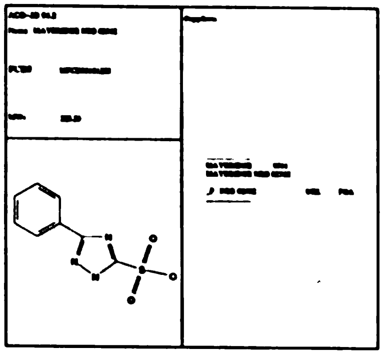

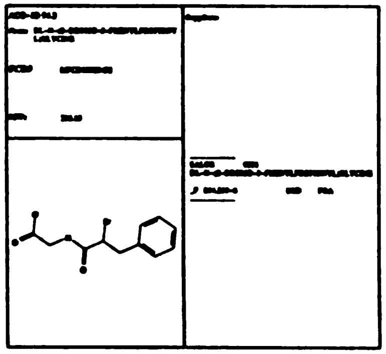

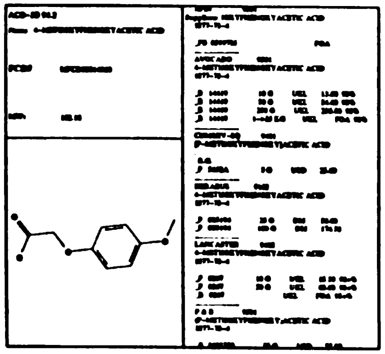

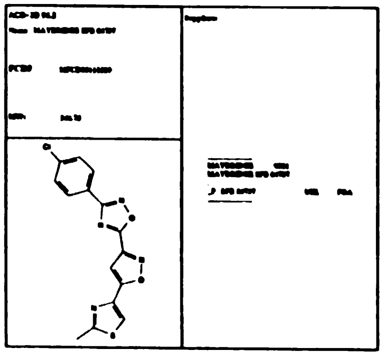

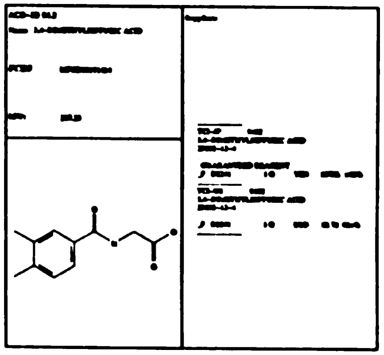

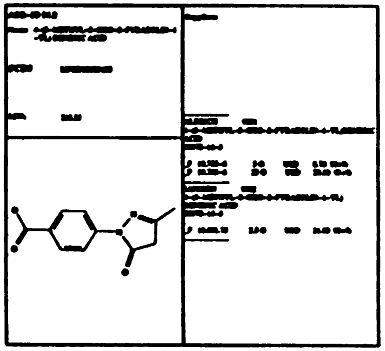
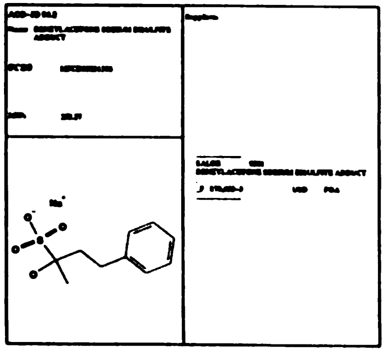
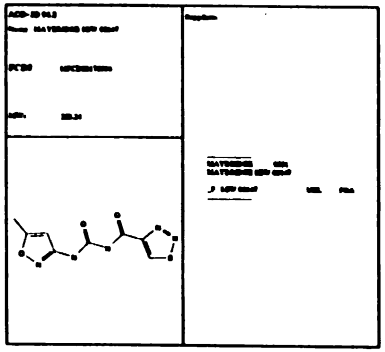
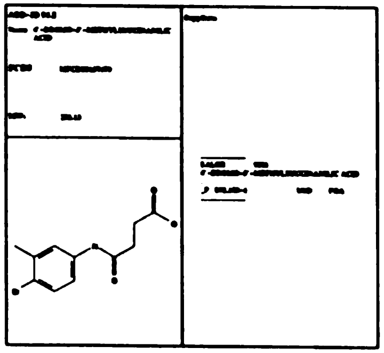
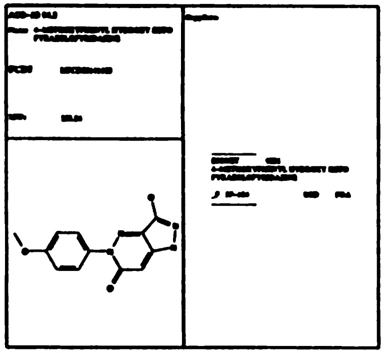
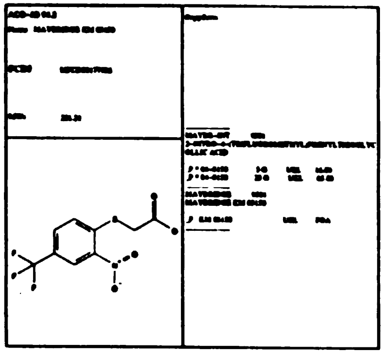
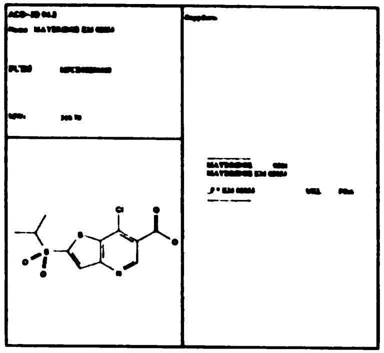
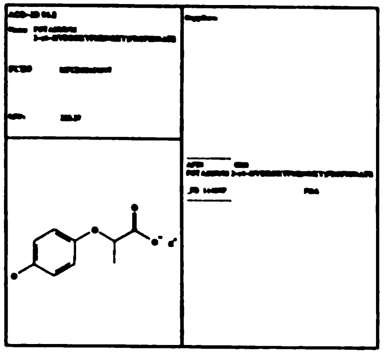
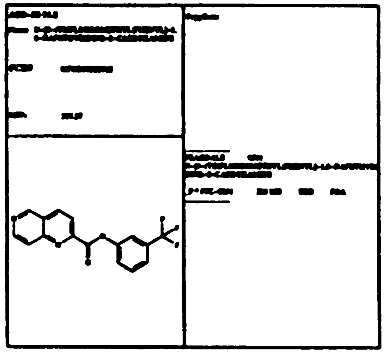
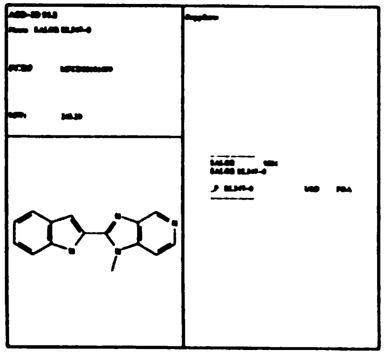
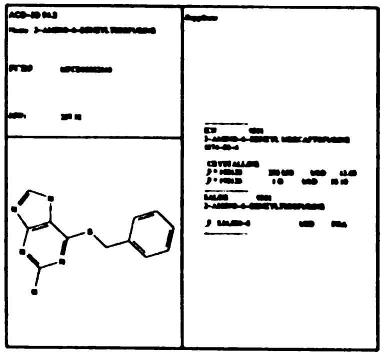
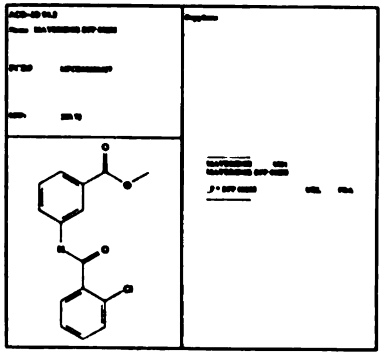

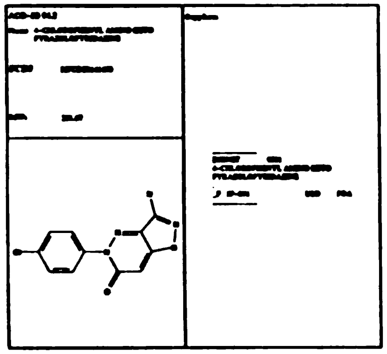

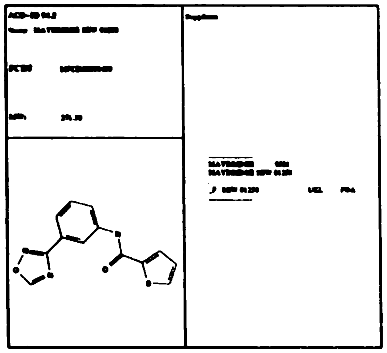

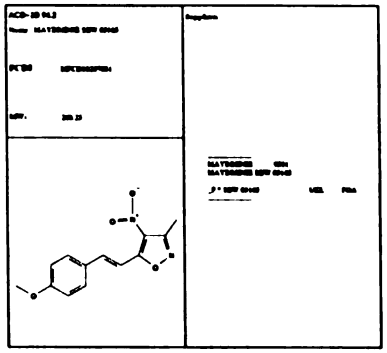

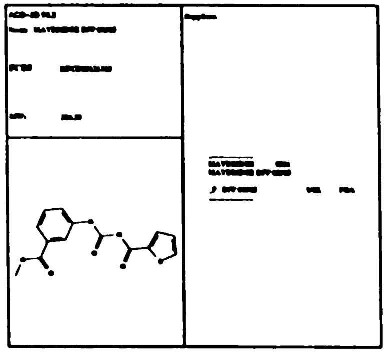

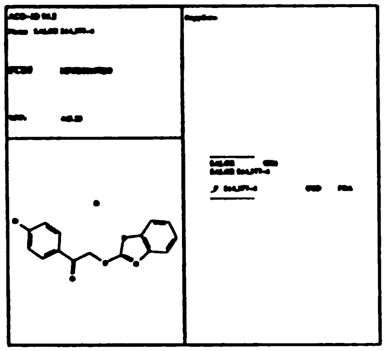

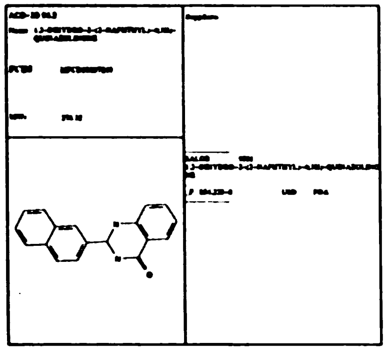

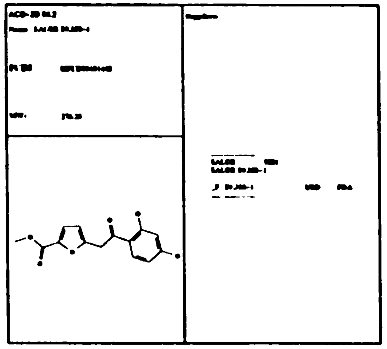

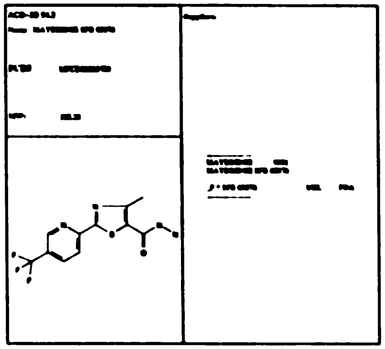

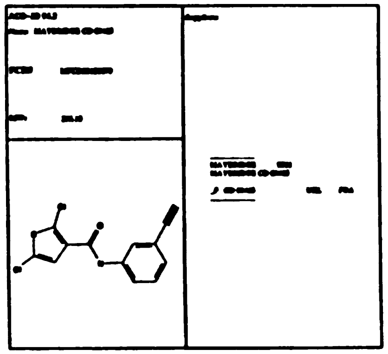

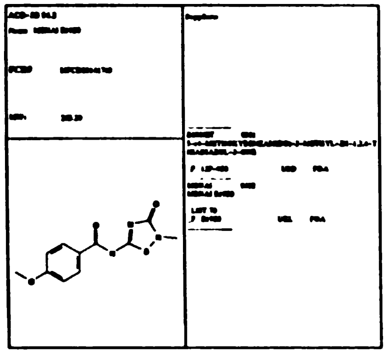

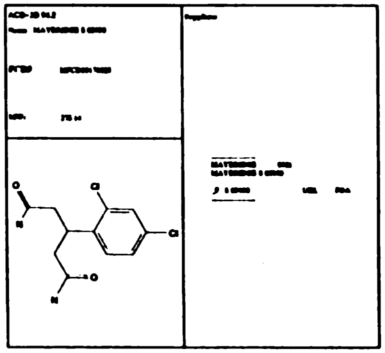

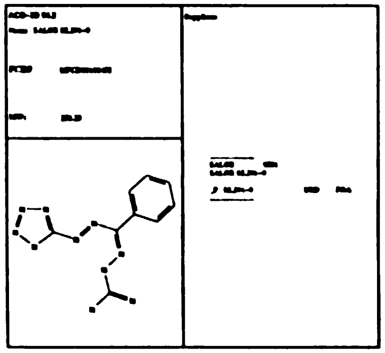

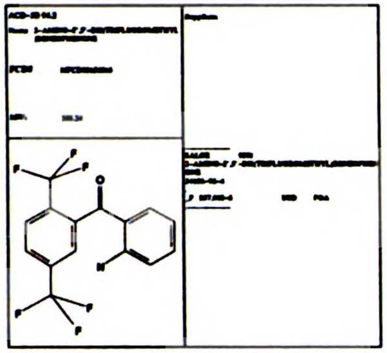
F
F
F
O
F
F
F

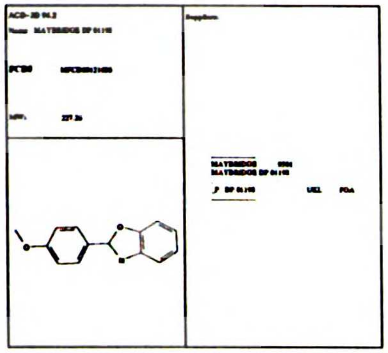

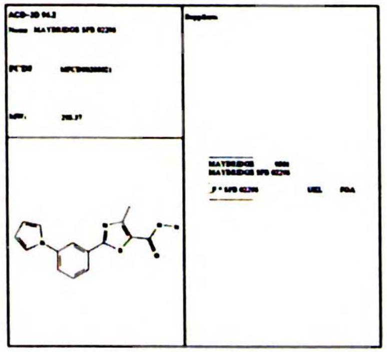

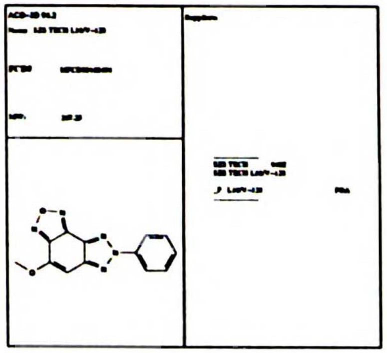

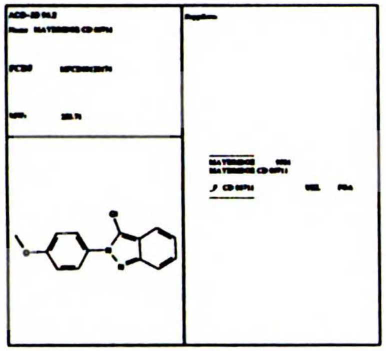

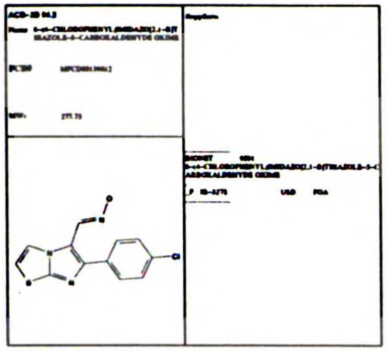
Cl

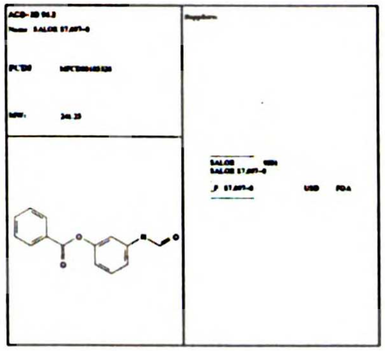

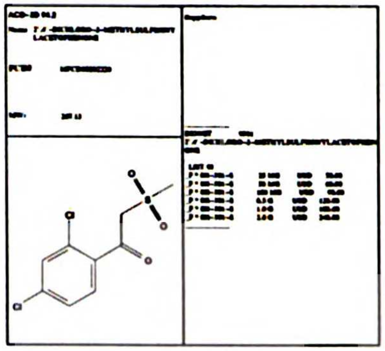
O
S
O
Cl
O
Cl

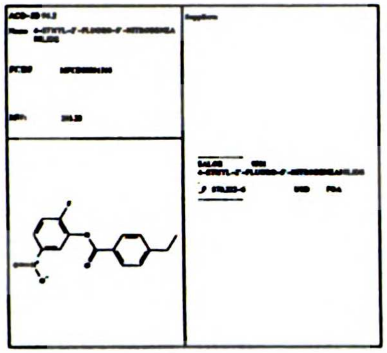

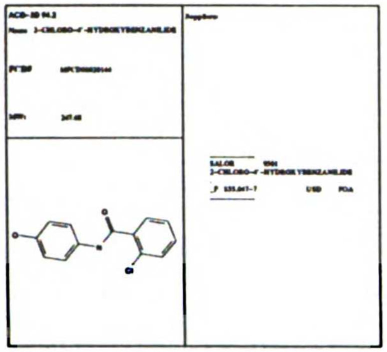
Cl

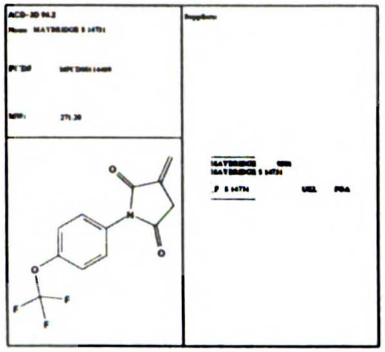
O
N
O
O
F
F
F

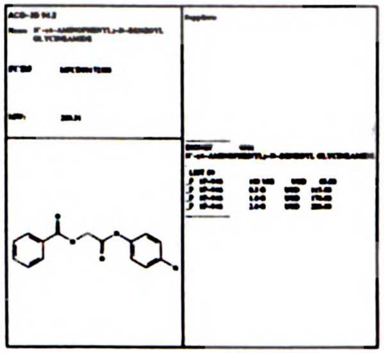

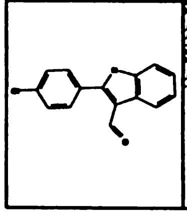
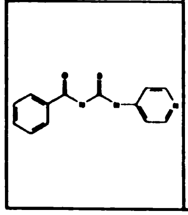
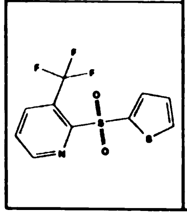
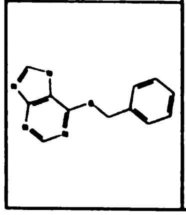
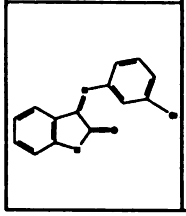
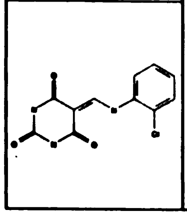
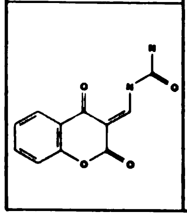
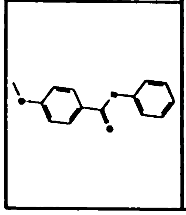
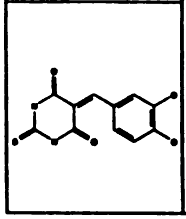
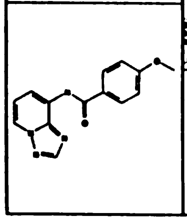
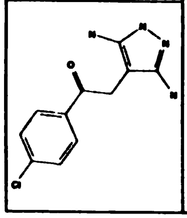
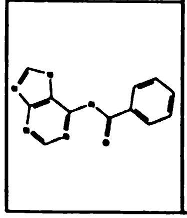

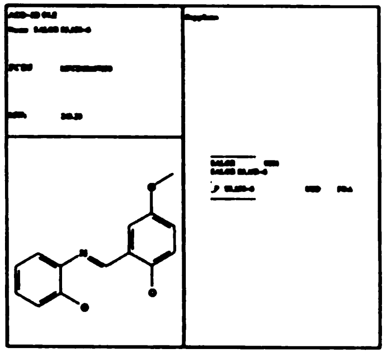

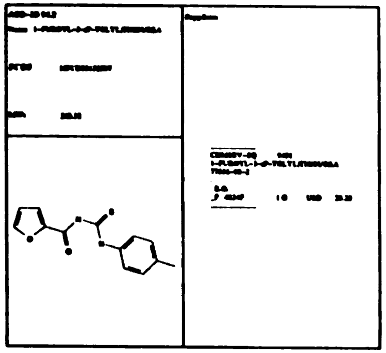

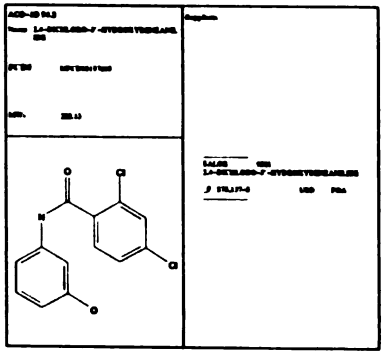

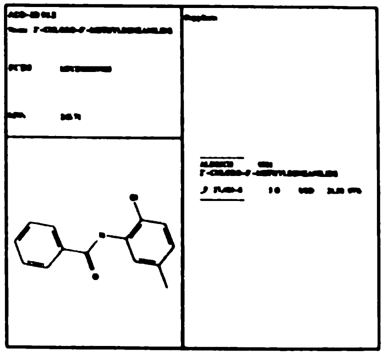

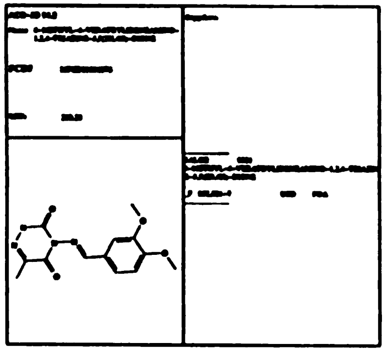

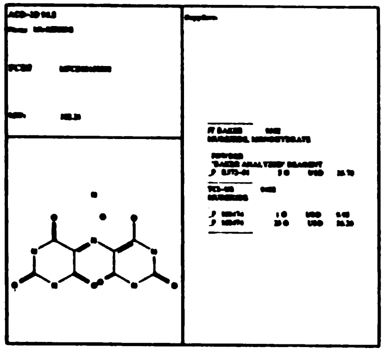

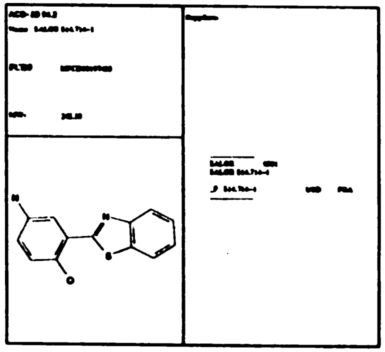

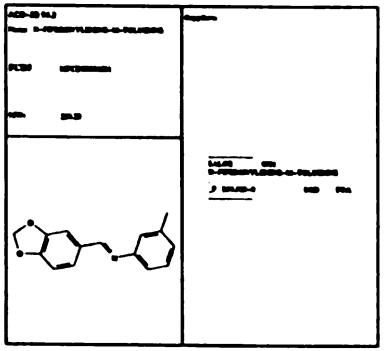

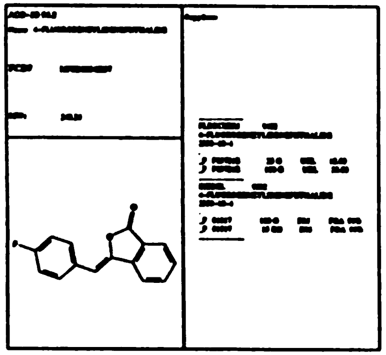

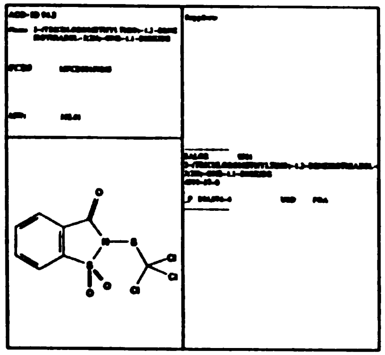

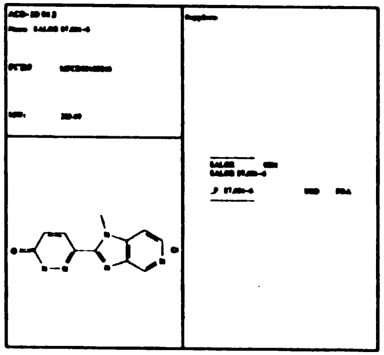

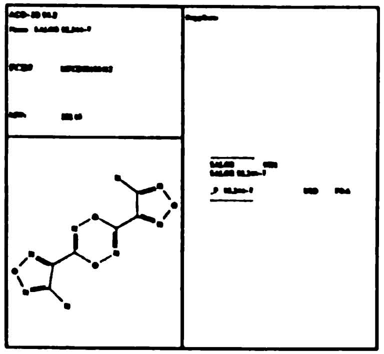

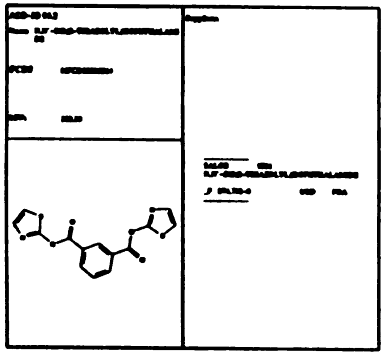

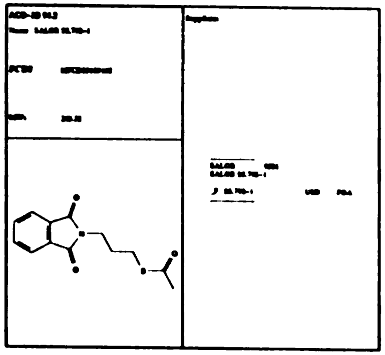

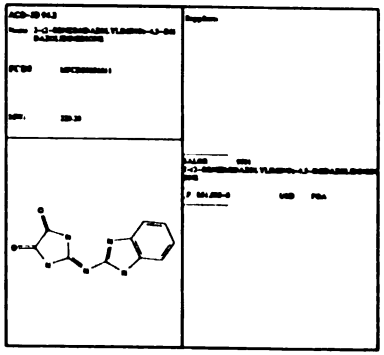

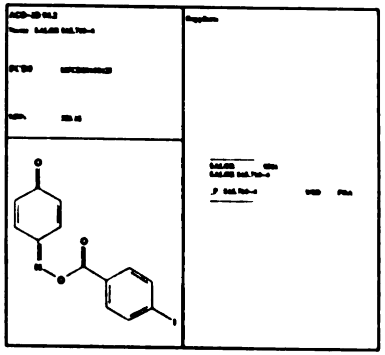

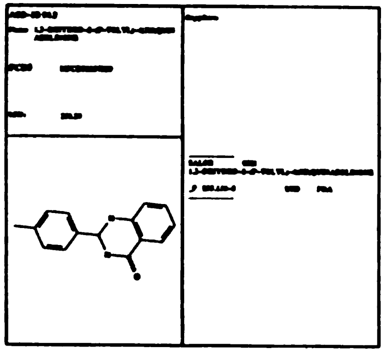

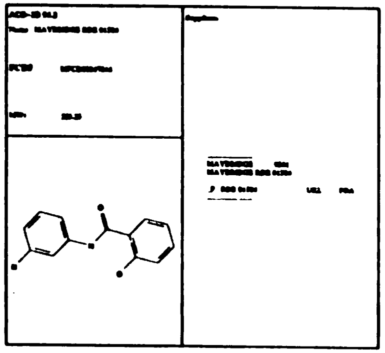

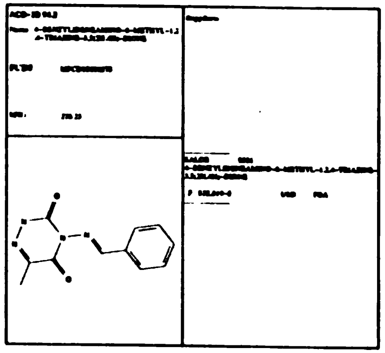

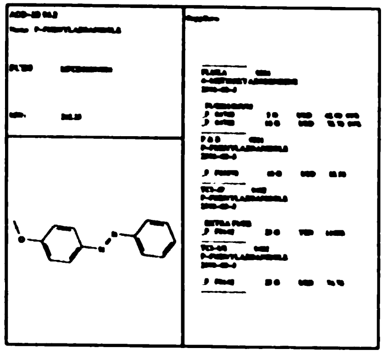

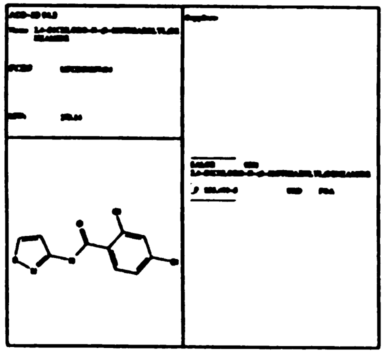

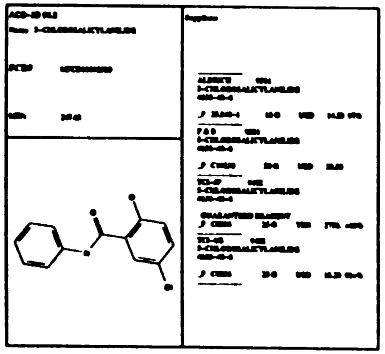

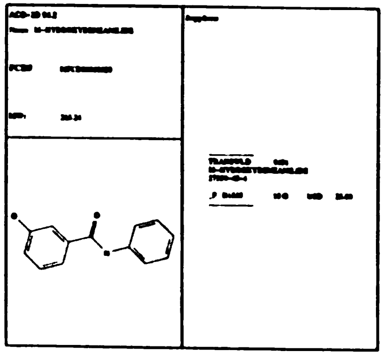

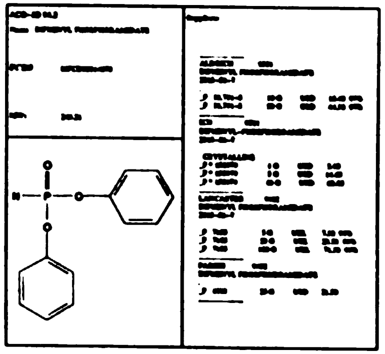

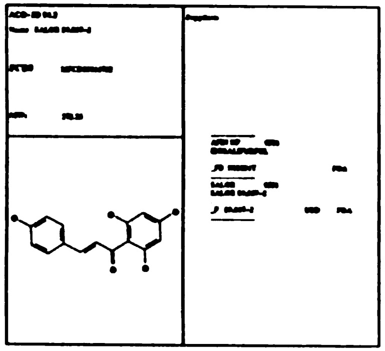

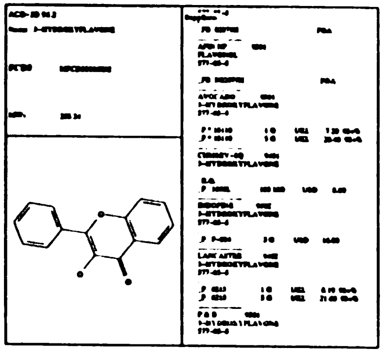

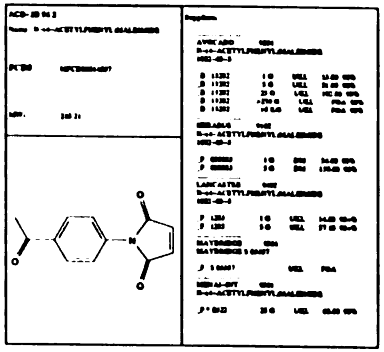

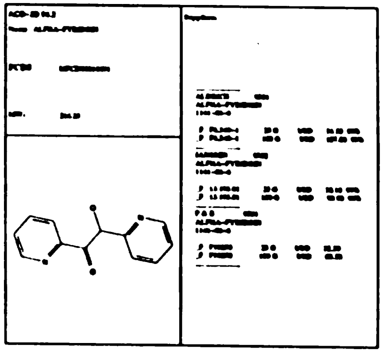

UC
San Francisco
LIBRARY

For reference

Not to be taken
from the room.